Proceedings of the 11th Conference on Applied and Industrial Mathematics, vol2

UNIVERSITY OF ORADEA ROMAI BUCHAREST

TEODOR MAGHIAR
(Editor-in-Chief)

ADELINA GEORGESCU
(Editor and Prefacer)

MIRCEA BALAJ
(Editor)

IOAN DZITAC
(Editor)

IOAN MANG
(Editor)

PROCEEDINGS

of

The 11th

Conference on Applied and Industrial Mathematics

May 29-31, 2003

Oradea, Romania CAIM 2003

Vol. 2

EDITURA UNIVERSITĂȚII DIN ORADEA

Descrierea CIP a Bibliotecii Naţionale a României
CONFERENCE ON APPLIED AND INDUSTRIAL MATHEMATICS-CAIM 2003
(11; 2003; Oradea)

Proceedings of the 11th Conference on applied and industrial mathematics-CAIM 2003: Oradea, May 29-31 2003 / editor-in-chief: Teodor Maghiar; editor and prefacer: Adelina Georgescu; co-editors: Mircea Bălaj, Ioan Dziţac, Ioan Mang.-Oradea: Editura Universităţii din Oradea, 2003. 2 vol. ISBN 973-613-330-3 **Vol. 2.** – 2003. Bibliogr.
Index
ISBN 973-613-332-X

I. Maghiar, Teodor (ed.)
II. Georgescu, Adelina (ed.)
III. Bălaj, Mircea (ed.)
IV. Dziţac, Ioan (ed.)
V. Mang, Ioan (ed.)

51-7(063)

Preface

Professor Dr. Adelina Georgescu, ROMAI President

This second (and last) volume contains part of papers presented to the conference on applied and Industrial mathematics (CAIM), held in Oradea, Romania, in the period May 29-31, 2003, and coorganized by University of Oradea and Romanian society of applied and industrial mathematics (ROMAI).

In the first part of the volume we include 25 contributions (most of them written in english) to research sections while in the second part - 8 contributions (written in Romanian) to education section.

There is a variety of topics reflecting the concern of various research teams and / or directions to which the CAIM 2003 participants belong. Some of these topics are traditional in CAIMs., e.g. fluid mechanics and its applications (to airspace and naval industries, ecology, meteorology, physiology); dynamical systems and bifurcation and their applications (to fluid dynamics, biology, medicine, communications security, economics). Other papers belong to the new and strong trend in information systems, e.g. computer science, artificial intelligence, and are concerned with: digital signature, image quality (when zoomed, compressed or decompressed), integrity in distributed database, computer packages for analysis of variance, genetic algorithms. These treatments are applications of code theory (cryptography), algebra, dispersional analysis and logic. It is for the first time that a paper of application of operational research to container loading was presented at CAIM.

Applied an industrial mathematics is directly related to pure mathematics, education in maths, particular sciences and industry. The first two domains are well represented in CAIMs. Researchers in physics are our collaborators from the very beginning. We remark that at CAIMs there are not so many economists, physicians, biologists, chemists as desired. Like throughout the world, the connection to respective domains are realized by physicists. It is also a different task, especially for ROMAI, to attract engineers directly involved into the productive activity. Partly this is due to the weakness of our industry and, consequently, to the reorientation of our good specialists (engineers) towards higher education, research or industrial units from other countries. In exchange, more and more specialists in computers, directly involved in industrial applications came towards ROMAI and CAIMs, in accordance with the trend throughout the world. In these circumstances our colleagues in ROMAI and CAIMs defined themselves as a selected group of specialists aiming to coordinate information and produce research related to the four above mentioned domains.

Having in view the preponderance of theoretical approaches in CAIMs papers, we encouraged fundamental research (of complex analysis, category theory, differential equations) too. This represents a promise for seniors research contribution in the future.

Apart from pure mathematicians, to CAIMs we invited high school teachers of maths to join us. In fact, more or less, they are responsible for the first stage in training maths with its two aspects: informative and formative. We had the proof of the large echo to our invitation and the manifest will of maths teachers to contribute to an applications - oriented teaching of maths. They are convinced that it is their duty to signal out to their scholars the newest achievements in maths and to motivate their lectury on the most arid parts of maths by attractive as well as useful examples from everyday life, industry, economy, society. At the same time they must create bridges between mathematics and other sciences and reveal their interconnections, in view of an appropiate reasoning in their future interconnected activities. These are the reasons why the second part of this volume contains the papers of the newly (namely in 2002) introduced section on education. This proved to be of a more and more increasing interest not only among maths teachers but also among students in maths and their professors. Some papers in this section plead for the introduction into school curricula of elements of new (e.g. fractal geometry) or very important (e.g. statistics and probability) branches of mathematics; some others adopt an interdisciplinary view point; others reveal the frequent occurrence in applications of certain mathematical topics less known even to mathematicians (e.g. related to calculus of variations). There is also the care for the formation of deep reasoning through geometry. We also draw attention to a paper devoted to agreeable teaching of maths through recreative games. Another paper treats an elementary topic of calculus which can create discomfort in complicated concrete applications.

We remark an optimal collaboration with the authors during the preparation of their works for publication. However, there are two papers whose authors was not possible to contact in due time, such that the reader is prayed to forgive us for the remained slips, in spite of our efforts to eliminate all of them.

We thank all authors from Romania, Republic of Moldova, Italy and Canada for providing the readers of these volumes with high level, clear, modern and useful papers.

Special thanks are addressed to the hard core of CAIMs participants, most of them ROMAI members, for the continuation of these prestigious conferences in Romania but with an international participation. Along with a few other scientific meetings in our country, CAIMs heavily contributed not only to the survival but also to the development of Romanian School of Mathematics, let it be pure or applied. Indirectly, through serious applications to industry, ecology, economics, medicine and communications, and through increasing level of maths education, CAIMs are helping the development of Romania and good relationships with other countries. They also created the opportunity for a renewal of the collaboration between researchers from Romania and their former colleagues who actually are practicing mathematics abroad. During all its existence, since 1992, ROMAI, and, so, CAIMs, benefited from material, scientific and moral support for these colleagues. We thank to them vividly, even if, by various reasons, they are no longer ROMAI members and / or CAIMs participants.

We address our warm thanks to Oradea Organizing committee and especially to Prof. Dr. Ioan Dzitac, constantly benefiting to the important support of the Rector, Prof. Dr. Theodor Maghiar, for their decisive contribution to the notable success of CAIM 2003: the number of participants exceeded 150 and the contributions were more than 85.

We also thank to all those who made possible the issue of these Proceedings and especially to Prof. Dr. Ioan Mang, Prof. Dr. Mircea Balaj and to Assoc. Prof. Dr. Ioan Dzitac's young collaborators Daniel Erzse and Horea Oros.

Let us meet again to CAIM 2004 in Pitesti, October 15-17.

Bucharest 2004-05-02

The remainder estimation in terms of the third derivative for the successive approximations method applied to ODE's

Alexandru Bica
Department of Mathematics, University of Oradea,
Str. Armatei Romane no.5, 410087, Oradea, Romania
e-mail: smbica@yahoo.com, abica@uoradea.ro

Abstract. In this paper we obtain a new remainder estimation for the error in the numerical method to solve Cauchy's problems for first order ordinary differential equations using the successive approximations method. In this article we improve the results from [8].

Keywords: successive approximations method, perturbed trapezoid quadrature formula
2000 Mathematics Subject Classification: 34K28, 65D30, 65D32.

1. Introduction

The successive approximations method to solve ODE's use the equivalence between the Cauchy's problem (1) and the Volterra integral equation (3), and apply to this integral equation the Banach's fixed point principle and a quadrature formula.

Let $a, b > 0$, $x_0, y_0 \in \mathbb{R}$ and $f : [x_0 - a, x_0 + a] \times [y_0 - b, y_0 + b] \to \mathbb{R}$ a continuous function which verifies the Lipschitz condition in the second argument. Then, the following Cauchy's problem,

$$(1) \qquad \begin{cases} y' = f(x, y) \\ y(x_0) = y_0 \end{cases}$$

has in the space $C^1[x_0 - h, x_0 + h]$ an unique solution, which can be obtained by the successive approximations method starting from any $y \in C^1[x_0 - h, x_0 + h]$ (in particular, we can start from y_0), where $h = \min(a, \frac{b}{M})$ and $M \in \mathbb{R}_+$ is such that $|f(x, y)| \leq M$, $\forall (x, y) \in [x_0 - a, x_0 + a] \times [y_0 - b, y_0 + b]$.

The Lipschitz condition in the second argument is: $\exists L > 0$ such that

$$(2) \qquad |f(x, u) - f(x, v)| \leq L\,|u - v|\,,\ \forall x \in [x_0 - a, x_0 + a], \forall u, v \in [y_0 - b, y_0 + b].$$

The Cauchy's problem (1) is equivalent to the following integral equation,

$$(3) \qquad y(x) = y_0 + \int_{x_0}^{x} f(s, y(s))ds.$$

Applying Banach's fixed point principle to the integral equation (3) we obtain the sequence of successive approximations,

$$(4) \qquad \begin{array}{c} y_0(x) = y_0, \quad \forall x \in [x_0, x_0 + h] \\ y_m(x) = y_0 + \int_{x_0}^{x} f(s, y_{m-1}(s))ds,\ \forall x \in [x_0, x_0 + h], \forall m \in \mathbb{N}^*. \end{array}$$

In [7, pages 87-95], at page 84-95, D.V.Ionescu proves the uniform convergence on $I = [x_0 - h, x_0 + h]$, of the sequence $(y_m)_{m \in \mathbb{N}}$ given in (4). Using the sequence (4) and a uniform partition of $[x_0, x_0 + h]$, D.V.Ionescu gives a numerical method to approximate the solution of (1). In this method he applies the trapezoidal quadrature rule in [9], to compute the integrals from (4) on the knots of the uniform partition.

The successive approximations method and the trapezoidal quadrature rule applied to Fredholm and Volterra integral equations can be viewed in [5].

In [8], using the quadrature formula of K.Petr (see [11]),

$$(5) \qquad \int_a^b f(x)dx = \frac{b - a}{2} \cdot [f(a) + f(b)] - \frac{(b - a)^2}{12} \cdot [f'(b) - f'(a)] + R(f)$$

with the remainder estimation,

$$(6) \qquad |R(f)| \le \frac{(b-a)^5}{720} \cdot \left\| f^{IV} \right\|$$

D.V.Ionescu obtains a numerical method for the problem (1) in which the remainder estimation is obtained by the method from [7] and [9] and by the inequality (6). The inequality (6) holds for smooth functions $f \in C^4(D)$, where $D = [x_0 - a, x_0 + a] \times [y_0 - b, y_0 + b]$. Unfortunately, the fourth derivative $\frac{d^4 f(t,x(t))}{dt^4}$ have 13 terms, and therefore, increase the terms in the remainder estimation. This is the reason for which we consider that we can stop to the third derivative in the estimation of the remainder, trying to use an adequate quadrature formula.

The quadrature formula of Petr is a particular case of the Obreschkoff's quadrature formula (see [10] and [6]). These formulas (of Petr and Obreschkoff) are presented in the general case in [6] at page 55, where (81) and (81') is the Obreschkoff's formula and (82) is the Petr's formula:

$$(7) \qquad \begin{aligned} &\int_a^b f(x)dx = \tfrac{C_k^1}{C_{2k}^1} \cdot (b-a)[f(a)+f(b)] - \tfrac{C_k^2}{C_{2k}^2} \cdot \tfrac{(b-a)^2}{2!} \cdot [f'(b) - f'(a)] + \\ &+ ... + (-1)^{k-1} \tfrac{C_k^k}{C_{2k}^k} \cdot \tfrac{(b-a)^k}{k!} \cdot [f^{(k-1)}(b) + (-1)^{k-1} f^{(k-1)}(a)] + R_k(f) \end{aligned}$$

with

$$(8) \qquad R_k(f) = (-1)^k \frac{(k!)^2}{(2k+1)!} (b-a)^{2k+1} \cdot \frac{1}{(2k)!} f^{(2k)}(\zeta).$$

The formula (5)-(6) is the particular case, $k = 2$, of the formula (7)-(8).

Here, we use a recent remainder estimation in the formula (5) obtained by N.S.Barnett and S.S.Dragomir in [1] and [2]. We sumarize the results from [1] and [2] in the following inequality,

$$\left| \int_a^b f(x)dx - \frac{b-a}{2}[f(a)+f(b)] + \frac{(b-a)^2}{12}[f'(b) - f'(a)] \right| \le$$

$$(9) \qquad \le \begin{cases} \frac{(b-a)^4}{160} \cdot \|f'''\|, & \text{if } f \in C^3[a,b] \\ \frac{(b-a)^5}{720} \cdot \left\| f^{IV} \right\|, & \text{if } f \in C^4[a,b]. \end{cases}$$

Here, we consider $f \in C^3[a,b]$ and use the following quadrature formula, from [1] :

$$(10) \qquad \int_a^b f(x)dx = \frac{b-a}{2}[f(a)+f(b)] - \frac{(b-a)^2}{12}[f'(b) - f'(a)] + R(f)$$

with the remainder estimation,

$$(11) \qquad |R(f)| \le \frac{(b-a)^4}{160} \cdot \|f'''\|.$$

Using a uniform partition of the interval $[a,b]$,

$$\Delta : a = x_0 < x_1 < ... < x_{n-1} < x_n = b, \quad x_i = a + \frac{i(b-a)}{n}, \forall i = \overline{0,n},$$

in [1], N.S.Barnett and S.S.Dragomir obtains the following quadrature rule,

$$(12) \qquad \int_a^b f(x)dx = \frac{b-a}{2n}[f(a) + 2\sum_{i=1}^{n-1} f(x_i) + f(b)] - \frac{(b-a)^2}{12n^2}[f'(b) - f'(a)] + R_n(f)$$

with the remainder estimation,

$$(13) \qquad |R_n(f)| \le \frac{(b-a)^4}{160n^3} \cdot \|f'''\|.$$

If $f \in C^4[a,b]$, then, the remainder estimation of the same quadrature rule, according to [2] and [8], is,

$$|R_n(f)| \le \frac{(b-a)^5}{720n^4} \cdot \left\| f^{IV} \right\|, \tag{14}$$

In [3], using the sequence of successive approximations and the quadrature rule (12)-(13), we obtain a numerical method to solve the delay integral equation,

$$x(t) = \int_{t-\tau}^{t} f(s, x(s))ds,$$

which arises in the study of the spread of certain infectious diseases. In [4] we use the same quadrature rule to solve ordinary Volterra integral equations and present a comparison between the numerical methods which use the trapezoidal quadrature rule and the quadrature rule (12)-(13). In [4] we show that, for a fixed error $\varepsilon = 10^{-4}$, the trapezoidal numerical method requires six iterations and the numerical method based on the formulas (12)-(13) require only four iterations.

2. The numerical method and the remainder estimation

Let Δ an uniform partition of $[x_0, x_0 + h]$,

$$\Delta : x_0 < x_1 < ... < x_{n-1} < x_n = x_0 + h, \quad x_i = x_0 + \frac{ih}{n}, \forall i = \overline{1,n}.$$

On the knots $x_i, i = \overline{1,n}$, the sequence of successive approximations (4) is,

$$\begin{aligned} y_0(x_i) &= y_0, \quad \forall i = \overline{0,n}. \\ y_m(x_i) &= y_0 + \int_{x_0}^{x_i} f(s, y_{m-1}(s))ds, \ \forall i = \overline{0,n}, \forall m \in \mathbb{N}^*. \end{aligned} \tag{15}$$

If $f \in C^3(D)$, then from the relations (4), we have that $y_n \in C^3$ $[x_0, x_0 + h]$, $\forall m, \in \mathbb{N}$ and for this reason, the functions

$$F_m : [x_0, x_0 + h] \to \mathbb{R}, \ F_m(x) = f(x, y_m(x)), \ \forall x \in [x_0, x_0 + h], \forall m \in \mathbb{N} \tag{16}$$

lies in the space C^3 $[x_0, x_0+h]$. To compute the integrals from (15) we use the quadrature rule (12)-(13), and obtain:

$$\begin{aligned} y_m(x_i) &= y_0 + \int_{x_0}^{x_i} F_{m-1}(s)ds = y_0 + \frac{h}{2n}[F_{m-1}(x_0) + 2\sum_{j=1}^{i-1} F_{m-1}(x_j) + F_{m-1}(x_i)] - \\ &\frac{h^2}{12n^2}[F'_{m-1}(x_i) - F'_{m-1}(x_0)] + R_{m,i}(f) = y_0 + \frac{h}{2n}[f(x_0, y_0) + 2\sum_{j=1}^{i-1} f(x_j, y_{m-1}(x_j)) \\ &+ f(x_i, y_{m-1}(x_i))] - \frac{h^2}{12n^2}[\frac{\partial f}{\partial x}(x_i, y_{m-1}(x_i)) + \frac{\partial f}{\partial y}(x_i, y_{m-1}(x_i)) \cdot y'_{m-1}(x_i) - \\ &- \frac{\partial f}{\partial x}(x_0, y_0) - \frac{\partial f}{\partial y}(x_0, y_0) \cdot y'_{m-1}(x_0)] + R_{m,i}(f), \quad \forall i = \overline{1,n}, \forall m \in \mathbb{N}^*. \end{aligned} \tag{17}$$

From (4) we obtain,

$$y'_m(x) = f(x, y_{m-1}(x)), \ \forall x \in [x_0, x_0 + h], \ \forall m \in \mathbb{N}^*. \tag{18}$$

and by (17) we have,

$$\begin{aligned} y_m(x_i) &= y_0 + \frac{h}{2n}[f(x_0, y_0) + 2\sum_{j=1}^{i-1} f(x_j, y_{m-1}(x_j)) + f(x_i, y_{m-1}(x_i))] - \\ &- \frac{h^2}{12n^2}[\frac{\partial f}{\partial x}(x_i, y_{m-1}(x_i)) + \frac{\partial f}{\partial y}(x_i, y_{m-1}(x_i)) \cdot f(x_i, y_{m-2}(x_i)) - \end{aligned}$$

(19) $$-\frac{\partial f}{\partial x}(x_0,y_0)-\frac{\partial f}{\partial y}(x_0,y_0)\cdot f(x_0,y_0)]+R_{m,i}(f),\quad \forall i=\overline{1,n},\forall m\in\mathbb{N}^*.$$

and the remainder estimation is,

(20) $$|R_{m,i}(f)|\le \frac{h^4}{160n^3}\cdot\left\|F'''_{m-1}\right\|,\quad \forall i=\overline{1,n},\forall m\in\mathbb{N}^*.$$

After elementary calculus we have,

$$F'''_{m-1}(x)=\frac{\partial^3 f}{\partial x^3}(x,y_m(x))+3\frac{\partial^3 f}{\partial x^2\partial y}(x,y_m(x))\cdot y'_m(x)+3\frac{\partial^3 f}{\partial x\partial y^2}(x,y_m(x))\cdot$$
$$\cdot[y'_m(x)]^2+\frac{\partial^3 f}{\partial y^3}(x,y_m(x))\cdot[y'_m(x)]^3+3\frac{\partial^2 f}{\partial x\partial y}(x,y_m(x))\cdot y''_m(x)+$$

(21) $$3\frac{\partial^2 f}{\partial y^2}(x,y_m(x))\cdot y'_m(x)\cdot y''_m(x)+\frac{\partial f}{\partial y}(x,y_m(x))\cdot y'''_m(x),\ \forall x\in[x_0,x_0+h],\ \forall m\in\mathbb{N}.$$

and,

$$y''_m(x)=\frac{\partial f}{\partial x}(x,y_{m-1}(x))+\frac{\partial f}{\partial y}(x,y_{m-1}(x))\cdot y'_{m-1}(x),$$
$$y'''_m(x)=\frac{\partial^2 f}{\partial x^2}(x,y_{m-1}(x))+2\frac{\partial^2 f}{\partial x\partial y}(x,y_{m-1}(x))\cdot y'_{m-1}(x)+\frac{\partial^2 f}{\partial y^2}(x,y_{m-1}(x))\cdot$$

(22) $$\cdot[y'_{m-1}(x)]^2+\frac{\partial f}{\partial y}(x,y_{m-1}(x))\cdot y''_{m-1}(x),\ \forall x\in[x_0,x_0+h],\forall m\in\mathbb{N}^*.$$
$$y'_0(x)=y''_0(x)=y'''_0(x)=0,\ \forall x\in[x_0,x_0+h].$$

Let

$$\left\|\frac{\partial^\alpha f}{\partial x^{\alpha_1}\partial y^{\alpha_2}}\right\|=\max\{\left|\frac{\partial^\alpha f(x,y)}{\partial x^{\alpha_1}\partial y^{\alpha_2}}\right|:x\in[x_0,x_0+h],y\in[y_0-b,y_0+b]\}$$

for $|\alpha|\le 3$, $\alpha_1+\alpha_2=|\alpha|$, $\alpha_1,\alpha_2\in\{0,1,2,3\}$, and

$$M_1=\max\{\left\|\frac{\partial f}{\partial x}\right\|,\left\|\frac{\partial f}{\partial y}\right\|\},$$
$$M_2=\max\{\left\|\frac{\partial^2 f}{\partial x^2}\right\|,\left\|\frac{\partial^2 f}{\partial x\partial y}\right\|,\left\|\frac{\partial^2 f}{\partial y^2}\right\|\}$$
$$M_3=\max\{\left\|\frac{\partial^3 f}{\partial x^3}\right\|,\left\|\frac{\partial^3 f}{\partial x^2\partial y}\right\|,\left\|\frac{\partial^3 f}{\partial x\partial y^2}\right\|,\left\|\frac{\partial^3 f}{\partial y^3}\right\|\}.$$

Then, from (18), (21) and (22) we have,

$$|F'''_m(x)|\le M_3+3MM_3+3M_3M^2+M_3M^3+3M_1M_2(M+1)+$$
$$+3MM_1M_2(M+1)+M_1[M_2+2MM_2+M_2M^2+M_1^2(M+1)=M_3(M+1)^3+$$

(23) $$+4M_1M_2(M+1)^2+M_1^3(M+1)=M''',\ \forall x\in[x_0,x_0+h],\forall m\in\mathbb{N},$$

and therefore, the inequality (20) becames:

(24) $$|R_{m,i}(f)|\le\frac{h^4M'''}{160n^3},\ \forall i=\overline{1,n},\forall m\in\mathbb{N}^*.$$

We see that the estimation from the inequality (24) does not depend on i and m.

The relations (19) and (24) lead to the following algorithm :

$$y_m(x_0)=y_0,\ \forall m\in\mathbb{N}\text{ and }y_0(x_i)=y_0,\ \forall i=\overline{0,n},$$
$$y_1(x_i)=y_0+\frac{h}{2n}[f(x_0,y_0)+2\sum_{j=1}^{i-1}f(x_j,y_0(x_j))+f(x_i,y_0(x_i))]-$$
$$-\frac{h^2}{12n^2}[\frac{\partial f}{\partial x}(x_i,y_0(x_i))-\frac{\partial f}{\partial x}(x_0,y_0)]+R_{1,i}(f)=y_0+\frac{h}{2n}[f(x_0,y_0)+$$

$$+2\sum_{j=1}^{i-1} f(x_j,y_0)+f(x_i,y_0)]-\frac{h^2}{12n^2}[\frac{\partial f}{\partial x}(x_i,y_0)-\frac{\partial f}{\partial x}(x_0,y_0)]+$$

$$+R_{1,i}(f)=\overline{y_1(x_i)}+R_{1,i}(f),\ \forall i=\overline{1,n} \tag{25}$$

$$y_2(x_i)=y_0+\frac{h}{2n}[f(x_0,y_0)+2\sum_{j=1}^{i-1} f(x_j,\overline{y_1(x_j)}+R_{1,j}(f))+f(x_i,\overline{y_1(x_i)}+R_{1,i}(f))]$$

$$-\frac{h^2}{12n^2}[\frac{\partial f}{\partial x}(x_i,\overline{y_1(x_i)}+R_{1,i}(f))+\frac{\partial f}{\partial y}(x_i,\overline{y_1(x_i)}+R_{1,i}(f))\cdot f(x_i,y_0)-\frac{\partial f}{\partial x}(x_0,y_0)$$

$$-\frac{\partial f}{\partial y}(x_0,y_0)\cdot f(x_0,y_0)]+R_{2,i}(f)=y_0+\frac{h}{2n}[f(x_0,y_0)+2\sum_{j=1}^{i-1} f(x_j,\overline{y_1(x_j)})+$$

$$+f(x_i,\overline{y_1(x_i)})]-\frac{h^2}{12n^2}[\frac{\partial f}{\partial x}(x_i,\overline{y_1(x_i)})+\frac{\partial f}{\partial y}(x_i,\overline{y_1(x_i)})\cdot f(x_i,y_0)-\frac{\partial f}{\partial x}(x_0,y_0)$$

$$-\frac{\partial f}{\partial y}(x_0,y_0)\cdot f(x_0,y_0)]+\overline{R_{2,i}(f)}=\overline{y_2(x_i)}+\overline{R_{2,i}(f)},\ \forall i=\overline{1,n} \tag{26}$$

and

$$\left|\overline{R_{2,i}(f)}\right|\le |R_{2,i}(f)|+\frac{h}{2n}(2L\sum_{j=1}^{i-1}|R_{1,j}(f)|+L\,|R_{1,i}(f)|)+$$

$$+\frac{h^2}{12n^2}[\left\|\frac{\partial^2 f}{\partial x\partial y}\right\|\cdot|R_{1,i}(f)|+M\left\|\frac{\partial^2 f}{\partial y^2}\right\|\cdot|R_{1,i}(f)|]\le|R_{2,i}(f)|+Lh\cdot\frac{h^4M'''}{160n^3}$$

$$+\frac{h^2}{12n^2}M_2(M+1)\cdot\frac{h^4M'''}{160n^3}\le[1+hL+\frac{h^2}{12n^2}M_2(M+1)]\cdot\frac{h^4M'''}{160n^3},\ \forall i=\overline{1,n}. \tag{27}$$

By induction, for $m\in\mathbb{N}$, $m\ge 3$, we obtain :

$$y_m(x_i)=y_0+\frac{h}{2n}[f(x_0,y_0)+2\sum_{j=1}^{i-1} f(x_j,\overline{y_{m-1}(x_j)}+\overline{R_{m-1,j}(f)})+f(x_i,\overline{y_{m-1}(x_i)}+$$

$$+\overline{R_{m-1,j}(f)})]-\frac{h^2}{12n^2}[\frac{\partial f}{\partial x}(x_i,\overline{y_{m-1}(x_i)}+\overline{R_{m-1,j}(f)})+\frac{\partial f}{\partial y}(x_i,\overline{y_{m-1}(x_i)}+$$

$$+\overline{R_{m-1,j}(f)})\cdot f(x_i,\overline{y_{m-2}(x_i)}+\overline{R_{m-2,j}(f)})-\frac{\partial f}{\partial x}(x_0,y_0)-\frac{\partial f}{\partial y}(x_0,y_0)\cdot f(x_0,y_0)]$$

$$+R_{m,i}(f)=y_0+\frac{h}{2n}[f(x_0,y_0)+2\sum_{j=1}^{i-1} f(x_j,\overline{y_{m-1}(x_j)})+f(x_i,\overline{y_{m-1}(x_i)})]-$$

$$-\frac{h^2}{12n^2}[\frac{\partial f}{\partial x}(x_i,\overline{y_{m-1}(x_i)})+\frac{\partial f}{\partial y}(x_i,\overline{y_{m-1}(x_i)})\cdot f(x_i,\overline{y_{m-2}(x_i)})-\frac{\partial f}{\partial x}(x_0,y_0)-$$

$$-\frac{\partial f}{\partial y}(x_0,y_0)\cdot f(x_0,y_0)]+\overline{R_{m,i}(f)}=\overline{y_m(x_i)}+\overline{R_{m,i}(f)},\ \forall i=\overline{1,n},\ \forall m\ge 3. \tag{28}$$

Firstly, for the remainder estimation we obtain the reccurent inequality:

$$\left|\overline{R_{m,i}(f)}\right|\le|R_{m,i}(f)|+\frac{h}{2n}[L\left|\overline{R_{m-1,i}(f))}\right|+2L\sum_{j=1}^{i-1}\left|\overline{R_{m-1,j}(f)}\right|]+$$

$$+\frac{h^2}{12n^2}[\left\|\frac{\partial^2 f}{\partial x\partial y}\right\|\cdot\left|\overline{R_{m-1,i}(f))}\right|+\left\|\frac{\partial f}{\partial y}\right\|L\cdot\left|\overline{R_{m-2,i}(f))}\right|+M\left\|\frac{\partial^2 f}{\partial y^2}\right\|\cdot$$

$$\cdot\left|\overline{R_{m-1,i}(f))}\right|]\le\frac{h^4M'''}{160n^3}+\frac{hL}{2n}(\left|\overline{R_{m-1,i}(f))}\right|+2\sum_{j=1}^{i-1}\left|\overline{R_{m-1,j}(f)}\right|)+$$

$$\frac{h^2}{12n^2}[M_2(M+1)\left|\overline{R_{m-1,i}(f))}\right|+M_1L\left|\overline{R_{m-2,i}(f))}\right|],\ \forall i=\overline{1,n},\ \forall m\in\mathbb{N},m\ge 2. \tag{29}$$

For $i=\overline{1,n}$, let

$$|\rho_{2,i}| = \max\{\left|\overline{R_{2,j}(f)}\right| : j=\overline{1,i}\}.$$

From (27) we have,

$$|\rho_{2,i}| \le [1+hL+\frac{h^2}{12n^2}M_2(M+1)]\cdot\frac{h^4M'''}{160n^3} \le$$

$$\le [1+hL+\frac{h^2}{12n^2}(M_2(M+1)+M_1L)]\cdot\frac{h^4M'''}{160n^3},\ \forall i=\overline{1,n}. \tag{30}$$

From (29) and (30) it follows,

$$\left|\overline{R_{3,i}(f)}\right| \le |R_{3,i}(f)| + [hL+\frac{h^2}{12n^2}(M_2(M+1)+M_1L)]\cdot|\rho_{2,i}| \le (1+[hL+$$

$$+\frac{h^2}{12n^2}(M_2(M+1)+M_1L)]+[hL+\frac{h^2}{12n^2}(M_2(M+1)+M_1L)]^2)\frac{h^4M'''}{160n^3},\ \forall i=\overline{1,n}. \tag{31}$$

By induction, for $m\ge 3$, we denote for $q\in\{m-2,m-1\}$,

$$\left|\widetilde{R_{q,i}(f)}\right| = \max\{\left|\widetilde{R_{q,j}(f)}\right| : j=\overline{1,i}\}$$

and

$$|\rho_{m-1,i}| = \max\{\left|\widetilde{R_{m-1,i}(f)}\right|, \left|\widetilde{R_{m-2,i}(f)}\right|\},\ \forall i=\overline{1,n}.$$

Then, we obtain, from (31), the inequalities:

$$\left|\widetilde{R_{m-1,i}(f)}\right| \le (1+[hL+\frac{h^2}{12n^2}(M_2(M+1)+M_1L)]+...+$$

$$+[hL+\frac{h^2}{12n^2}(M_2(M+1)+M_1L)]^{m-2})\cdot\frac{h^4M'''}{160n^3}$$

and

$$\left|\widetilde{R_{m-2,i}(f)}\right| \le (1+[hL+\frac{h^2}{12n^2}(M_2(M+1)+M_1L)]+...+$$

$$+[hL+\frac{h^2}{12n^2}(M_2(M+1)+M_1L)]^{m-3})\cdot\frac{h^4M'''}{160n^3}\ ,\forall i=\overline{1,n},$$

and consequently, by (29), it follows that,

$$\left|\overline{R_{m,i}(f)}\right| \le |R_{m,i}(f)| + [hL+\frac{h^2}{12n^2}(M_2(M+1)+M_1L)]\cdot|\rho_{m-1,i}| \le$$

$$\le \frac{h^4M'''}{160n^3} + [hL+\frac{h^2}{12n^2}(M_2(M+1)+M_1L)]\cdot\frac{h^4M'''}{160n^3}\cdot$$

$$\cdot\sum_{k=0}^{m-2}[hL+\frac{h^2}{12n^2}(M_2(M+1)+M_1L)]^k = (1+[hL+\frac{h^2}{12n^2}(M_2(M+1)+M_1L)]+$$

$$+...+[hL+\frac{h^2}{12n^2}(M_2(M+1)+M_1L)]^{m-1})\cdot\frac{h^4M'''}{160n^3} =$$

$$= \frac{1-[hL+\frac{h^2}{12n^2}(M_2(M+1)+M_1L)]^m}{1-[hL+\frac{h^2}{12n^2}(M_2(M+1)+M_1L)]}\cdot\frac{h^4M'''}{160n^3}\ ,\forall i=\overline{1,n},\ \forall m\in\mathbb{N}, m\ge 3. \tag{32}$$

In this way, we obtain in (25), (26) and (28) the sequence $(\overline{y_m(x_i)})_{m\in\mathbb{N}}$ which approximates the values $y_m(x_i)$, $m\in\mathbb{N}$ on the knots x_i , $i=\overline{1,n}$ with an error for which the estimation (32) holds.

Theorem 1. *If $Lh < \frac{11}{12}$ and $f \in C^3([x_0 - a, x_0 + a] \times [y_0 - b, y_0 + b])$ then, for $n \in \mathbb{N}$, $n > h\sqrt[2]{M_2(M+1) + M_1 L}$, the sequence $(\overline{y_m(x_i)})_{m\in\mathbb{N}}$ approximates on the knots x_i , $i = \overline{1,n}$, the solution y^* of the Cauchy's problem (1) with the error estimation :*

$$(33) \qquad \left|y^*(x_i) - \overline{y_m(x_i)}\right| \leq \frac{(Lh)^m}{1 - Lh}(|y_0| + Mh) + \\ + \frac{h^4 M'''}{160n^3(1 - [hL + \frac{h^2}{12n^2}(M_2(M+1) + M_1 L)])}, \ \forall i = \overline{1,n}, \forall m \in \mathbb{N}, m \geq 2.$$

Proof. From the Banach's fixed point principle, we have,

$$|y^*(x) - y_m(x)| \leq \frac{(Lh)^m}{1 - Lh} \cdot \|y_0 - y_1\|, \ \forall x \in [x_0, x_0 + h], \ \forall m \in \mathbb{N}^*$$

and

$$\|y_0 - y_1\| = \max\{\left|y_0 - \int_{x_0}^{x} f(s, y_0)ds\right| : x \in [x_0, x_0 + h]\} \leq |y_0| + Mh.$$

Then,

$$(34) \qquad |y^*(x_i) - y_m(x_i)| \leq \frac{(Lh)^m}{1 - Lh}(|y_0| + Mh), \ \forall i = \overline{1,n}, \forall m \in \mathbb{N}^*.$$

Since $Lh < \frac{11}{12}$ and $n > h\sqrt[2]{M_2(M+1) + M_1 L}$, we have that $hL + \frac{h^2}{12n^2}(M_2(M+1) + M_1 L) < 1$, and from (32) it obtains,

$$(35) \qquad \left|y_m(x_i) - \overline{y_m(x_i)}\right| = \left|\overline{R_{m,i}(f)}\right| \leq \frac{h^4 M'''}{160n^3(1 - [hL + \frac{h^2}{12n^2}(M_2(M+1) + M_1 L)])}$$

, $\forall i = \overline{1,n}$, $\forall m \in \mathbb{N}, m \geq 2$. The inequality (33) follows from (34) and (35). □

Remark 1. If $f \in C^4([x_0 - a, x_0 + a] \times [y_0 - b, y_0 + b])$, then for

$$M_4 = \max\{\left\|\frac{\partial^4 f}{\partial x^i \partial y^j}\right\| : i, j = \overline{0,4}, \ i + j = 4\}$$

and after analogous calculus as in (21), (22) and (23) we obtain the fourth derivative $F_m^{(IV)}(x)$ which has 13 terms,

$$F_m^{(IV)}(x) = \frac{\partial^4 f}{\partial x^4}(x, y_m(x)) + 4\frac{\partial^4 f}{\partial x^3 \partial y}(x, y_m(x)) \cdot y'_m(x) + \frac{\partial^4 f}{\partial x^4}(x, y_m(x)) \cdot \\ \cdot [y'_m(x)]^4 + 4\frac{\partial^4 f}{\partial x \partial y^3}(x, y_m(x)) \cdot [y'_m(x)]^3 + 3\frac{\partial^4 f}{\partial x^3 \partial y}(x, y_m(x)) \cdot [y'_m(x)]^2 + \\ 3\frac{\partial^4 f}{\partial x^2 \partial y^2}(x, y_m(x)) \cdot [y'_m(x)]^2 + 6\frac{\partial^3 f}{\partial x^2 \partial y}(x, y_m(x)) \cdot y''_m(x) + 12\frac{\partial^3 f}{\partial x \partial y^2}(x, y_m(x)) \cdot \\ \cdot y'_m(x) \cdot y''_m(x) + 6\frac{\partial^3 f}{\partial y^3}(x, y_m(x)) \cdot [y'_m(x)]^2 \cdot y''_m(x) + 4\frac{\partial^2 f}{\partial x \partial y}(x, y_m(x)) \cdot y'''_m(x) + \\ 3\frac{\partial^2 f}{\partial y^2}(x, y_m(x)) \cdot [y''_m(x)]^2 + 4\frac{\partial^2 f}{\partial x^2}(x, y_m(x)) \cdot y'_m(x) \cdot y'''_m(x) + \frac{\partial f}{\partial y}(x, y_m(x)) \cdot y_m^{IV}(x)$$

and the following estimations hold:

$$\|y_m\| \leq Mh, \quad \|y'_m\| \leq M, \quad \|y''_m\| \leq M_1(M+1), \\ \|y'''_m\| \leq M_2(M+1)^2 + M_1^2(M+1), \ \forall m \in \mathbb{N}^*, \\ \left|y_m^{IV}(x)\right| \leq M''', \forall x \in [x_0, x_0 + h], \forall m \in \mathbb{N}^*.$$

Therefore, we have

$$\left|F_m^{(IV)}(x)\right| \leq M_4(M+1)^4 + 6M_1 M_3(M+1)^2 + 3M_2 M_1^2(M+1)^2 + 4M_2^2(M+1)^3 +$$

$$+4M_2M_1^2(M+1)^2+M_1M'''=M^{IV},\ \forall x\in[x_0,x_0+h],\ \forall m\in\mathbb{N}.$$

Then, the inequality (24) became, according to (9),

$$|R_{m,i}(f)|\leq\frac{h^5M^{IV}}{720n^4},\ \forall i=\overline{1,n},\forall m\in\mathbb{N}^*. \tag{36}$$

The algorithm (25), (26) , (28) is the same, and the inequality (32) is in this case,

$$\left|\overline{R_{m,i}(f)}\right|\leq\frac{1-[hL+\frac{h^2}{12n^2}(M_2(M+1)+M_1L)]^m}{1-[hL+\frac{h^2}{12n^2}(M_2(M+1)+M_1L)]}\cdot$$

$$\cdot\frac{h^5M^{IV}}{720n^4},\ \forall i=\overline{1,n},\forall m\in\mathbb{N},m\geq 2. \tag{37}$$

Corollary 2. *If $f\in C^4([x_0-a,x_0+a]\times[y_0-b,y_0+b])$, under conditions of Theorem 1, the error estimation (33) became:*

$$\left|y^*(x_i)-\overline{y_m(x_i)}\right|\leq\frac{(Lh)^m}{1-Lh}(|y_0|+Mh)+ \tag{38}$$

$$+\frac{h^5M^{IV}}{720n^4(1-[hL+\frac{h^2}{12n^2}(M_2(M+1)+M_1L)])},\ \forall i=\overline{1,n},\forall m\in\mathbb{N},m\geq 2.$$

, $\forall i=\overline{1,n},\ \forall m\in\mathbb{N},m\geq 2$.

Proof. It is analogous with the proof of the previous theorem, where instead of inequality (32) is inequality (37). In this proof we use the above remark, too. □

Remark 2. The previous Corollary gives a concise error estimation for the numerical method presented in [8].

References

[1] N.S.Barnett, S.S.Dragomir, *A perturbed trapezoid inequality in terms of the third derivative and applications*, RGMIA Preprint, vol.4,no.2, (2001), 221-233.

[2] N.S.Barnett, S.S.Dragomir, *A perturbed trapezoid inequality in terms of the fourth derivative*, Korean J. Comput. & Appl. Math., vol.9, no.1, (2002), 45-60.

[3] A.Bica, C.Iancu, *On a delay integral equation in biomathematics*, J. of Concrete and Applicable Analysis (accepted).

[4] A.Bica, I.Mangrau, R.Mezei, *Numerical method for Volterra integral equations*, Proc. of the 11-th Conference on Applied and Industrial Math., 2003 Oradea, Romania, vol.1, 29-33.

[5] Gh.Coman, G.Pavel, I.Rus, I.A.Rus, *Introduction in the theory of operatorial equations*, Ed. Dacia, Cluj-Napoca, 1979 (in Romanian).

[6] D.V.Ionescu, *Numerical quadratures*, Ed. Tehnica, Bucuresti 1957 (in Romanian).

[7] D.V.Ionescu, *Differential and integral equations*, E.D.P., Bucuresti 1972 (in Romanian).

[8] D.V.Ionescu, *Aplicarea metodei aproximatiilor succesive in integrarea numerica a ecuatiilor diferentiale*, Studii si Cerc. Mat., Cluj-Napoca, 11, (1960), 273-286.

[9] D.V.Ionescu, *Integrarea numerica a ecuatiilor diferentiale*, Colocviul de mecanica, Bucuresti, 25-29 0ct. 1959.

[10] N.Obreschkoff, *Neue Quadraturformeln*, Abhandlungen der Preussischen Akademie der Wissenschaften, 1940, p.6-26.

[11] K.Petr, *Uber eine Formel fur numerische Berechnung der bestimen Integrale*, Casopis propestovani Matematiky a Fysiky, 44, (1915), 454-455.

The bifurcation codimension for the Goodwin's model

Codeci Elena, Codeci Daniel

CNVV Curtea de Arges
Sc nr. 1 Curtea de Arges
E-mail: codeci-lili@yahooo.com

Abstract. The Goodwin mathematical model is introduced. Then the eigenvalues corresponding to one of its equilibria are shown to be imaginary except at the origin and the axes of the parameter space. Thus, degenerated Hopf bifurcations of codimension at least equal to two occur.

1. Goodwin's model for the distribution of income

This represents a model of economic dynamics, which corresponds to an economic system containing workers and capitalists. The workers spend all their time income on daily consumption while the capitalist save their income.

On base on certain economical relations between the quantities that define the model and after several changes of coordinates we can find out that the associated mathematical model is the Cauchy problem $u(0) = u_0$, $v(0) = v_0$ for the Lotka-Volterra system of ordinary differential equations.

$$(1) \qquad \begin{cases} \dot{u} = (a - bv)u, \\ \dot{v} = (cu - d)v. \end{cases}$$

In (1) we have two state functions u and v and four real parameters a, b, c, d. For $bc \neq 0$, making the change of coordinates $u_1 = cu$ and $v_1 = bv$, (1) becomes the system

$$(2) \qquad \begin{cases} \dot{u_1} = u_1(a - v_1), \\ \dot{v_1} = v_1(u_1 - d). \end{cases}$$

where only just two parameters a and d remain.

The equilibrium points of the system (2) are $(u_1^*, v_1^*) = (0,0)$ and $(u_1^{**}, v_1^{**}) = (d, a)$. In the following we study the nature of the bifurcation corresponding to (u_1^{**}, v_1^{**}).

2. The codimension of the singularity for $a, d > 0$

First of all, we carry the equilibrium point $u^{**} = (d, a)$ at the origin by using the transformation $x = u_1 - d$, $y = v_1 - a$. In this way, system (2) becomes

$$(3) \qquad \begin{cases} \dot{x} = -dx - xy, \\ \dot{y} = ax + xy. \end{cases}$$

Using the notation $\overline{x} = (x, y)^T$ and $\overline{\alpha} = (d, a)$ the system (3) can also be written as

$$\dot{\overline{x}} = A(\overline{\alpha})\overline{x} + F(\overline{x}, \overline{\alpha}),$$

where $A(\overline{\alpha}) = \begin{pmatrix} 0 & -d \\ a & 0 \end{pmatrix}$ and $F(\overline{x}, \overline{\alpha}) = \begin{pmatrix} -xy \\ xy \end{pmatrix}$.

For the system (3) the origin is an equilibrium point for any $\overline{\alpha}$ and in particular, for $\overline{\alpha} = (0,0)$.

Let us now apply to (1) the method of normal form sin complex coordinates.

Thus, the eigenvalues $\lambda_{1,2}$ of A are the solutions of the characteristic equation

$$\lambda^2 + ad = 0 \text{ i.e. } \lambda_{1,2} = \pm\sqrt{ad}, \;\; \omega(\overline{\alpha}) = \sqrt{ad}.$$

By definition the inner product of two vectors $p, q \in \mathbb{C}^2$ is $\langle p, q \rangle = \overline{p_1} q_1 + \overline{p_2} q_2$, where $p = (p_1, p_2)^T$, $q = (q_1, q_2)^T$, $p_1, p_2, q_1, q_2 \in \mathbb{C}$.

Let $p(\overline{\alpha})$ and $q(\overline{\alpha})$ be the eigenvectors of $A(\alpha)$ and $A^T(\alpha)$ which satisfy the normalization condition $\langle p, q \rangle = 1$.

Therefore, $Aq = i\omega q$ and $A^T p = -i\omega p$. We choose $q = \begin{pmatrix} d \\ -i\omega \end{pmatrix}$ and $p = \begin{pmatrix} a \\ -i\omega \end{pmatrix}$, the normalization condition imposing $c = \frac{1}{2ad}$. Thus $q = \left(\frac{1}{2a}, -\frac{1}{2\sqrt{ad}}\right)^T$.

Now, introduce the new function $z = \langle p(\alpha), \overline{x}\rangle$. In this way, we have $x = zq(\alpha) + \overline{zq}(\alpha)$. Then the complex form of (4) becomes

$$\begin{aligned}
\dot{z} &= i\omega z + \langle p\left(\overline{\alpha}\right), F(zq\left(\overline{\alpha}\right) + \overline{zq}\left(\overline{\alpha}\right), \overline{\alpha})\rangle \\
&= i\omega z + \left\langle \begin{pmatrix} a \\ -i\omega \end{pmatrix}, F\left(zq_1 + \overline{zq}_1,\ zq_2 + \overline{zq}_2,\ \overline{\alpha}\right) \right\rangle \\
&= i\omega z + \left\langle \begin{pmatrix} a \\ -i\omega \end{pmatrix}, \begin{pmatrix} -(zq_1 + \overline{zq}_1)(zq_2 + \overline{zq}_2 \\ (zq_2 + \overline{zq}_1)(zq_2 + \overline{zq}_2) \end{pmatrix} \right\rangle \\
&= i\omega z - a(zq_1 + \overline{zq}_1) \cdot (zq_2 + \overline{zq}_2) + i\omega(zq_1 + \overline{zq}_1) \cdot (zq_2 + \overline{zq}_2) \\
= i\ &\omega z + (-a + i\omega)(q_1 q_2 + z\overline{z}(\overline{q}_1 q_2 + q_1 \overline{q}_2) + \overline{z}^2 \overline{q}_1 \overline{q}_2) \\
&= i\omega z + (-a + i\omega)\left[z^2\left(\frac{-i}{4a\sqrt{ad}}\right) + \overline{z}^{-2}\left(\frac{i}{4a\sqrt{ad}}\right)\right].
\end{aligned}$$

Let us denote $g(z, \overline{z}, \alpha) = \sum_{i+j\geq 2} g_{ij} z^i \overline{z^j}$.

In our case we have, $g_{20} = (-a+i\omega)\left(\frac{-i}{4a\sqrt{ad}}\right) = \frac{i}{4\sqrt{ad}} + \frac{1}{4a}$ and $g_{02} = (-a+i\omega)\left(\frac{i}{4a\sqrt{ad}}\right) = \frac{-i}{4\sqrt{ad}} + \frac{-1}{4a}$, $g_{11} = 0$ and $g_{ij} = 0$ for $i + j \geq 3$.

Taking into account the expressions of the first two Liapunov coefficients from [2], for our problem we find out that they are equal to zero, therefore, the Hopf singularity is degenerated and has the codimension at least equal to 2.

At this stage we think that bifurcations occur for $a = 0$ or $d = 0$ or $a = d = 0$.

References

[1] N. Giurgiteanu, *Economical and Biological Computational Dinamic*, .
[2] Y. A. Kuznetsov, *Elements of applied bifurcation theory*, Springer-Verlog, New York,1995..

Authentication of the message as part of the protocol with public key

Marieta Gâta
North University of Baia Mare
Department of Mathematics and Computer Science

Abstract. This paper gives an overview to the digital signing, authentication of a file and digital verifying. These cryptography operations make easier for developers to encrypt and decrypt messages, files, programs, passwords or any other data being transmitted over the Internet. In this paper we present how to create and manage digital certificates, how to digitally sign a message or file to guarantee that we can know the identity of author and that the data has not been modifying, or how to verify the digital sign.

Keywords: authenticate, digital signing, encryption/decryption

1. Digital signature. Generality

There are two main types of crypts: the encryption with public key and the encryption with private key. At present the used encryption on net or in internal way, of a firm, is mostly crypt with its public key, a combination of crypt with public key and crypt with secret key.

For the most systems of crypt, the encryption with public key uses intensely the authentication of the messages. The authentication of the messages represents a method where with messages addressee can verify the source and the validity of the source. The sender will utilize to crypt his secret key, signing thus the message. The secret key creates in the message frame a digital signature of the addressee which can be verified by the receiver (or somebody else, reason for which is used merely for this purpose in view - signature) through use of public key of the sender to decrypt digital signature.

Through digital signature, the receiver of a message can verify if the sender is indeed the source of the message. Because a digital signature can be created only by the holder of a private key, it certifies the identity of the message sender. Because a digital signature process the file and generates an unique number by virtue of the content of the file, date, hour, the verification of the signature avouches that nobody modified the file during or after the transmission of the message.

The way in which a program of applies the digital signatures appends a signature in the message frame and the kind in which the receiver of the message decodes the signature is illustrated in fig. 1.

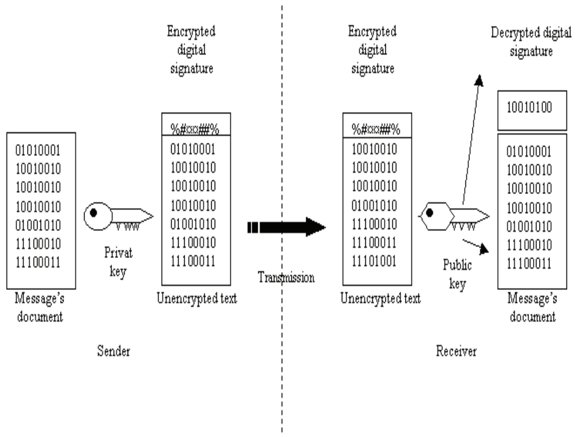

2. The creation of a digital signature

The encryption and decryption of files of big sizes through an algorithm with public key require a significant time. For this reason, algorithms with public key applies about files use usually digital signatures, which reduces substantially duration of transfer of the files, because the algorithm encrypt not only the signature.

The way in which an algorithm with public key creates digital signatures and it uses them for the signing of a file is illustrated in fig. 2.

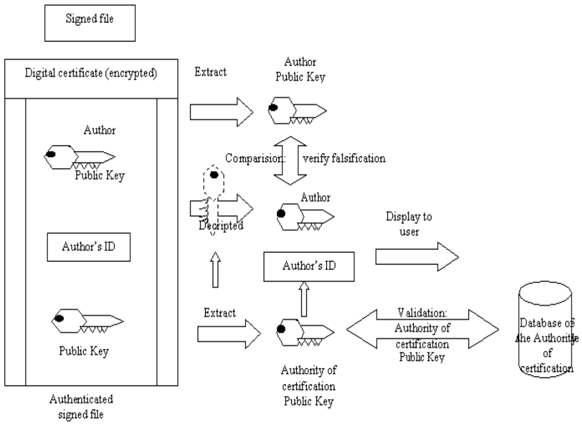

A digital signature uses the value of screening of the initial file, which has a role of checksum or finger mark of file. For instance, Authenticode from Microsoft (one among most widespread and used technology of digital signatures from net) sifts a certain file to a value on 128 or 160 of bits. At first, the program calculates a finger mark through the screening of the file, thereupon the finger mark is encrypted with the private key detained by the owner of the file. Through the combinations of the encrypted finger mark and the public key, the program creates the digital signature. In order to create the digital signature of a file by means of public and private keys, one follows the steps:

1. in the frame of the documents is marked out the fact how the digital signature contains the public key which the receiver of the file will use as his decrypt the finger mark;
2. the digital signature is created for file to the aim of signing that file;
3. the digital signature is attached to the original file.

3. The authentication of a file with help of a digital signatures

When the addressee receives the file marked with digital signature, the receiver can verify if whether modifications of the content of the files appeared between the moment of signing and the moment of the reception.

The way in which digital signature authenticates a file is illustrated in fig. 3.

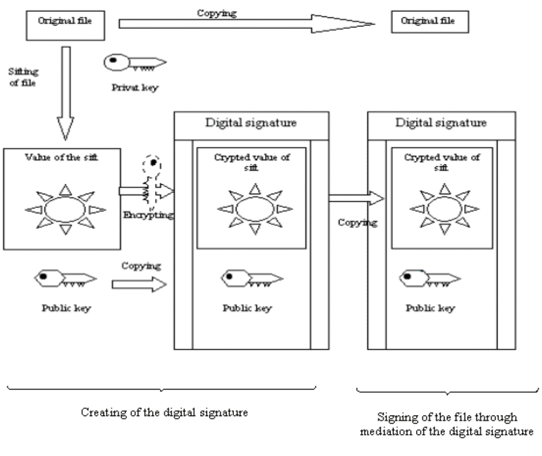

At the reception of the signed file, the user verifies the file through effectuation of the next steps:

1. the encrypted finger mark and the public public key is extracted from the frame of the digital signature;

2. the encrypted finger mark is decrypted by meansof the public key;
3. the original file for extracting a finger mark is sifted and this is compared to the value obtained to step 2.

If the values of the steps 2 and 3 are identical, the transfer is succeeded. If the values do not coincide, somebody modifies the file, or deliberates, or an error of transmission occured.

4. The verification of the digital signature and the certificates

In spite of all these safety measures, some problem remains unsolved anyway, even if to this aim Authenticode and another standards for digital signatures use Authorities of authentication. For the utilized Authenticode one must obtain a digital certificate from an Authority of authentication, this being a third firm. The Authorities of authentication certify to a user which receives a file that the person that signed the file is not a fictitious person and that the signature was not counterfeit of somebody else. A digital certificate is like a notarial authentication of documents. At the solicitation of a certificate, Authority of authentication will verify the identity of the persons and will send the digital certificate with information about person who solicited the certificate and a copy of the public key. The private key of the Authority of authentication encrypts the certificate.

In signing a component, Authenticode attaches to this digital signature also the digital certificate. When the receiver receive the file that contains the digital signature and the digital certificate, can verify whether the signature became or not forged.

The way in which the receiver verifies the digital signature and the digital certificate is illustrated in fig. 4.

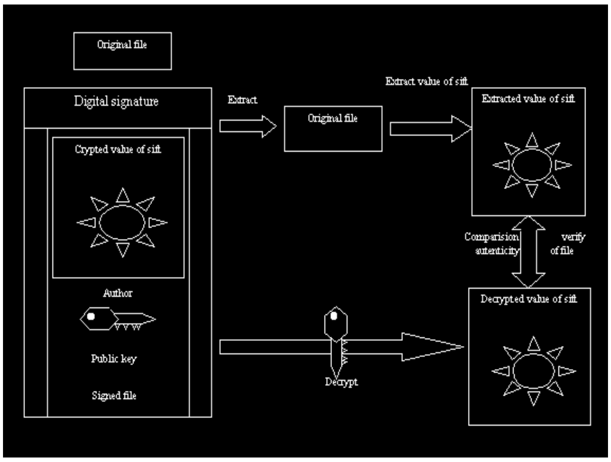

Authenticode verifies the digital signature through comparision of the public key of the titular, included in the digital signature, with its copy from the digital certificate. The user can access the informations about titular which belong in the digital certificate for found out the identity of titular. User can trust in the authenticity of the signature because the Authority of authentication verified the identity of the persons.

Strategy Authenticode is banked on two suppositions. In forefront, the user can not calculate easy the private key on the strength of public key. Specialists estimate that the break of the digital keys of 1024 bits used by Authenticode requires 90 milliards of years MIPS (millions of instructions on second), that is a milliard of computers which execute a milliard of instructions on second needs 90 years to broke the signature of a person. However, the time for burglarious of a code can be less, as proven with many inexpugnable codes.

References

[1] Bockmann C. J., Klander L., Tang L. *Visual basic developer's library*, Ed. Teora, Bucuresti, 2002.
[2] Meekness A. J., Borscht P. C., Vanstone S. A. *Handbook of applied cryptography*, CRC Press, Bon raton, 2001.

[3] Patriciu V. V. *Cryptography and the security of the nets of computers with application in C and Pascal*, Ed. Tehnica, Bucuresti, 1994.

[4] Patriciu V. V. *The security of the electronic commerce*, Ed. All, Bucuresti, 2001.

[5] http://www.microsoft.com (*Authenticode Security Increased in Internet Explorer*).

On the saddle-node bifurcations in the demand-supply model

Constantin Georgescu,
Adelina Georgescu

Dept of Applied Mathematics,
Univ. of Piteti

Abstract.
The saddle-node bifurcations corresponding to nonhyperbolic singularities characterized by a zero eigenvalue in a demand-supply model are studied.

1. Schema dinamică şi echilibrele sale nehiperbolice

Lucrarea de faţă face parte dintr-un studiu mai amplu privind modelul cerere-ofertă. Prezentăm aici cîteva aspecte legate de bifurcaţia şa-nod care apare în schema dinamică generată de problema Cauchy pentru sistemul de ecuaţii [1], [2]

$$(1)\qquad \begin{cases} \dot{u} = au - \frac{1}{2c}v + \beta, \\ \dot{v} = 2cu - \frac{1}{2}v^2, \end{cases}$$

$(a, \beta, c) \in \Omega = \{(a, \beta, c) \in \mathbb{R}^{*3} | 1 - 4a\beta c > 0\}$, ce descrie un model de cerere-ofert

Fie $(a, \beta, c) \in \Omega$, arbitrar fixat si fie (u_0, v_0) unul din cele două echilibre ale schemei dinamice (1), corespunzătoare. Pentru uşurinaa scrierii, în primele trei seciuni ale lucrării vom renunţa la indicii zero ai parametrului. Schimbarea de coordonate

$$(2)\qquad \begin{cases} u = x_1 + u_0, \\ v = x_2 + v_0 \end{cases}$$

transformă schema dinamică (1) cu echilibrul (u_0, v_0), în schema dinamică

$$(3)\qquad \begin{cases} \dot{x}_1 = ax_1 - \frac{1}{2c}x_2, \\ \dot{x}_2 = 2cx_1 - v_0x_2 - \frac{1}{2}x_2^2, \end{cases}$$

cu echilibrul $(0, 0)$, iar noul cîmp de vectori este

$$(4)\qquad \mathbf{F}(\mathbf{x}) = \begin{pmatrix} ax_1 - \frac{1}{2c}x_2 \\ 2cx_1 - v_0x_2 - \frac{1}{2}x_2^2, \end{pmatrix}$$

unde $\mathbf{x} = (x_1, x_2)$.

Printr-un calcul direct se găseşte că $v_0 \in \left\{\gamma, \frac{2}{a} - \gamma\right\}$, $\gamma = \frac{1}{a}(1+\sqrt{1 - 4a\beta c})$, i $\gamma \in \begin{cases} (-\infty, 0), & a < 0 \\ (0, +\infty), & a > 0. \end{cases}$

În acest fel, valorile proprii ale liniarizatei schemei dinamice (1) în jurul originii, depind explicit doar de a şi γ.

2. Echilibrele de tip şa-nod

Să notăm $\mathcal{S} = \left\{(a, \gamma) \in \mathbb{R}^{*2} | \lambda_1 \neq 0, \lambda_2 = 0\right\}$ (i.e. $\mathcal{S}$ este acea submulţime din spaţiul parametrilor (a, γ) ce corespund singularităţilor nehiperbolice cu o singură valoare proprie zero) (fig. 1).

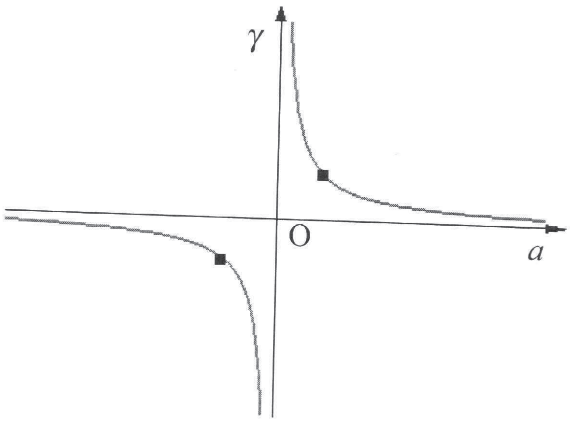

Mulţimea $\mathcal{S}$.

Propoziţie 1. *Orice punct de echilibru nehiberbolic (u_0, v_0) corespunzător lui $(a, \gamma) \in \mathcal{S}$ este o singularitate şa-nod a cîmpului de vectori $\mathbf{F}(\mathbf{x})$.*

Demonstraţie. Valorile proprii ale matricei

$$A = D\mathbf{F}(0,0) \left(= \begin{pmatrix} a & -\frac{1}{2c} \\ 2c & -v_0 \end{pmatrix} \right)$$

sunt soluţii ale ecuaţiei $\lambda^2 - (Tr\mathbf{A})\lambda = 0$ (i.e. $\lambda_1 = a - v_0$ i $\lambda_2 = 0$). Corespunzor lor se gesc vectorii proprii $\mathbf{w}_1 = \begin{pmatrix} a \\ 2c \end{pmatrix}$ i respectiv $\mathbf{w}_2 = \begin{pmatrix} 1 \\ 2ac \end{pmatrix}$. Să trecem la baza $\mathcal{B} = \{\mathbf{w}_1, \mathbf{w}_2\}$ i, corespunzător, să facem schimbarea de coordonate $\mathbf{x} = \mathbf{T}\mathbf{y}$, unde $\mathbf{T} = \begin{pmatrix} a & 1 \\ 2c & 2ac \end{pmatrix}$ şi $\mathbf{y} = (y_1, y_2)$. Atunci din (3) obţinem $\dot{\mathbf{x}} = \mathbf{F}(\mathbf{x}) \Leftrightarrow \mathbf{T}\dot{\mathbf{y}} = \mathbf{F}(\mathbf{T}\mathbf{y}) \Leftrightarrow \dot{\mathbf{y}} = \mathbf{T}^{-1}\mathbf{F}(\mathbf{T}\mathbf{y}) \Leftrightarrow \dot{\mathbf{y}} = \mathbf{T}^{-1}[\mathbf{X}_1(\mathbf{T}\mathbf{y}) + \mathbf{X}_2(\mathbf{T}\mathbf{y})]$, unde $\mathbf{F}(\mathbf{x}) = \mathbf{X}_1(\mathbf{x}) + \mathbf{X}_2(\mathbf{x}) + O(|\mathbf{x}|^3), \mathbf{X}_i \in \mathcal{H}_i$, iar $\mathcal{H}_i$ este spaţiul polinoamelor vectoriale omogene de grad i, $i = \overline{1,2}$, $\Leftrightarrow \dot{\mathbf{y}} = (\mathbf{T}^{-1}\mathbf{A}\mathbf{T})\mathbf{y} + \mathbf{T}^{-1}\mathbf{X}_2(\mathbf{T}\mathbf{y})$.

Deoarece $\mathbf{T}^{-1}\mathbf{A}\mathbf{T} = \begin{pmatrix} a - v_0 & 0 \\ 0 & 0 \end{pmatrix}$ şi

$$\mathbf{T}^{-1}\mathbf{X}_2(\mathbf{T}\mathbf{y}) = \frac{1}{2c(a^2-1)} \begin{pmatrix} 2ac & -1 \\ -2c & a \end{pmatrix} \left[-2c^2(y_1 + ay_2)^2 \begin{pmatrix} 0 \\ 1 \end{pmatrix} \right] =$$
$$= \begin{pmatrix} \frac{c}{a^2-1} \\ \frac{-ac}{a^2-1} \end{pmatrix} (y_1 + ay_2)^2$$

se găseşte că

$$(5) \qquad \begin{pmatrix} \dot{y}_1 \\ \dot{y}_2 \end{pmatrix} = \begin{pmatrix} a - v_0 & 0 \\ 0 & 0 \end{pmatrix} \begin{pmatrix} y_1 \\ y_2 \end{pmatrix} + K \begin{pmatrix} y_1^2 + 2ay_1y_2 + a^2y_2^2 \\ -ay_1^2 - 2a^2y_1y_2 - a^3y_2^2 \end{pmatrix}$$

unde am notat $K = \frac{c}{a^2-1}$.

În baza $\mathcal{B}$ operatorul Lie $L^2_{\mathbf{J}} : H_2 \longrightarrow H_2$, ($\mathbf{J}$ fiind forma Jordan a lui $\mathbf{A}$) are vectorii proprii $\mathbf{y}^{\mathbf{m}}\mathbf{e}_i$ ($\mathbf{e}_i$, $i = \overline{1,2}$ vectorii bazei canonice din $\mathbb{R}^2$) i, corespunzător, valorile proprii $\Lambda^2_{\mathbf{m},i} = m_1\lambda_1 - \lambda_i$, $i = \overline{1,2}, \mathbf{m} = (m_1, m_2)$ cu $m_1 + m_2 = 2$. (i.e. $m \in \mathbb{Z}^2_+(2)$.)

Fie transformarea de funcţii

$$(6) \qquad \mathbf{y} = \mathbf{z} + \mathbf{h}_2(\mathbf{z}),$$

unde $\mathbf{h}_2(\mathbf{z}) = \sum\limits_{m.i} h_{m.i}\mathbf{z}^m\mathbf{e}_i$, $\mathbf{z} = (z_1, z_2)$, $h_{m.i} = \frac{X_{m.i}}{\Lambda_{m.i}}$ i $X_{m.i} = a_{i1+\mathrm{pr}_2\mathbf{m}}$, $i = \overline{1,2}$, iar

$$(a_{ij})_{i=\overline{1,2},\, j=\overline{1,3}} = K \begin{pmatrix} 1 & 2a & a^2 \\ -a & -2a^2 & -a^3 \end{pmatrix}.$$

Conform teoriei formelor normale [3], [4], [5], rezultă tabelul

m_1	m_2	$\Lambda^2_{\mathbf{m}.1}$	$\Lambda^2_{\mathbf{m}.2}$	$X_{\mathbf{m}.1}$	$X_{\mathbf{m}.2}$	$h_{\mathbf{m}.1}$	$h_{\mathbf{m}.2}$
2	0	λ_1	$2\lambda_1$	K	$-aK$	K/λ_1	$-aK/(2\lambda_1)$
1	1	0	λ_1	$2aK$	$-2a^2K$	$-$	$-2a^2K/\lambda_1$
0	2	$-\lambda_1$	0	a^2K	$-a^3K$	$-a^2K/\lambda_1$	$-$

Termenii rezonanţi corespund lui $\mathbf{m}.i$ din tabel, pentru care $\Lambda^2_{\mathbf{m}.i}$ sunt nuli. Prin schimbarea de funcţii necunoscute (6), cu

$$\mathbf{h}_2(\mathbf{z}) = \frac{K}{\lambda_1}z_1^2\begin{pmatrix}1\\0\end{pmatrix} - \frac{a^2K}{\lambda_1}z_2^2\begin{pmatrix}1\\0\end{pmatrix} - \frac{aK}{2\lambda_1}z_1^2\begin{pmatrix}0\\1\end{pmatrix} - \frac{2a^2K}{\lambda_1}z_1z_2\begin{pmatrix}0\\1\end{pmatrix}$$

i.e.

$$\mathbf{h}_2(\mathbf{z}) = \frac{K}{\lambda_1}\begin{pmatrix} z_1^2 - a^2z_2^2 \\ -\frac{a}{2}z_1^2 - 2a^2z_1z_2\end{pmatrix},$$

ecuaţia (5) devine

$$\text{(7)} \qquad \dot{\mathbf{z}} = \mathbf{Az} - D\mathbf{h}_2(\mathbf{z})\mathbf{Az} + \mathbf{Ah}_2(\mathbf{z}) + \mathbf{X}_2(\mathbf{z}) + O(|\mathbf{z}|^3),$$

în care

$$\begin{aligned} \mathbf{Az} &= \begin{pmatrix}\lambda_1 z_1\\0\end{pmatrix}, \quad \mathbf{Ah}_2(\mathbf{z}) = \begin{pmatrix}Kz_1^2 - a^2Kz_2^2\\0\end{pmatrix} \\ D\mathbf{h}_2(\mathbf{z})\mathbf{Az} &= \tfrac{K}{\lambda_1}\begin{pmatrix} 2z_1 & -2a^2z_2^2 \\ -az_1 - 2a^2z_2 & -2a^2z_1\end{pmatrix}\begin{pmatrix}\lambda_1 z_1\\0\end{pmatrix} = \\ &= K\begin{pmatrix}2z_1^2\\ -az_1^2 - 2a^2z_1z_2\end{pmatrix}, \end{aligned}$$

Deci, avem

$$\dot{z} = \begin{pmatrix}\lambda z_1 - 2Kz_1^2 + Kz_1^2 - a^2Kz_2^2 + Kz_1^2 + 2aKz_1z_2 + a^2Kz_2^2 \\ +aKz_1^2 + 2a^2z_1z_2 - aKz_1^2 - 2a^2Kz_1z_2 - a^3Kz_2^2\end{pmatrix}.$$

Această ultimă formă a ecuaţiei (5) arată că toţi termenii nerezonanţi se reduc, astfel că în cele din urmă (5) devine

$$\text{(8)} \qquad \begin{cases}\dot{z}_1 = \lambda_1 z_1 + a_2 z_1 z_2 + O(|\mathbf{z}|^3),\\ \dot{z}_2 = b_2 z_2^2 + O(|\mathbf{z}|^3),\end{cases}$$

unde $a_2 = 2aK,\ b_2 = -a^3K$, iar $|\mathbf{z}| = \sqrt{z_1^2 + z_2^2}$. Se subînţelege că $\mathbf{z} \longrightarrow 0$.

Relaţia (8) este o formă normală a lui (3) în care coeficientul lui z_2^2, $b_2 = -a^3K \neq 0$. Comparând (8) cu (2.4.5) din [3], rezultă că echilibrul nehiperbolic (u_0, v_0) este o singularitate şa-nod nedegenerată

3. Dinamica pe varietatea centrală

Să studiem dinamica în jurul punctului nehiperbolic de tip şa-nod, (u_0, v_0), folosind metoda varietăţii centrale. Astfel, deoarece matricea $\mathbf{A} = D\mathbf{F}(0,0)$, are o singură valoare proprie nulă rezultă că pentru orice $(a, \gamma) \in \mathcal{S}$, sistemul dinamic asociat lui (3) este un punct de bifurcaţie de codimensiune 1 al schemei dinamice (3). Conform teoremei varietăţii centrale există varietatea centrală W^c şi ea este 1-dimensională

Varietatea centrală este tangentă în origine, la varietatea liniară E^c cu care se identifică local (i.e. pe o vecinătate convenabil aleasă a originii) (fig.2).

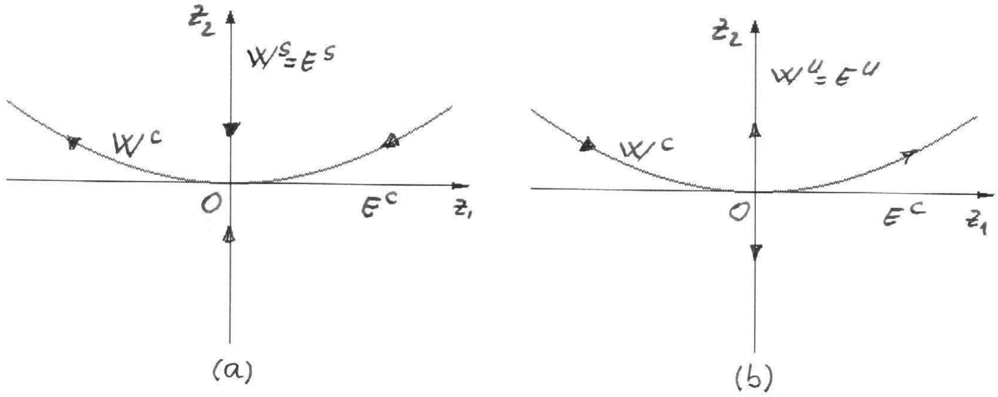

Pentru sistemul (8) se găseşte ([3], [4]) că local, varietatea centrală W^c poate fi reprezentată prin graficul funcţiei netede $V : \mathbb{R} \longrightarrow \mathbb{R},\ z_1 = V(z_2)$, unde $V(z_2) = b_2 z_2^2 + O(z_2^3)$, i.e. $W^c = \{(z_1, z_2) | z_1 = V(z_2)\}$ i are [3] ecuaţia $z_1 = 0$, până la ordinul trei. Conform principiul reducerii [3], [4], local, într-o vecinătate a originii, sistemul (8) este topologic echivalent cu sistemul

$$(9)\qquad \begin{cases} \dot{z}_1 = \lambda_1 z_1, \\ \dot{z}_2 = b_2 z_2^2. \end{cases}$$

Prima ecuaţie a lui (9) este liniară iar soluiile ei cresc/descresc exponenţial. A doua ecuaţie a lui (9) este restricţia la varietatea centrală a sistemului (8). Prin urmare, dinamica sistemului (8) este esenţial determinată de această restricţie.

Astfel, pentru orice $(a, \gamma) \in \mathcal{S}$, punctul de echilibru care este de tip şa-nod, are trei direcii atractive şi una repulsivă (fig. 2 (a)), sau una atractivă şi trei repulsive (fig.2 (b)), după cum $\lambda_1 < 0$, sau respectiv $\lambda_1 > 0$.

4. Desfăşurarea versală a singularităţii şa-nod

Până acum am studiat dinamica de fază pentru un sistem dinamic generat de problema Cauchy pentru sistemul de e. d. o. (3). Acest sistem dinamic are originea drept şa-nod şi este caracterizat de un parametru tridimensional (a_0, β_0, c_0) arbitrar fixat în spaţiul de control Ω. Deci, de fapt, în loc de (3) avem

$$(10)\qquad \begin{cases} \dot{x}_1 = a_0 x_1 - \frac{1}{2c_0} x_2, \\ \dot{x}_2 = 2c_0 x_1 - v_0 x_2 - \frac{1}{2} x_2^2. \end{cases}$$

Pentru fiecare $(a_0, \gamma_0) \in \mathcal{S}$, sistemul (1), fiind o bifurcaţie de codimensiune 1, se scufundă într-o familie uniparametrică de sisteme dinamice. Când (a_0, γ_0) parcurge $\mathcal{S}$, sistemul dinamic corespunzător lui (1) parcurge această familie, care la rândul ei, se află în schema dinamică generată atunci când (a, γ) parcurge domeniul Ω' corespunzător lui Ω. Evident, pentru fiecare $(a_0, \gamma_0) \in \mathcal{S}$, sistemul dinamic (1) este structural instabil (i.e. o bifurcaţie), şi el corespunde unui câmp de vectori care are în origine o singularitate. Pentru a caracteriza această bifurcaţie trebuie să variem pe (a, γ) Ω' într-o vecinătate a lui (a_0, γ_0). Acestei varieri a lui (a, γ) îi corespunde o deformare, desfăşurare a câmpului de vectori, care scrisă sub forma normală se numeşte desfăşurare versală (universală a singularităţii şa-nod (3) şi este determinată de familia locală de câmpuri vectoriale [3]

$$(11)\qquad \mathbf{F}(\mathbf{z}, \varepsilon) = \begin{pmatrix} \lambda_1 z_1 + a_2 z_1 z_2 \\ \varepsilon + b_2 z_2^2 \end{pmatrix} + O(|\mathbf{z}|^3).$$

Pentru $\varepsilon = 0$, (1) se reduce la forma normală (8), corespunzătoare bifurcaţiei (3). Prin urmare, forma normală a schemei dinamice corespunzătoare acestei desfăşurări universale este

(12) $\quad \dot{\mathbf{z}} = \mathbf{F}(\mathbf{z}, \varepsilon)$.

Să studiem dinamicile generate de (3) când termenii $O(|\mathbf{z}|^3)$ se neglijează. Pentru $b_2\varepsilon < 0$ schema dinamică generată de (3) are echilibrele $\mathbf{z}^*_{\pm}(\varepsilon) = \begin{pmatrix} 0 \\ \pm\omega(\varepsilon) \end{pmatrix}, \omega(\varepsilon) = \sqrt{\frac{\varepsilon}{-b_2}}$ şi pentru $b_2\varepsilon > 0$ nu are echilibre. În jurul acestor echilibre avem

(13) $\quad \det D\mathbf{F}(\mathbf{z}^*_{\pm}(\varepsilon), \varepsilon) = \pm 2b_2\lambda_1\omega(\varepsilon) + O(\varepsilon) \left(\stackrel{not}{=} \mathcal{P}^*_{\pm}\right)$

şi

(14) $\quad TrD\mathbf{F}(\mathbf{z}^*_{\pm}(\varepsilon), \varepsilon) = \lambda_1 \pm O(\sqrt{\varepsilon}) \left(\stackrel{not}{=} \mathcal{S}^*_{\pm}\right)$.

Din (4) i (5) rezultă că pentru $\lambda_1 < 0$, $\mathbf{z}^*_{+}(\varepsilon)$ este nod atractiv ($\mathcal{S}^*_{+} < 0$, $\mathcal{P}^*_{+} > 0$) şi $\mathbf{z}^*_{-}(\varepsilon)$ este şa ($\mathcal{S}^*_{-} < 0$, $\mathcal{P}^*_{-} < 0$), iar pentru $\lambda_1 > 0$, $\mathbf{z}^*_{+}(\varepsilon)$ este şa ($\mathcal{S}^*_{+} > 0$, $\mathcal{P}^*_{+} < 0$) şi $\mathbf{z}^*_{-}(\varepsilon)$ este nod repulsiv ($\mathcal{S}^*_{-} > 0$, $\mathcal{P}^*_{-} > 0$).

Prin urmare în $\varepsilon = 0$, există o bifurcaţie şa-nod: când parametrul $\mu = (a, \gamma) \in \mathcal{S}$, cele două echilibre, şaua şi nodul, se ciocnesc (coincid), formând un singur echilibru şa-nod, ca apoi să se desfacă iarăşi în echilibrele distincte şa şi nod. Diagrama de bifurcaţie dinamică locală corespunzătoare acestei bifurcaţii este dată în fig.3 (a) pentru cazul $\lambda_1 < 0$, i.e. $a < v_0$, şi în fig.3 (b) pentru cazul $\lambda_1 > 0$, i.e. $a > v_0$.

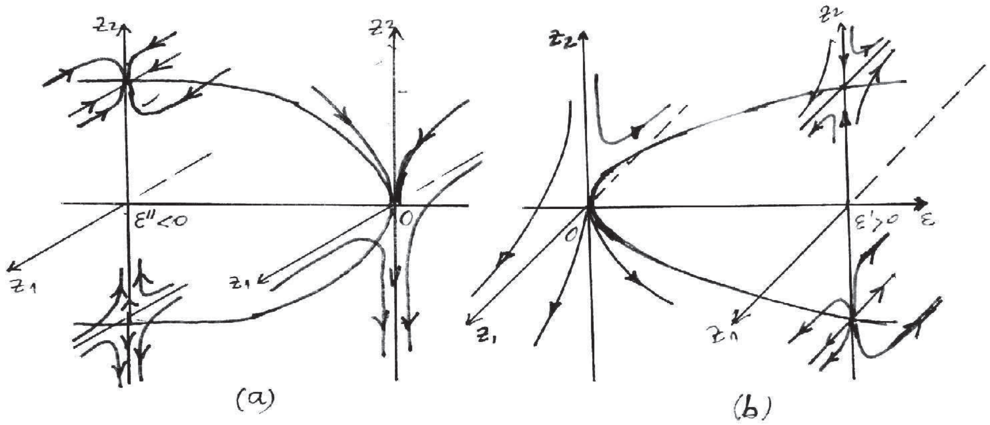

În cazul $b_2(= -\frac{a^3c}{a^2-1}) > 0$, (fig.3(a)), deoarece şaua şi nodul apar pentru *epsilon* < 0, bifurcaţia şa-nod este subcritică pe când în cazul $b_2 < 0$ (fig. 3(b)) bifurcaţia şa-nod este supercritică deoarece şaua şi nodul apar pentru *epsilon* > 0.

În [3] se dă forma normală (9) fără a se specifica expresia noului parametru ε în funcţie de cei vechi. Pentru a determina această expresie mai sunt necesare anumite transformări de parametru, de timp şi eventual introducerea de noi funcţii de stare. Aceasta va face obiectul unei alte lucrări.

References

[1] Ungureanu, L., Ungurenu, L., *Elemente de dinamica economica*, Editura Universităţii din Piteşti, 2000.
[2] Tu, P. N. V., *Dynamical systems,* Springer, Berlin, 1994.
[3] Arrowsmith, D.K., Place, C.M. *An introduction to dynamical systems,* Cambridge University Press, 1990.
[4] Kuznetsov, Y.A., *Elements of applied bifurcation theory,* Springer, New York, 1998.
[5] Sterpu, M., *Dinamică şi bifurcaţii pentru doua modele Van Der Pol generalizat,* Editura Universităţii din Piteşti, 2001.

Amorphous Viral Operator

Eugen Laslo, Dan Noje
Department Of Mathematics, University Of Oradea
Armatei Române 5, 3700 Oradea, Romania.
E-mail: lasloeugen@yahoo.com, dnoje@uoradea.ro

Abstract. In the context of genetic algorithms a new type of variation operator called Amorphous Viral operator that works with Linear Viruses is introduced. This new variation operator is a generalization of the Gene Viral and Linear Viral Operators.
Keywords: genetic algorithms, genetic operators, viral operators, variation operators

1. Introduction

Inspired from the nature, Genetic Algorithms where introduced to solve in an optimal way, problems that have not a convenient solution by standard methods [1], [2], [3]. The genetic algorithms where deeply studied for their numerous applications [5].

Recently in the genetic algorithms where introduced some new entities and variation operators [4], [6], [7] that simulate the action of some kind of natural viruses on the chromosomes.

In [6] the virus is considered to be an entity of the form

$$vir_p = (\lambda_1, \lambda_2, ..., \lambda_p),$$

where $\lambda_i,\ i = \overline{1,p}$ are genes that belong to the same set as the genes of the chromosomes of the considered population. The set of all viruses is denoted by Vir.

A chromosome of the population is an entity of the form

$$crom = (x_1, x_2, ..., x_n)$$

and the set of all chromosomes is denoted by $Crom$.

In [6] it was introduced the entity called gene virus, which is a virus that have only one gene and which is denoted by $gvir$. The set of all gene viruses is denoted by $GVir$.

In [6] it was also introduced a new genetic operator called Gene Viral Operator that corresponds to the action of the gene virus on chromosomes. The Gene Viral Operator

$$GVO_k : Crom \times GVir \to Crom$$

is defined as follows

$$GVO_k\,(crom, gvir) = icrom,$$

where $icrom$ represents the infected chromosome and is one of the form

$$icrom = (x_1, x_2, ..., x_{k-1}, \lambda, x_{k+1}, ..., x_n)$$

with $1 \leq k \leq n$.

It is obvious that the index k represents the position of the chromosome gene that is replaced by the virus gene.

As a generalization of Gene Viral Operator, in [7] it was introduced the Linear Viral Operator. This variation operator substitutes a sequence of genes from the considered chromosome with the genetic material of a linear virus of type vir_p. The set of all viruses of type vir_p was denoted by Vir_p.

Let us consider that the replacing process starts with the gene k of the considered chromosome. It has also to be assumed that the considered chromosome is of length n. It follows that in order to complete the replacing process, the following inequality has to be fulfilled

$$k \leq n - p + 1.$$

The Linear Viral Operator

$$LVO_{k,p} : Crom \times Vir_p \to Crom$$

is defined as follows

$$LVO_{k,p}\left(crom, vir_p\right) = icrom,$$

where *icrom* is one of the type

$$icrom = \left(x_1, x_2, ..., x_{k-1}, \lambda_1, ..., \lambda_p, x_{k+p}, ..., x_n\right).$$

It is obvious that if $p = 1$ we obtain the Gene Viral Operator. Denoting by C_{GVO_k} the class of Gene Viral Operators and by $\mathsf{C}_{LVO_{k,p}}$ the class of Linear Viral Operators we may write $\mathsf{C}_{GVO_k} \subset \mathsf{C}_{LVO_{k,p}}$.

2. Amorphous Viral Operator

In this section we introduce a new type of viral operator, called *Amorphous Viral Operator*, as a generalization of the Linear Viral Operator. The Linear Viral Operator is replacing a contiguous sequence of genes of a considered chromosome by the genetic material of a linear virus. The Amorphous Viral Operator is also using a linear virus to modify the genetic material of a chromosome, but it is not necessary replacing a contiguous sequence of genes. The linear viruses used for infection process by the Amorphous Viral operator are from the set Vir_p.

In what follows we consider a population of chromosomes. A chromosome from the population is of the type

$$crom = \left(x_1, x_2, ..., x_{k-1}, x_k, x_{k+1}, ..., x_n\right)$$

and, obviously, that $crom \in Crom$.

From the above considerations it follows that the number n of genes of the chromosomes has to be greater than or equal to the number p of genes of the considered viruses.

From the above considerations the Amorphous Viral Operator is defined by

Definition 1. The Amorphous Viral Operator is the variation operator

$$AVO_{\{k_1,k_2,...,k_p\}} : Crom \times Vir_p \rightarrow Crom$$

defined as follows:

$$LVO_{\{k_1,k_2,...,k_p\}}\left(crom, vir_p\right) = icrom,$$

where *icrom* is a infected chromosome obtained from *crom* by replacing the genes x_{k_i} with the genes λ_i of the linear virus, for all $i \in \{1, 2, ..., p\}$.

Remark 3. *icrom* is also a chromosome from the set *Crom*, since the gene of the gene virus belong to the same set as the genes of the chromosomes of the population.

It is easy to see that using the same virus and the same chromosome, but some different values of indexes k_i for the Amorphous Viral Operators we can obtain totally different results.

It has to be mentioned that if in the used codification not all genes have the same domain of values, than the virus genes has to correspond to the chromosome genes that are going to be replaced, otherwise the resulted chromosome will be a nonviable one.

Remark 4. If in the definition of the Amorphous Viral Operator we consider $p = 1$, than we obtain the definition of the Gene Viral Operator.

Let us denote by $\mathsf{C}_{AVO_{\{k_1,k_2,...,k_p\}}}$ the class of the Amorphous Viral Operators.

Theorem 1. *For $k = k_1$ we have*

$$\mathsf{C}_{GVO_k} \subset \mathsf{C}_{AVO_{\{k_1,k_2,...,k_p\}}}.$$

Proof. The proof is obvious. □

The Amorphous Viral Operator can be interpreted somehow as a composition of some Gene Viral Operators, as follows.

Example 2. For $p = 3$ we have

$$AVO_{\{2,6,3\}}\left(\left(x_1,...,x_{10}\right),\left(\lambda_1,\lambda_2,\lambda_3\right)\right) =$$
$$= GVO_2\left(AVO_{\{6,3\}}\left(\left(x_1,...,x_{10}\right),\left(\lambda_2,\lambda_3\right)\right),\left(\lambda_1\right)\right)$$
$$= GVO_2\left(GVO_6\left(AVO_{\{3\}}\left(\left(x_1,...,x_{10}\right),\left(\lambda_3\right)\right),\left(\lambda_2\right)\right),\left(\lambda_1\right)\right).$$

From Theorem 1 we have that $AVO_{\{3\}} = GVO_3$. Thus :

$$AVO_{\{2,6,3\}}\left(\left(x_1,...,x_{10}\right),\left(\lambda_1,\lambda_2,\lambda_3\right)\right) =$$
$$= GVO_2\left(GVO_6\left(GVO_3\left(\left(x_1,...,x_{10}\right),\left(\lambda_3\right)\right),\left(\lambda_2\right)\right),\left(\lambda_1\right)\right).$$

Remark 5. If in the definition of the Amorphous Viral Operator we consider $k_1, k_2, ..., k_p$ as consecutive numbers, $k_1 \geq 1$ and $k_1 \leq n - p + 1$, then we obtain the definition of Linear Viral Operator.

Theorem 3. *Under conditions of Remark 5 we have that* $\complement_{LVO_{k,p}} \subset \complement_{AVO_{\{k_1,k_2,...,k_p\}}}$.

Proof. The proof is obvious. □

Sometimes, the Amorphous Viral Operator can be interpreted as a composition of some Linear Viral Operators as follows

Example 4. Using Theorem 3 we have

$$AVO_{\{2,3,4,7,8,9\}}\left(\left(x_1,...,x_{10}\right),\left(\lambda_1,\lambda_2,\lambda_3,\lambda_4,\lambda_5,\lambda_6\right)\right) =$$
$$= LVO_{2,3}\left(LVO_{7,3}\left(\left(x_1,...,x_{10}\right),\left(\lambda_4,\lambda_5,\lambda_6\right)\right),\left(\lambda_1,\lambda_2,\lambda_3\right)\right).$$

Using Theorems 1 and 3 we have that sometimes, the Amorphous Viral Operator can be interpreted as a composition of some Linear Viral Operators and Gene Viral Operators as follows:

Example 5. For $p = 6$ we have that

$$AVO_{\{9,3,4,5,6,8\}}\left(\left(x_1,...,x_{10}\right),\left(\lambda_1,\lambda_2,\lambda_3,\lambda_4,\lambda_5,\lambda_6\right)\right) =$$
$$= GVO_9\left(LVO_{3,4}\left(GVO_8\left(\left(x_1,...,x_{10}\right),\left(\lambda_6\right)\right),\left(\lambda_2,\lambda_3,\lambda_4,\lambda_5\right)\right),\left(\lambda_1\right)\right).$$

As a conclusion, the Amorphous Viral Operator is a generalization of Gene Viral Operator and Linear Operator too.

3. Use of amorphous viral operator

This viral operator raises as a consequence of problems for genetic algorithms which imply long chromosomes. In the existing theory for genetic algorithms using mutation types [5] there exists a multitude of solutions with long genes chromosomes which may give a and the long genes chromosomes convergence. The viral operators were introduced for solving this shortcoming. We designed this virus in order to use it in approximation theory.

The general idea of using genetic algorithms in Approximation Theory raises from the difficulty of implementing computation of best approximation polynomials using Remez algorithms. This algorithm is designed using chromosomes of fixed or variable length. The gene for this genetic algorithm is of the form $G = n, a_0, a_1, ..., a_n$, and may be interpreted as a polynomial of order n, $P : [a, b] \to \mathbb{R}$, $P(x) = a_0 + a_1x + ... + a_nx^n$. The matching function for this chromosome is defined based on some distance between continuous functions. With a choice of genetic operators based on [5] the algorithm will converge to best approximation polynomial of order n.

By minimizing the matching function (i.e. distance between the given function f and the polynomial P) one obtains some best approximation polynomial. For example, let $f : [a, b] \to \mathbb{R}$ and if the matching function is

$$\phi_{match}(P) = d(f, P) = \sum_{i=0}^{n} |f(x_i) - P(x_i)|$$

then for $\phi_{match}(P) = 0$ the polynomial P is the Lagrange interpolation polynomial.

If

$$\phi_{match}(P) = d(f, P) = \int_a^b |f(x) - P(x)| dx,$$

i.e. the distance in $L^1[a, b]$ space of all integrable functions, then by minimizing $\phi_{match}(P)$ one obtains best approximation polynomial in the mean (or the $L^1[a, b]$ space).

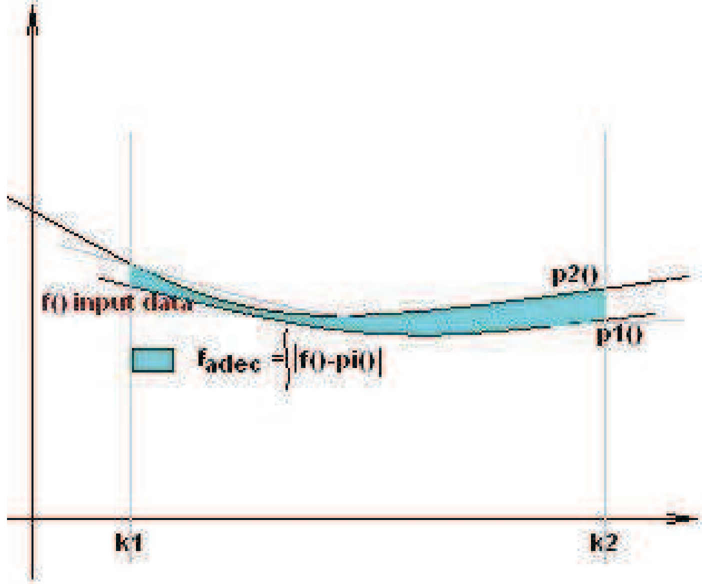

Figure 1. Mapping function for best polynomial approximation

The shortcoming of these genetic algorithms for computing best approximations of high degree is that it is a time consuming task. The amorphous viral operator reduces considerably the computation cost, since it can modify the degree of the polynomial or it can give preliminary information on some coefficients. For example, if the algorithm of searching for a polynomial of degree 100 and a 5^{th} degree polynomial approximation on an interval is accurate enough, then the virus modifies the degree of the polynomial. Also, if during some preliminary processing we know that it will contain the term $5x^2$, then its coefficient can be set to 5 and p to minim 2 by using the amorphous viral operator.

References

[1] Box, G. E. P., Evolutionary operation: a method of increasing industrial productivity, Applied Statistics, 6(1957) 81-101;

[2] Dumitrescu, D., Algoritmi genetici si strategii evolutive-aplicatii in inteligenta artificiala si in domenii conexe, Editura Albastra, Cluj-Napoca, 2000.

[3] Fraser, A. S., Simulation of genetic systems by automatic digital computers, Australian Journal of Biological Science, 10(1957), 484-491.

[4] Holland, J. , Adaptation in Natural and Artificial Systems, University of Michigan Press, Ann Arbor (1975).

[5] Laslo, E., Noje, D. (2003), Gene Viral Operator, Proceedings of the Symposium "Zilele Academice Clujene" Computer Science Section, submitted

[6] Laslo, E., Noje, D., Linear Viral Operator, Proceedings of the Symposium "Zilele Academice Clujene" Computer Science Section, submitted, (2003).

[7] Shimojima, K., Kubota, N., Fukuda, T., Virus-Evolutionary Genetic Algorithm for fuzzy controller Optimization, Studies in Fuzzyness and Soft Computing, 8 (1996), 367-388.

Bifurcation problems for the equation $div(g(|\nabla f|^2)\nabla f) + \lambda f = 0$

B.V.Loginov, K.M.Petrov

Ulyanovsk State Technical University, L.Shevtsova str.54-"b"-2-35, Ulyanovsk, Russia
e-mail: loginov@ulstu.ru
Sophia Technical University, Bulgaria 2304 Pernik, Gagarin str.36-51

Abstract. Bifurcation problems for the equation $div(g(|\nabla f|^2)\nabla f) + \lambda f = 0$ are investigated. Particular cases of boundary value problems for this equation can be found in capillary surfaces theory and in the problems of Rayleigh-Taylor instability. Bifurcation theory methods under group invariance conditions are used.

1. Introduction

Considered the nonlinear eigenvalue problem for the equation

$$(\nabla, g(|\nabla f|^2)\nabla f) + \lambda f = 0, \qquad (x, y) \in \Omega \subset R^2 \tag{1}$$

with one of the boundary conditions

$$f|_{\partial\Omega} = 0 \quad (a) \qquad \frac{\partial f}{\partial n}|_{\partial\Omega} = 0 \quad (b) \tag{2}$$

The problem (1),(2a) for $g(u) = (1 + u)^{-1/2}$ occurs in capillary surfaces theory [1,2], the problem (1),(2b) - in the theory of Rayleigh-Taylor instability [3,4]. It is supposed that

$$g(u) = 1 + a_1 u + a_2 u^2 + \cdots \tag{3}$$

is a given analytic function in some neighborhood of the point $u = 0$. The indicated problems inherit the symmetry of the domain Ω just as the relevant bifurcation equations (BEq)[5]. As in [4] we consider here the cases of square (rectangular) and circular domains Ω and use group analysis methods in branching theory [5,6]. Special attention is payed to bifurcation from multiple eigenvalues. The results of our previous work [4] follow from those presented here.

These investigations are supported by RFBR, grant N 0101-00019 relative to the first author.

2. Rectangular or square domain Ω

For the rectangular domain Ω our problems take the form ($\varepsilon = \lambda - \lambda_0$)

$$f_{xx} + f_{yy} + \lambda_0 f = -\varepsilon f - a_1[f_{xx}f_y^2 + f_{yy}f_x^2 + 3f_{xx}f_x^2 + 3f_{yy}f_y^2 + 4f_x f_y f_{xy}] + \cdots \tag{4}$$

$$\Lambda_a : f(\pm a, y) = 0, \quad f(x, \pm b) = 0; \quad \Lambda_b : f_x(\pm a, y) = 0, \quad f_y(x, \pm b) = 0; \tag{5}$$

in the functional spaces $C^{2+\alpha}(\Omega; \Lambda) \to C^\alpha(\Omega)$. The bifurcation points of (4),(5) are the eigenvalues of the linearized operator $B : C^{2+\alpha}(\Omega; \Lambda) \to C^\alpha(\Omega)$

$$\lambda_0 = \lambda_{m,n} = \frac{\pi^2}{4}(\frac{m^2}{a^2} + \frac{n^2}{b^2}), \quad m, n > 0 \quad for(a); \quad m, n \geq 0 \quad for(b) \tag{6}$$

with relevant eigenfunctions

$$\varphi_a = f_{m,n} = \frac{1}{\sqrt{ab}} \sin\frac{m\pi}{2a}(x + a) \sin\frac{n\pi}{2b}(y + b), \; \varphi_b = f_{m,n} = \frac{1}{\sqrt{ab}} \cos\frac{m\pi}{2a}(x + a) \cos\frac{n\pi}{2b}(y + b) \tag{7}$$

2.1. λ_0 **is a simple eigenvalue.** Here Lyapounov-Schmidt method [7] allows to obtain the representation of the bifurcating solutions in the form of the convergent series pf powers of $\varepsilon^{1/2}$. For both problems (4),(5) the equivalent BEq has the form

$$\xi\varepsilon = L_{30}\xi^3 + \cdots, \quad L_{30} = \frac{a_1\pi^4}{2^8 a^5 b^5}[8(n^4a^4 + b^4m^4) + (n^2a^2 + m^2b^2)^2]$$

Its investigation allows to prove the following result

Theorem 1. *For a rectangular domain Ω the problems (1),(2a) and (1),(2b) in some neighborhoods of the simple eigenvalues (6) have analytical in $\varepsilon^{1/2}$ solutions*

$$f(x,y;\varepsilon) = \pm(L_{30}^{-1}\varepsilon)^{\frac{1}{2}}\varphi + O(|\varepsilon|), \quad sign\varepsilon = signa_1 \tag{8}$$

where φ is the relevant to λ_0 eigenfunction (7).

2.2. **Square domain Ω.** For a square domain in dimensionless variables one can set $a = b = 1$. Then the eigenvalues take the form $\lambda_0 = \lambda_{m,n} = \frac{\pi^2}{4}(m^2+n^2)$ and their multiplicities are equal to the number of representations of the integer $(m^2 + n^2)$ as the sum of two squares m^2 and n^2, $\quad m, n > 0$. From Theorem 1 it follows

Corollary 2. *For a square domain Ω and simple eigenvalue $\lambda_{n,n} = \frac{n^2\pi^2}{2}$ the problems (4),(5) have the analytical in $\varepsilon^{1/2}$ solutions*

$$f(x,y;\varepsilon) = \pm\frac{8}{\sqrt{5}n^2\pi^2}\sqrt{\frac{\varepsilon}{a_1}}\begin{cases}\sin\frac{n\pi}{2}(x+1)\sin\frac{n\pi}{2}(y+1), & for(a)\\ \cos\frac{n\pi}{2}(x+1)\cos\frac{n\pi}{2}(y+1), & for(b)\end{cases} + O(|\varepsilon|), \ sign\varepsilon = signa_1 \tag{9}$$

.

If $m \neq n$, then in general the eigenvalue λ_0 is 2-multiple with eigenfunctions $\varphi_1 = f_{m,n}$, $\varphi_2 = f_{n,m}$; for example $m^2 + n^2 = 5, (m, n) = (2, 1), (1, 2)$. Here, when $m \neq n$, according to the inherited group symmetry of the square $(\xi_1 \to \xi_2 \to \xi_1)$, the BEq has the form of the system

$$\xi_1\varepsilon = a_1A\xi_1^3 + a_1B\xi_1\xi_2^2 + \cdots, \quad \xi_2\varepsilon = a_1B\xi_1^2\xi_2 + a_1A\xi_2^3 + \cdots,$$

where

$$A = \frac{\pi^4}{2^8}(9m^4 + 2m^2n^2 + 9n^4), \quad B = \frac{\pi^4}{2^6}(m^4 + 6m^2n^2 + n^4)$$

Theorem 3. *For a square domain Ω and 2-multiple eigenvalue $\lambda_0 = \frac{\pi^2}{4}(m^2 + n^2), m \neq n$, the problems (4),(5) have analytical in $\varepsilon^{1/2}$ solutions (all signs combinations are possible)*

$$f(x,y;\varepsilon) = \sqrt{\frac{\varepsilon}{a_1}}\frac{1}{\sqrt{A+B}}[\pm f_{m,n}(x,y) \pm f_{n,m}(x,y)] + O(|\varepsilon|)$$

$$f(x,y;\varepsilon) = \pm\sqrt{\frac{\varepsilon}{a_1}}\frac{1}{\sqrt{A}}f_{m,n}(x,y) + O(|\varepsilon|),$$

$$f(x,y;\varepsilon) = \pm\sqrt{\frac{\varepsilon}{a_1}}\frac{1}{\sqrt{A}}f_{n,m}(x,y) + O(|\varepsilon|), \quad sign\varepsilon = signa_1$$

2.3. **One case of high dimensional degeneration of the linearized operator.** Let us consider the case $(m, n) = (m_1, n_1), (n_1, m_1), (m_2, m_2)$, i.e. $m_1^2 + n_1^2 = 2m_2^2$. Example of such situation is $(m, n) = (7, 1), (1, 7), (5, 5)$. Here

$$\lambda_0 = \frac{\pi^2}{4}(m_1^2 + n_1^2) = \frac{\pi^2}{2}m_2^2 \tag{10}$$

with 3-dimensional $N(B)$ consisting of the corresponding eigenfunctions (7). According to the symmetry of the square $(\xi_1 \to \xi_2 \to \xi_1, \xi_3)$ the branching system has the form

$$\xi_1\varepsilon = a_1A\xi_1^3 + a_1B\xi_1\xi_2^2 + a_1C\xi_1\xi_3^3 + \cdots$$

$$\xi_2\varepsilon = a_1B\xi_1^2\xi_2 + a_1A\xi_2^3 + a_1C\xi_2\xi_3^2 + \cdots$$

$$\xi_3\varepsilon = a_1C\xi_1^2\xi_3 + a_1C\xi_2^2\xi_3 + a_1D\xi_3^3 + \cdots$$

where $A=\frac{\pi^4}{2^8}(9m_1^4+2m_1^2n_1^2+9n_1^4)$, $\quad B=\frac{\pi^4}{2^6}(m_1^4+6m_1^2n_1^2+n_1^4)$, $\quad C=\frac{\pi^4}{2^4}m_2^2(m_1^2+n_1^2)=\frac{m_2^4\pi^4}{2^3}$, $\quad D=\frac{5m_2^4\pi^4}{2^6}$. Its investigation allows to prove the following assertion

Theorem 4. *For a square domain Ω and 3-multiple eigenvalue (10), the problems (4),(5) have the following analytical in $\varepsilon^{1/2}$ by $\varepsilon^{1/2}$ solutions (all signs combinations are possible):*

I. $\xi_3=0\Rightarrow$ *solutions of Theorem 2;*

II. $\xi_1=\xi_2$ *or* $\xi_1=-\xi_2\Rightarrow \xi_1=\pm[\frac{(C-D)\varepsilon}{a_1[2C^2-(A+B)D]}]^{1/2}=\pm\xi_2=\pm\frac{8}{\sqrt{21}m_2^2\pi^2}\sqrt{\frac{\varepsilon}{a_1}}$,

$\xi_3=\pm[\frac{(2C-A-B)\varepsilon}{a_1[2C^2-(A+B)D]}]^{1/2}=\pm\frac{8}{\sqrt{21}m_2^2\pi^2}\sqrt{\frac{\varepsilon}{a_1}}$, $\quad sign\varepsilon=sign a_1$,

$$f(x,y;\varepsilon)=\pm\frac{8}{\sqrt{21}m_2^2\pi^2}\sqrt{\frac{\varepsilon}{a_1}}[\pm f_{m_1,n_1}(x,y)\pm f_{n_1,m_1}(x,y)\pm f_{m_2,n_2}(x,y)]+O(|\varepsilon|);$$

III. $\xi_1\neq\pm\xi_2,\quad \xi_3\neq 0\Rightarrow \xi_1=\pm\xi_1^0=\pm\sqrt{\frac{\varepsilon}{a_1}\frac{C-D}{C^2-AD}}=\pm\sqrt{\frac{\varepsilon}{a_1}}\frac{8\sqrt{3}}{\pi^2\sqrt{19m_2^4+20m_1^2n_1^2}}$,

$$\xi_2=0,\ \xi_3=\pm\xi_3^0=\pm\sqrt{\frac{\varepsilon}{a_1}\frac{C-A}{C^2-AD}}=\pm\frac{8}{\pi^2m_2^2}\sqrt{\frac{\varepsilon(7m_2^4-2(m_1^4+n_1^4))}{a_1(19m_2^4+20m_1^2n_1^2)}},$$

or $\xi_1=0,\quad \xi_2=\pm\xi_1^0,\quad \xi_3=\pm\xi_3^0\Rightarrow$

$f(x,y;\varepsilon)=\pm\xi_1^0f_{m_1,n_1}(x,y)\pm\xi_3^0f_{m_2,m_2}(x,y)+O(|\varepsilon|)$
$f(x,y;\varepsilon)=\pm\xi_1^0f_{n_1,m_1}(x,y)\pm\xi_3^0f_{m_2,m_2}(x,y)+O(|\varepsilon|)$, $\ sign\varepsilon=sign[a_1(7m_2^4-2(m_1^4+n_1^4))]$.

3. Circular domain Ω

For a circular domain Ω the problems (1),(2) allow continuous rotations-reflections group O(2) and, in polar coordinates, have the form

$$(\Delta+\lambda_0)f=f_{\rho\rho}+\frac{1}{\rho}f_\rho+\frac{1}{\rho^2}f_{\theta\theta}+\lambda_0f=-\varepsilon f-\frac{a_1}{\rho^2}[\rho f_\rho^3-$$
$$-\frac{1}{\rho}f_\rho f_\theta^2+f_{\rho\rho}f_\theta^2+4f_\rho f_\theta f_{\rho\theta}+f_{\theta\theta}f_\rho^2+3\rho^2f_{\rho\rho}f_\rho^2+\frac{3}{2\rho^2}f_{\theta\theta}f_\theta^2]+\cdots \tag{11}$$

$$\Lambda_a: f(r_0,\theta)=0,\quad \Lambda_b: f_\rho(r_0,\theta)=0 \tag{12}$$

Bifurcation points are $\lambda_0=\lambda_{m,n}=(\frac{\kappa_m^{(n)}}{r_0})^2$ with relevant zero-subspaces $N(B)=span\{\varphi_1(\rho,\theta)=\mathcal{I}_n(\frac{\kappa_m^{(n)}}{r_0}\rho)\cos n\theta,\quad \varphi_2(\rho,\theta)=\mathcal{I}_n(\frac{\kappa_m^{(n)}}{r_0}\rho)\sin n\theta\}$, where $\mathcal{I}_n(x)$ is the Bessel function of index n and $\kappa_m^{(n)}=\mu_m^{(n)}$ is its m-th root ($\mathcal{I}_n(\mu_m^{(n)})=0$) for the problem (a), $\kappa_m^{(n)}=\nu_m^{(n)}$ is the m-th root of its derivative (${\mathcal{I}'}_n(\nu_m^{(n)})=0$) for the problem (b) [8]. Here (see [8])

$$\int_0^{r_0}\rho\mathcal{I}_n^2(\frac{\kappa_m^{(n)}}{r_0}\rho)d\rho\int_0^{2\pi}\left\{\begin{matrix}\cos^2n\theta\\ \sin^2n\theta\end{matrix}\right\}d\theta=\left\{\begin{matrix}\beta_{m,n}=\frac{r_0^2\pi}{2}[{\mathcal{I}'}_n(\mu_m^{(n)})]^2, & \text{for (a)}\\ \alpha_{m,n}=\frac{r_0^2\pi}{2}[1-\frac{n^2}{(\nu_m^{(n)})^2}]\mathcal{I}_n^2(\nu_m^{(n)}), & \text{for (b)}\end{matrix}\right.$$

The BEqs for both problems inherit the group symmetry O(2) and have the form

$$A\xi_1\varepsilon+B\xi_1(\xi_1^2+\xi_2^2)+\cdots=0,\quad A\xi_2\varepsilon+B\xi_2(\xi_1^2+\xi_2^2)+\cdots=0$$

where $A_a=-\beta_{m,n}<0,\quad A_b=-\alpha_{m,n}<0$,

$$B=a_1\left[\frac{3\pi}{2}(\frac{\kappa_m^{(n)}}{r_0})^3\int_0^{r_0}\mathcal{I}_n'^3(\frac{\kappa_m^{(n)}}{r_0}\rho)\mathcal{I}_n(\frac{\kappa_m^{(n)}}{r_0}\rho)d\rho+\frac{\pi}{2}\frac{\kappa_m^{(n)}}{r_0}n^2\int_0^{r_0}\frac{1}{\rho^2}{\mathcal{I}'}_n(\frac{\kappa_m^{(n)}}{r_0}\rho)\mathcal{I}_n^3(\frac{\kappa_m^{(n)}}{r_0}\rho)d\rho+\right.$$
$$+\frac{\pi}{2}n^4\int_0^{r_0}\frac{1}{\rho^3}\mathcal{I}_n^4(\frac{\kappa_m^{(n)}}{r_0}\rho)d\rho+\frac{\pi}{4}(\frac{\kappa_m^{(n)}n}{r_0})^2\int_0^{r_0}\frac{1}{\rho}\mathcal{I}_n^4(\frac{\kappa_m^{(n)}}{r_0}\rho)d\rho-$$

$$-\frac{5\pi}{4}\left(\frac{\kappa_m^{(n)}n}{r_0}\right)^2\int\limits_0^{r_0}\frac{1}{\rho}\mathcal{I}_n'^2\left(\frac{\kappa_m^{(n)}}{r_0}\rho\right)\mathcal{I}_n^2\left(\frac{\kappa_m^{(n)}}{r_0}\rho\right)d\rho+\frac{9\pi}{4}\left(\frac{\kappa_m^{(n)}}{r_0}\right)^4\int\limits_0^{r_0}\rho\mathcal{I}_n'^2\left(\frac{\kappa_m^{(n)}}{r_0}\rho\right)\mathcal{I}_n^2\left(\frac{\kappa_m^{(n)}}{r_0}\rho\right)d\rho\Bigg],$$

$\kappa_m^{(n)}=\mu_m^{(n)}$ for (a), $\kappa_m^{(n)}=\nu_m^{(n)}$ for (b).

According to the general theory [5-7] the obtained families of solutions are represented in the form of convergent series in $\varepsilon^{1/2}$ in some neighborhood of $\varepsilon=0$.

Theorem 5. *For circular domain Ω the problems (11),(12) in some neighborhoods of the bifurcation points $\lambda_0=\lambda_{m,n}$ have one-parametric families of solutions*

$$f(x,y;a)=\left(-\frac{A\varepsilon}{B}\right)^{1/2}\mathcal{I}_n\left(\frac{\kappa_m^{(n)}}{r_0}\rho\right)\cos n(\theta+\alpha)+O(|\varepsilon|),$$
$$sign\varepsilon=signB,$$

where α is the free parameter of the rotation group O(2).

Remark 6. Variational methods of bifurcation theory are supposed to apply to these problems.

References

[1] Finn, R., Equilibrium capillary surfaces, Springer, Berlin, 1986; Moscow, Mir, 1989.

[2] Nakao, M., A bifurcational problem for a quasilinear elliptic boundary value problem, Nonlinear Analysis. TMA, **14** 3(1990), 251-262.

[3] Pimbley, G.H., Stationary solutions of the problem of Rayleigh-Taylor instability, J. Math. Anal. Appl., **55** 1(1976), 170-206.

[4] Loginov, B.V., Petrov, K.M., Bifurcation of stationary solutions in problem of Rayleigh-Taylor instability, Univ. Annual Appl.Math., Sophia Technical University, **27** 1(1998), .

[5] Loginov, B.V., Branching theory of solutions of nonlinear equations under group invariance conditions, Fan Tashkent. 1985. (Russian).

[6] Loginov, B.V., Group analysis methods for construction and investigation of the bifurcation equation, Applications of Mathematics, **37** 4(1992), 241-248.

[7] Vainberg, M.M., Trenogin, V.A. Branching, Theory of solutions of nonlinear equations, Nauka, Moscow, 1969; Engl. transl. Noordhoff, Leyden, 1974.

[8] Tikhonov, A.N., Samarsky, A.A., Mathematical physics equations, Nauka, Moscow, 1972. (Russian)

Image contrast modifiers using vectorial MV-algebras

D. Noje, B. Bede, V. Kos
Department of Mathematics, University of Oradea
Armatei Romane 5, 3700 Oradea, Romania
E-mail: dnoje@uoradea.ro, bbede@uoradea.ro, vkos@uoradea.ro

Abstract. In this paper we present some numerical methods used to improve the digital image contrast. The algebraic support of these numerical methods is the RGB model organized as a vectorial MV-algebra.
Keywords: MV-algebras, Vectorial MV-algebras, Many Valued Logics, Image processing
2000 Mathematics Subject Classification: 06D35, 06B23, 65XX

1. Introduction

It is well known that after image compression and decompression or after image zooming there are some losses of image quality. These losses of quality are mainly produced by the approximations used during the image processing. It is easy to see that the contrast of the obtained image is not as good as of the original one.

The aim of this paper is to provide some numerical methods to improve the quality of the obtained image by improving its contrast.

In order to provide these numerical methods the vectorial MV-algebra structure of RGB model [2] is used .

2. Algebraic structures used

In 1958, C.C. Chang introduced a new type of algebras as support for many-valued logic [3]. In the meantime, these algebras were deeply studied due to their applications in many domains. In [2] where Vectorial MV-algebras are introduced as a special type of MV-algebras as the algebraic support of some approximation methods used for image processing.

First will recall some basic definitions that we use later. An MV-algebra [4] is an algebra $\langle A, \oplus, \neg, 0_A \rangle$ with a binary operation $\oplus$, a unary operation $\neg$ and a constant 0_A satisfying the following equations:

MV1) $x \oplus (y \oplus z) = (x \oplus y) \oplus z$;
MV2) $x \oplus y = y \oplus x$;
MV3) $x \oplus 0_A = x$;
MV4) $\neg\neg x = x$;
MV5) $x \oplus \neg 0_A = \neg 0_A$;
MV6) $\neg (\neg x \oplus y) \oplus y = \neg (\neg y \oplus x) \oplus x$.

Remark 7. On each MV-algebra A the constant 1_A and the operations $\odot$ and $\ominus$ defined as follows:

i) $1_A = \neg 0_A$;
ii) $x \odot y = \neg (\neg x \oplus \neg y)$;
iii) $x \ominus y = x \odot \neg y$.

On each MV-algebra A we say that $x \leq y$ iff x and y satisfy one of the equivalent conditions:

i) $\neg x \oplus y = 1_A$;
ii) $x \odot \neg y = 0_A$;
iii) $y = x \oplus (y \ominus x)$;
iv) there is an element $z \in A$ such that $x \oplus z = y$.

The distance function $d : A \times A \to A$ is defined by

$$d(x, y) = (x \ominus y) \oplus (y \ominus x).$$

Proposition 1. *In every MV-algebra A we have:*

i) $d(x,y) = 0_A$ *iff* $x = y$;
ii) $d(x,y) = d(y,x)$;
iii) $d(x,y) \leq d(x,y) \oplus d(y,z)$;
iv) $d(x,y) = d(\neg x, \neg y)$;
v) $d(x \oplus s, y \oplus t) \leq d(x,y) \oplus d(s,t)$.

For more details on MV-algebras we recomend [3] and [4].

In what follows we will recall the definition of vectorial MV-algebras [2] and some of their basic properties.

We say that an MV-algebra A is a vectorial MV-algebra, if a multiplicative operation $\bullet : \mathbb{R}_+ \times A \to A$ is defined having the following properties:

i) $1 \bullet x = x$ for any $x \in A$;
ii) $(a+b) \bullet x = a \bullet x \oplus b \bullet x$ for any $x \in A$ and $a, b \in \mathbb{R}_+$;
iii) $a \bullet (b \bullet x) \leq (a \cdot b) \bullet x$ for any $x \in A$ and $a, b \in \mathbb{R}_+$;
iv) $d(a \bullet x, a \bullet y) \leq a \bullet d(x,y)$ for any $x, y \in A$ and $a \in \mathbb{R}_+$;

Proposition 2. *Let A be a vectorial MV-algebra.*

i) $(a_1 + ... + a_n) \bullet x = a_1 \bullet x \oplus ... \oplus a_n \bullet x$ *for any* $x \in A$ *and* $a_1, .., a_n \in \mathbb{R}_+$;
ii) *for any* $n \in N$ *and* $x \in A$ *we have* $nx = n \bullet x$ *where* $nx = x \oplus x \oplus ... \oplus x$ *(n times)*;
iii) $\lambda \bullet 0_A = 0_A$ *for any* $\lambda \in \mathbb{R}_+$.
iv) $a \bullet x \leq b \bullet x$ *for any* $x \in A$ *and* $a, b \in R_+$, *where* $a \leq b$.

3. Vectorial MV-algebra structure of RGB model

RGB model [5] is one of the most well known color models used for digital image processing. In this model one color is obtained combining red, green and blue which represents the basic colors components. It means that we can consider the color of a pixel as a triplet of red, green and blue and the RGB model as the set

$$RGB = \left\{(r,g,b) \,|r,g,b \in \left[0, 2^t - 1\right]\right\}$$

where t represents the number of bits on which the color component is stored in computer's memory.

Let us consider $c_1 = (r_1, g_1, b_1), c_2 = (r_2, g_2, b_2) \in RGB$. In [1] a binary operation $\oplus_{RGB}$, an unary operation $\neg_{RGB}$ and a constant 0_{RGB} are defined as follows:

i) $c_1 \oplus_{RGB} c_2 = (r_1 \oplus r_2, g_1 \oplus g_2, b_1 \oplus b_2)$ where $r_1 \oplus r_2 = \min(2^t - 1, r_1 + r_2)$ and so on;
ii) $\neg_{RGB} c = (\neg r, \neg g, \neg b)$ where $\neg r = 2^t - 1 - r$ and so on;
iii) $0_{RGB} = (0,0,0)$.

It is easy to see that $\langle RGB, \oplus_{RGB}, \neg_{RGB}, 0_{RGB} \rangle$ is an MV-algebra.

We also introduce the following:

i) $1_{RGB} = (2^t - 1, 2^t - 1, 2^t - 1)$;
ii) $c_1 \odot c_2 = (r_1 \odot r_2, g_1 \odot g_2, b_1 \odot b_2)$ where $r_1 \odot r_2 = \max(0, r_1 + r_2 - 2^t + 1)$ and so on;
iii) $c_1 \ominus c_2 = (r_1 \ominus r_2, g_1 \ominus g_2, b_1 \ominus b_2)$ where $r_1 \ominus r_2 = \max(0, r_1 - r_2)$ and so on;
iv) $d(c_1, c_2) = (d(r_1, r_2), d(g_1, g_2), d(b_1, b_2))$ where $d(r_1, r_2) = |r_1 - r_2|$ and so on.

In [2] the following external operation $\bullet_{RGB} : \mathbb{R}_+ \times RGB \to RGB$ was introduced

$$a \bullet_{RGB} c = (a \bullet r, a \bullet g, a \bullet b) \text{ where } a \bullet r = \min\left(2^t - 1, a \cdot r\right) \text{ and so on.}$$

It is also proved that $\langle RGB, \oplus_{RGB}, \neg_{RGB}, 0_{RGB}, \bullet_{RGB} \rangle$ is a vectorial complete MV-algebra.

4. Contrast modifiers

In this section some numerical methods used to modify the contrast, in order to improve the quality of digital images, are presented.

Let us assume that the image has the resolution $M \times N$, i.e. it has M rows of pixels and N pixels on each row. We also assume that pixel's color is one element of the

$$RGB = \left\{(r,g,b) \,|r,g,b \in \left[0, 2^t - 1\right]\right\}$$

set.

It follows that an image can be interpreted as

$$F : [1, M] \times [1, N] \to RGB,$$

where $F(i, j)$ represents the color of the pixel situated on row i and column j, for all $i \in [1, M]$ and $j \in [1, N]$.

Therefore we can assume that a contrast modifier is a mapping

$$H : RGB \to RGB$$

that will modify the color of each pixel of an image.

Since any element of RGB set is one of the form $c = (r, g, b)$ with $r, g, b \in [0, 2^t - 1]$, it follows that the contrast modifier has to correct each component of the color c. Thus we can assume that

$$H(c) = (h(r), h(g), h(b)), \tag{1}$$

where

$$h : \left[0, 2^t - 1\right] \to \left[0, 2^t - 1\right],$$

represents the modifier of one component of the considered color.

In what follows the way of choosing the function h is presented. Suppose that x is the original and x' is the obtained value of the color component by using function h. Then x' has to fulfill the following properties:

$$x' \in \left[0, 2^t - 1\right]; \tag{2}$$

$$\text{if } x < \frac{2^t - 1}{2} \text{ then } x' \leq x; \tag{3}$$

$$\text{if } x > \frac{2^t - 1}{2} \text{ then } x' \geq x; \tag{4}$$

$$\text{if } x \in \left\{0, \frac{2^t - 1}{2}, 2^t - 1\right\} \text{ then } x' = x. \tag{5}$$

All these conditions lead us to define function h as follows:

$$h(x) = x \bullet \left(1 - \frac{\lambda \cdot \sin\left(\frac{2\pi x}{2^t - 1}\right)}{100}\right),$$

where $\lambda \in [0, 100]$.

Since

$$0 \leq 1 - \frac{\lambda \cdot \sin\left(\frac{2\pi x}{2^t - 1}\right)}{100} \leq 1$$

it follows that

$$h(x) = x \cdot \left(1 - \frac{\lambda \cdot \sin\left(\frac{2\pi x}{2^t - 1}\right)}{100}\right). \tag{6}$$

Using relation (1) and (6) we obtain that

$$\begin{aligned} H(r, g, b) &= \\ &= \left(r \cdot \left(1 - \frac{\lambda \cdot \sin\left(\frac{2\pi r}{2^t - 1}\right)}{100}\right), g \cdot \left(1 - \frac{\lambda \cdot \sin\left(\frac{2\pi g}{2^t - 1}\right)}{100}\right), b \cdot \left(1 - \frac{\lambda \cdot \sin\left(\frac{2\pi b}{2^t - 1}\right)}{100}\right)\right). \end{aligned} \tag{7}$$

It is easy to see that using the modifier H, each color component of a pixel is modified with a quantity determined by its original value.

Let us remind that a color c is a triple of form (r, g, b). Let us denote

$$m = \frac{r+g+b}{3}.$$

Then we can rewrite the conditions (2), (3), (4) and (5) in the form:

$$r', g', b' \in \left[0, 2^t - 1\right];$$

$$\text{if } m < \frac{2^t-1}{2} \text{ then } m' \le m;$$

$$\text{if } m > \frac{2^t-1}{2} \text{ then } m' \ge m;$$

$$\text{if } r, g, b \in \left\{0, 2^t - 1\right\} \text{ then } r' = r,\ g' = g \text{ and } b' = b.$$

Using these conditions, the contrast modifier can be defined as follows:

$$H'(r, g, b) = \tag{8}$$

$$= \left(r \cdot \left(1 - \frac{\lambda \cdot \sin\left(\frac{2\pi m}{2^t-1}\right)}{100} \right), g \cdot \left(1 - \frac{\lambda \cdot \sin\left(\frac{2\pi m}{2^t-1}\right)}{100} \right), b \cdot \left(1 - \frac{\lambda \cdot \sin\left(\frac{2\pi m}{2^t-1}\right)}{100} \right) \right).$$

The difference between H and H' is that H' modifies each color component with a quantity determined by the average of the original values of the color components.

5. Experimental results

In this section some experimental results using the contrast modifiers H and H', defined as in (7), (8) are presented. These modifiers are applied on some zoomed images that present loose of quality.

The images are the following:

Figure 1. Image 1 obtained after zooming process, after applying 3 times modifier H with $\lambda = 10$ and after applying modifier H' with $\lambda = 1$.

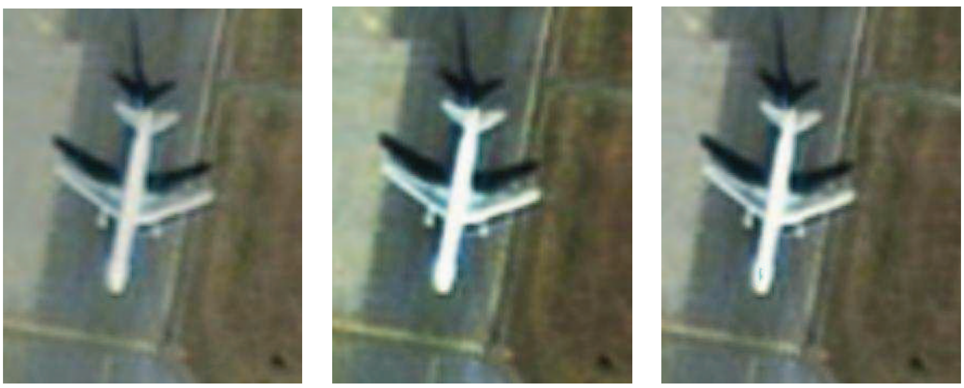

Figure 2. Image 2 obtained after zooming process, after applying 2 times modifier H with $\lambda = 10$ and after applying modifier H' with $\lambda = 15$.

It is easy to see that the quality of the images obtained using contrast modifiers H and H' is better. We can also see that H offers a better result than H'. These results are proving the utility of using the contrast modifiers H and H'.

References

[1] Chang, C.C., (1958) Algebraic analysis of many-valued logic, Trans. Amer. Math. Soc. **88**, 467-490.

[2] Cignoli, R., D'Ottaviano, I.M.L., Mundici, D., Algebraic foundations of many-valued reasoning, Kluwer, Dordrecht, Trends in Logic, 2000.

[3] Ionescu, F., Grafica in realitatea virtuala, Ed. Tehnica, Bucuresti, 2000.

[4] D. Noje, B. Bede, MV-algebra structure of RGB model, Studia Univ. Babeş-Bolyai, Informatica, **XLVI**, 1(2001), 77-86.

[5] Noje, D., Bede, B., Vectorial MV-algebras, Soft Computing, **7** (2003), 258-262.

On a differential inequality

Georgia Irina Oros and Adriana Cătaş
"Babeş-Bolyai" University
Department of Mathematics
Cluj-Napoca, România.
University of Oradea
Department of Mathematics
România.

Abstract. We find conditions on the complex-valued functions A and B, defined in the unit disc U such that the differential inequality

$$Re\,[A(z)p^2(z)+B(z)p(z)-\alpha(zp'(z))^2+\beta(zp'(z))+\gamma]>0$$

implies $Re\,p(z)>0$, where $\alpha\geq 0$, $\beta\in\mathbb{R}$, $\gamma<\dfrac{\alpha n^2}{4}+\dfrac{\beta n}{2}$ and $p\in\mathcal{H}[1,n]$.

Keywords: differential subordination, dominant

2000 Mathematics Subject Classification: 30C80

1. Introduction and preliminaries

Let $\mathcal{H}[U]$ denote the class of holomorphic functions in the unit disc

$$U=\{z\in\mathbb{C}:\quad |\,z\,|<1\}.$$

For $a\in\mathbb{C}$ and $n\in\mathbb{N}^*$ let

$$\mathcal{H}[a,n]=\{f\in\mathcal{H}[U],\quad f(z)=a+a_nz^n+a_{n+1}z^{n+1}+...,\ z\in U\}$$

and

$$\mathcal{A}_n=\{f\in\mathcal{H}[U],\quad f(z)=z+a_{n+1}z^{n+1}+a_{n+2}z^{n+2}+...,\ z\in U\}$$

with $\mathcal{A}_1=\mathcal{A}$.

In order to prove the new results we use the following lemma, which is a particular form of Theorem 2.3.i[1,p.35].

Lemma 1 (1,p.35)**.** *Let $\psi:\mathbb{C}^2\times U\to\mathbb{C}$ a function which satisfies*

$$Re\ \psi(\rho i,\sigma;z)\leq 0,$$

where $\rho,\sigma\in\mathbb{R}$, $\quad\sigma\leq-\frac{n}{2}(1+\rho^2)\quad z\in U\quad$ and $\quad n\geq 1$.
If $p\in\mathcal{H}[1,n]$ and

$$Re\ \psi\,(p(z),zp'(z);z)>0$$

then

$$Re\,p(z)\ >0.$$

2. Main results

Theorem 2. *Let $\alpha\geq 0$, $\beta\in\mathbb{R}$, $\gamma<\dfrac{\alpha n^2}{4}+\dfrac{\beta n}{2}$ and let n be a positive integer. Suppose that the functions $A,B:U\to\mathbb{C}$ satisfy*

$$(1)\qquad \begin{aligned}&(i)\ Re\,A(z)>-\frac{\alpha n^2}{2}-\frac{\beta n}{2}\\ &(ii)\ (ImB(z))^2\leq 4\left(\frac{\alpha n^2}{2}+\frac{\beta n}{2}+Re\,A(z)\right)\left(\frac{\alpha n^2}{4}+\frac{\beta n}{2}-\gamma\right)\end{aligned}$$

If $p\in\mathcal{H}[1,n]$ and

(2) $\quad Re\,[A(z)p^2(z) + B(z)p(z) - \alpha(zp'(z))^2 + \beta(zp'(z)) + \gamma] > 0$

then

$$Re\,p(z) > 0.$$

Proof. Let $\psi : \mathbb{C}^2 \times U \to \mathbb{C}$ be defined by

(3) $\quad \psi(p(z), zp'(z); z) = A(z)p^2(z) + B(z)p(z) - \alpha(zp'(z))^2 + \beta(zp'(z)) + \gamma$

From (2) we have

(4) $\quad Re\,\psi(p(z), zp'(z); z) > 0$ for $z \in U$.

For $\rho, \sigma \in \mathbb{R}$ satisfying $\sigma \leq -\frac{n}{2}(1+\rho^2)$, hence $-\sigma^2 \leq -\frac{n^2}{4}(1+\rho^2)^2$, and $z \in U$, by using (1) we obtain

$$Re\,\psi(\rho i, \sigma; z) = Re\,[A(z)(\rho i)^2 + B(z)\rho i - \alpha\sigma^2 + \beta\sigma + \gamma] = -\rho^2 Re\,A(z) - \rho\, Im\,B(z) -$$

$$-\alpha\sigma^2 + \beta\sigma + \gamma \leq -\rho^2 Re\,A(z) - \rho\, Im\,B(z) -$$

$$-\frac{\alpha n^2}{4}(1+\rho^2)^2 - \frac{\beta n}{2}(1+\rho^2) + \gamma \leq$$

$$\leq -\rho^2\, Re\,A(z) - \rho\, Im\,B(z) - \frac{\alpha n^2}{4} - \frac{\alpha n^2}{2}\rho^2 - \frac{\alpha n^2}{4}\rho^4 -$$

$$-\frac{\beta n}{2} - \rho^2\,\frac{\beta n}{2} + \gamma \leq$$

$$\leq -\frac{\alpha n^2}{4}\rho^4 - \rho^2\left(\frac{\alpha n^2}{2} + \frac{\beta n}{2} + Re\,A(z)\right) -$$

$$-\rho\, Im\,B(z) - \frac{\alpha n^2}{4} - \frac{\beta n}{2} + \gamma \leq 0.$$

By using Lemma A we have that $Re\,p(z) > 0$. $\square$

If $\alpha = 0$, then Theorem 1 can be rewritten as follows:

Corollary 3. *Let $\beta \in \mathbb{R}$, $\gamma < \frac{\beta n}{2}$ and let n be a positive integer. Suppose that the functions $A, B : U \to \mathbb{C}$ satisfy*

$$(5) \qquad \begin{aligned} &(i)\ Re\,A(z) > -\frac{\beta n}{2} \\ &(ii)\ (Im B(z))^2 \leq 4\left(\frac{\beta n}{2} + Re\,A(z)\right)\left(\frac{\beta n}{2} - \gamma\right) \end{aligned}$$

If $p \in \mathcal{H}[1, n]$ and

(6) $\quad Re\,[A(z)p^2(z) + B(z)p(z) + \beta(zp'(z)) + \gamma] > 0$

then

$$Re\,p(z) > 0.$$

If $\beta = 0$, then Theorem 1 can be rewritten as follows

Corollary 4. *Let* $\alpha \geq 0, \gamma < \dfrac{\alpha n^2}{4}$ *and let* n *be a positive integer. Suppose that the functions* $A, B : U \to \mathbb{C}$ *satisfy*

$$(7)\qquad \begin{aligned} &(i)\ Re\, A(z) > -\frac{\alpha n^2}{2} \\ &(ii)\ (Im B(z))^2 \leq 4\left(\frac{\alpha n^2}{2} + Re\, A(z)\right)\left(\frac{\alpha n^2}{4} - \gamma\right) \end{aligned}$$

If $p \in \mathcal{H}[1, n]$ *and*

$$(8)\qquad Re\left[A(z)p^2(z) + B(z)p(z) - \alpha(zp'(z))^2 + \gamma\right] > 0$$

then

$$Re\, p(z) > 0.$$

References

[1] Miller, S.S., Mocanu, P.T., Differential subordinations. Theory and applications, Marcel Dekker, New York, 2000.
[2] Oros, G.I., On a differential inequality I, 11th C0nference on Applied and Industrial Mathematics, CAIM 2003, May 29-31, 2003, Oradea, România, Proceedings, vol.I, 165-166.

A new differential inequality I

Georgia Irina Oros

Faculty of Mathematics and Computer Sciences
Babeş-Bolyai University, 3400 Cluj-Napoca, Romania

Abstract. We find conditions on the complex-valued functions A, B, C, D, E defined in the unit disc U such that the differential inequality

$$\text{Re}\,[A(z)p^2(z) + B(z)p(z) - C(z)(zp'(z))^2 + D(z)(zp'(z)) + E(z)] > 0$$

implies $\text{Re}\,p(z) > 0$, where $p \in \mathcal{H}[1, n]$.

Keywords: differential subordination, dominant

2000 Mathematics Subject Classification: 30C80

1. Introduction and preliminaries

Let $\mathcal{H}[U]$ denote the class of holomorphic functions in the unit disc

$$U = \{z \in \mathbb{C} : \; |z| < 1\}.$$

For $a \in \mathbb{C}$ and $n \in \mathbb{N}^*$ let

$$\mathcal{H}[a, n] = \{f \in \mathcal{H}[U], \; f(z) = a + a_n z^n + a_{n+1} z^{n+1} + \dots, \; z \in U\}$$

and

$$\mathcal{A}_n = \{f \in \mathcal{H}[U], \; f(z) = z + a_{n+1} z^{n+1} + a_{n+2} z^{n+2} + \dots, \; z \in U\}$$

with $\mathcal{A}_1 = \mathcal{A}$.

In order to prove the new results we shall use the following lemma, which is a particular form of Theorem 2.3.i [1, p. 35].

Lemma A. [1, p. 35] *Let $\psi : \mathbb{C}^2 \times U \to \mathbb{C}$ a function which satisfies*

$$\text{Re}\,\psi(\rho i, \sigma; z) \le 0,$$

where $\rho, \sigma \in \mathbb{R}$, $\sigma \le -\dfrac{n}{2}(1 + \rho^2)$, $z \in U$ and $n \ge 1$.

If $p \in \mathcal{H}[1, n]$ and

$$\text{Re}\,\psi(p(z), zp'(z); z) > 0$$

then

$$\text{Re}\,p(z) > 0.$$

2. Main results

Theorem 1. *Let n be a positive integer. Suppose that the functions $A, B, C, D, E : U \to \mathbb{C}$ satisfy*

(1)

i) $\text{Re}\,C(z) \ge 0$;

ii) $\text{Re}\,[2A(z) + n^2 C(z) + nD(z)] \ge 0$;

iii) $\text{Im}\,^2 B(z) \le 4\left[\text{Re}\,A(z) + \frac{n^2}{2}\text{Re}\,C(z) + \frac{n}{2}\text{Re}\,D(z)\right]\left[\frac{n^2}{2}\text{Re}\,C(z) + \frac{n}{2}\text{Re}\,D(z) - \text{Re}\,E(z)\right]$.

If $p \in \mathcal{H}[1, n]$ and

$$\text{Re}\,[A(z)p^2(z) + B(z)p(z) - C(z)(zp'(z))^2 + D(z)zp'(z) + E(z)] > 0 \tag{2}$$

then

$$\text{Re}\,p(z) > 0.$$

Proof. Let $\psi : \mathbb{C}^2 \times U \to \mathbb{C}$ be defined by

(3) $$\psi(p(z), zp'(z); z) = A(z)p^2(z) + B(z)p(z) - C(z)(zp'(z))^2 + D(z)zp'(z) + E(z).$$

From (2) we have

(4) $$\text{Re } \psi(p(z), zp'(z); z) > 0, \text{ for } z \in U.$$

For $\sigma, \rho \in \mathbb{R}$ satisfying $\sigma \leq -\frac{n}{2}(1+\rho^2)$, and $z \in U$, by using (1), we obtain:

$$\text{Re } \psi(\rho i, \sigma; z) = \text{Re } [A(z)(\rho i)^2 + B(z)\rho i - C(z)\sigma^2 + D(z)\sigma + E(z)]$$

$$-\rho^2 \text{Re } A(z) - \rho \text{Im } B(z) - \sigma^2 \text{Re } C(z) + \sigma \text{Re } D(z) + \text{Re } E(z) \leq$$

$$\leq -\rho^2 \text{Re } A(z) - \rho \text{Im } B(z) - \frac{n^2}{4}(1 + 2\rho^2 + \rho^4)\text{Re } C(z) - \frac{n}{2}(1+\rho^2)\text{Re } D(z) + \text{Re } E(z) \leq$$

$$\leq -\rho^4 \frac{n^2}{4} \text{Re } C(z) - \left[\rho^2 \left(\text{Re } A(z) + \frac{n^2}{2}\text{Re } C(z) + \frac{n}{2}\text{Re } D(z)\right) + \right.$$

$$\left. + \rho \text{Im } B(z) + \frac{n^2}{4}\text{Re } C(z) + \frac{n}{2}\text{Re } D(z) - \text{Re } E(z)\right] \leq 0.$$

By using Lemma A we have that Re $p(z) > 0$. □

If $E(z) \equiv 0$, then Theorem can be rewritten as follows:

Corollary 2. *Let n be a positive integer. Suppose that the functions $A, B, C, D : U \to \mathbb{C}$ satisfies*
i) Re $C(z) \geq 0$
ii) Re $2A(z) \geq -\text{Re } [n^2 C(z) + nD(z)]$
iii) Im $^2 B(z) \leq 4 \left[\text{Re } A(z) + \frac{n^2}{2}\text{Re } C(z) + \frac{n}{2}\text{Re } D(z)\right] \left[\frac{n^2}{2}\text{Re } C(z) + \frac{n}{2}\text{Re } D(z)\right]$..
If $p \in \mathcal{H}[1, n]$ and

$$\text{Re } [A(z)p^2(z) + B(z)p(z) - C(z)(zp'(z))^2 + D(z)zp'(z)] > 0$$

then

$$\text{Re } p(z) > 0.$$

If $A(z) = 1 + z$, $B(z) = 3 + 2z$, $C(z) = 2 + z$, $D(z) = 3 - 2z$, $n = 1$, then in this case from Corollary 1 we deduce

Example 1. If $p \in \mathcal{H}[1, 1]$ and

$$\text{Re } [(1+z)p^2(z) + (3+2z)p(z) - (2+z)(zp'(z))^2 + (3-2z)zp'(z)] > 0$$

then

$$\text{Re } p(z) > 0.$$

If $A(z) = 1 + \frac{z}{2}$, $B(z) = 2 - z$, $C(z) = 2 - 2z$, $D(z) = z$, $n = 2$, then in this case from Corollary we deduce:

Example 2. If $p \in \mathcal{H}[1, 2]$ and

$$\text{Re } \left[\left(1 + \frac{z}{2}\right) p^2(z) + (2-z)p(z) - (2-2z)(zp'(z))^2 + z(zp'(z))\right] > 0$$

then

$$\text{Re } p(z) > 0.$$

If $D(z) \equiv 0$, then Theorem can be rewritten as follows:

Corollary 3. *Let n be a positive integer. Suppose that the functions $A, B, C, E : U \to \mathbb{C}$ satisfyies:*
i) Re $C(z) \geq 0$
ii) Re $A(z) \geq \dfrac{-n^2}{2}$Re $C(z)$
iii) Im $^2 B(z) \leq 4\left[\text{Re } A(z) + \frac{n^2}{2}\text{Re } C(z)\right]\left[\frac{n^2}{2}\text{Re } C(z) - \text{Re } E(z)\right]$.
If $p \in \mathcal{H}[1, n]$ and

$$\text{Re } [A(z)p^2(z) + B(z)p(z) - C(z)(zp'(z))^2 + E(z)] > 0$$

then

$$\text{Re } p(z) > 0.$$

If $A(z) = 1 - \dfrac{z}{2}$, $B(z) = i(1 + z)$, $C(z) = 1 - z$, $E(z) = \dfrac{z}{2}$, $n = 1$, then in this case from Corollary 2 we deduce

Example 3. If $p \in \mathcal{H}[1, 1]$ and

$$\text{Re } \left[\left(1 - \frac{z}{2}\right)p^2(z) + i(1 + z)p(z) - (1 - z)(zp'(z))^2 + \frac{z}{2}\right] > 0$$

then

$$\text{Re } p(z) > 0.$$

If $C(z) \equiv 0$, then Theorem can be rewritten as follows:

Corollary 4. *Let n be a positive integer. Suppose that the functions $A, B, D, E : U \to \mathbb{C}$ satisfy*
i) Re $2A(z) \geq -n$Re $D(z)$
ii) Im $^2 B(z) \leq 4\left[\text{Re } A(z) + \frac{n}{2}\text{Re } D(z)\right]\left[\frac{n}{2}\text{Re } D(z) - \text{Re } E(z)\right]$.
If $p \in \mathcal{H}[1, n]$ and

$$\text{Re } [A(z)p^2(z) + B(z)p(z) + D(z)zp'(z) + E(z)] > 0$$

then

$$\text{Re } p(z) > 0.$$

If $A(z) = z$, $B(z) = \dfrac{1 + z}{1 - z}i$, $D(z) = 1 - z$, $E(z) = -z$, $n = 2$, then in this case from Corollary 3 we deduce

Example 4. If $p \in \mathcal{H}[1, 2]$ and

$$\text{Re } \left[zp^2(z) + \frac{1 + z}{1 - z}ip(z) - (1 - z)zp'(z) - z\right] > 0$$

then

$$\text{Re } p(z) > 0.$$

If $E(z) = \dfrac{n^2}{4}C(z) + \dfrac{n}{2}D(z)$, then Theorem can be rewritten as follows:

Remark 8. If $B(z) \equiv 0$, $C(z) \equiv \alpha \geq 0$, $D(z) \equiv 0$, $E(z) = \beta \leq \dfrac{\alpha n^2}{4}$, we obtain Theorem 2 from [2].

References

[1] Miller, S.S., Mocanu, P.T., Differential subordinations. Theory and applications, Marcel Dekker, New York, 2000.
[2] Oros, G.I., On a differential inequality I, 11th C0nference on Applied and Industrial Mathematics, CAIM 2003, May 29-31, 2003, Oradea, România, Proceedings, vol.I, 165-166.

A probability interpretation for the zeta function of Riemann and some technical regularization for spectral representation

Fabian Todor
University of Montreal

Riemann considers the zeta function of Euler given by the following formula

(1) $$\zeta(s) = \sum_{n=1}^{\infty} 1/n^s = \prod_p (1 - 1/p^s)^{-1}$$

where $s = \sigma + it$ is a complex number; the infinite product is over all the prime numbers, and the Dirichlet series (1) is convergent for $\sigma > 1$.

The investigations of Riemann lead to the following definition

(2) $$\xi(s) = (1/2)s(s-1)\pi^{-s/2}\Gamma(s/2) \cdot \zeta(s);$$

where Γ is the gamma function.

The famous Riemann hypothesis asserts that all roots of $\xi(s)$ lie on the line $\Re\ s = \sigma = 1/2$. We also have the functional equation $\xi(s) = \xi(1-s)$ and the Hadamard factorization theorem $\xi(s) = \xi(0) \cdot \prod_\rho (1 - s/\rho) \cdot e^{s/\rho}$, where ρ ranges over the roots of the equation $\xi(\rho) = 0$, and these roots lie in the strip $0 < \sigma < 1$.

The appellation *Riemann ξ-function* is also used in reference to: $\Xi(t) = \xi(1/2 + it)$.

The Riemann hypothesis is equivalent to: “all the zeros of $\Xi(t)$ are real”.

The representation integral of function (1) is given by

(3) $$\zeta(s) = 1/(\Gamma(s)) \cdot \int_0^\infty dt \cdot t^{s-1}/(e^t - 1)$$

where $\Gamma(s) = \int_0^\infty t^{s-1} \cdot e^{-t} dt$.

If we really consider the identity

(4) $$\begin{aligned} n^{-s} &= (1/\Gamma(s)) \cdot \int_0^\infty dt \cdot t^{s-1} \cdot e^{-nt}; \text{ and} \\ \sum_{n=0}^{\infty} e^{-nt} &= (1/(e^t - 1)) \end{aligned}$$

we get relation (3).

This representation (3) is unique only for $s \neq 1$, and shows that $\zeta(s)$ can by analytically continued except for $s = 1$, where it has a single pole with residue 1.

The analytical continuity is realized by transformation

$$\int_0^\infty = \int_0^1 + \int_1^\infty \text{ and } t/(e^t - 1) = \sum_{k=1}^{\infty} B_k \cdot t^k/k!;$$

where B_k are the Bernoulli numbers, and we have

(5) $$\zeta(s) = (1/\Gamma(s)) \cdot \sum_{k=1}^{\infty} (1/(k+s-1)) \cdot B_k/k! + (1/\Gamma(s)) \cdot \int_1^\infty dt \cdot t^{s-1}/(e^t - 1)$$

For $s = 1$ we have the Laurent series

(6) $$\zeta(s) = (1/(1-s)) + \gamma + \gamma_1(s-1) + \gamma_2(s-1)^2 + \dots$$

where $\gamma =$ the Euler-Mascheroni constant.

The deterministic statements can be proved by probabilistic reasoning. For now, it is clear that the probabilistic method is a very powerful tool for proving results in discrete mathematics. There are more examples that illustrate the fact that, probabilistic arguments may be (counter-intuitive) valuables for the probabilistic interpretation of the Riemann function. I state "counter-intuitive" arguments even if in general and historically (was the other way around) the deterministic methods used for the approximation of random phenomena conducted to the development of statistical and probabilistic methods which are applicable today with success to random events.

Only in [2] may be found four examples for the connection between the Riemann function and the probability theory. Thus table 1 may be read:

$$\Sigma;$$
$$S_1 = 2/\pi^2 \cdot \sum_{n=1}^{\infty} \varepsilon_n/n^2;$$
$$S_2 = 2/\pi^2 \cdot \sum_{n=1}^{\infty} (\varepsilon_n + \eta_n)/n^2;$$
$$C_1 = 2/\pi^2 \cdot \sum_{n=1}^{\infty} \varepsilon_n/(n-1/2)^2;$$
$$C_2 = 2/\pi^2 \sum_{n=1}^{\infty} (\varepsilon_n + \eta_n)/(n-1/2)^2;$$
$$E[\Sigma];$$
$$\frac{2^{1-2s}-1}{1-2s} \cdot \frac{(2)^s}{(\pi)^s} 2\epsilon(2s);$$
$$(2/\pi)2\epsilon(2s);$$
$$\Gamma(s+1)2^{s+1}(2/\pi)^{2s+1} \mathrm{L}_\chi(2s+1);$$
$$\frac{2^{2s+1}-1}{s+1} \cdot \frac{(2)^{s+1}}{(\pi)^{s+1}} \cdot \epsilon(2s+2).$$

where ε_n and η_n are random variables with the gamma(1) or standard exponential distribution $P(\varepsilon_n \geq x) = e^{-x}$, $x \geq 0$; and $L_\chi(s) = \sum_{n=1}^{\infty} (-1)^{n-1}/(2n-1)^s$ is the Dirichlet L-function (modulo 4 and $\Re s > 0$).

The **important result**, which we infer, is the following

In [2] it is noticed that the "Li's criterion for Riemann Hypothesis" which consists in the following sentence: The Riemann hypothesis: $\xi(\rho) = 0 \Rightarrow \Re\rho = 1/2$ is equivalent to the sequence of inequalities $\lambda_n > 0$ for $n = 1,\ 2, \ldots$ where

$$\text{(7)} \qquad \lambda_n = 1/(n-1)! \cdot d^n/ds^n (s^{n-1} \cdot \log \xi(s))\big|_{s=1} = \sum_\rho [1 - (1 - 1/\rho)^n]$$

Here Σ_ρ is the limit as $T \to \infty$ of a sum over the zeros ρ of ξ with $|\rho| \leq T$, with repetition of zeros by multiplicity.

By the moment problem of Hamburger H. (see [5]) "The necessary and sufficient condition for the existence of a non decreasing function $f(x)$, $-\infty < x < \infty$ with an infinity of points of growth and such that

$$\text{(8)} \qquad \int_{-\infty}^{\infty} x^n \cdot f(x) dx = s_n,\ n = 1,\ 2,\ \ldots$$

is that the sequence $\{s_n,\ n = 1,\ 2,\ \ldots\}$ is to be positive definite".

By an elementary binomial expansion, from (7), we have

$$\text{(9)} \qquad \lambda_n = n \sum_{i=0}^{n-1} \begin{pmatrix} n-1 \\ i \end{pmatrix} \cdot k_{n-i}/(n-i)!$$

and the $k_n = d^n/ds^n \left[\log \xi(s)\right]_{s=1}$ is the n cumulant of the variable $V = \log(1/Y)$ and $E(Y^s) = 2 \cdot \xi(s)$ (see[2]).

To apply the moment problem of Hamburger we must substitute

(10) $$s_n = \sum_{i=0}^{n-1} \binom{n-1}{i} \cdot s_i \cdot k_{n-i},$$

where $s_0 = 1$, $s_1 = k_1 = d/ds\,[\log\xi(s)]_{s=1}$.

Another consequence of (3) is the functional equation or reflection formula

(11) $$\zeta(s) = 2^s \pi^{s-1} \cdot \sin(\pi s/2) \cdot \Gamma(1-s) \cdot \zeta(1-s)$$

or

$$\Gamma(s/2) \cdot \zeta(s) = \pi^{s-1/2} \cdot \Gamma((1-s)/2) \cdot \zeta(1-s).$$

Due to $s = -m + \varepsilon$ we have $1/\Gamma(-m+\varepsilon) = (-1)^m \cdot m!\varepsilon(1 + O(\varepsilon))$; also we have

$$t/(e^t - 1) = \sum_{k=1}^{\infty} B_k t^k / k!$$

and

$$\begin{aligned} B_0 &= 1, \\ B_1 &= -1/2, \\ B_2 &= 1/6, \\ B_3 &= 0, \\ B_4 &= -1/30, \\ B_5 &= 0, \ \ldots \end{aligned}$$

We have

$$\begin{aligned} \lim \zeta(-m+\varepsilon) &= (-1)^m B_{m+1}/(m+1), \\ \zeta(0) &= -1/2; \\ \zeta(-2n) &= 0; \\ \zeta(1-2n) &= -B_{2n}/2n \ n = 1,\ 2,\ 3,\ \ldots \end{aligned}$$

and because

$$f(t) = t/(1-e^{-t}) = t + t/(e^t - 1)$$

we have $f(t) = t + f(-t)$ implying the result: $f^{(k)}(0) = B_k$ for $k \neq 1$ $f''(0) = 1 + B_1$; $f^{(k)}(0) = B_k = 0$ where $k = 2m+1$ and $m = 1,\ 2,\ 3,\ \ldots$ Also we have: $\zeta(2n) = (-1)^{n+1} \cdot (2\pi)^{2n} \cdot B_{2n}/2(2n)!$ for n=1,2,3,... Due to $\zeta(\bar{s}) = \bar{\zeta}(s)$; in Riemann Hypothesis in $s = 1/2 + i\gamma$ it is sufficiently to have $\gamma > 0$.

By Riemann it is known (see [7], [8]) that if $\gamma \leq T$ the number of zeros are approximated by $T(\log T)/2\pi$. If we assume the sequence $0 \leq \gamma_1 \leq \gamma_2 \leq \gamma_3 \leq \ldots$ then the normal average is $\bar{\gamma}_j = \gamma_j \cdot \log\gamma_j/2\pi$ and the standard distance is $X_j = \bar{\gamma}_{j+1} - \bar{\gamma}_j$ even if there is no random variable for j$\to\infty$ but it is possible to approximate it by the Gaudin distribution (see: the A.Odlyzko work for $j = 2.10^{20}$)

After, these definitions and considerations, we introduce three (see [3], [4]) new generalized forms for the function $\zeta_t(s)$ and consequently for the Riemann function $\xi(s)$:

(12) $$\zeta_t(s) = \sum_{m=1}^{\infty} m^{-s} \cdot f(mt)$$

where m =integer, and

(13) $$F(s,\ t) = \sum_{m=1}^{\infty} \lambda_m^{-s} \cdot f(t \cdot \lambda_m)$$

and also

(14) $$\zeta_A(s) = \sum_{m=1}^{\infty} \lambda_m^{-s};$$

where $\{\lambda_m\}$ are the eigenvalues of an operator A, $s \in \mathbb{C}$, $t \in \mathbb{R}$, $t > 0$.

Likewise we have

$$\zeta_0(s) = \sum_{m-1}^{\infty} m^{-s} \cdot f(0) = f(0) \cdot \zeta(s) \text{ and } F(s,\ 0) = f(0) \cdot \zeta_A(s).$$

The series $F(s,\ t)$ generalizes the heat-kernel expansion which appears as particular case for $s = 0$ and $f(\lambda_m \cdot t) = e^{-t\lambda_m}$, providing

$$F(0,\ t) = \sum_{m=1}^{\infty} e^{-t\lambda_m}.$$

If the operator A has m discrete eigenvalues, then, by definition,

$$\zeta_A(s) = \mathrm{Tr}(A^{-s}) = \sum_{n=1}^{m} (\lambda_n)^{-s}; \tag{15}$$

obviously that even if $m \to \infty$ there is a generalization of $\zeta(s)$ due to the eigenvalues that are not always integers.

Example (see [6]). If we do not know the eigen values of the operator A from the heat equation we can obtain some information about the generalized zeta function by studying the equation

$$d/dt(F(x,\ y,\ t)) + AF(x,\ y,\ t) = 0; \tag{16}$$

here x and y represent points in the four dimensional spacetime manifold, t is a fifth dimension. With initial conditions $F(x,\ y,\ 0) = \delta(x,\ y)$ the heat kernel F represents the diffusion over the spacetime manifold in parameter time t of a unit quantity of heat (or ink) placed at the point y at $t = 0$. One can express F in terms of the eigenvalues and eigenfunctions of operator A, namely

$$F(x,\ y,\ t) = \sum_n \exp(-\lambda_n t)\Phi_n(x)\Phi_n(y); \tag{17}$$

for $x = y$, one obtains

$$Y(t) = \int \mathrm{Tr}F(x,\ x,\ t)(g_0)^{1/2} \cdot d^4x = \sum_n \exp(-\lambda_n t); \tag{18}$$

the g_0 and Φ_0 are the background fields. The generalized zeta function is related to $Y(t)$ by a Mellin transform:

$$\zeta_A(s) = \sum_n{}' \lambda_n^{-s} = 1/\Gamma(s) \cdots \int_0^{\infty} t^{s-1} \cdot Y(t) \cdot dt \tag{19}$$

A number of authors have obtained asymptotic expansions for F and Y, valid as $t \to 0^+$. If the operator A is a second order Laplacian type operator on a four dimensional compact manifold, then $Y(t) \sim \sum_n B_n \cdot t^{n-2}$ where the coefficients B_n are integrals over the manifold of scalar polynomials in the metric, the curvature tensor and its covariant derivatives, which are of order 2n in the derivatives of the metric. About the (16), (17), (18), and (19) see [2].

As far as the Zeta-function is concerned, regularization and renormalization procedures are essential issues in contemporary physics (see [4]).Assuming the corresponding Hamiltonian operator, H, that has a spectral decomposition of the form (think, as simplest case, of a quantum harmonic oscillator) $\{\lambda_I,\ \varphi_i\}$, $i \in I$, with I a set of indices(which can be discrete, continuous, mixed, multiple etc.), then the quantum vacuum energy is obtained as follows

$$\sum_{i \in I} (\varphi_i,\ H\varphi_i) = \mathrm{Tr}H = \sum_{i \in I} \lambda_i = \sum_{i \in I} \lambda_i^{-s}\Big|_{s=-1} = \zeta_H(-1)$$

where ς_H is the zeta function corresponding to the operator H. The formal sum over the eigenvalues is usually ill-definited, and the last step involves analytic continuation, inherent to the definition of the zeta-function itself.

For a probability interpretation we consider the probability models concerning basic properties of ζ and ξ following the representation of ξ as the Mellin transform, involving the density of a probability distribution on the real line and connection with the theory of Brownian motion.

References

[1] Alexander, K.S., Baclwaski, K., Rota, G.C., *A stochastic interpretation of the Riemann zeta function*, Proc. Natl. Acad. Sci. USA, **90** (1993), 697-699.

[2] Bianne, P., Pitman, J., Yor, M., *Probability laws related to the Jacobi teta and Riemann zeta functions,and brownian excursions*, Bulletin of the AMS, **38**, 4(2001).

[3] Elizalde, E., Odintsov, S., Romeo, A., Bytsenko, A. and Zerbini, S., *Zeta Regularization Techniques with Applications*, World Scientific, Singapore, 1994.

[4] Encyclopedia of Mathematics, supp.Vol.III, Kluwer Academic Publisher, Dordrecht, 2001, 333-456

[5] Hamburger, H., *Übereine Erweiterung des Stieltjessen Momentenprobems*, Math. Ann. **81**, (1920), **82**, (1921).

[6] Hawking, S.W., *Zeta function regularization of path integrals in curved spacetime*, Commun. Math. Phys. **55** (1977), 133-148.

[7] Katz, N.M., Sarnak, P., *Zeros of zeta functions and symmetry*, Bulletin of the AMS, **36**, 1(1999).

[8] Tracy, C.A., Widom, H., *Level-spacing distributions and the airy kernel*, Commun. Math. Phys. **159** (1994), 151-174.

Some mathematical models in cancer theory

Mariana Trifan

Department of Applied Mathematics,
University of Pitesti, Romania
E-mail: mariana_trifan@yahoo.com

Abstract. Cancer is one of the principal research field because it is one of the greatest killers in the world. The formulation of the cancer evolution and the subsequent treatment focuses on the heterogeneous nature of the cancer and the drug resistance effects. Mathematical modelling of biomedical phenomena can be extremely helpful in analyzing factors that may contribute to the complexity intrinsic in insufficiently understood developmental processes and diseases. Some mathematical models of cancer dynamics and treatment, represented by partial differential equations (PDE) and ordinary differential equations (ODE), are presented.

Keywords: cancer, tumor, proliferation, model

1. Introduction

Cancer (= neoplasm = malignance) is the result of aberrate growth of a type cell (may be any one of the body), a modified cell respecting to its initial state, which obtains different properties [1]. Normally, the body cells growth (as number and/or size) is controlled. Naturally, the cells have a well established location in body that they do not leave. Unlike a normal cell, the tumor cell may detach itself from the tumor (original tumor), it may go inside the blood-stream or lymphatic stream (in addition to blood circulation there exists the lymphatic circulation, through ganglions and lymphatic vessels) and it fastens on another of the region body. It is in this way that metastasis (second tumors) appear [2]. Moreover, cancer cells develop faster than normal cells, they secret substances that accelerate their development and possess ,,factories" for ,,building aids" more active than the normal cells.

Uncontrolled evolution of cells leads to tumor formation. The *tumor* represents a pathological excrescence. Tumors can be *benign* and *malignant*. The distinction between benign and malignant tumors is based on many criteria: degree of differentiation, rate of growth, local invasion and metastatic ability [3].

Huge tumor diversion does not permit one unique classification. Some basic criteria of classification are: histological membership (epithelial, conjunctive, muscular); morphological characteristics; macro-organic location; spread characteristic; malignance degree; metastasis feature.

However, last few years it has been adopted an unique international classification after TNM system: T(1-2-3-4)-tumor, N(0-1-2-3)-lymphatic ganglions, M(0-1)-metastasis.

2. Mathematical models

. Let us present a few mathematical models on cancer.

Kinetic model. Cancer growth is looking at as an interaction between various independent compartments of the body. The model considers the cell development and the metastasis resulting in the formation of new tumor masses.

In metastasis stage the cancer cells are migrating to various regions through blood-stream and, by means of it, they may attach to and spread inside a tissue. Nevertheless, the tumor cells missing the blood-stream may be eliminated out of body by the immune system or by any action based on drug administration, or death by apoptosis (programmed death of cells). Thus, only a small cells fraction that escape from a primary tumor survive and forms a new tumor. It is taken into account the cells death, unsuccessful cell attachment and plasma clearance too.

Mathematically the above reasoning are expussed in the following form [4]

$$\begin{cases} \dfrac{dT_{tum}}{dt} = \alpha r T_{tum}\left(1 - \dfrac{T_{tum}}{T_0}\right) - \beta k_{f1} T_{tum} + k_{r1} T_{plas}, \\ \dfrac{dT_{plas}}{dt} = \beta k_{f1} T_{tum} - k_{r1} T_{plas} + n(-k_{f2} T_{plas} + \beta k_{r2} T_{new}) - \delta c T_{plas}, \\ \dfrac{dT_{new}}{dt} = \alpha r T_{new}\left(1 - \dfrac{T_{new}}{T_0}\right) + k_{f2} T_{plas} - \beta k_{r2} T_{new}, \end{cases}$$

where T_0 is the *equilibrium cell concentration in the tumor*;
T_{tum} is the *cell concentration of the original tumor*;
T_{plas} is the *cancer cell concentration in the plasma*;
T_{new} is the *cell concentration of new and developing tumor*;
r is the *specific growth rate*;
n is the *number of new tumors* being developed simultaneously;
$k_{f1},\ k_{f2},\ k_{r1},\ k_{r2}$ are the *rate constants*;
α, β, δ are the *relative drug efficiency factors.*

In [4] an example of cancer growth and development for some values of parameters and different therapy (e.g. EGFR therapy, adoptive therapy, antibody therapy) is presented.

Temporal model. A brain tumor is a dynamical system in which cancer cells grow and spread overwhelming good brain cells. Their location, how quickly they grow and spread will affect the cancer spreads [5].

Cancer brain cells grow fast. The tumor such as GBM (glioblastoma multiforme) has many billions of cells and it is necessary more than one treatment. In GBM case the death is caused by the tumor burden and the expansion into the normal tissue.

The temporal model does not take into account the second aspects of disease [6]. Let n_t be the number of tumor cells at time t. Then the model represents the time derivative, denoted by $\dot{n}_t$, of tumor burden by formula

$$\dot{n}_t = p n_t - k_t n_t,$$

where p is the *proliferation rate*; k_t is the *killing rate* at time t.

In absence of the treatment the tumor increases exponentially at rate p. This is why the treatment(e.g. radiotherapy and chemotherapy) corresponds to **log-kill hypothesis**: a certain percentage of cancer cells (not a certain absolute number) will be killed with each course of treatment. In other words, the I log cell kill rate will kill 90% of tumor cells, the II log cell kill rate will kill 99% of tumor cells, the III log cell kill rate will kill 99.9% of tumor cells etc [7].

Tumor cure probability (TCP) is computed using the Poisson hypothesis

$$TCP = exp\ (-f n_t),$$

where T is the *treatment duration*, f is the *clonogenic tumor cells fraction* (cells able of repopulating the tumor). Thus this model contains four parameters: the proliferation rate, p; the killing rate, k (for various treatments); clonogenic fraction, f; the initial number of tumor cells, n_0.

Quantitative model. This is an other model to study GBM growth and it relies on proliferation and diffusion.

Net proliferation rate and migration rate of cells are the basic parameters in quantitative model. This model corresponds to the following law [8]: the rate of change of the tumor cell population density is equal to the diffusion of the tumor cells in white and grey matter plus the net proliferation of the tumor cells. Mathematically it has the form

$$\frac{\partial c}{\partial t} = \nabla(D(x)\nabla c) + \rho c,$$

where
$c(x, t)$ is the *tumor cells concentration* at location x and time t;

$D(x)$, a function of x position in brain, is the *diffusion coefficient* with $D(x) = D_w, D_g$ constants for x in white and grey matter, respectively. Biologically is observed that $D_w > D_g$;

ρ represents the *net proliferation rate* of GBM;

∇ is the *differentiation (nabla) operator*.

A consequence of modelling cellular diffusion is the impossibility to establish boundary between malignant and normal tissues.

Deterministic model. It is used for the immunological and therapeutic control of human immunodeficiency virus (HIV). Being infected with HIV the immune system obtained an anti-HIV response. This response includes HIV-specific cytotoxic T lymphocytes (CTLs) and antibodies [9].

The (4-dimensional) deterministic model is obtained from Nowak-May model and it reads

$$\begin{aligned}\dot{x} &= s - \beta(1-\tau)xv - \mu_1 x,\\ \dot{y} &= \beta(1-\tau)xv - \mu_2 y - pyz,\\ \dot{v} &= ky - \mu_3 v,\\ \dot{z} &= cyz - \mu_4 z,\end{aligned}$$

where

x are CD4+T *noninfected cells*;

y are CD4+T *infected cells*;

v is the *virus*;

z are CTLs;

s is the *source* of CD4+T cells;

β is the *infection rate*;

τ represents the *effectiveness of anti-body therapy*;

p is the *clearance rate* of cells infected with CTLs;

k is the *virions* HIV *number* per infected cell;

c is the CTLs *production rate*;

μ_1, μ_2, μ_4 are *natural death parameters* of the x, y, z populations, respectively;

μ_3 is *clearance rate parameter of the virus.*

Lymphocytes-tumor interaction model. This model is used to study the temporal behavior at periodical administration of immunotherapy treatment.

Reformulating the „predator-prey” model, we obtain the lymphocytes-tumor interaction model, comprising new terms of tumor aggressiveness, the lymphocytes diffusion, the effect of cytokine on the tumor. It takes into account the lymphocytes death thanks to increase of malignant cells population, flux of lymphocytes towards the place of interaction and the effect of cytokine administrated doses [10].

Let X and Y be the number of malignant cells and lymphocytes, respectively. The malignant cells rate and lymphocytes growth rate are described by the following system of ODE

$$\begin{aligned}\frac{dX}{dt} &= aX - bXY,\\ \frac{dY}{dt} &= dXY - fY - kX + u,\end{aligned}$$

where

a is the coefficient of proportionality between growth rate and X;

b is the coefficient of proportionality between decrease rate and frequency of interaction with lymphocytes;

f is the coefficient of proportionality between natural death of malignant cells and tumor area of interaction with lymphocytes;

k is the coefficient of proportionality between growth of malignant cells and tumor area of interaction with lymphocytes;

u is the diffusion process of lymphocytes that takes place in tumor neighborhood at a constant lymphocytes flux.

This model describes possible stages of tumor. A „curious" phenomenon, observed in experience, consists in tumor evolution as a result of interaction between immune system and immunotherapy. This evolution can be justified using certain values of parameters.

Heterogeneous tumor model. This model is applied to study of breast cancer.

Tumor progression appear as a result of changes caused by expansion of tumor cells population. It is often described as a lot of lesions that can be recognized morphologically. Because biologically are determined two pathways (linear and nonlinear) [11], mathematically these pathways are interpreted as compartmental models with transition rate.

The linear model contains seven parameters. They govern the transition rates in and out of six stages of the tumor (three of ductal carcinoma in situ DCIS and three of invasive ductal carcinoma IDC). ODE of cells concentrations with atypical hyperplasia (c_0) and six different stages ($c_1, c_2, c_3, c_4, c_5, c_6$) of the tumor, as a function of time t are the following

$$\frac{dc_0}{dt} = -k_0 c_0, \quad \frac{dc_1}{dt} = k_0 c_0 - k_1 c_1, \quad \frac{dc_2}{dt} = k_1 c_1 - k_2 c_2,$$
$$\frac{dc_3}{dt} = k_2 c_2 - k_3 c_3, \quad \frac{dc_4}{dt} = k_3 c_3 - k_4 c_4, \quad \frac{dc_5}{dt} = k_4 c_4 - k_5 c_5,$$
$$\frac{dc_6}{dt} = k_5 c_5 - k_6 c_6.$$

The first three constant rates are interpreted as the result of mutations accumulation affecting cell proliferation and morphological structure. The next rates are interpreted as a result of mutations accumulation affecting cell invasion.

The nonlinear model contains three parameters. They correspond to three rate constants determining transition between stages: k_0 corresponds to transition of stages for DCIS, k_1 – from DCIS to IDC, k_2 – to transition of stages for IDC. The ODE of this model read

$$\frac{dc_0}{dt} = -k_0 c_0, \quad \frac{dc_1}{dt} = k_0 c_0 - k_0 c_1 - k_1 c_1, \quad \frac{dc_2}{dt} = k_0 c_1 - k_0 c_2 - k_1 c_2,$$
$$\frac{dc_3}{dt} = k_0 c_2 - k_0 c_3 - k_1 c_3, \quad \frac{dc_4}{dt} = k_1 c_1 - k_2 c_4, \quad \frac{dc_5}{dt} = k_1 c_2 + k_2 c_4 - k_2 c_5,$$
$$\frac{dc_6}{dt} = k_2 c_5 + k_1 c_3 - k_2 c_6.$$

For the nonlinear model biologically the growth rates k_0 and k_2 can be interpreted as the result of mutations accumulation affecting cell proliferation and morphological structure, while k_1 rate – as a result of mutations accumulation affecting cell invasion. In this model they are no longer constants.

References

[1] *Enciclopedie medicala populara*, Ed. - Redactia principala a Enciclopediei Sovietice Moldovenesti, Chisinau, 1984.

[2] http://medcab.go.ro.

[3] Peterson, B. E., *Oncology*, Medicine, Moscow, 1980. (Russian).

[4] Siddharta, J., *Kinetic model for designing cancer therapy*, Cancer Cell International, **2**(13) (2002).

[5] http://virtualtrials.com.

[6] Skipper, H. et al., *Experimental evaluation of potential anticancer agents. XIII. On the criteria and kinetics associated with „curability" of experimental leukemia*, Cancer Chemother. Rep., **34** (1964), 1 - 111.

[7] Pfeiffer, C., Pharm., D., BCPS, BCOP, *Carcinogenesis/ Tumor resistance and principles of chemotherapy*, Fall, 2002.

[8] Swanson, K.R., Alvord Jr., E. C., Murray, J.D., *A quantitative model for differential motility of gliomas in grey and white matter*, Cell Prolif., **33** (2000), 317-329.

[9] Gumel, A. B., Moghadas, S. M., *HIV control in vivo: Dynamical analysis*, Elsevier Science, Amsterdam, 2003.

[10] Sotolongo-Costa, O., Morales Molina, L., Rodriguez Perez, D., *Behavior of tumors under nonstationary therapy*, Physica D, **178** (2003), 242-253.

[11] Subramanian, B., Axelrod, D. E., *Progression of heterogeneous breast tumors*, J. Theor. Biol., **210** (2001), 107-119.

On the variation of the stationary states for an excitable model

Asupra variatiei starilor stationare ale unui model de excitatie

Adela Ionescu
University of Craiova, Univ. College Drobeta Tr. Severin
22 Decembrie 1989 Str., G5-III-3, 1100 Craiova, 0251125136,
E-mail: adaion@hotmail.com

Abstract. This paper deals with an activator-inhibitor model with different sources, i.e. a Gierer-Meinhardt dynamical system, in its normalized form. Some properties related to the variation of the stationary states of this excitable model, with respect to the parameters variation are investigated. There were chosen five parameters groups, used also in experimental studies, related to another group of eight parameters. The graphical comparative analysis consists in five plots of 40 points each, and is realized with the MAPLE program. The main conclusion is that there exist specific parameter values (larger than the unity) for which the evolution of stationary states cannot be controlled.

1. Introducere

Modelarea matematică a mediilor excitabile a găsit în cinetica chimică o mare varietate de modele moleculare specifice, toate stând la baza mecanismelor morfogenezei [7]. Dintre mecanismele moleculare specifice, cele de tip activator-inhibitor sunt cele mai mult legate de procesele biochimice cunoscute şi, pentru valori limitative ale parametrilor lor, corespund condiţiilor de bază ale ecuaţiilor fundamentale care descriu generarea pattern-urilor [2]. Pentru a avea un volum de calcul rezonabil, prezentăm modelul de tip activator-inhibitor cu surse diferite. Aşa cum au arătat Gierer şi Meinhardt [1,2], acest model are la bază fenomenul inhibiţiei laterale. El a fost studiat atât din punct de vedere analitic, cât şi numeric de către M.I.Granero-Porati, A.Porati, D.Zanacca [3,4]. Întrucât în această lucrare ne interesează numai variaţia temporală, vom neglija derivatele spaţiale (presupunând constanele de difuzie D_a, D_h suficient de mici). Vom considera, deci, sistemul

$$(1)\qquad \begin{cases} \dot{a} = \frac{c\rho a^2}{h} - \mu a + \rho\rho_0, \\ \dot{h} = -\gamma h + c_1 \rho a^2, \end{cases}$$

unde a reprezintă concentraţia activatorului, h concentraţia inhibitorului, $\rho\rho_0$ este concentraţia sursă pentru activator, iar ρ cea pentru inhibitor; μ şi γ sunt coeficienţii de degradare ai lui a şi respectiv h, iar c şi c_1 sunt legaţi de producţiile lui a şi respectiv h.

Prin adimensionalizare, s-a găsit [4] următoarea formă normalizată a sistemului (1)

$$(2)\qquad \begin{cases} \frac{dA}{d\tau} = -A + \frac{\rho A^2}{H} + \rho\rho_0', \\ \frac{dH}{d\tau} = F(\rho A^2 - H), \end{cases}$$

în care normalizarea este

$$(3)\qquad \begin{cases} \rho_0' = \frac{\rho_0}{\gamma} \cdot \frac{c_1}{c},\ F = \frac{\gamma}{\mu},\ t = \frac{\tau}{\mu} \\ A = a \cdot \frac{\mu}{\gamma} \cdot \frac{c_1}{c},\ H = h \cdot \frac{\mu^2}{\gamma} \cdot \frac{c_1}{c^2}. \end{cases}$$

În urma studiului pantei dH/dA a curbei soluţie în jurul unicului punct fix (A_0, H_0), s-a stabilit că în condiţiile

$$(4)\qquad \rho\rho_0 < \gamma \cdot \frac{c}{c_1},\quad \rho\rho_0 < \gamma \cdot \frac{c}{c_1} \cdot \frac{\mu - \gamma}{\mu + \gamma},$$

i.e. $\mu > \gamma$, există un ciclu limită. Astfel, inhibitorul nu se echilibrează rapid şi oscilaţiile în sistem sunt rapid obţinute.

În [5] s-a regăsit acest rezultat, folosindu-se teoria varietăţii centrale.

2. Variaţia stărilor staţionare ale modelelor excitabile

Vom considera doar sisteme activator-inhibitor (1) cu surse diferite, întrucât acestea permit o abordare cu un volum mai mic de calcul. Toţi parametrii sunt pozitivi, iar funcţiile de stare a şi h iau valori reale.

Forma (1) este adecvată unei analize temporale, ea fiind utilizată şi de Granero şi Porati [4] pentru organizarea temporală într-un câmp morfogenetic.

S-a arătat că, în cazul acestui model, pot exista oscilaţii autoîntreţinute când un parametru de ordine, legat de constantele de depreciere ale morfogenezei, trece printr-o valoare critică. Rezultatele analitice sunt în acord cu rezultatele numerice ale lui Gierer şi Meinhardt.

Să considerăm forma normalizată (2) cu normalizarea (3). Datorită normalizării (3), numărul parametrilor modelului (1) al lui Gierer şi Meinhardt a scăzut de la şase la trei. Acest fapt facilitează mult calculele analitice.

Unica stare staţionară a lui (2) este

$$A_0, H_0 = (1 + \rho\rho_0^{'}, \rho(1 + \rho\rho_0^{'})^2). \tag{5}$$

În [5] s-a analizat existenţa unei varietăţi centrale pentru sistemul (2) liniarizat în jurul acestei stări ca şi fluxul pe varietatea centrală.

În [6] se face o analiză grafică comparativă a variaţiei stărilor de echilibru de pe varietatea centrală şi a variaţiei stării de echilibru (A_0,H_0) a sistemului (2) în funcţie de parametri, pentru a observa diferenţa de comportament a traiectoriilor în cazul sistemului redus pe varietatea centrală şi al celui iniţial. Aici considerăm cinci seturi de valori pentru ρ_0, c, c_1, μ şi γ, folosite şi în studiile experimentale din [2]. Parametrul ρ_0' se află din relaţia $(3)_1$ iar pentru ρ vom considera un şir de opt valori apropiate:

$$\rho \in \{1/2, 1/3, 1/4, 1/5, 1/6, 1/7, 1/8, 1\}.$$

Astfel, dacă pentru fiecare din următoarele cinci seturi de valori ale parametrilor ce compun pe $\rho_0^{'}$:

$$a)\begin{cases} \rho_0 = 0,01 \\ c = 5 \cdot 10^{-5} \\ \mu = \gamma = 0,0025 \\ c_1 = 1,5 \cdot 10^{-4} \end{cases}, b)\begin{cases} \rho_0 = 6 \cdot 10^{-4} \\ c = 0,05 \\ \mu = \gamma = 0,001 \\ c_1 = 0,025 \end{cases}, c)\begin{cases} \rho_0 = 6 \cdot 10^{-4} \\ c = 0,05 \\ \gamma = 0,0045 \\ c_1 = 0,025 \end{cases},$$

$$d)\begin{cases} \rho_0 = 6 \cdot 10^{-4} \\ c = 0,05 \\ \gamma = 0,01 \\ c_1 = 0,025 \end{cases}, e)\begin{cases} \rho_0 = 7,5 \cdot 10^{-4} \\ c = 0,05 \\ c_1 = 0,025 \\ \gamma = 0,0045 \end{cases}$$

dăm lui ρ o variaţie în şirul de valori precizate, obţinem patruzeci de puncte dispuse în cinci grafice. Acestea se regăsesc în figurile 1-5.

Poziţia echilibrului (A_0, H_0) în spaţiul fazelor pentru cele cinci seturi de valori ale parametrilor ρ_0, ρ, γ, μ, c şi c_1

3. Concluzii

Graficele de mai sus au fost realizate cu ajutorul programului matematic de calcul MAPLE (Maple V Release IV), cu ajutorul procedurii speciale de calcul *pointplot2D* adaptată pentru perechile (A_0,H_0) în cele cinci cazuri menţionate în Secţiunea 2. În primul rând se observă că toate graficele (dar mai ales ultimele trei) corespund unei variaţii neliniare a coordonatelor lui A_0 şi H_0 ca funcţii de ρ. Apoi, în toate cele cinci cazuri, se observă că odată cu creşterea lui ρ - şi anume începând de la ρ=1- variaţia stării de echilibru înregistrează o evoluţie bruscă, încât se poate conjectura că pentru valori ale lui ρ mai mari decât unitatea evoluţia devine greu de controlat, sistemul putând să se comporte ca un sistem

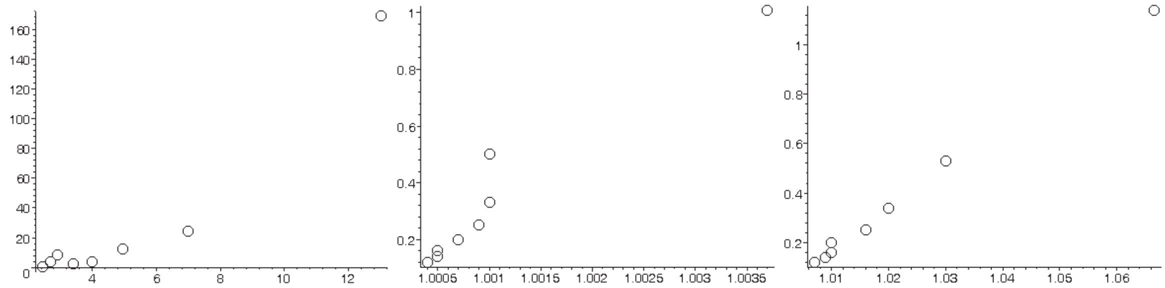

Figure 1. a) b) c)

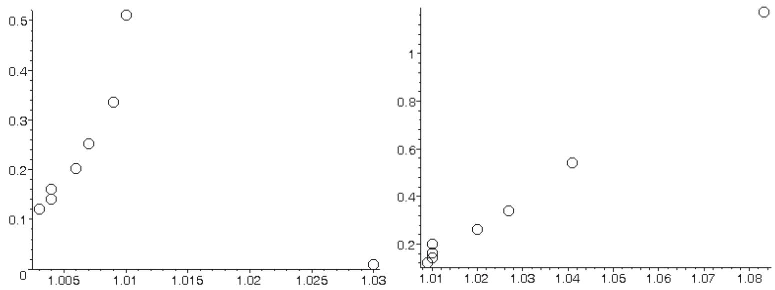

Figure 2. c) d)

"departe de echilibru". Spre deosebire de cazul sistemului redus care evidenţiază o variaţie liniară [6], situaţia analizată aici se datorează numărului mare de parametri care induc neliniarităţi puternice în model.

References

[1] Gierer, A., H. Meinhardt, *A theory of biological pattern formation*. Kybernetik **12** (1970), 30-39.

[2] Gierer, A., H. Meinhardt. *Biological pattern formation involving lateral inhibition*, Lect. on Math. in Life Sciences,**7**, Springer, Berlin, 1974.

[3] Granero-Porati, M.I., A.Porati, D. Zanacca *A bifurcation analysis of pattern formation in a diffusion governed morphogenetic field*, J. Math. Biol. **4** (1977), 21-27.

[4] Granero-Porati, M.I., A.Porati, *Temporal organization in a morphogenetic field*. J. Math. Biol. **20** (1984), 133-137.

[5] Ionescu ,A., A. Georgescu, *Existence of a center manifold for a biological model*, Proceedings of the Conference on Applied and Industrial Mathematics, 1996, Pitesti.

[6] Ionescu ,A., *Stabilitatea structurală a oscilatorilor biologici. Contribuţii de interes analitic*, Teză de doctorat, Univ. "Politehnică" Bucureşti, 2002.

[7] Murray, J.D., *Mathematical biology*, Biomathematics **19**, Springer, Berlin, 1989.

Determination of an exremal domain for the functions of class S

Determinarea unui domeniu extremal pentru functiile din clasa S

Iovanov Miodrag
Universitatea ,,C.Brâncuşi" Tg-Jiu

Abstract. Let S be the class of all holomorphic and univalent functions on the unit discus $|z| < 1$. In the present paper, given $r > 0$ we compute $\max \mathrm{Re} f(z)$ for $\mathrm{Re} z f'(z) = 0$, $|z| = r$. We use the Schiffer-Goluzin variational method. Inside $\Omega_e = \{z : |z| > z_e\}$ any straight line paralel to the x axis crosses $f(|z| = r)$ in at most one point.

1. Fie S clasa funcţiilor $f(z) = z + a_2 z^2 + \dots, f(0) = 0, f'(0) = 1$ olomorfe şi univalente în discul unitate $|z| < 1$.

Pentru prima dată Petru T. Mocanu [2] a pus problema determinării lui z_e cu Re $z_e = \max_{f \in S} \mathrm{Re} f(z)$ când $\mathrm{Re} z f'(z) = 0$, $|z| = r$, $r > 0$ dat.

Geometric aceasta se exprimă astfel:

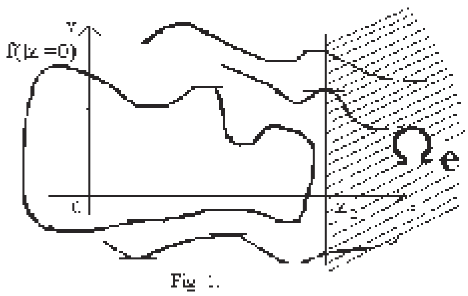

Figure 1

În regiunea haşurată Ω_e) orice pararelă (Re $(z) >$ Re (z_e)) la Ox, intersectează $f(|z| = r)$, într-un singur punct. Deoarece clasa S este compactă, există o astfel de regiune. În această lucrare vom rezolva această problemă folosind metoda variaţională a lui Schiffer-Goluzin [1].

2. Fie $|z| = r$ şi fie $f \in S$ cu Rez f'(z)=0, funcţia extremală pentru care este atins $\max \mathrm{Re} f(z)$, $f \in S$. Să cosiderăm o variaţie f^*(z) a funcţiei $f(z)$ dată de formula lui Schiffer-Goluzin [1],

(1) $\quad f^*(z) = f(z) + \lambda V(z; \zeta; \psi) + O(\lambda^2), |\, \zeta| < 1,\ \lambda > 0$

ψ real, unde

$$\begin{aligned} V(z;\zeta;\psi) &= e^{i\psi} \frac{f^2(z)}{f(z) - f(\zeta)} - e^{i\psi} f(z) \left[\frac{f(\zeta)}{\zeta f'(\zeta)} \right] - e^{i\psi} \cdot \frac{z f'(z)}{z - \zeta} \cdot \zeta \cdot \left[\frac{f(\zeta)}{\zeta f'(\zeta)} \right]^2 \\ &\quad + e^{-i\psi} \cdot \frac{z^2 f'(z)}{1 - \bar{\zeta} z} \cdot \bar{\zeta} \overline{\left[\frac{f(\zeta)}{\zeta f'(\zeta)} \right]}. \end{aligned} \tag{2}$$

Se ştie că pentru λ suficient de mic, funcţia $f^*(z)$ aparţine clasei S. Să considerăm o variaţie z^* a lui z

$$z^* = z + \lambda h + O(\lambda^2),\ \ h = \left. \frac{\partial z^*}{\partial \lambda} \right|_{\lambda = 0}$$

care satisface condiţiile :

(3) $\quad |z^*| = r$ şi $Re z^* f^{*'}(z^*) = 0$

Observăm că

$$|z^*|^2 = |z|^2 + 2\lambda \mathrm{Re}(\overline{z}h) + O(\lambda^2) = r^2.$$

Deoarece $|z| = r$ din relaţia de mai sus obţinem

$$\mathrm{Re}(\overline{z}h) = 0. \tag{4}$$

Înlocuind pe z cu z^* în expresia lui $f^*(z)$ avem: $z^* f^{*'}(z^*) = A + B\lambda + O(\lambda^2)$ unde $A = hf'(z)$, $B = hf'(z) + zhf''(z) + zV'(z;\zeta;\psi)$. Condiţia $\mathrm{Re} z^* f^{*'}(z^*) = 0$ din relaţia (3) devine

$$\mathrm{Re}\left\{h(f'(z) + zf"(z)) + zV'(z;\zeta;\psi)\right\} = 0 \tag{5}$$

Deoarece $f(z)$ este extremală, avem relatia $\mathrm{Re} f^*(z^*) \leq \mathrm{Re} f(z)$ care este echivalentă cu:

$$\mathrm{Re}\left\{f(z) + \lambda hf'(z) + \cdots + \lambda V(z;\zeta;\psi) + O(\lambda^2)\right\} \leq \mathrm{Re} f(z)$$

sau cu

$$\mathrm{Re}\left\{hf' + V(z;\zeta;\psi)\right\} \leq 0. \tag{6}$$

Din (5) in care ţinem seama de (4) (i.e. $\overline{h} = -\frac{\overline{z}}{z}h$) şi (6) obţinem

$$h = \frac{z\overline{z} \cdot V^{'}(z;\zeta;\psi) + z^2 \cdot \overline{V^{'}(z;\zeta;\psi)}}{-zf'(z) - z^2 f'' + \overline{z \cdot f'(z)} + \overline{z^2} \cdot \overline{f''(z)}}. \tag{7}$$

In continuare folosim notaţiile

$$f = f(z), w = f(\zeta), l = f'(z), m = f^{''}(z), V = (z;\zeta;\psi), V^{'} = V_z^{'}(z;\zeta;\psi),$$

cu care relaţiile (6) şi (7) devin

$$\mathrm{Re}\left\{pzV' + V\right\} \tag{8}$$

unde $p = \frac{zl - \overline{z} \cdot \overline{l}}{-zl - z^2 m + \overline{z} \cdot \overline{l} + \overline{z^2} \cdot \overline{m}}$ (p real).

I. Presupunem că $\mathrm{Im}(zl + z^2 m) \neq 0$. Calculând pe V' din (2) si înlocuind în relaţia (8) expresiile lui V şi V' obţinem relaţia

$$\mathrm{Re}\left[e^{i\psi}(E - GF)\right] \leq 0, \tag{9}$$

unde

$$\begin{aligned}
E &= \frac{f\left[(-f - 2pzl)w + f^2 + pzlf\right]}{(f-w)^2}, \\
F &= \left(\frac{w}{\zeta w'}\right)^2, \\
G &= f + \frac{zl}{z-\zeta}\zeta - \frac{\overline{z}^2 \cdot \overline{l}}{(1-\overline{z}\zeta)^2}\zeta + +pzl + \frac{pz\left[z(z-\zeta)m - \zeta \cdot l\right] \cdot \zeta}{(z-\zeta)^2} \\
&\quad - \frac{pz\left[\overline{z}^2(1-\zeta \cdot \overline{z}) \cdot \overline{m} + \overline{z} \cdot \overline{l} \cdot (2 - \zeta \cdot \overline{z})\right] \cdot \zeta}{(1 - \overline{z} \cdot \zeta)^2}
\end{aligned}$$

Doarece ψ este arbitrar, din relaţia (8) rezultă că funcţia extremală $w = f(\zeta)$ trebuie să satisfacă următoarea ecuaţie diferenţială ordinara

$$\left(\frac{\zeta \cdot w'}{w}\right)^2 \cdot \frac{f\left[(-f - 2pzl)w + f^2 + pzlf\right]}{(f-w)^2} = \frac{\sum\limits_{k=0}^{4} t_k \zeta^k}{(z-\zeta)^2(1 - \overline{z} \cdot \zeta)^2} \tag{10}$$

unde

$$\begin{aligned}
t_0 &= z^2(f+pzl)+f;\\
t_1 &= -2zf(1+r^2)+z^2l-\overline{z}^2\overline{l}-2plz^2(1-r^2)+pz^3m-pr^2(\overline{mz}+2\overline{l});\\
t_2 &= f(r^4+4r^2+1)-zl(2r^2+1)-\overline{z}\cdot\overline{l}(2r^2+r^4)+\\
&\quad +pzl(r^4+4r^2+1)-pz(2r^2\cdot zm+mz+l)+pz\left[2r^2(\overline{m}\cdot\overline{z}+2\cdot\overline{l})+r^4(\overline{m}\cdot\overline{z}+\overline{l})\right];\\
t_3 &= -2f\overline{z}(1-2\overline{r})+r^2zl(\overline{z}+2)-\overline{z}^2\overline{l}(1+2r^2)+\\
&\quad +r^2(-2r^2+mr^2z+2mz-\overline{mz}-2\overline{l}-2r^2\overline{zm}-2r^2\overline{l});\\
t_4 &= f\overline{z}^2+p\left[\overline{m}(z^4-\overline{z}^4)+\overline{z}^2(lz-\overline{l}\cdot\overline{z})\right].
\end{aligned}$$

Funcţia extremală $w=f(\zeta)$ transformă discul unitate într-un domeniu fără puncte exterioare. Pentru a justifica acest lucru este suficient să presupunem că acest domeniu are un punct exterior w_0 şi să considerăm funcţia de variaţie:

$$f^*(z)=f(z)+\lambda e^{i\psi}\frac{f^2(z)}{f(z)-w_0},\quad \lambda>0,\quad \psi \text{ real}, f^{''}\in S$$

3. Se ştie că funcţia extremală $w=f(\zeta)$ transformă discul unitate $|\zeta|<1$, în întreg planul, tăiat de-a lungul unui număr finit de arce analitice. Fie $q=e^{i\theta}$, punctul de pe cercul $|\zeta|=1$ care corespunde extremităţii unei astfel de tăieturi în care $w'(q)=0$ şi fie $\zeta=q$ rădăcină dublă pentru polinomul $\sum\limits_{k=0}^{4} t_k\zeta^k$. Atunci putem scrie :

$$\sum_{k=0}^{4} t_k\zeta^k=(1-\overline{q}\cdot\zeta)^2\left(a_0+a_1\zeta+a_2\zeta^2\right).$$

Din expresiile găsite ale coeficienţilor t_k , $k=\overline{0,4}$ rezultă că putem lua $a_0=t_0$, $a_1=-2kq$, $a_2=q^2\cdot t_4$, astfel ca (10) se mai poate scrie astfel

$$\left(\frac{\zeta w'}{w}\right)^2\cdot\frac{f\left[(-f-2pzl)w+f^2+pzlf\right]}{(f-w)^2}=\frac{(1-overlineq\zeta)^2(t_0-2kq\zeta+q^2t_4\zeta^2)}{(z-\zeta)^2(1-\overline{z}\cdot\zeta)^2}\tag{11}$$

4. Extragând radicalul din ecuaţia (11) si integrând obţinem

$$\int_0^w\frac{\sqrt{f\left[(-f-2pzl)\,w+f^2+pzlf\right]}}{w(f-w)}dw=\int_0^\zeta\frac{(1-\overline{q}\zeta)\sqrt{t_0-2kq\zeta+q^2t_4\zeta^2}}{\zeta(z-\zeta)(1-\overline{z}\zeta)}d\zeta.\tag{12}$$

Fie I_1 integrala din stânga relatiei (12). Observăm că $I_1=\sqrt{f(-f-2pzl)}\int\frac{\sqrt{w+a^2}}{w(f-w)}dw$ unde am notat $\frac{f^2+pzlf}{-f-2pzl}=a^2$. Cu substituţia $w=u^2-a^2$, $dw=2udu$ obţinem $I_1=\sqrt{f(-f-2pzl)}\int\frac{-2u^2du}{(u^2-a^2)(u^2-b^2)}$, $b^2=a+f$. sau echivalent

$$I_1=\frac{\sqrt{f-(-f-2pzl)}}{b^2-a^2}\cdot\ln\left[\left(\frac{u-a}{u+a}\right)^a\cdot\left(\frac{u+b}{u-b}\right)^b\right]\tag{13}$$

unde $u=\sqrt{w+a^2}$.

Fie I_2 integrala din dreapta relaţiei (12)

$$I_2=\int\frac{(1-\overline{q}\zeta)\sqrt{t_0-2kq\zeta+q^2t_4\zeta^2}}{\zeta(z-\zeta)(1-\overline{z}\zeta)}d\zeta.$$

Avem

$$q^2t_4\zeta^2-2kq\zeta+t_0=q^2t_4\cdot(\zeta-\zeta_1)(\zeta-\zeta_2)$$

unde $\zeta_{1,2}=\frac{k\pm\sqrt{k^2-t_0t_4}}{t_4}\overline{q}$. Notând $k-\sqrt{k^2-t_0t_4}=\delta$, observând că $\zeta_1=\frac{\delta}{t_4}\overline{q}$ şi că $\zeta_2=\frac{t_0}{\delta}\overline{q}$, rezultă imediat $\sqrt{q^2t_4-2kq\zeta+t_0}=\sqrt{q^2t_4}\sqrt{(\zeta-\frac{\delta}{t_4}\overline{q})(\zeta-\frac{t_0}{\delta}\overline{q})}$.

Pentru calculul lui I_2 facem substituţia

$$(14)\qquad \sqrt{(\zeta-\frac{\delta}{t_4}\overline{q})(\zeta-\frac{t_0}{\delta}\overline{q})}=v(\zeta-\frac{\delta}{t_4}\overline{q})$$

Din (14) obţinem

$$(15)\qquad \zeta=\sigma\cdot\frac{v^2-\alpha^2}{v^2-1}\ \text{cu}\ \sigma=\frac{\delta}{t_4}\overline{q}\ \text{şi}\ \alpha^2=\frac{t_0t_4}{\delta^2}.$$

Notând $\beta^2=\frac{\sigma\alpha^2-z}{\sigma-z}$, $\gamma^2=\frac{1-\overline{z}\sigma\alpha^2}{1-\overline{z}\sigma}$ un calcul elementar conduce la

$$(16)\qquad I_2=\frac{2\sigma q(1-\overline{q}\sigma)(1-\alpha^2)^2\sqrt{t_4}}{(\sigma-z)(1-\overline{z}\sigma)}\int\frac{v^2(v^2-\delta^2)}{(v^2-1)(v^2-\alpha^2)(v^2-\beta^2)(v^2-\gamma^2)}dv.$$

Descompunând integrandul lui I_2 in fractii simple şi introducând notatiile $\frac{1-\delta^2}{2(1-\alpha^2)(1-\beta^2)(1-\gamma^2)}\overset{not}{=}\tau_1$; $\frac{\alpha(\alpha^2-\delta^2)}{2(\alpha^2-1)(\alpha^2-\beta^2)(\alpha^2-\gamma^2)}=\tau_2$; $\frac{\beta(\beta^2-\delta^2)}{2(\beta^2-1)(\beta^2-\alpha^2)(\beta^2-\gamma^2)}=\tau_3$; $\frac{\gamma(\gamma^2-\delta^2)}{2(\gamma^2-1)(\gamma^2-\alpha^2)(\gamma^2-\beta^2)}=\tau_4$; $\mu=\frac{2\sigma q(1-\overline{q}\sigma)(1-\alpha^2)^2\cdot\sqrt{t_4}}{(\sigma-z)(1-\overline{z}\sigma)}$ gasim

$$(17)\qquad I_2=\mu\left[\tau_1\ln\frac{v-1}{v+1}+\tau_2\ln\frac{v-\alpha}{v+\alpha}+\tau_3\ln\frac{v-\beta}{v+\beta}+\tau_4\ln\frac{v-\gamma}{v+\gamma}\right].$$

Din relaţia (14) observăm că

$$(18)\qquad v(\zeta)=\sqrt{\frac{\zeta-\frac{t_0}{\delta}\overline{q}}{\zeta-\frac{\delta}{t_4}\overline{q}}},\ \ v(0)=\pm\alpha$$

iar din $w=u^2-a^2$ obţinem

$$(19)\qquad u(\zeta)=\sqrt{w(\zeta)-\frac{f^2+2pzlf}{f+2pzl}},\ \ u(0)=\pm a$$

Cu ajutorul relaţiilor (13) şi (17) relaţia (12) devine:

$$(20)\qquad I_1\left.\right|_0^w=I_2\left.\right|_0^\zeta$$

Pentru $\zeta=0$ din (13), (17) şi (12') obţinem constanta (care provine din cei doi membri ai relaţiilor (13) şi (17) corespunzători lui $\frac{u-a}{u+a}$ din $\frac{v-\alpha}{v+\alpha}$ (din stânga)): $\ln(-1)^{\frac{a\sqrt{f(-f-2pzl)}}{b^2-a^2}+\mu\tau_2}$, obţinută în membrul stâng al egalităţii(12'). Astfel (12') se mai scrie :

$$(21)\qquad \left\{\begin{array}{l}\left[\left(\frac{a-u(\zeta)}{a+u(\zeta)}\right)^a\cdot\left(\frac{u(\zeta)+b}{u(\zeta)-b}\cdot\frac{a+b}{a-b}\right)^b\right]^{\frac{\sqrt{f(-f-2pzl)}}{b^2-a^2}}=\\ =\left[\left(\frac{v(\zeta)-1}{v(\zeta)+1}\right)^{\tau_1}\cdot\left(\frac{\alpha-v(\zeta)}{\alpha+v(\zeta)}\right)^{\tau_2}\cdot\left(\frac{v(\zeta)-\beta}{v(\zeta)+\beta}\cdot\frac{\alpha+\beta}{\alpha-\beta}\right)^{\tau_3}\left(\frac{v(\zeta)-\gamma}{v(\zeta)+\gamma}\cdot\frac{\alpha-\gamma}{\alpha+\gamma}\right)^{\tau_4}\right]^\mu.\end{array}\right.$$

Relaţia (21) reprezintă sub formă implicită ecuaţia pe care o verifică funcţia extremală $w=w(\zeta)$, care realizează $\max_{f\in S}\mathrm{Re}f(z)$.

II. Să presupunem acum că $\mathrm{Im}(zl+z^2m)=0$. În acest caz din expresia lui p, trebuie ca $zl-\overline{z}\overline{l}=0$. Cum $zl+\overline{z}\overline{l}=0$ rezultă $zl=0$. Dacă $l=0(|z|=r>0)$ atunci $\overline{l}=0$. Din relaţia (6) rezultă că $w(\zeta)$ trebuie să verifice condiţia

$$(22)\qquad \mathrm{Re}\left\{e^{i\psi}\left[\frac{f^2}{f-w}-f\left(\frac{w}{\zeta w^{/}}\right)^2\right]\right\}\leq 0.$$

Cum ψ este arbitrar, real rezultă că $w(\zeta)$ verifică următoarea ecuaţie diferenţială ordinara

$$(23)\qquad \left(\frac{w}{\zeta w^{/}}\right)^2=\frac{f}{f-w}.$$

sau $\frac{\sqrt{f}dw}{w\sqrt{f-w}} = \frac{d\zeta}{\zeta}$. Prin integrare rezultă

$$(24) \qquad \int_0^w \frac{\sqrt{f}dw}{w\sqrt{f-w}} = \int_0^\zeta \frac{d\zeta}{\zeta}.$$

si cu notaţia $\sqrt{f-w} = t$, obţinem

$$(25) \qquad \ln \frac{\sqrt{f-w} - \sqrt{f}}{\sqrt{f-w} + \sqrt{f}} |_0^w = \ln \zeta|_0^\zeta .$$

în membrul stâng subînțelegând limitele pentru t corespunzatoare limitelor pentru w. Formal avem

$$\begin{cases} \ln \frac{\sqrt{f-w}-\sqrt{f}}{\sqrt{f-w}+\sqrt{f}} - \ln \frac{\sqrt{f-w}-\sqrt{f}}{\sqrt{f-w}+\sqrt{f}} |_0 = \ln \zeta - \ln \zeta |_{\zeta=0} , \\ \text{şi} \\ \ln \frac{\sqrt{f-w}-\sqrt{f}}{\sqrt{f-w}+\sqrt{f}} + \ln \left(\frac{\zeta(\sqrt{f-w}+\sqrt{f})^2}{-w} \right) |_{\zeta=0} = \ln \zeta. \end{cases}$$

Riguros, în loc de ζ=0 si w=0 se ia respective $\zeta=\epsilon$ si $w=\eta(\epsilon)$ astfel încât $\eta\sim\epsilon$ pentru $\epsilon\to 0$ si apoi se trece la limita pentru $\epsilon\to 0$. Rezulta $\ln \left(\frac{\sqrt{f}-\sqrt{f-w}}{\sqrt{f}+\sqrt{f-w}} \cdot 4f \right) = \ln \zeta$ şi deci, de unde avem $\frac{\sqrt{f}-\sqrt{f-w}}{\sqrt{f}+\sqrt{f-w}} = \frac{\zeta}{4f}$, astfel ca

$$(26) \qquad w(\zeta) = \frac{16\zeta f^2(z)}{(4f(z)+z)^2}.$$

Cum $f(z)$ era considerată extremală (26) implica imediat $w(z) = \frac{z}{4}$. Observăm că şi condiţia

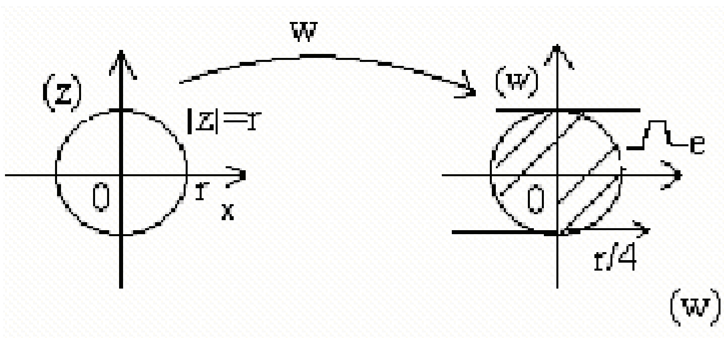

Figure 2

$\mathrm{Re} zw^{/}(z) = 0$ dă $x = 0 (z = x + iy)$. Atunci $\overline{z} = \max \mathrm{Re} w(z) = 0$ şi deci pentru $z_e = 0$ şi $\forall |z| > |z_e|$, orice paralelă la Ox întâlneşte $f(|z| = r)$ într-un singur punct.

Acest caz banal îl excludem, el arătând că problema are sens.

Din I şi II, rezultă că funcţia extremală care corespunde regiunii exterioare Ω_e din fig 1, este dată sub formă implicită de ecuaţia (21).

5. Mai rămâne să precizăm cum determinăm pe θ . Pentru aceasta în (11) facem pe $\zeta \to z$; după simplificări şi prin înmulţirea egalităţii prin $\overline{z}^3\overline{l}$ obţinem

$$r^3(r^2-1)l\overline{l} \cdot p = (1-\overline{q}z)^2 \cdot \left(t_0 - 2kqz + q^2 \cdot t_4 \cdot z^2\right) \cdot \overline{z^3} \cdot \overline{l}$$

sau , echivalent,

$$(27) \qquad r^3(r^2-1)l\overline{l} \cdot p = (\overline{z} - \overline{q}r^2)^2 \cdot (t_0\overline{z}\overline{l} - 2kq\overline{l}r^2 + q^2 t_4 \overline{l} z \cdot r^2).$$

Deoarece p este real, rezulta ca $r^3(r^2-1)l\overline{l}p$ este real astfel ca din relaţia (27) obţinem urmatorul sistem cu două ecuaţii din care aflăm pe θ şi k

$$(28) \qquad \begin{cases} r^3(r^2-1)\overline{l}\overline{l}p = \mathrm{Re}\left[\left(\overline{z} - \overline{q}r^2\right)^2 \left(t_0\overline{z}\overline{l} - 2kq\overline{l}r^2 + q^2t_4\overline{l}zr^2\right)\right] \\ \mathrm{Im}\left[\left(\overline{z} - \overline{q}r^2\right)\left(t_0\overline{z}\overline{l} - 2kq\overline{l}r^2 + q^2t_4\overline{l}zr^2\right)\right] = 0 \end{cases}$$

Cu θ şi k astfel determinaţi funcţia extremală din ecuaţia (25) este bine determinată şi cu ajutorul ei găsim $\mathrm{Re} z_e = \max_{f \in S} \mathrm{Re} f(z)$ cu proprietatea geometrică enunţată : în domeniul $\Omega_e = \{z : \ |z| > |z_e|\}$, orice paralelă la axa Ox intersectează $f(|z| = r)$ într-un singur punct (eventual în cel mult unul).

References

[1] Goluzin, G.M., Geometriceskaia teoria complecsnogo peremenogo, Moscva-Leningrad, 1952.

[2] Mocanu, P.T., O problemă extremală în clasa funcţiilor univalente, Universitatea Babeş Bolyai-Cluj Napoca, Facultatea de Matematică, 1998.

Cusp bifurcation in a problem of microeconomic dynamics

Laura Ungureanu

Let K_t be the capital of a firm at the time t and let L_t be the number of workers. Then the production force reads $y_t = F(K_t, L_t)$. The dynamics of the capital depends on the politics of development of the firm involving the net profit π_t, the dividends covering by the actionaries δ_t (where $\delta_t \pi_t$ represents the dividends and $(1-\delta_t)\pi_t$ are the remaining investments), the capital depreciation by a coefficient μ_t and the income obtained by liquidation of the damped actives at the revenue costs λ_t. Let γ_t be the rate of change of the capital, such that $\pi_t = \gamma_t y_t$. Then [2], [3]

$$\begin{cases} \dot{K}(t) = \gamma_t(1-\delta_t)F(K_t, L_t) - \mu_t(1-\lambda_t)K_t \\ \dot{L}(t) = \alpha_1 K + \alpha_2 L - \alpha_0 \end{cases}$$

where the dot over quantities represents the differentiation with respect to time. If $y_t = AK^\alpha L^\beta$ and the production has an increasing physical efficiency, i.e. $\alpha + \beta > 1$, the above equations become

$$\begin{cases} \dot{x} = cx^2y + bx \\ \dot{y} = x + \alpha_2 y - 1 \end{cases} \tag{1}$$

where we choose $\alpha = 2$, $\beta = 1$, $x = \beta_1 K_t$, $y = \beta_2 L_t$, $\beta_1 = \alpha_1/\alpha_0$, $\beta_2 = 1/\alpha_0$ for $\alpha_0 \neq 0$, $\alpha_1 \neq 0$, $a = A\gamma_t(1-\delta_t)$, $b = -\mu_t(1-\lambda_t)$, $c = a\alpha_0^2/\alpha_1$. In this way the new state functions x and y are proportional to the capital and working force respectively. In addition, the number of parameters was reduced from eight to three.

Let $P_0(b_0, b_0, -4b_0^2)$, $b_0 \neq 0$ the fixed point on curve $\gamma = \left\{\alpha_2 = b, c = -4b^2\right\}$. In the point P_0 the system (1) admits the point of equilibrium nonhiperbolic double $\bar{\mathbf{u}}_2 = \bar{\mathbf{u}}_3 = (1/2, 1/2b_0)$. For these values we expect that a Bogdanov-Takens or a degenerated Bogdanov-Takens occur..

For the easiness calculi, the existing theories presuppose ab initio that the singularity is in origin space phases and she corresponds the origin from the space parameters. Ergo we bring $\bar{\mathbf{u}}_2$ on in origin marks from plan and the point P_0 in origin marks from the space with the aid of parameters change of coordinate $x_1 = x - 1/2$, $y_1 = y - 1/2b_0$ and change of parameters $\alpha_2' = \alpha_2 - b_0$, $b' = b - b_0$, $c' = c + 4b_0^2$.

Then (1) becomes

$$\begin{cases} \dot{x}_1 = \frac{b'}{2} + \frac{c'}{8b_0} + (\frac{c'}{2b_0} + b' - b_0)x_1 + (\frac{c'}{4} - b_0^2)y_1 + \\ \quad +(\frac{c'}{2b_0} - 2b_0)x_1^2 + (c' - 4b_0^2)x_1y_1 + (c' - 4b_0^2)x_1^2y_1, \\ \dot{y}_1 = \frac{\alpha_2'}{2b_0} + x_1 + (\alpha_2' + b_0)y_1. \end{cases} \tag{2}$$

The linearized system, around the equilibrium $(x_1, y_1) = (0, 0)$ is defined by the matrix $A = \begin{pmatrix} \frac{c'}{2b_0} + b' - b_0 & \frac{c'}{4} - b_0^2 \\ 1 & \alpha_2' + b_0 \end{pmatrix} \neq \mathbf{O}_2$. In the point $(\alpha_2', b', c') = (0, 0, 0)$ the system (2) becomes

$$\begin{cases} \dot{x}_1 = -b_0x_1 - b_0^2y_1 - 2b_0x_1^2 - 4b_0^2x_1y_1 - 4b_0^2x_1^2y_1, \\ \dot{y}_1 = x_1 + b_0y_1. \end{cases} \tag{2'}$$

In addition we have $A(0,0,0) = \begin{pmatrix} -b_0 & -b_0^2 \\ 1 & b_0 \end{pmatrix}$, $\det A(0) = 0$, $trA(0) = 0$ and therefore $s_1 = s_2 = 0$. But $A(\mathbf{0}) \neq \mathbf{O}_2$. This show that the point $\bar{\mathbf{u}}_2 (= \bar{\mathbf{u}}_3)$ is a singularity with double zero.

Brought the matrix $A(0,0,0)$ to canonical form(Jacobi) consider the vectors $\mathbf{v}_1 = (-b_0, 1)$, $\mathbf{v}_2 = (\frac{1}{1+b_0^2}, \frac{b_0}{1+b_0^2})$ which verify the conditions $A\mathbf{v}_1 = 0$, $A\mathbf{v}_2 = \mathbf{v}_1$, $\langle \mathbf{v}_1, \mathbf{v}_2 \rangle = 0$. Changing the canonic base $\mathcal{B} = \{\mathbf{e}_1 = (1,0), \mathbf{e}_2 = (0,1)\}$ with base $\mathcal{B}' = \{\mathbf{v}_1, \mathbf{v}_2\}$ formula of changes the coordinates are:

$$\begin{cases} x_1 = -b_0x_2 + \frac{1}{1+b_0^2}y_2, \\ y_1 = x_2 + \frac{b_0}{1+b_0^2}y_2 \end{cases}$$

and transform the system(2) in the system

$$(3)\qquad \begin{cases} \dot{x}_2 = \frac{\alpha_2'}{2b_0} + \alpha_2' x_2 + y_2, \\ \dot{y}_2 = \frac{b'}{2} + \frac{c'}{8b_0} + (\alpha_2' b_0 - b' b_0 - \frac{c'}{4})x_2 + (\frac{c'}{2b_0} + b')y_2 + (2b_0^3 - \frac{c' b_0}{2})x_2^2 + (\frac{c'}{2b_0} - 2b_0)y_2^2 + \\ \qquad b_0^2(c' - 4b_0^2)x_2^3 - 2b_0(c' - 4b_0^2)x_2^2 y_2 + (c' - 4b_0^2)x_2 y_2^2 \end{cases}$$

which for $\alpha_2' = b' = c' = 0$ has the form

$$(3)'\qquad \begin{cases} \dot{x}_2 = y_2, \\ \dot{y}_2 = 2b_0^3 x_2^2 - 2b_0 y_2^2 - 4b_0^4 x_2^3 + 8b_0^3 x_2^2 y_2 - 4b_0^2 x_2 y_2^2. \end{cases}$$

Proposition 1. *The system(3) is topologically equivalent with the system*

$$(4)\qquad \begin{cases} \dot{x}_3 = \frac{\alpha_2'}{2b_0} + 2\alpha_2' x_3 + y_3 + 3\alpha_2' b_0 x_3^2 + 2\alpha_2' b_0 x_3^3 - 8b_0^3 x_3^3 y_3 - 4\alpha_2' b_0^3 x_3^4, \\ \dot{y}_3 = \frac{b'}{2} + \frac{c'}{8b_0} + \alpha_2' b_0 x_3 + (\frac{c'}{2b_0} + b' + \alpha_2')y_3 + (2b_0^3 - \frac{c' b_0}{2} + b' b_0^2 + \alpha_2' b_0^2)x_3^2 + \\ \qquad + \frac{c'}{2b_0} y_3^2 + 6\alpha_2' b_0 x_3 y_3 + b_0^2(\frac{3c' b_0^2}{2} + 2\alpha_2' b_0^3 + 2b' b_0^3 - 4b_0^4)x_3^3 + \\ \qquad +(18\alpha_2' b_0^2 - 2c' b_0 + 8b_0^3)x_3^2 y_3 + 4b_0^2 x_3 y_3^2. \end{cases}$$

Proof. With the nonlinear transformation of coordinate

$$(5)\qquad \begin{cases} x_2 = x_3 - b_0 x_3^2, \\ y_2 = y_3 - 2b_0 x_3 y_3 \end{cases}$$

the system (3) becomes (4). □

Corollary 2. *The system (3) ′ is topologically equivalent with*

$$(4)'\qquad \begin{cases} \dot{x}_3 = y_3 - 8b_0^3 x_3^3 y_3, \\ \dot{y}_3 = 2b_0^3 x_3^2 - 4b_0^4 x_3^3 + 8b_0^3 x_3^2 y_3 + 4b_0^2 x_3 y_3^2 + 6b_0^5 x_3^4 - 16b_0^4 x_3^3 y_3 + 20b_0^3 x_3^2 y_3^2. \end{cases}$$

Proposition 3. *The system (4) is topologically equivalent with the system*

$$(6)\qquad \begin{cases} \dot{x}_4 = \frac{\alpha_2'}{2b_0} + \alpha_2' x_4 + y_4 + 3\alpha_2' b_0 x_4^2 + (-\frac{2\alpha_2' b_0^3}{3} + \frac{8b_0^3}{3})x_4^3 - 8b_0^3 x_4^3 y_4 - 4\alpha_2' b_0^3 x_4^4, \\ \dot{y}_4 = \frac{b'}{2} + \frac{c'}{8b_0} + \alpha_2' b_0 x_4 + (\frac{c'}{2b_0} + b' + \alpha_2')y_4 + (2b_0^3 - \frac{c' b_0}{2} - 3\alpha_2' b_0^2)x_4^2 + \\ \qquad + \frac{c' b_0}{2} y_4^2 + 6\alpha_2' b_0 x_3 y_3 + (-\frac{38}{3}\alpha_2' b_0^3 + \frac{14}{3} b' b_0^3 + \frac{17}{6} c' b_0^2 - 4b_0^4)x_4^3 + \\ \qquad +(10\alpha_2' b_0^2 - 2c' b_0 + 8b_0^3)x_4^2 y_4 + (-16b' b_0^4 + \frac{20}{3} c' b_0^2 + 402\alpha_2' b_0^3)x_4^3 y_4 + \\ \qquad +(\frac{16}{3} b' b_0^4 + \frac{1}{6} c' b_0^3 + \frac{34}{3}\alpha_2' b_0^4 + \frac{14}{3} b_0^5)x_4^4 + (-2c' b_0 + 20b_0^3)x_4^2 y_4^2 \end{cases}$$

Proof. Let $\mathcal{H}_2^3$ the vectorial space of matrix $\begin{pmatrix} \xi_1 \\ \xi_2 \end{pmatrix}$ where ξ_1, ξ_2 are polynomial homogeneous of the degree three with two the variables, and let the linear map $L_A^3 : \mathcal{H}_2^3 \to \mathcal{H}_2^3$,

$L_A^3 \begin{pmatrix} \xi_1 \\ \xi_2 \end{pmatrix} = \begin{pmatrix} \frac{\partial \xi_1}{\partial x} & \frac{\partial \xi_1}{\partial y} \\ \frac{\partial \xi_2}{\partial x} & \frac{\partial \xi_2}{\partial y} \end{pmatrix} \begin{pmatrix} 0 & 1 \\ 0 & 0 \end{pmatrix} \begin{pmatrix} \xi_1 \\ \xi_2 \end{pmatrix} - \begin{pmatrix} 0 & 1 \\ 0 & 0 \end{pmatrix} \begin{pmatrix} \xi_1 \\ \xi_2 \end{pmatrix}$, any ploughes be the matrix $\begin{pmatrix} \xi_1 \\ \xi_2 \end{pmatrix} \in \mathcal{H}_2^3$. If $\mathcal{R}^3 = \mathrm{Im} L_A^3$ and $\mathcal{C}^3 = Ker L_{A^*}^3$. than $\mathcal{H}_2^3 = \mathcal{R}^3 \oplus \mathcal{C}^3$.

If $\xi = \begin{pmatrix} 0 \\ -4b_0^4 x_3^3 + 8b_0^3 x_3^2 y_3 + 4b_0^2 x_3 y_3^2 \end{pmatrix}$ then $\xi = L_A^3(H) + \begin{pmatrix} \frac{8}{3} b_0^3 x_3^3 \\ -4b_0^4 x_3^3 \end{pmatrix}$, where $H = \begin{pmatrix} \frac{2}{3} b_0^2 x_3^3 \\ \frac{8}{3} b_0^3 x_3^3 + 2b_0^2 x_3^2 y_3 \end{pmatrix}$.
The calculations for determination of the transformation (5) are very laborious and we not present here. This result make us to consider the transformation of coordination

$$(7)\qquad \begin{cases} x_3 = x_4 + \frac{2}{3} b_0^2 x_4^3, \\ y_3 = y_4 + \frac{8}{3} b_0^3 x_4^3 + 2b_0^2 x_4^2 y_4, \end{cases}$$

and the system (4) becomes (6). □

Corollary 4. *The system (4) ′ is topologically equivalent with the system*

$$(6)' \qquad \begin{cases} \dot{x}_4 = y_4 + \frac{8b_0^3}{3}x_4^3 - 8b_0^3x_4^3y_4, \\ \dot{y}_4 = 2b_0^3x_4^2 - 4b_0^4x_4^3 - 16b_0^4x_4^3y_4 + \frac{14}{3}b_0^5x_4^4 + 20b_0^3x_4^2y_4^2. \end{cases}$$

Proposition 5. *The system (6) is topologically equivalent with the system*

$$(8) \qquad \begin{cases} \dot{x}_5 = y_5, \\ \dot{y}_5 = \frac{b'}{2} + \frac{c'}{8b_0} + \alpha_2'b_0x_5 + (\frac{c'}{2b_0} + b' + \alpha_2')y_5 + (2b_0^3 - \frac{c'b_0}{2} - 3\alpha_2'b_0^2)x_5^2 + \\ \qquad + \frac{c'}{2b_0}y_5^2 + 4\alpha_2'b_0x_5y_5 + (\frac{2}{3}\alpha_2'b_0^3 - 2b'b_0^3 + \frac{1}{2}c'b_0^2 - 4b_0^4)x_5^3 + \\ \qquad +(-2\alpha_2'b_0^2 - 2c'b_0 + 8b_0^3)x_5^2y_5 + (-16b_0^4 + 4c'b_0^2 - 8\alpha_2'b_0^3)x_5^3y_5 + \\ \qquad +(\frac{16}{3}b'b_0^4 + \frac{1}{6}c'b_0^3 + \frac{26}{3}\alpha_2'b_0^4 + \frac{14}{3}b_0^5)x_5^4 + (-2c'b_0 + 20b_0^3)x_5^2y_5^2 \end{cases}$$

Proof. The system(8) is obtained from the system(6) through the transformation

$$(9) \qquad \begin{cases} x_4 = x_5, \\ y_4 = y_5 - \frac{8}{3}b_0^3x_5^3 + 8b_0^3x_5^3y_5 \end{cases}$$

□

Corollary 6. *The system (6)′ is topologically equivalent with the system*

$$(8)' \qquad \begin{cases} \dot{x}_5 = y_5, \\ \dot{y}_5 = 2b_0^3x_5^2 - 4b_0^4x_5^3 + 8b_0^3x_5^2y_5 - 16b_0^4x_5^3y_5 + \frac{14}{3}b_0^5x_5^4 - 4b_0^3x_5^2y_5^2. \end{cases}$$

Remark 9. The system (8)′ is a normal form of three order for the system (3)′.

So far, if neglect the order three terms of , we have

$$\begin{cases} \dot{x}_5 = y_5, \\ \dot{y}_5 = 2b_0^3x_5^2. \end{cases}$$

Hence, the point $\overline{\mathbf{u}}_2$ corresponds to a degenerated Bogdanov-Takens bifurcation point for a system

$$\begin{cases} \dot{x}_5 = y_5, \\ \dot{y}_5 = \alpha x_5^2 + \beta x_5y_5, \end{cases}$$

with $\alpha \neq 0$, $\beta = 0$.

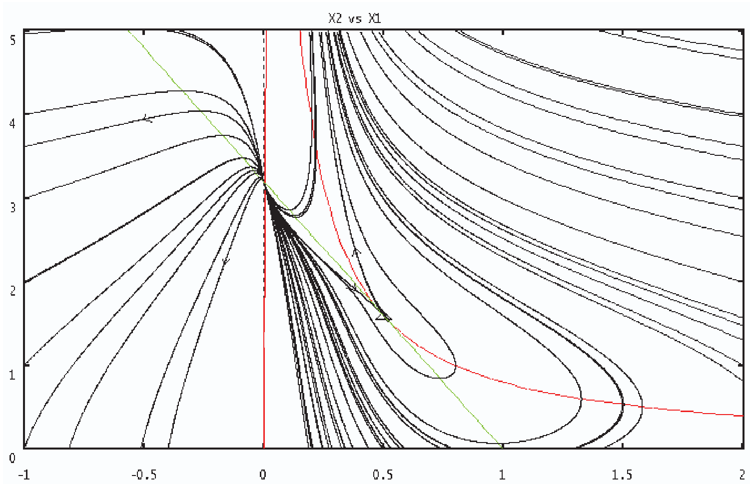

FIGURE 1. The phase portrait for a point from curve γ .

Theorem 7. *The system(8) has in origin a cusp bifurcation. (of codimension ≥ 3).*

Proof. The second equation of the system (8) can be written

$$\dot{y}_5 = F(x_5, \lambda) + y_5 G(x_5, \lambda) + y_5^2 Q(y_5, x_5, \lambda)$$

where $\lambda = (\alpha_2', b', c')$, $F(x_5, \lambda) = \frac{b'}{2} + \frac{c'}{8b_0} + \alpha_2' b_0 x_5 + (2b_0^3 - \frac{c' b_0}{2} - 3\alpha_2' b_0^2) x_5^2 + (\frac{2}{3}\alpha_2' b_0^3 - 2b' b_0^3 + \frac{1}{2} c' b_0^2 - 4b_0^4) x_5^3 + (\frac{16}{3} b' b_0^4 + \frac{1}{6} c' b_0^3 + \frac{26}{3}\alpha_2' b_0^4 + \frac{14}{3} b_0^5) x_5^4$, $G(x_5, \lambda) = \frac{c'}{2b_0} + b' + \alpha_2' + \frac{c'}{2b_0} y_5^2 + 4\alpha_2' b_0 x_5 + (-2\alpha_2' b_0^2 - 2c' b_0 + 8b_0^3) x_5^2 + (-16 b_0^4 + 4c' b_0^2 - 8\alpha_2' b_0^3) x_5^3$, $Q(x_5, y_5, \lambda) = (-2c' b_0 + 20 b_0^3) x_5^2 + \frac{c'}{2b_0}$ and the condition for the cusp bifurcation [1] : $F(0,0) = 0$, $G(0,0) = 0$, $\frac{\partial F}{\partial x_5}(0,0) = 0$, $\frac{\partial G}{\partial x_5}(0,0) = 0$, $\frac{\partial^2 F}{\partial x_5^2}(0,0) = 4b_0^3 \neq 0$, are verify. □

References

[1] Dumortier F., Roussarie R., Sotomayor J., *Generic 3-parameter families of vector fields on the plane, unfolding a singularity with nilpotent linear part. The cusp case of codimension 3,* Ergodic Th.&Dynam. Sys.**7**, 375-413, 1987.

[2] Gheorghe Oprescu, Mathematics for economists, Ed. Fundatiei "Romania de Maine", Bucharest, 1996 (Romanian)

[3] Laura Ungureanu, Liviu Ungureanu, Elements of dynamics economics, Ed. Univ. Piteşti, 2000

Observaţii metodice asupra compunerii funcţiilor

Liliana Antonescu şi Georgia Irina Oros
Grup şcolar "Al. Roman"
Str. Ciocârliei, nr. 1 bis, Aleşd
Universitatea Babeş-Bolyai
Facultatea de Matematică şi Informatică, Cluj-Napoca

Abstract. În această lucrare punem în evidenţă o metodă simplă care dă posibilitatea elevilor de a înţelege compunerea funcţiilor definite pe intervale diferite şi a obţinerii domeniului de definiţie pentru fiecare ramură.

1. Introducere şi preliminarii

Fie funcţiile $f : A \to B$ şi $g : B \to C$. Să observăm că domeniul de definiţie al funcţiei g coincide cu codomeniul funcţiei f. Această situaţie ne permite să facem următoarele consideraţii. Fie $a \in A$, atunci elementul $f(a)$ aparţine lui B. Prin funcţia g elementului $f(a)$ îi corespunde elementul $g(f(a))$ din C. Astfel, oricărui element $a \in A$, ii putem asocia un element unic $g(f(a))$ din mulţimea C. Am definit astfel o funcţie $h : A \to C$, $h(x) = g(f(x))$, pentru orice $x \in A$. Funcţia h se numeşte compusa funcţiilor g şi f şi se notează $g \circ f$ (citim g compus cu f), $(g \circ f)(x) = g(f(x))$. Pentru realizarea compunerii funcţiilor cu mai multe braţe elevii au nevoie de stăpânirea cunoştinţelor legate de rezolvarea sistemelor de inecuaţii.

2. Rezolvări concrete

I. Fie $f : \mathbb{R} \to \mathbb{R}$, $f(x) = 3x + 4$ şi $g : \mathbb{R} \to \mathbb{R}$,

$$g(x) = \begin{cases} 2x+3 & \text{dacă} \quad x < 3 \\ x+1 & \text{dacă} \quad x \geq 3. \end{cases}$$

Să se calculeze: a) $f \circ g$, b) $g \circ f$.

a) Avem

$$\begin{aligned}(f \circ g)(x) &= f(g(x)) = 3g(x) + 4 = \begin{cases} 3(2x+3)+4 & \text{dacă} \quad x < 3 \\ 3(x+1)+4 & \text{dacă} \quad x \geq 3 \end{cases} \\ &= \begin{cases} 6x+13 & \text{dacă} \quad x < 3 \\ 3x+7 & \text{dacă} \quad x \geq 3 \end{cases}\end{aligned}$$

b) $$(g \circ f)(x) = g(f(x)) = \begin{cases} 2f(x)+3 & \text{dacă} \quad f(x) < 3 \\ f(x)+1 & \text{dacă} \quad f(x) \geq 3 \end{cases} = \begin{cases} 6x+11 & \text{dacă} \quad x < -\dfrac{1}{3} \\ 3x+5 & \text{dacă} \quad x \geq -\dfrac{1}{3} \end{cases}$$

II. Fie $f : \mathbb{R} \to \mathbb{R}$,

$$f(x) = \begin{cases} 2x-3 & \text{dacă} \quad x < 0 \\ 7x & \text{dacă} \quad x \geq 0 \end{cases}$$

şi $g : \mathbb{R} \to \mathbb{R}$,

$$g(x) = \begin{cases} x^2 & \text{dacă} \quad x \leq -2 \\ 2x-1 & \text{dacă} \quad x > -2 \end{cases}$$

Să se calculeze: a) $f \circ g$, b) $g \circ f$.

a)

$$\begin{aligned}(f \circ g)(x) &= f(g(x)) = \begin{cases} 2g(x)-3 & \text{dacă} \quad g(x) \leq 0 \\ 7g(x) & \text{dacă} \quad g(x) > 0 \end{cases} \\ &= \begin{cases} 2x^2-3 & \text{dacă} \quad x^2 \leq 0 \text{ şi } x \leq -2 \\ 7x^2 & \text{dacă} \quad x^2 > 0 \text{ şi } x \leq -2 \\ 2(2x-1)-3 & \text{dacă} \quad 2x-1 \leq 0 \text{ şi } x > -2 \\ 7(2x-1) & \text{dacă} \quad 2x-1 > 0 \text{ şi } x > -2 \end{cases} = \begin{cases} 7x^2 & \text{dacă} \quad x \in (-\infty, -2] \\ 4x-5 & \text{dacă} \quad x \in \left(-2, \dfrac{1}{2}\right] \\ 14x-7 & \text{dacă} \quad x \in \left(\dfrac{1}{2}, \infty\right) \end{cases}\end{aligned}$$

b)

$$
\begin{aligned}
(g\circ f)(x) &= g(f(x)) = \begin{cases} [f(x)]^2 & \text{dacă} \quad f(x)\le -2\\ 2f(x)-1 & \text{dacă} \quad f(x) > -2\end{cases}\\
&= \begin{cases} (2x-3)^2 & \text{dacă} \quad 2x-3\le -2 \text{ şi } x\le 0\\ 2(2x-3)-1 & \text{dacă} \quad 2x-3 > -2 \text{ şi } x\le 0\\ (7x)^2 & \text{dacă} \quad 7x\le -2 \text{ şi } x>0\\ 2\cdot 7x-1 & \text{dacă} \quad 7x > -2 \text{ şi } x>0\end{cases} = \begin{cases} 4x^2-12+9 & \text{dacă} \quad x\le 0\\ 14x-1 & \text{dacă} \quad x>0\end{cases}
\end{aligned}
$$

III. Fie $f:\mathbb{R}\to\mathbb{R}$,

$$
f(x) = \begin{cases} x^2-3x+1 & \text{dacă} \quad x<-2\\ 5 & \text{dacă} \quad -2\le x\le 1\\ x-3 & \text{dacă} \quad x>1\end{cases}
$$

şi $g:\mathbb{R}\to\mathbb{R}$,

$$
g(x) = \begin{cases} x-1 & \text{dacă} \quad x\le -1\\ -2 & \text{dacă} \quad -1\le x<3\\ x^3-4 & \text{dacă} \quad x\ge 3\end{cases}
$$

Să se calculeze: a) $f\circ g$, b) $g\circ f$.

$$
\begin{aligned}
\text{a) } (f\circ g)(x) &= f(g(x)) = \begin{cases} [g(x)]^2-3g(x)+1 & \text{dacă} \quad g(x)<-2\\ 5 & \text{dacă} \quad -2\le g(x)\le 1\\ g(x)-3 & \text{dacă} \quad g(x)>1\end{cases}\\
&= \begin{cases} (x-1)^2-3(x-1)+1 & \text{dacă} \quad x-1<-2 \text{ şi } x\le -1\\ 5 & \text{dacă} \quad -2\le x-1\le 1 \text{ şi } x\le -1\\ x-1-3 & \text{dacă} \quad x-1>1 \text{ şi } x\le -1\\ (-2)^2-3(-2)+1 & \text{dacă} \quad -2<-2 \text{ şi } -1\le x<3\\ 5 & \text{dacă} \quad -2\le -2\le 1 \text{ şi } -1\le x<3\\ -2-3 & \text{dacă} \quad -2>1 \text{ şi } -1\le x<3\\ (x^2-4)^2-3(x-3)+1 & \text{dacă} \quad x^3-4<-2 \text{ şi } x\ge 3\\ 5 & \text{dacă} \quad -2\le x^2-4\le 1 \text{ şi } x\ge 3\\ x^2-4-3 & \text{dacă} \quad x^2-4>1 \text{ şi } x\ge 3\end{cases}\\
&= \begin{cases} x^2-5x+5 & \text{dacă} \quad x<-1\\ 5 & \text{dacă} \quad -1\le x<3\\ x^2-7 & \text{dacă} \quad x\ge 3\end{cases}
\end{aligned}
$$

$$
\begin{aligned}
\text{b) } (g\circ f)(x) &= g(f(x)) = \begin{cases} f(x)-1 & \text{dacă} \quad f(x)\le -1\\ -2 & \text{dacă} \quad -1\le f(x)<3\\ [f(x)]^2-4 & \text{dacă} \quad f(x)\ge 3\end{cases}\\
&= \begin{cases} x^2-3x+1-1 & \text{dacă} \quad x^2-3+1\le -1 \text{ şi } x<-2\\ -2 & \text{dacă} \quad -1\le x^2-3x+1<3 \text{ şi } x<-2\\ (x^2-3x+1)^2-4 & \text{dacă} \quad x^2-3x+1\ge 3 \text{ şi } x<-2\\ 5-1 & \text{dacă} \quad 5\le -1 \text{ şi } -2\le x\le 1\\ -2 & \text{dacă} \quad -1\le 5<3 \text{ şi } -2\le x\le 1\\ 25-4 & \text{dacă} \quad 5\ge 3 \text{ şi } -2\le x\le 1\\ x-3-1 & \text{dacă} \quad x-3\le -1 \text{ şi } x>1\\ -2 & \text{dacă} \quad -1\le x-3<3 \text{ şi } x>1\\ (x-3)^2-4 & \text{dacă} \quad x-3\ge 3 \text{ şi } x>1\end{cases}\\
&= \begin{cases} x^4-6x^3+11x^2-6x-3 & \text{dacă} \quad x\in(-\infty,-2)\\ 19 & \text{dacă} \quad x\in[-2,1]\\ x-4 & \text{dacă} \quad x\in(1,2]\\ -2 & \text{dacă} \quad x\in[2,6)\\ x^2-6x+5 & \text{dacă} \quad x\in[6,\infty)\end{cases}
\end{aligned}
$$

References

[1] Stănescu, I., Cunţan, I., *Algebră. Manual pentru clasa a IX-a*, Editura Ananda Kali, Sibiu, 1999.
[2] Galea, G., *Matematică. Manual pentru clasa a IX-a*, Editura Colosseum, Bucureşti, 1995.
[3] Mihalca, D., *Algebră. Exerciţii şi probleme pentru clasa a IX-a*, Editura Teora, Bucureşti, 1999.
[4] Petrică, I., Lazăr, I., *Probleme de algebră pentru liceu*, vol. I, Editura Petrion, Bucureşti, 1995.

Fluid dynamics of expanding and contracting tube: a case study of methods of series summation

O. D. MAKINDE and M. O. ADEBAYO
Applied Mathematics Department, University of the North,
Private Bag X1106, Sovenga 0727, South Africa

Abstract. The fluid dynamics of expanding and contracting tube is investigated mathematically using both the Navier-Stokes and continuity equations for an incompressible viscous fluid. The problem admits similarity solution, thereby reducing the unsteady Navier-Stokes equations to a parameter dependent fourth order nonlinear ordinary differential equation. Analytical solutions are constructed for the problem using perturbation technique together with a new special type of Hermite-Padé approximants and important properties of the overall structure of the flow are discussed. The model is appropriate to simulate wind tunnel tests on rheological phenomenon in physiological systems.

Keywords: Expanding and contracting tube, Hermite-Padé approximants, bifurcation.
2000 Mathematics Subject Classification: 76E25.

1. INTRODUCTION

Fluid flow through an expanding and contracting tube is a complex problem due to the interaction between the tube-wall and the flowing fluid, Heil (1997). Expanding and contracting tubes are easily deformed by negative transmural pressure owing to marked reduction of rigidity. Thus, they show a considerable nonlinearity and reveal various complicated phenomena. It is usually used to simulate biological flows such as blood flow in arteries or veins, flow of urine in urethras and airflow in the bronchial airways. These investigations are very useful for the study and prediction of many diseases, as the lung disease (asthma and emphysema), or the cardiovascular diseases (heart stroke). The major research goal remains, the full understanding of the flow structure and the mechanism driving this flow. Many previous theoretical works on flow in collapsible tubes concentrated on the development and analysis of simpler models, by reducing the spatial dimension of the problem, which involve a number of ad-hoc assumptions e.g. Contrad (1969), Grotberg (1971), Flaherty et al. (1972), Cowley (1982), Bonis & Ribreau (1987) etc. Experimental example of the work that have been done on collapsible tube includes the one performed with finite-length elastic tubes whose upstream and downstream ends are held open (i.e. Starling-resistor, Brower & Scholten 1975, Bertram 1986). Inside a pressure chamber, thin-walled elastic tube (made of latex rubber) is mounted on two rigid tubes. Fluid (liquid or gas) typically water or air respectively is driven through the tube, either by applying a controlled pressure-drop between the ends of the rigid tubes or by controlling the flow rate. If the external presssure exceeds the fluid pressure by a sufficiently large amount, the tube buckles non-axisymmetrically, which then leads to a nonlinear relation between pressure-drop and flow rate. At sufficiently large Reynolds numbers, the system produces self-excited oscillations, and exhibits hysteresis in transitions between dynamical states, multiple modes of oscillations (each having distinct frequency range), rich and complex nonlinear dynamics (Bertram et al. 1990). The inertia and resistance of the fluid in the supporting rigid tubes have an important influence on the system's overall dynamics. This experiment forms the basis for most recent theoretical investigations due to its three-dimensional nature. Meanwhile, Bertram & Pedley (1982), Bertram & Raymond (1991) investigated two-dimensional channel theoretical model with one wall of the channel been replaced by a membrane under longitudinal tension, viscous flow is driven through the channel by an imposed pressure-drop. The variation between the external pressure and the internal flow determine the deformation of the membrane. The dynamics of the problem is described by nonlinear ODE's whose numerical solutions exhibit oscillatory behaviour reminiscent of that observed in experiments. Despite the difficulties of producing two-dimensional flows experimentally, this system still attracted considerable theoretical attentions. Since it avoid the complications of three-dimensional flows found in the Starling-resistor, while still exhibiting phenomena such as flow limitation and self-excited oscillations.

Meanwhile, mathematical model of physical phenomena often results in nonlinear equations for some unknown function. Usually the problems cannot be solved exactly. The solutions of these nonlinear systems are dominated by their singularities: physically, a real singularity controls the local behaviour of a solution. There is a long tradition in applied mathematics to solve nonlinear problems by expansion in powers of some "small" perturbation parameter. The advantage of this approach is that it reduces the original nonlinear problem to a sequence of linear problems (Makinde, 1999). However, it is not always possible to find an unlimited number of terms of power series. Often it is possible to obtain a finite number of terms of that series and these may contain a remarkable amount of information. One can reveal the solution behaviour near the critical points by analysing partial sum (Makinde, 2001). Over the last quarter century, highly specialised techniques have been developed to improved the series summation and also used to extract the required information of the singularities from a finite number of series coefficients. The most frequently used methods include Domb-Sykes(1957), Shafer (1974), Hunter and Guerrieri (1980), Sergeev (1986), Drazin and Tourigny (1996), Sergeev and Goodson (1998), Makinde et al. (2002), etc.

In this paper, we investigate the flow of a viscous incompressible fluid in a collapsible tube. A special type of Hermite-Padé approximants technique is presented and utilised to analyse the flow structure. The chief merit of this new method is its ability to reveal the dominant singularity in the flow field together with solution branches of the underlying problem in addition to the one represented by the original series. In Sections 2 & 3, we establish the mathematical formulation for the problem. With the benefit of twenty years of advances in computing hardware, we are able to find many terms of the solution series as presented in Section 4. The methods used to sum the series are described in Section 5. In Section 6, we discuss the pertinent results.

2. Mathematical formulation

The problem under consideration is that of transient flow of a viscous incompressible fluid in a collapsible tube. Take a cylindrical polar coordinate system (r, θ, z) where *0z* lies along the centre of the tube, *r* is the distance measured radially and θ is the azimuthal angle. Let *u* and *v* be the velocity components in the directions of *z* and *r* increasing respectively. It is assumed that the tube's wall is at $r = a_0\sqrt{(1-\alpha t)}$, where α is a constant of dimension $[T^1]$ which characterizes unsteadiness in the flow field, a_0 is the characteristic radius of the tube at time $t = 0$ as shown in fig. 1;

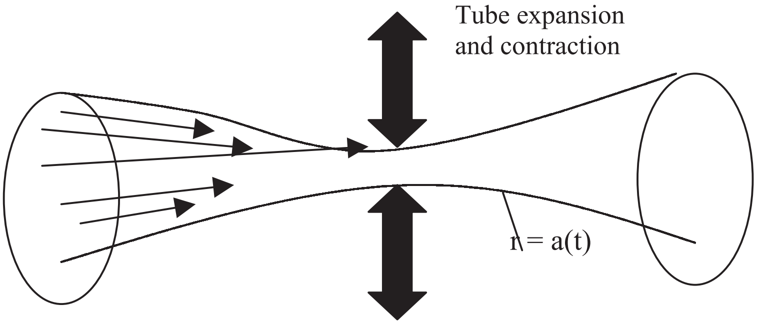

Fig. 1. Schematic diagram of the problem.

Then, for axisymmetric unsteady viscous incompressible flow, the Navier-Stokes equations are

$$\frac{\partial u}{\partial t} + u\frac{\partial u}{\partial z} + v\frac{\partial u}{\partial r} = -\frac{1}{\rho}\frac{\partial P}{\partial z} + \upsilon\nabla^2 u\,, \tag{2.01}$$

$$\frac{\partial v}{\partial t}+u\frac{\partial v}{\partial z}+v\frac{\partial v}{\partial r}=-\frac{1}{\rho}\frac{\partial P}{\partial r}+\upsilon(\nabla^2 v-\frac{v}{r^2}), \tag{2.02}$$

where $\nabla^2=\partial^2/\partial r^2+\partial/r\partial r+\partial^2/\partial z^2$, P is the pressure, ρ the density and υ the kinematic viscosity of the fluid. The equation of continuity is

$$\frac{\partial}{\partial r}(rv)+r\frac{\partial u}{\partial z}=0. \tag{2.03}$$

The appropriate boundary conditions are

Regularity of solution along z-axis, i.e.

$$\frac{\partial u}{\partial r}=0,\ v=0, \qquad \text{on} \quad r=0. \tag{2.04}$$

The axial and normal velocities at the wall are prescribed as

$$u=0,\ v=\frac{da}{dt}, \qquad \text{on} \quad r=a(t). \tag{2.05}$$

We introduce the stream-function Ψ and vorticity ω in the following manner:

$$u=\frac{1}{r}\frac{\partial\Psi}{\partial r} \quad \text{and} \quad v=-\frac{1}{r}\frac{\partial\Psi}{\partial z}, \tag{2.06}$$

$$\omega=\frac{\partial v}{\partial z}-\frac{\partial u}{\partial r}=-\frac{1}{r}\frac{\partial^2\Psi}{\partial z^2}-\frac{1}{r}\frac{\partial^2\Psi}{\partial r^2}+\frac{1}{r^2}\frac{\partial\Psi}{\partial r}. \tag{2.07}$$

Eliminating pressure P from (2.01) and (2.02) by using (2.06) and (2.07) we get

$$\frac{\partial\omega}{\partial t}+\frac{1}{r}\frac{\partial(\Psi,\omega)}{\partial(r,z)}+\frac{\omega}{r^2}\frac{\partial\Psi}{\partial z}=\upsilon\left[\nabla^2\omega-\frac{\omega}{r^2}\right], \quad \omega=-\nabla^2\Psi, \tag{2.08}$$

$$\frac{\partial\Psi}{\partial r}=0,\ \frac{\partial\Psi}{\partial z}=-a\frac{da}{dt}, \qquad \text{on} \quad r=a(t), \tag{2.09}$$

$$\frac{\partial}{\partial r}\left(\frac{1}{r}\frac{\partial\Psi}{\partial r}\right)=0,\ \frac{\partial\Psi}{\partial z}=0, \qquad \text{on} \quad r=0. \tag{2.10}$$

We introduce the following transformation;

$$\eta=\frac{r}{a_0\sqrt{(1-\alpha t)}},\ \Psi=\frac{a_0^2\alpha zF(\eta)}{2},\ \omega=-\frac{\alpha zG(\eta)}{2a_0\left(\sqrt{1-\alpha t}\right)^3}. \tag{2.11}$$

Substituting equation (2.11) into equations (2.08)-(2.10), we obtain

$$\frac{d}{d\eta}\left[\frac{1}{\eta}\frac{d(\eta G)}{d\eta}\right]=R\left[\frac{G}{\eta}\frac{dF}{d\eta}-F\frac{d}{d\eta}\left(\frac{G}{\eta}\right)+\eta\frac{dG}{d\eta}+3G\right],\ G=\frac{d}{d\eta}\left(\frac{1}{\eta}\frac{dF}{d\eta}\right), \tag{2.12}$$

$$\frac{dF}{d\eta}=0,\ F=1, \qquad \text{on} \quad \eta=1, \tag{2.13}$$

$$\frac{d}{d\eta}\left(\frac{1}{\eta}\frac{dF}{d\eta}\right)=0,\ F=0, \qquad \text{on} \qquad \eta=0, \tag{2.14}$$

where $R=a_0^2\alpha/2\upsilon$ is the local Reynolds number ($R>0$ represents contraction while $R<0$ represents expansion of the tube's wall).

3. METHOD OF SOLUTION

To solve equations (2.12)-(2.14), it is convenient to take a power series expansion in the flow local Reynolds number R, i.e.,

$$F=\sum_{i=0}^{\infty}F_iR^i,\ G=\sum_{i=0}^{\infty}G_iR^i, \tag{3.01}$$

substitute (3.01) into equations (2.12) –(2.14) and collecting the coefficients of like powers of R, we obtain the following;

Zeroth Order:

$$\frac{d}{d\eta}\left(\frac{1}{\eta}\frac{d(\eta G_0)}{d\eta}\right)=0,\ G_0=\frac{d}{d\eta}\left(\frac{1}{\eta}\frac{dF_0}{d\eta}\right), \tag{3.02}$$

$$\frac{dF_0}{d\eta}=0,\ \ F_0=1, \qquad \text{on} \qquad \eta=1, \tag{3.03}$$

$$\frac{d}{d\eta}\left(\frac{1}{\eta}\frac{dF_0}{d\eta}\right)=0,\ \ F_0=0, \qquad \text{on} \qquad \eta=0, \tag{3.04}$$

Higher Order ($n\geq 1$):

$$\frac{d}{d\eta}\left(\frac{1}{\eta}\frac{d(\eta G_n}{d\eta}\right)=R\left[\sum_{i=0}^{n-1}\left(\frac{G_i}{\eta}\frac{dF_{n-i-1}}{d\eta}-F_i\frac{d}{d\eta}\left(\frac{G_{n-i-1}}{\eta}\right)\right)+\eta\frac{dG_{n-1}}{d\eta}+3G_{n-1}\right],\ G_n=\frac{d}{d\eta}\left(\frac{1}{\eta}\frac{dF_n}{d\eta}\right), \tag{3.05}$$

$$\frac{dF_n}{d\eta}=0,\ \ F_n=0, \qquad \text{on} \qquad \eta=1, \tag{3.06}$$

$$\frac{d}{d\eta}\left(\frac{1}{\eta}\frac{dF_n}{d\eta}\right)=0,\ \ F_n=0, \qquad \text{on} \qquad \eta=0. \tag{3.07}$$

We have written a MAPLE program that calculates successively the coefficients of the solution series. In outline, it consists of the following segments:

(1) Declaration of arrays for the solution series coefficients e.g. F= array(0..43), G=array (0..43).
(2) Input the leading order term and their derivatives i.e. F_0 , G_0.
(3) Using a MAPLE loop procedure, iterate to solve equations (3.05)-(3.07) for the higher order terms i.e. F_n, G_n, n=1,2,3,….
(4) Compute the skin friction and axial pressure gradient coefficients.

Details of the MAPLE program can be found in the appendix. Some of the solution stream-function and vorticity are then given as follows:

$$F(\eta) = (2\eta^2 - \eta^4) + \frac{R\eta^2}{36}(\eta^2 - 1)^2(\eta^2 - 10) + \frac{R^2\eta^2}{1940400}(\eta^2 - 1)^2(2\eta^6 - 101\eta^4 + 596\eta^2 - 1057) + O(R^3), \tag{3.08}$$

$$G(\eta) = -8\eta + \frac{2Rr}{3}(2\eta^4 - 12\eta^3 + 7) - \frac{R^2\eta}{135}(3\eta^8 - 105\eta^6 + 480\eta^4 - 705\eta^2 + 271) + O(R^3). \tag{3.09}$$

The wall skin friction is given by

$$\tau_w = -\mu \frac{\partial u}{\partial r} = -\frac{\alpha\mu z}{2a_0\left(\sqrt{(1-\alpha t)}\right)^3} \frac{d}{d\eta}\left(\frac{1}{\eta}\frac{dF}{d\eta}\right) \quad \text{at } \eta = 1, \tag{3.10}$$

where μ is the coefficient of dynamic viscosity. From the axial component of the Navier-Stokes equations, the pressure drop in the longitudinal direction can be obtained. Let

$$\frac{\partial P}{\partial z} = \frac{\mu\alpha z A}{2a_0^2(1-\alpha t)^2}, \tag{3.11}$$

we substitute (2.11) together with (3.11) into (1.01) and obtain

$$A = \frac{1}{\eta}\frac{d}{d\eta}\left[\eta\frac{d}{d\eta}\left(\frac{1}{\eta}\frac{dF}{d\eta}\right)\right] - R\left(\left(\frac{1}{\eta}\frac{dF}{d\eta}\right)^2 - \frac{F}{\eta}\frac{d}{d\eta}\left(\frac{1}{\eta}\frac{dF}{d\eta}\right) + \eta\frac{d}{d\eta}\left(\frac{1}{\eta}\frac{dF}{d\eta}\right) + \frac{2}{\eta}\frac{dF}{d\eta}\right). \tag{3.12}$$

4. Computer Extended Series Solution

In order to investigate the flow structure at moderately large Reynolds numbers, we expand H=-G(η) at η=1 and A representing wall skin friction and axial pressure gradient parameters respectively, in powers of the Reynolds number R, i.e.

$$H = 8 + 2R - \frac{56R^2}{135} + \frac{3389R^3}{22680} - \frac{5104949R^4}{81648000} + \frac{12136339R^5}{143700480} + \ldots \tag{4.01}$$

$$A = 8 + \frac{38R}{3} - \frac{152R^2}{135} + \frac{3287R^3}{7560} - \frac{15420829R^4}{81648000} + \frac{133921837R^5}{1539648000} + \ldots \tag{4.02}$$

We compute the first 44 coefficients of the above series as shown in Table (4.01) below. The signs of the coefficients alternate after the second term and are monotonically decreasing in magnitude. Hence, the convergence of the series may be limited by a singularity on the negative real axis.

Table (4.01): *Computation showing the coefficients of skin friction (H) and the axial pressure gradient (A).*

I	*H*[I]	*A*[I]
0	8.00000000000000000000	8.00000000000000000000
1	2.00000000000000000000	12.6666666666666666666
2	-0.4148148148148148148148	-1.125925925925925925925
3	0.1494268077601410934744	0.4347883597883597883597
4	-0.0625238707622966882226	-0.1888696477562218302959

5	0.0281519333361540151663	0.0869821134441119009020
6	-0.0132724706996553826849	-0.0416211775640870658507
7	0.0064643388160512792644	0.0204834857891982133353
8	-0.0032265990912916592118	-0.0103027895546493893152
9	0.0016417802495310663793	0.0052732235273090776156
10	-0.0008484311187308859129	-0.0027377428203082558834
11	0.0004440820648382163006	0.0014383673576706599757
12	-0.0002349402466731163546	-0.0007633259858988316029
13	0.0001254305567430137767	0.0004085881358779705208
14	-0.0000674917367212586422	-0.0002203406416769250305
15	0.0000365642147638740717	0.0001195992765265208744
16	-0.0000199277638520420002	-0.0000652907605394189572
17	0.0000109183831428787684	0.0000358248604550732079
18	$-0.6010425269329513\text{1}\times10^{-5}$	-0.0000197465699469006895
19	$0.33226732632656363\times10^{-5}$	0.0000109288257549187453
20	$-0.18438486165334343\times10^{-5}$	$-0.6070983316920430\times10^{-5}$
21	$0.10267460443666857\times10^{-5}$	$0.33837697772319878\times10^{-5}$
22	$-0.57354398864899106\times10^{-6}$	$-0.18917804092095402\times10^{-5}$
23	$0.32130638137606970\times10^{-6}$	$0.10606127724960538\times10^{-5}$
24	$-0.18047552471895858\times10^{-6}$	$-0.59615721680683764\times10^{-6}$
25	$0.10161859240932710\times10^{-6}$	$0.33588889421710805\times10^{-6}$
26	$-0.5734608688398468\times10^{-7}$	$-0.18966368143603949\times10^{-6}$
27	$0.32429391236793735\times10^{-7}$	$0.10731428830386769\times10^{-6}$
28	$-0.18374451829805262\times10^{-7}$	$-0.60835082276469294\times10^{-7}$
29	$0.10429735365447369\times10^{-7}$	$0.345476396215183357\times10^{-7}$
30	$-0.59301252514417988\times10^{-8}$	$-0.19651710560692073\times10^{-7}$
31	$0.33770651565496140\times10^{-8}$	$0.111957897005567141\times10^{-7}$
32	$-0.1926006091458700\times10^{-8}$	$-0.63876388090257912\times10^{-8}$
33	$0.10999677996265670\times10^{-8}$	$0.364938537339216432\times10^{-8}$
34	$-0.62902978347529542\times10^{-9}$	$-0.20876544368137609\times10^{-8}$
35	$0.36016306705767121\times10^{-9}$	$0.119570938332980531\times10^{-8}$
36	$-0.20645924643932868\times10^{-9}$	$-0.68563344512564036\times10^{-9}$
37	$0.11848122398245690\times10^{-9}$	$0.393578321549529340\times10^{-9}$
38	$-0.68064353071254785\times10^{-10}$	$-0.22616151458953450\times10^{-9}$
39	$0.39140086061786793\times10^{-10}$	$0.130086427859861979\times10^{-9}$
40	$-0.22528604394664139\times10^{-10}$	$-0.74894526488293995\times10^{-10}$
41	$0.12978885564204897\times10^{-10}$	$0.431572279542049867\times10^{-10}$
42	$-0.74836362617043105\times10^{-11}$	$-0.24889966117313476\times10^{-10}$
43	$0.43185993904897869\times10^{-11}$	$0.143663202118368715\times10^{-10}$

5. SERIES IMPROVEMENT TECHNIQUE: (A NEW APPROACH)

The main tool of this paper is a simple technique of series summation based on the generalization of Padé approximants and may be described as follows. Let us suppose that the partial sum

$$U_{N-1}(\lambda) = \sum_{i=0}^{N-1} a_i \lambda^i = U(\lambda) + O(\lambda^N) \text{ as } \lambda \to 0, \tag{5.01}$$

is given. We are concerned with the bifurcation study by analytic continuation as well as the dominant behaviour of the solution by using partial sum (5.01). We expect that the accuracy of the critical parameters will ensure the accuracy of the solution. It is well known that the dominant behaviour of a solution of a linear ODE can often be written as Guttmann (1989)

$$U(\lambda) \approx \begin{cases} K(\lambda_C - \lambda)^{\alpha} & \text{for} \quad \alpha \neq 0, 1, 2, \ldots \\ K(\lambda_C - \lambda)^{\alpha} \ln|\lambda_C - \lambda| & \text{for} \quad \alpha = 0, 1, 2, \ldots \end{cases} \quad \text{as } \lambda \to \lambda_C \tag{5.02}$$

where K is some constant and λ_c is the critical point with the exponent α. However, we shall make the simplest hypothesis in the contest of nonlinear problems by assuming the $U(\lambda)$ is the local representation of an algebraic function of λ. Therefore, we seek an expression of the form

$$F_d(\lambda, U_{N-1}) = A_{0N}(\lambda) + A_{1N}^d(\lambda)U^{(1)} + A_{2N}^d(\lambda)U^{(2)} + A_{3N}^d(\lambda)U^{(3)}, \tag{5.03}$$

such that

$$A_{0N}(\lambda)=1, \; A_{iN}(\lambda) = \sum_{j=1}^{d+i} b_{ij}\lambda^{j-1}, \tag{5.04}$$

and

$$F_d(\lambda, U) = O(\lambda^{N+1}) \quad \text{as } \lambda \to 0, \tag{5.05}$$

where $d \geq 1$, i =1, 2, 3. The condition (5.04) nomalises the F_d and ensures that the order of series A_{iN} increases as i and d increase in value. There are thus 3(2+d) undetermined coefficients b_{ij} in the expression (5.03). The requirement (5.05) reduces the problem to a system of N linear equations for the unknown coefficients of F_d. The entries of the underlying matrix depend only on the N given coefficients a_i. Henceforth, we shall take

$$N=3(2+d), \tag{5.06}$$

so that the number of equations equals the number of unknowns. Equation (5.05) is a new special type of Hermite-Padé approximants. Both the algebraic and differential approximants form of equation (5.05) are considered. For instance, we let

$$U^{(1)}=U, \;\; U^{(2)}=U^2, \;\; U^{(3)}=U^3, \tag{5.07}$$

and obtain a cubic Padé approximant. This gives an extension of the idea of quadratic Padé approximants by Shafer (1974) and Sergeev (1986). Furthermore, Sergeev and Goodson (1998), Drazin and Tourigny (1996) had also suggested a similar form of higher order algebraic approximants. Generally, this enables us to obtain solution branches of the underlying problem in addition to the one represented by the original series. In the same manner, we let

$$U^{(1)}=U, \;\; U^{(2)}=DU, \;\; U^{(3)}=D^2U, \tag{5.08}$$

in equation (5.04), where D is the differential operator given by $D=d/d\lambda$. This leads to a second order differential approximants. It is an extension of the integral approximants idea by Hunter and Baker (1979) and enables us to obtain the dominant singularity in the flow field i.e. by equating the coefficient $A_{3N}(\lambda)$ in the equation (5.05) to zero. The critical exponent α_N can easily be found by using Newton's polygon algorithm. However, it is well known that, in the case of algebraic equations, the only singularities that are structurally stable are simple turning points. Hence, in practice, one almost invariably obtains α_N =1/2. If we assume a singularity of algebraic type as in equation (5.02), then the exponent may be approximated by

$$\alpha_N = 1 - \frac{A_{2N}(\lambda_{CN})}{DA_{3N}(\lambda_{CN})}. \tag{5.09}$$

Using the above procedure, we performed series summation and improvement study on the solution series obtained in Table (4.01). Our results show the dominant singularity in the flow field to be R_c=-1.6739367347720807 (which corresponds to the radius of convergence and the turning point in the flow field) with the critical exponent α_C =0.5 as shown in the table (5.01). We also noticed that $A \sim A_{-1}/R$ and $H \sim H_{-1}/R$ as $R \to 0$ on the secondary solution branch where $A_{-1} \approx$-280.98050 and $H_{-1} \approx$-67.6702067. It is noteworthy to mention that the wall shear stress $H \to 0$ as $R \to$-1.6431409627402, i.e., separation and possible flow reversal occur due to tube wall expansion.

Table (5.01): Computation showing the dominant singularity, secondary solution branch asymptotic behaviour and critical exponent.

d	N	R_C	A_{-1}	H_{-1}	α_C
1	9	-1.6863617034262282	-------------	-------------	0.331632240
3	15	-1.6739700125855259	-276.48020	67.3394184	0.498634106
5	21	-1.6739367218509650	-281.11885	67.6661825	0.498726578
7	27	-1.6739367371687654	-280.98120	67.6702443	0.500000000
9	33	-1.6739367347718036	-280.98046	67.6702065	0.500000000
11	39	-1.6739367347720807	-280.98050	67.6702067	0.500000000
12	42	-1.6739367347720807	-280.98050	67.6702067	0.500000000

6. Graphical results and discussion

In fig.6.01, we observed that the fluid axial velocity profile is parabolic with maximum value at centerline and minimum at the plates. It is interesting to note that the fluid axial velocity generally decreases with an increase in tube contraction due to the strong influence of the negative transmural pressure owing to marked reduction of rigidity (i.e. R>0). In reality, this is possible, since contraction brings about a reduction in the tube's cross-sectional area, hence, decreasing the amount of flow passing through the compressed region. Table 5.01, shows the convergence of the dominant singularity R_c in the flow field together with its corresponding exponent α_c, as well as the asymptotic behaviour of wall skin friction and pressure gradient as the flow Reynolds number tends to zero. It is noteworthy also that R_c is the bifurcation point and lies in the negative real axis of the flow Reynolds number R, i.e. the region representing tube's contraction. This critical value of Reynolds number enables the biomedical engineers to determine accurately the maximum expansion of the tube walls due to the variation in the tube's external and internal pressure i.e. $a_0 = \sqrt{2\upsilon R_c/\alpha}$. Figs.6.02 and 6.03 show the sketch of bifurcation diagrams for the skin friction and fluid axial pressure gradient parameters. For tube's contraction i.e. R>0, only one solution branch exist i.e. type I. This is the primary solution branch and it shows that the wall skin friction and fluid axial pressure gradient increase with increase in R. In the expansion region, i.e. R < 0, two solution branches are identified (i.e. type I, II). A simple turning point with exponent α_c=0.5 exsits between type I and type II solution branches i.e. R_c. We observed that the type II solution is physically unreasonable but mathematically interesting. It is interesting to note that the turning point here also corresponds to the dominant singularity in the flow field.

Finally, in this paper, we have proposed a new form of series summation and improvement technique based on the generalizations of Padé approximants, i.e. a special type of Hermite-Padé approximant. We have applied this method to investigate the problem of squeezing flow in parallel plates viscometer with great success. The chief novelty of this procedure is its ability to reveal the dominant singularities together with solution branches of the underlying nonlinear problem in addition to the branch represented locally by the original series. Generally, we have found that this new method is very competitive. However, we have not yet developed a theory that would explain its strengths and limitations and so we have relied on intelligent numerical investigation.

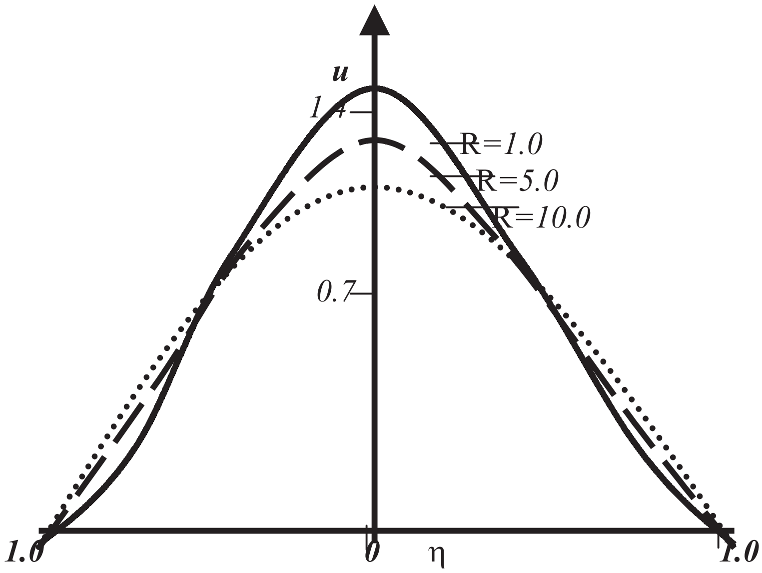

Fig. 6.01 Axial velocity profile during tube contraction (R>0).

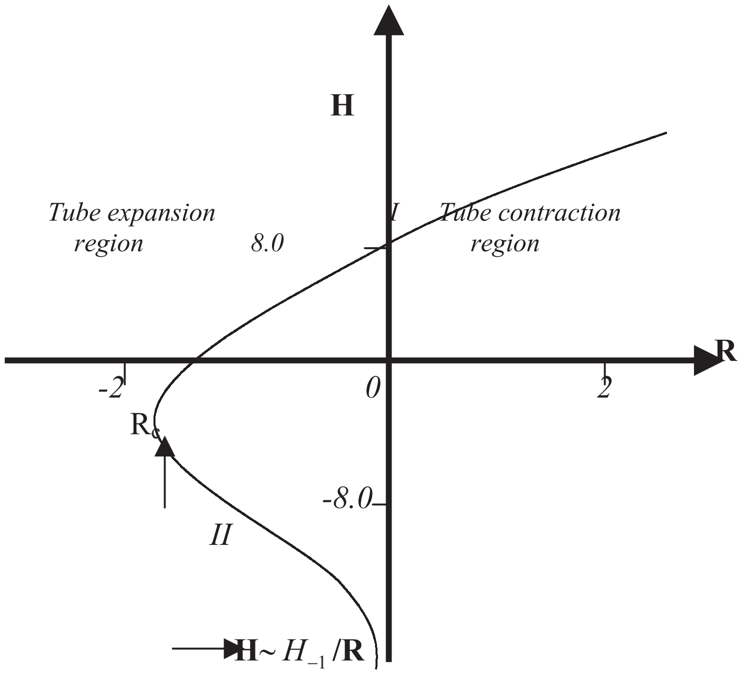

Fig. 6.02 A sketch of bifurcation diagram for skin friction.

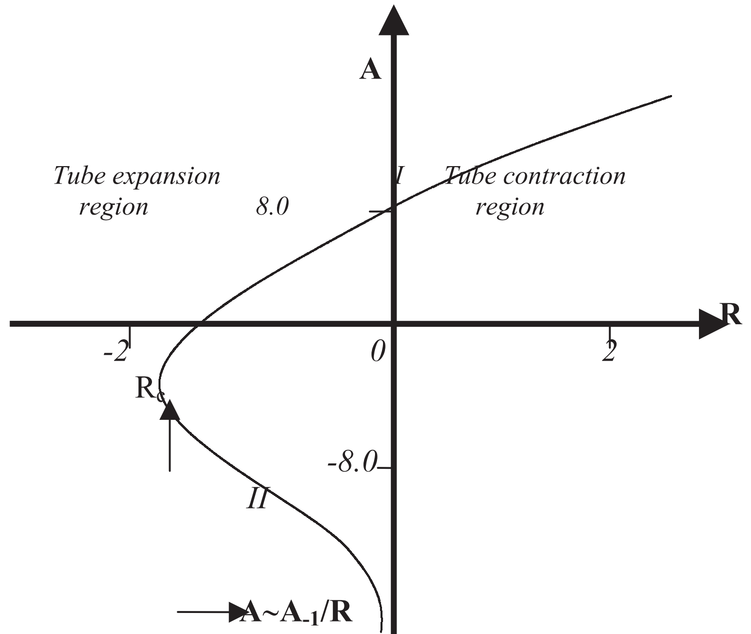

Fig. 6.03 A sketch of bifurcation diagram for axial pressure gradient.

Appendix

A1: The Maple procedure to solve the equations (3.05) to (3.07).

```
#  Here we declare the arrays to store the computed results
          F:=array(0..34): G:=array(0..34): Fr:=array(0..34): Gr:=array(0..34):
# Here we input the zero order solution F[0] and G[0].
          F[0]:=(2*r^2-r^4): G[0]:=-8*r:
          Fr[0]:=diff(F[0],r): Gr[0]:=diff(G[0],r):
# This computes the higher order teams i.e. n>0.
          for n from 1 by 1 to 43 do
          A1:=normal(1/r*sum(g[i]*fr[n-i-1]+f[i]*(g[n-i-1]/r-gr[n-i-1]),i=0..n1)):
          A2:=normal(r*gr[n-1]+3*g[n-1]):
          A:=R*(A1+A2):
          A1:=0:A2:=0:  g11:=normal(r*(int(A,r)+K)):
          A:=0: g1:=normal(int(g11,r)/r):
          g11:=0: f11:=normal(r*(int(g1,r)+M)):
          f1:=normal(int(f11,r)):
          r:=1: K:=normal(solve(f11=0,K): M:=normal(solve(f1=0,M)):
          r:='r':
          f11:=0: F[n]:=normal(f1):
          f1:=0:  G[n]:=normal(g1):
          g1:=0: Fr[n]:=normal(diff(F[n],r)): Gr[n]:=normal(diff(G[n],r)):
          K:='K': M:='M': print(F[n]); print(G[n]);
# Here we compute the wall skin friction coefficients.
          print(evalf(sub(r=1,G[n])));
          od: quit();
```

Reference

[1] Bertram, C. D., Unstable equilibrium behaviour in collapsible tubes, *J. Biomech.* **19** (1986), 61-69.

[2] Bertram, C. D., and Pedley, T. J., A mathematical model of unsteady collapsible tube behaviour, *J. Biomech.* **15** (1982), 39-50.
[3] Bertram, C. D., and Raymond, C. J., Measurements of wave speed and compliance in a collapsible tube during self-excited oscillations: A test of the choking hypothesis, *Med. Biol. Eng. Comput.* **29** (1991), 493-500.
[4] Bertram, C. D., Raymond, C. J., and Pedley, T. J., Mapping of instabilities for flow through collapsible tubes of deferring length, *J. Fluids. Struct.* **4** (1990), 125-153.
[5] Bertram, C. D., Raymond, C. J., and Pedley, T. J., Application of nonlinear dynamics concepts to the analysis of self- excited oscillations of a collapsible tube conveying a fluid, *J. Fluids. Struck.* **5** (1991), 391-287.
[6] Bonis, M., and Ribreau, C., Etude de quelques proprietes de I'ecoulement dans une conduite collabable, *La Houille Blanche* **3-4** (1987), 165-173.
[7] Brower, R. W., and Scholten, C., Experimental evidence on the mechanism for the instability of flow in collapsible vessels, *Med. Biol. Engng* **13** (1975), 839-845.
[8] Contrad, W. A., Pressure-flow relationship in collapsible tubes, *IEEE Trans. Bio-Med. Engng BME*-**16** (1969), 284-295.
[9] Cowley, S. J., Elastic jumps in fluid -filled elastic tubes, *J. Fluid Mech.* **116** (1982), 459-473.
[10] Cowley, S. J., On the wavetrains associated with elastic jumps on fluid- filled elastic tubes, *Q. J. Mech. Appl. Math.* **36** (1983), 289-312.
[11] Domb, C and Sykes, M. F., On the susceptibility of a ferromagnetic above the Curie point, *Proc. R. Soc. London, Ser. A,* **240** (1957), 214-228.
[12] Drazin, P. G., and Tourigny, Y., Numerical study of bifurcations by analytic continuation of a function defined by a power series, *SIAM J. Appl. Math.* **56** (1996), 1-18.
[13] Elad, D., Kamm, R. D., and Shapiro, A. H., Choking phenomena in a lung-like model, *ASME J. Biomech. Engng* **109** (1987), 1-9.
[14] Flaherty, J. E., Keller, J. B., and Rubinow, S. I., Post buckling behaviour of elastic tubes and rings with opposite sides in contact, *SIAM J. Appl. Math***.** **23** (1972), 446 – 455.
[15] Grotberg, J. B., Pulmonary flow and transport phenomena, *Ann. Rev. Fluid Mech.* **26** (1971), 529-571.
[16] Guttamann, A. J., Asymptotic analysis of power –series expansions, Phase Transitions and Critical Phenomena, *C. Domb and J. K. Lebowitz, eds.* Academic Press, New York, (1989) pp. 1-234.
[17] Hunter, C., and Guerrieri, B., Deducing the properties of singularities of functions from their Taylor series coefficients, *SIAM J. Appl. Math.,* **39** (1980), 248-263.
[18] Hunter, D. L. and Baker G. A., Methods of series analysis III: Integral approximant methods, *Phys. Rev. B* **19** (1979), 3808-3821.
[19] Heil, M., Stokes flow in collapsible tubes-computational and experiment, *J. Fluid Mech.,* **353** (1997), 285-312.
[20] Makinde, O. D., Extending the utility of perturbation series in problems of laminar flow in a porous pipe and a diverging channel, *Jour. of Austral. Math. Soc. Ser. B* **41** (1999), 118-128.
[21] Makinde, O. D., Heat and mass transfer in a pipe with moving surface: Effects of viscosity variation and energy dissipation, *Quaestiones Mathematicae,* **24** (2001), 97-108.
[22] Makinde, O. D., Motsumi, T. G., and Ramollo, M. P., Squeezing flow between parallel plates: A bifurcation study*, Far East Jour. Appl. Math.,.* **9,** 2 (2002), 81-94.
[23] Shafer, R. E., On quadratic approximation, *SIAM J. Numer.Anal.,* **11** (1974), 447-460.
[24] Sergeev, A. V. A recursive algorithm for Padé–Hermite approximations, *U.S.S.R. Comput. Math. Phys.* **26** (1986), 17-22.
[25] Sergeev, A. V. and Goodson, A. Z. Summation of asymptotic expansions of multiple-valued functions using algebraic approximants: Application to anharmonic oscillators, *J. Phys., A: Math. Gen.* **31** (1998), 4301-4317.

Project of a hybric-heuristical algorithm
Progetto di un algoritmo ibrido-euristico

L. Marra

Abstract. Starting with the analysis of some algorithms of CLP we introduce the concept of metabox and establish an algorithm which provides good results for volumetric reasons, for the weight balancing and for the management of the boarding and unloading. A special attention is drawn to the fragility of the objects contained in the package. This is the crucial problem for the senders. It is implied in the most transports.

Sommario. Partendo dall'analisi di alcuni algoritmi del CLP si introduce il concetto di metascatola e si mette a punto un algoritmo che oltre a fornire dei buoni risultati per quanto riguarda la resa volumetri-ca, raggiunge buoni risultati per quanto riguarda il bilanciamento del peso e la gestione delle operazioni di carico e scarico. Particolare attenzione viene posta poi al problema della fragilità degli oggetti contenuti nel pacco, problema cruciale per gli spedizionieri e che coinvolge la maggior parte dei trasporti.

1. Introduzione

Si affronta il progetto e lo sviluppo di un algoritmo per la soluzione del problema relativo al caricamento di un container (CLP). Le basi di tale algoritmo sono euristiche e si sono fatte delle scelte con il dichiarato obiettivo di rispondere contemporaneamente ad alcune delle diverse problematiche presentate dal CLP quali, entrando nello specifico, la resa volumetrica (AVU[1]), la stabilità, il bilanciamento del peso ed un'agevole gestione delle operazioni di carico e scarico. Si sono attinte idee dai modelli di vari studiosi che si è cercato poi di migliorare ed è quindi per questo motivo che l'algoritmo che s'introdurrà, oltre che essere euristico, è stato chiamato anche ibrido.

I modelli presi in considerazione sono quelli di Bischoff e Davies [25], quello di Gehring-Menschner-Meyer [11] ed infine quello di Bischoff-Ratcliff [19] per cui l'algoritmo proposto non è del tutto innovativo ma ha fondamentalmente l'intento di sperimentare l'efficienza di una serie di regole euristiche costituenti un sistema di caricamento che mira al conseguimento di diversi scopi, in particolare quello di una buona performance volumetrica. Inoltre, giacché una delle caratteristiche adottate è quella di concepire il caricamento del container per sezioni verticali (muri) indipendenti, il metodo si presterebbe anche a rispondere ad esigenze del tipo multi-drop[2] ma ciò andrebbe ovviamente a discapito di un buon riempimento complessivo del container stesso.

Ad ogni modo l'algoritmo è stato tradotto in un software (in linguaggio Matlab®) ed è stato fornito di un'interfaccia grafica del cui concepimento teorico si parlerà in un prossimo lavoro.

1.2 Obiettivi ed approccio risolutivo dell'algoritmo

Riprendendo quanto affermato, lo sviluppo dell'algoritmo ibrido-euristico per la risoluzione del CLP si propone il raggiungimento contemporaneo dei seguenti obiettivi:

A. Ottenimento di una buona efficienza volumetrica.
B. Sistemazione geometrica delle scatole in modo da garantire un'adeguata stabilità dell'intero carico.
C. Agevole manovrabilità nelle operazioni di carico e scarico.
D. Possibilità di gestione di carichi del tipo multi-drop.
E. Possibilità di operazioni di *post-processing* mirate a realizzare una distribuzione bilanciata del peso all'interno del container.

---

[1] Acronimo di *Average Volume Utilization* (ossia utilizzazione media del volume)
[2] Trattasi dell'ipotesi di un carico che è suddiviso in più di una destinazione

I punti C, D ed E si possono concretizzare pensando ad un caricamento del container per sezioni (muri) indipendenti. Ora, tali sezioni potrebbero immaginarsi tanto in senso orizzontale quanto in senso verticale; ai fini, però, del perseguimento dell'altro obiettivo B, è ovvio far ricadere la scelta su un riempimento per sezioni verticali e ciò in virtù dei risultati negativi prodotti dall'analisi di stabilità del metodo GMM che prevede al contrario la sistemazione del carico per strati orizzontali.

Riguardo infine al punto A si è deciso di realizzare la costruzione di ogni singolo muro attraverso l'impiego di "metascatole" che possono essere definite come un insieme di scatole appartenenti ad una stessa tipologia (quindi scatole omogenee) e raggruppate tra loro spazialmente in modo da apparire come un'unica grande scatola. Va da sé che, al limite, per metascatola si può anche intendere il singolo pacco! Il motivo di una tale scelta risiede ovviamente nel tentativo di rendere la strategia di caricamento migliore da un punto di vista dell'occupazione del container e ciò sulla base di due considerazioni empiriche: la prima scaturisce dalla natura stessa del CLP per cui, essendo il problema di fondo quello di colmare uno spazio assegnato con un numero di oggetti, più piccoli, di varie dimensioni, è evidente che si otterrà una sistemazione tanto

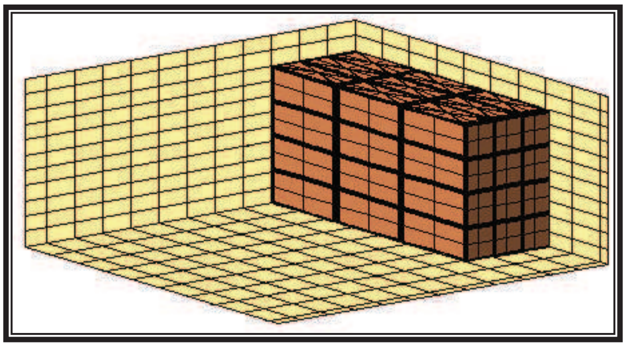

Figura 1.Esempio di metascatola costituita da 36 scatole omogenee, ossia appartenenti ad una stessa tipologia

migliore quanto più sarà efficiente la combinazione di tali oggetti nel processo di allocazione ed è quindi altrettanto evidente che, in tal senso, non esiste combinazione più vantaggiosa di quella di affiancare tra loro oggetti di identiche dimensioni. La seconda considerazione guarda, invece, ad un altro fatto oggettivo vale a dire che una metascatola offre, agli eventuali altri pacchi che potrebbero trovare posto su di essa, una superficie d'appoggio certamente superiore a quella offerta da una scatola singola.

Chiaramente un simile modo di agire si discosta da quanto previsto dal metodo BR di Bischoff-Ratcliff che considera sempre il concetto di muro (sezione verticale del container), ma con la differenza che esso è formato da colonne o subcolonne aventi come base un'unica scatola. D'altra parte, in quel metodo, la strategia impiegata è votata alla gestione di carichi multi-drop per i quali, nel processo di riempimento del singolo muro, ove verranno assegnati oggetti aventi tutti la stessa destinazione, in effetti, il numero di tipologie e la relativa numerosità delle scatole da piazzare sono piuttosto limitati. Ma questa è una possibilità che, di fatto, non è esclusa a priori dall'algoritmo ibrido-euristico che, per come definisce la metascatola, arriva a contemplare anche, come caso limite, situazioni come quelle considerate in BR. In altre parole, considerata una generica tipologia di pacchi, la filosofia è quella di costruire metascatole grandi se la disponibilità di pacchi è grande, e metascatole più piccole (colonne, subcolonne o addirittura un unico pezzo) se viceversa la disponibilità è più piccola.

Quello che in realtà si riduce, pensando ad un riempimento del container tramite metascatole, è la possibilità di effettuare operazioni di *swapping*[3] tra le parti indipendenti del carico per il bilanciamento del peso. E' evidente, infatti, che quanto più piccole sono le parti in cui viene frazionato l'intero carico, tanto maggiori saranno le possibilità di scambiare tra di loro le varie parti per una più omogenea distribuzione delle masse. E sotto questo aspetto il metodo BR è certamente più performante, poiché prevede, oltre alla suddivisione del carico complessivo in muri, la suddivisione dei muri in colonne isolate. Tuttavia va anche detto che questo elemento di vantaggio si manifesta essenzialmente quando si ha a che fare con carichi

[3] Sostituzione, scambio

debolmente eterogenei, mentre per carichi più eterogenei la differenza diventa più lieve giacché, a parità di volume totale del carico, un maggior numero di tipologie vuol dire mediamente un minor numero di scatole per tipologia e quindi l'impossibilità di costruire metascatole relativamente grandi.

Rispetto al metodo BR, viceversa, la costituzione di metascatole garantisce una migliore stabilità e ciò grazie ad un impaccamento che è compatto proprio perché formato da scatole appartenenti ad una stessa tipologia. Stavolta, esattamente al contrario di quanto visto poc'anzi, gli effetti positivi della stabilità sono più presenti nell'ipotesi di carichi debolmente eterogenei e meno in quella di carichi maggiormente eterogenei.

In definitiva il layout di carico risultante dalle scelte operate, è frutto di un problema di taglio tridimensionale, essendo costituito da una serie d'unità ciascuna descrivibile sempre come un set ghigliottinabile: la prima regione d'indagine è costituita dal volume del container che è suddivisibile in muri, quindi ogni muro risulterà composto da metascatole, ed infine ogni metascatola da scatole di tipo omogeneo. L'organizzazione finale si presenta quindi come una struttura gerarchica che si può tranquillamente accostare a quella tipica dei frattali.

Si conclude il paragrafo ricordando la natura euristica dell'algoritmo realizzato, quindi sottolineando la consapevolezza riguardo alle varie penalità che una tale scelta comporta. Fra tutte, l'appena ricordata suddivisione del carico in una sequenza di set ghigliottinabili che vuol dire frammentazione a più livelli dello spazio da colmare e, in definitiva, una ridotta capacità in termini di utilizzazione del volume.

1.3 Procedura risolutiva generale

Anzitutto viene fissato un sistema di riferimento cartesiano solidale con il container come quello rappresentato in figura 2.6. L'origine coincide con il vertice inferiore sinistro del back-end[4] del container mentre gli assi x, y, z coincidono rispettivamente con la sua lunghezza (o profondità), larghezza ed altezza.

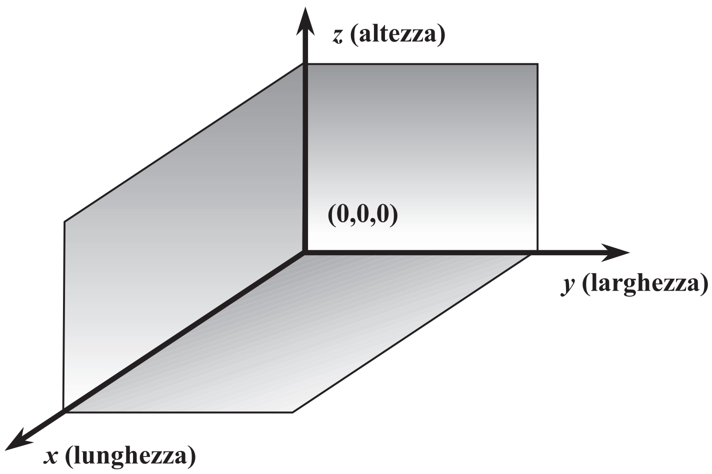

Figura 2.: Sistema di riferimento adottato. L'origine coincide con il vertice in basso a sinistra del *back-end* del container

L'idea di base, quindi, è quella di riempire il container per sezioni (muri) verticali cominciando dal fondo fino ad arrivare al limite del suo lato accessibile. Per quanto riguarda le dimensioni delle sezioni, esse hanno tutte larghezza ed altezza coincidenti con le rispettive dimensioni del container, mentre la profondità e variabile

[4] Ossia la parete verticale del container opposta rispetto a quella d'accesso

dipendendo dalla metascatola che per prima viene allocata nell'operazione di costruzione del muro. In pratica viene utilizzata la definizione per cui la profondità di ogni muro coincide con la dimensione della metascatola (per tale ragione indicata con l'acronimo di LDB[5]) che, dopo il posizionamento, risulta parallela alla lunghezza del container. Il caricamento avrà termine con la costruzione dell'ultimo muro che è possibile individuare grazie all'utilizzo di una variabile RD[6] che conserva, aggiornandolo alla fine della costruzione di ogni muro, il valore della profondità residua del container ancora disponibile per l'alloggiamento di ulteriori pacchi.

In realtà, nella definizione di profondità delle varie sezioni verticali, esiste un'eccezione che riguarda proprio l'ultimo muro. La procedura risolutiva infatti, dopo la costruzione del muro i-simo, effettua sempre un confronto tra la profondità residua del container e quella che dovrebbe essere la profondità del muro successivo (l'i+1-simo): se dal confronto risulta che c'è ancora spazio disponibile, allora si mantiene il muro i-simo e viene avviata la costruzione dell'i+1-simo; viceversa, se lo spazio non è sufficiente, allora il muro i-simo viene smantellato e la profondità residua del container (qual era prima della edificazione dello stesso muro i-simo) viene fissata come profondità dell'ultimo muro. Pertanto, per i primi muri, la profondità è fissata dalla prima metascatola allocata, per l'ultimo è invece fissata dalla profondità residua del container.

Ritornando per un attimo al tema su dimensioni e sistemi di riferimento, è importante notare che tutti gli oggetti considerati, siano essi muri, scatole, metascatole o spazi da allocare, avendo in comune la medesima forma geometrica (e cioè quella di un parallelepipedo), sono tutti individuati in uno stesso modo e cioè attraverso le coordinate del loro vertice più prossimo all'origine del container; in particolare, però, per le metascatole e per le singole scatole il riferimento al sistema cartesiano di figura 2. è indiretto nel senso che, almeno in un primo momento, la loro posizione non è definita rispetto all'origine del container, bensì rispetto a quella del proprio muro d'appartenenza (ossia rispetto al punto del muro definito con la sigla LLBC[7] che serve per individuarne, a sua volta, la posizione).

Entrando ancor di più nel merito delle modalità di realizzazione di un singolo muro, va detto che il principio fondamentale al quale si fa riferimento è quello che, da un lato individua degli spazi da colmare, mentre dall'altro ricerca, all'interno del sotto-set di scatole ancora da caricare, quelle tipologie che meglio si adattano al loro riempimento. Il procedimento è pertanto di tipo iterativo. La generica iterazione è infatti innescata al piazzamento di ogni metascatola, operazione questa che ha due importanti conseguenze: la prima è che si aggiorna la lista delle scatole non ancora caricate, la seconda è che lo spazio ove è stata effettuata l'allocazione risulta partizionato in spazi più piccoli. Prima però di considerare tale frammentazione, è opportuno distinguere il caso della collocazione della prima metascatola del muro da quella di una qualsiasi altra metascatola utilizzata per il suo completamento. Infatti nel primo caso lo spazio risulta suddiviso in tre sottospazi e cioè uno occupato, che è quello dove è sistemata la metascatola, e altri due liberi situati superiormente e lateralmente alla metascatola stessa. Nel secondo caso, invece, i sottospazi generati sono quattro: uno occupato dalla metascatola e altri tre liberi, vale a dire i due del caso precedente più un terzo che si sviluppa frontalmente alla metascatola fino a raggiungere il limite della profondità del muro (e che in effetti non può esistere nel primo caso essendo proprio la prima metascatola del muro a fissarne la profondità).

Ad ogni modo, ciascuno degli spazi via via prodotti è rappresentato con un vettore riga le cui componenti ne contengono le informazioni relative alle dimensioni, alle coordinate e, in alcuni frangenti, relative al volume. Inoltre essi sono successivamente impilati in una lista del tutto simile a quella prevista dal metodo GMM, gestita con tecnica LIFO[8] per cui si tenterà sempre di colmare per primo l'ultimo spazio entrato in elenco. Ovviamente si farà in modo che ad entrare per ultimi nella lista siano gli spazi che, secondo prefissati criteri, hanno priorità maggiore nel processo di riempimento. Un tentativo di allocazione di uno spazio può produrre due risultati: un successo o un insuccesso. Nel primo caso ci sarà produzione di ulteriori tre spazi liberi, nel secondo caso lo spazio verrà semplicemente eliminato dalla lista. Il discorso verrà ripreso ed approfondito ulteriormente nei prossimi paragrafi ove si parlerà più dettagliatamente dell'iter seguito per la realizzazione di un muro.

Si preferisce, invece, fare adesso alcune considerazioni riguardo al set di scatole che costituiscono l'ordine di carico. Innanzitutto, come da prassi adottata dagli altri algoritmi analizzati nei capitoli precedenti, sono prese in considerazione solo scatole non deformabili con dimensioni rettangolari. Quindi in

---

[5] Acronimo di *Layer Determining Box*
[6] Acronimo di *Residual depth*
[7] Acronimo di *Low Left Bottom Corner*
[8] Acronimo di *Larst In First Out*

Figura 3.: Foglio di calcolo Excel→ ove sono raccolte le informazioni sull'ordine di carico. Ogni riga

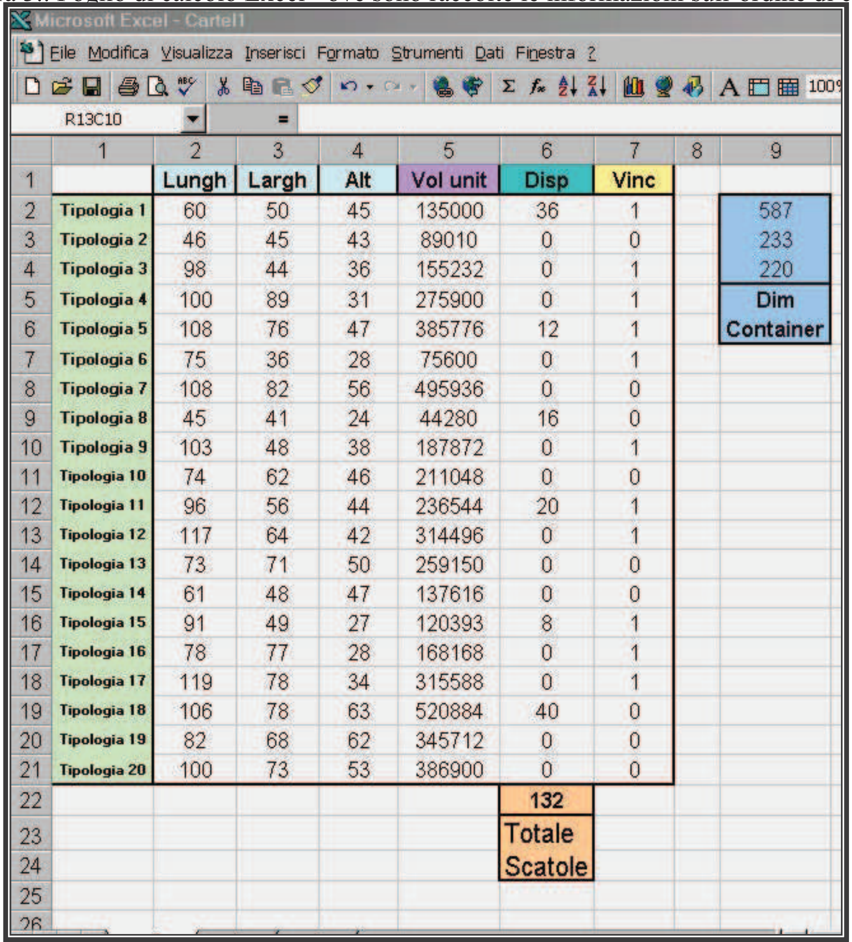

	1	2	3	4	5	6	7	8	9
1		Lungh	Largh	Alt	Vol unit	Disp	Vinc		
2	Tipologia 1	60	50	45	135000	36	1		587
3	Tipologia 2	46	45	43	89010	0	0		233
4	Tipologia 3	98	44	36	155232	0	1		220
5	Tipologia 4	100	89	31	275900	0	1		Dim
6	Tipologia 5	108	76	47	385776	12	1		Container
7	Tipologia 6	75	36	28	75600	0	1		
8	Tipologia 7	108	82	56	495936	0	0		
9	Tipologia 8	45	41	24	44280	16	0		
10	Tipologia 9	103	48	38	187872	0	1		
11	Tipologia 10	74	62	46	211048	0	0		
12	Tipologia 11	96	56	44	236544	20	1		
13	Tipologia 12	117	64	42	314496	0	1		
14	Tipologia 13	73	71	50	259150	0	0		
15	Tipologia 14	61	48	47	137616	0	0		
16	Tipologia 15	91	49	27	120393	8	1		
17	Tipologia 16	78	77	28	168168	0	1		
18	Tipologia 17	119	78	34	315588	0	1		
19	Tipologia 18	106	78	63	520884	40	0		
20	Tipologia 19	82	68	62	345712	0	0		
21	Tipologia 20	100	73	53	386900	0	0		
22						132			
23						Totale			
24						Scatole			
25									

corrisponde ad una tipologia (nell'esempio ne sono considerate 20) rispetto alla quale, nelle varie colonne, sono riportati nell'ordine i seguenti dati: dimensioni della scatola, volume unitario, numero di scatole (numerosità della tipologia), eventuale vincolo sul posizionamento in altezza. Infine, in un riquadro più piccolo sulla destra, vengono inseriti i dati relativi alle dimensioni del container.

un foglio di calcolo Excel→ (riportato in figura 3.6), insieme alle dimensioni del container dove verranno collocate, vengono inseriti tutti i dati che le concernono, ovvero dimensioni, volume unitario, numerosità ed eventuale presenza di un vincolo sul posizionamento in altezza[9]. Quest'ultimo, in particolare, è un dato molto importante; infatti, essendo la logica dell'algoritmo quella di piazzare le scatole in modo da ottenere la più efficiente utilizzazione possibile del volume del container, è lampante che esso, nella ricerca della collocazione migliore, valuti tutte le loro orientazioni[10]. Con la presenza di un vincolo, invece, che obbliga tra l'altro a orientare la relativa scatola in modo che la dimensione vincolata coincida con la sua altezza[11], le possibilità delle orientazioni si riducono notevolmente, per l'esattezza a due che sono quelle corrispondenti alle possibili permutazioni delle dimensioni di base. Naturalmente, questo discorso sulle orientazioni fatto per una scatola, rimane assolutamente valido anche per una metascatola se si considera che, per definizione, essa è ottenuta affiancando e sovrapponendo scatole della stessa tipologia ed orientate tutte nello stesso modo.

---

[9] Tale informazione è affidata ad un indicatore booleano che è posto a "1" quando il vincolo sussiste, altrimenti a "0"

[10] In assenza di vincoli una scatola può essere collocata in 6 modi possibili ossia due (corrispondenti alle possibili permutazioni delle due dimensioni di base) per ciascuno dei tre criteri (corrispondenti alle 3 dimensioni) con cui si può fissare l'altezza

[11] E' difatti per questo che si parla di vincolo sul posizionamento in altezza!

L'ultima rilevante osservazione sulla procedura risolutiva generale dell'algoritmo, riguarda un'operazione di pre-processamento effettuata proprio sulla lista dell'ordine di carico e che, pertanto, precede l'avvio della routine relativa alla costruzione dei muri. Una volta acquisiti i dati dal foglio di calcolo Excel→**,**
Figura 4.: Flowchart illustrante la procedura risolutiva generale proposta dall'algoritmo ibrido-*euristico*

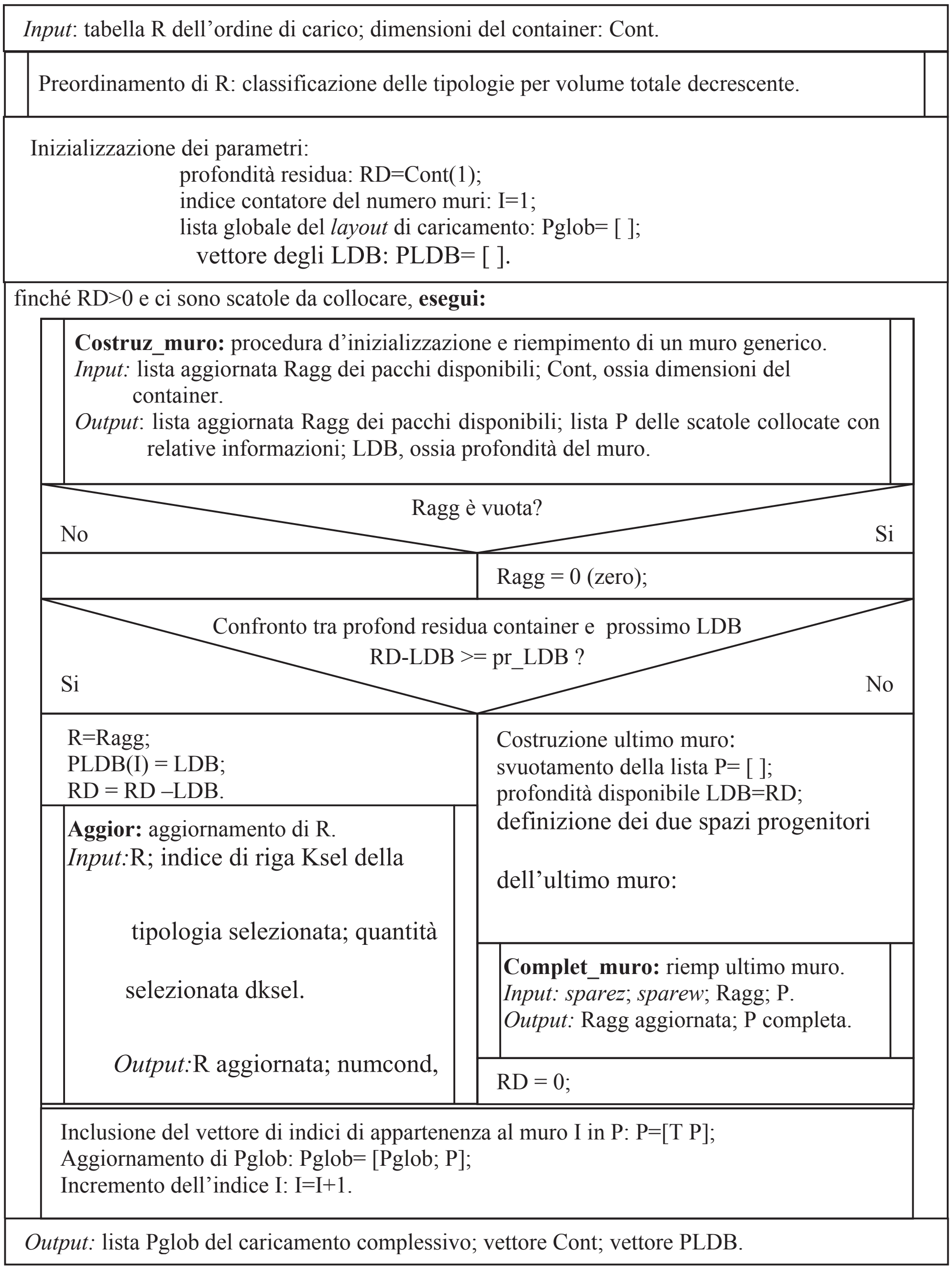

Figura 5.: Flowchart della procedura di costruzione dei muri "Costruz_muro"

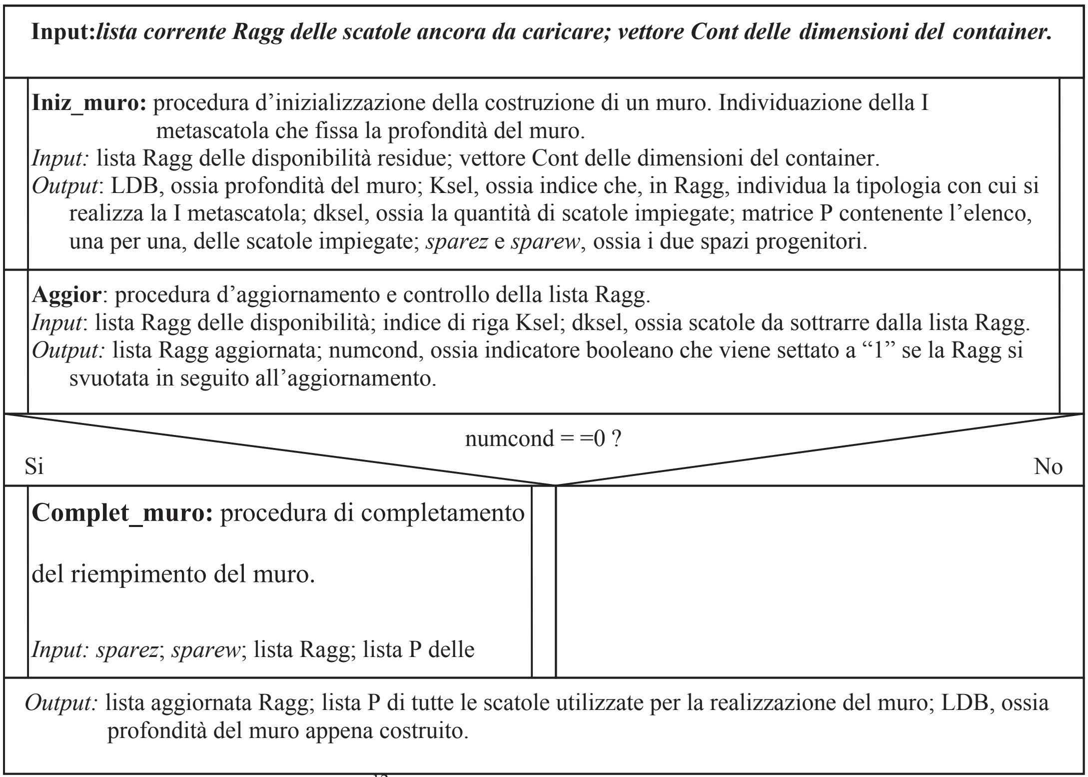

essi vengono, infatti, inseriti in una matrice[12] che viene immediatamente elaborata e riorganizzata in modo tale che la prima riga corrisponda alla tipologia a volume totale[13] maggiore, mentre l'ultima a quella a volume totale minore. In altri termini viene operata una riclassificazione delle tipologie disponibili per volume totale decrescente e, ancora una volta, la ragione che spinge verso questa scelta è da ricercarsi nell'obiettivo di massimizzare la resa volumetrica del caricamento. Il ragionamento che si fa è il seguente: se è vero che è opportuno pensare alla formazione di metascatole[14] e se è vero che un oggetto tanto più è voluminoso, tanto più è difficile sperare di collocarlo andando avanti nel processo di riempimento del container, allora risulta logico cercare di collocare per prima le metascatole più grandi che, verosimilmente, saranno appunto quelle creabili con le scatole della tipologia a volume totale maggiore.

A conclusione del paragrafo, in figura 4., si riporta il flowchart che descrive, abbastanza analiticamente, la procedura risolutiva (del problema del CLP) proposta dall'algoritmo ibrido-euristico. La lettura dei paragrafi successivi aiutano a perfezionarne la comprensione.

1.4 Realizzazione dei muri: procedura "Costruz_muro"

L'algoritmo ibrido-euristico affida l'operazione di costruzione dei muri alla *routine* "Costruz_muro", di cui si può apprezzare il *flowchart* funzionale nella figura 5. Ebbene tale *routine*, come si evince dallo stesso *flowchart*, si avvale a sua volta di altre due *subroutine* ciascuna delle quali si occupa, in pratica, di una delle due fasi attraverso cui si compie la realizzazione di un muro. Il riempimento di una generica sezione verticale del container, in effetti, avviene in due passi successivi:

I passo: inizializzazione del muro attraverso la collocazione di un'opportuna metascatola che ne fisserà la profondità. Di questa fase si occupa la *subroutine* "Iniz_muro";

II passo: completamento del muro inizializzato attraverso la collocazione di un'opportuna serie di metascatole che dovranno tentare di colmare al meglio gli spazi generati dalla prima metascatola. Di quest'altra fase si occupa, invece, la *subroutine* "Complet_muro". Ora, poiché le due procedure

---

[12] Denominata R e che ha tante righe quante sono le tipologie in gioco

[13] Per volume totale di una tipologia s'intende il prodotto del volume unitario della singola scatola per il numero di scatole che la compongono

[14] Cfr. par. 2

d'inizializzazione e di completamento di un muro introdotte hanno in comune solo l'obiettivo, che è quello solito dell'occupazione ottimale del volume del container, mentre per il resto agiscono con tecniche e/o regole empiriche piuttosto differenti, si è preferito affrontarne la trattazione separatamente.

1.4.1 Inizializzazione di un muro

Nella fase d'inizializzazione di un muro, poiché non si pongono a priori limitazioni sulle dimensioni della prima metascatola (le cui misure, d'altra parte, dipenderanno dalla numerosità delle scatole ancora da caricare), teoricamente si ha disposizione tutto lo spazio residuo che resta da occupare (nel caso di costruzione del primo muro, addirittura l'intero container!). E' per tale ragione che, in questo primo stadio operativo, si cercherà sempre di piazzare per prima la più grossa metascatola che, in base delle disponibilità delle varie tipologie, si è in grado di realizzare. Pertanto la regola empirica dominante che si utilizza in questa sede, come già accennato precedentemente, è quella che guarda al principio secondo cui tanto più grande è un oggetto,

Figura 6.: Esempio di "unità logiche": a sinistra il caso di una parete (formata da 3 colonne ognuna composta da 4 pacchi), a destra quello di due pareti.

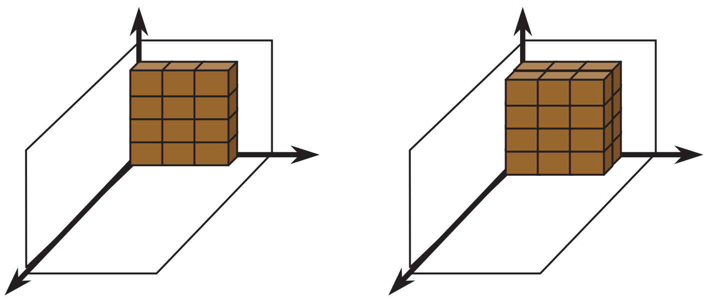

tanto più si abbassano le probabilità di sistemarlo andando avanti nel processo di caricamento.

Detto ciò, è evidente che la procedura d'inizializzazione di un muro creerà la sua metascatola attingendo alla tipologia con volume totale maggiore e che, per il pre-processamento effettuato dall'algoritmo subito dopo l'acquisizione dei dati dal foglio di calcolo Excel, coincide con la prima in testa alla lista di carico. Il problema successivo diventa quindi quello di organizzare le scatole selezionate in modo da ottenere la più grossa metascatola possibile il che è funzione sia delle dimensioni della singola scatola, sia della presenza o meno di un vincolo sul posizionamento in altezza (che vuol dire, rispettivamente un numero minore o maggiore di soluzioni esplorabili), sia infine delle dimensioni dello spazio da colmare[15]. Il modo di agire generale prevede che, fissata una dimensione come altezza, si affidi ad un'altra *routine* ("Permutaz_1") il compito di individuare quale sarà la più grossa *unità logica* realizzabile, scegliendola tra le soluzioni ottenibili dalla permutazione delle due dimensioni di base della scatola.

Per *unità logiche* s'intendono delle metascatole che derivano da un raggruppamento di pacchi che abbia almeno una dimensione finale prossima a quelle dello spazio in questione. In pratica i raggruppamenti di cui si parla sono due: *colonna* e *parete*. La prima è l'insieme del massimo numero di pacchi che si possono disporre uno sopra l'altro fino a colmare l'altezza dello spazio; la seconda è il numero massimo di colonne[16] che possono essere affiancate tra di loro fino a colmare la larghezza dello spazio. Quindi una colonna è colmante rispetto ad una dimensione (altezza), mentre una parete lo è rispetto a due dimensioni (altezza e larghezza). Ebbene per *unità logiche* s'intenderà o un multiplo intero di pareti o un multiplo intero di colonne (tali comunque da non arrivare a formare una parete).

Introdotte queste definizioni, si passa ora in rassegna l'iter risolutivo completo della procedura d'inizializzazione che si sviluppa attraverso le seguenti tappe:

---

[15] Si ricorda che una generica sezione verticale da colmare ha sempre larghezza ed altezza coincidenti con quelle del container, mentre profondità (prima che venga fissata dal posizionamento della prima metascatola) coincidente con la sua lunghezza residua (RD).

[16] Al limite potrebbe anche essere una!

1. Viene fissata come altezza una delle dimensioni della scatola[17].
2. In base al numero delle scatole disponibili, si verifica anzitutto se si possono costruire unità logiche formate da un numero intero di pareti considerando, allo scopo, le soluzioni offerte dalle due possibili permutazioni delle dimensioni di base. Nell'ipotesi in cui si possono costruire pareti (almeno una) sia ponendo le scatole in un verso, sia ponendole nel verso ottenuto ruotandole, rispetto ad un'asse verticale, di 90°, si preferirà l'orientazione che realizza l'unità logica col maggior numero di scatole (il che vuol dire, in pratica, metascatola più voluminosa). Nella particolare eventualità in cui, con entrambe le orientazioni, si realizzano unità logiche utilizzanti lo stesso numero di scatole, allora si opterà per quella che le dispone con la più piccola dimensione (di base) parallela alla lunghezza del container[18]. Nel caso in cui, invece, il numero delle scatole è insufficiente per formare anche solo una parete (comunque si orientino le dimensioni di base), allora si passa al punto successivo.
3. Verificato che non c'è il numero di pacchi sufficiente per costruire neppure una parete, la procedura prosegue valutando se esiste la possibilità di costruire unità logiche formate da colonne (almeno una). In caso affermativo, si sceglie di orientare le scatole ponendo, stavolta, parallelamente alla lunghezza del container, la dimensione (di base) maggiore. La giustificazione risiede nella volontà (quando si hanno almeno due colonne) di offrire, agli eventuali pacchi che dovessero posizionarsi su tale metascatola, una superficie d'appoggio con dimensioni più omogenee[19]. In caso negativo, quando cioè non si può costruire neppure una colonna, si passa invece al punto successivo.
4. Verificato che non c'è il numero di pacchi sufficiente per costruire né una parete né una colonna, infine la procedura piazzerà semplicemente quelli disponibili (organizzandoli in subcolonne) e lo farà orientandoli così come descritto al punto 2.

Comunque sia, seguendo le istruzioni riportate nei quattro passi precedenti, che nell'insieme costituiscono la procedura "Permutaz_1", rimane individuata una certa metascatola (formata da pareti, da colonne o da subcolonne). A questo punto, se la tipologia cui ci si sta riferendo ha il vincolo sul posizionamento in altezza, allora tale metascatola sarà effettivamente la prima del muro in costruzione, altrimenti si dovrà ripetere per altre due volte (considerando a turno, come altezza, una delle altre due dimensioni) la suddetta procedura. In quest'ultima ipotesi la prima metascatola del muro dovrà essere scelta tra le tre individuate dalla routine "Permutaz_1" (una per ciascuna delle tre volte che viene applicata). Il compito di scegliere spetta alla procedura "Iniz_muro" che, ovviamente, opterà per quella formata dal maggior numero di pacchi.

Con la creazione ed il piazzamento della prima metascatola ha termine la fase di inizializzazione del muro. Infatti, dopo tale operazione, restano individuate completamente le sue caratteristiche e cioè la profondità e due spazi liberi contigui alla metascatola, indicati come sparez e sparew, delle cui tecniche di riempimento (per il completamento del muro) si parlerà nel paragrafo seguente.

---

[17] Inizialmente si lascia come altezza la dimensione così come riportata nel *datasheet* di Excel, ossia la più piccola delle tre (infatti, al di là delle orientazioni con cui verranno posizionate all'interno del container, lunghezza, larghezza e altezza sono definite rispettivamente come la dimensione maggiore, media e minore della scatola). Tale scelta si effettua in previsione del fatto che, se la tipologia considerata ha il vincolo sul posizionamento in altezza, rimane l'unica opzione possibile.

[18] Si adotta, quindi, un criterio che è conservativo rispetto alla profondità del container. La filosofia è quella di rendere disponibile un volume maggiore per la costruzione dei muri successivi

[19] Ovviamente il criterio evocato è intuitivo e non è quindi detto che corrisponda, sempre, alla soluzione migliore

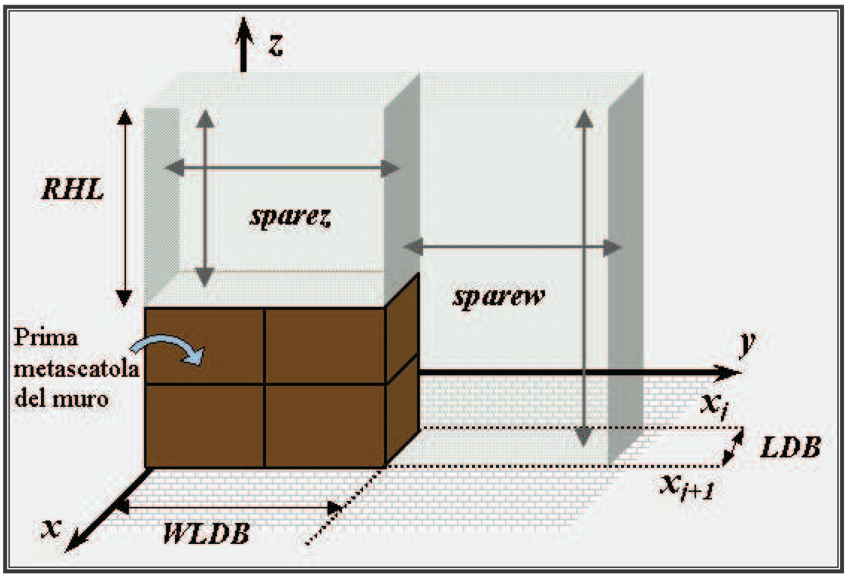

Figura 7.: Spazi progenitori “sparez” e “sparew” generati in seguito al piazzamento della prima metascatola. RHL, WLDB e LDB sono le grandezze attraverso cui tali spazi vengono definiti. In particolare con LDB si indica anche la profondità del muro.

1.4.2 Completamento di un muro

Il completamento della costruzione di un muro si perfeziona con il riempimento degli spazi progenitori sparez e sparew rappresentati in figura 7.6. Indicate con x_j e x_{j+1} le coordinate estreme, relative all’asse x, della profondità del generico muro j-mo, tali spazi sono analiticamente descrivibili come i luoghi dei punti:

$$\text{spare z} = \{(x, y, z) : x_j \leq x \leq x_{j+1}, 0 \leq y \leq \text{WLDB}, \text{HLDB} \leq z \leq \text{Hcont}\}$$

$$\text{spare w} = \{(x, y, z) : x_j \leq x \leq x_{j+1}, \text{WLDB} \leq y \leq \text{Wcont}, 0 \leq z \leq \text{Hcont}\}$$

ove i valori WLDB ed HLDB indicano rispettivamente larghezza ed altezza della metascatola, mentre Hcont e Wcont indicano altezza e larghezza del container. La procedura che l’algoritmo ibrido-euristico deputa all’adempimento di questa seconda fase della costruzione di un muro è la “Complet_muro”. Essa inizia con l’inserire gli spazi sparez e sparew (ovvero due vettori riga che ne contengono le informazioni relative a dimensioni, coordinate e volume) in una lista L, quindi applica una procedura ricorsiva di riempimenti degli spazi che, per costruzione, prima si occupa dello spazio superiore e poi di quello laterale.

Pertanto, complessivamente, sono avviati due cicli, uno per ogni spazio progenitore. Per ciascuno di tali cicli viene dapprima inizializzata una lista temporanea W (contenente inizialmente il solo spazio progenitore considerato, ma cui si aggiungono di volta in volta quelli prodotti dalla collocazione di ogni metascatola), dunque si evoca una subroutine (la “Riemp_spaz”) la cui funzione è quella di individuare, tra tutte le tipologie che hanno ancora pacchi da piazzare, quella che è in grado di formare la metascatola che colmi al meglio lo spazio in esame; spazio che è quello progenitore alla prima iterazione, uno generico della lista W per le iterazioni successive e fino ad esaurimento della lista stessa.

In effetti la collocazione di una metascatola all'interno di uno spazio generico implica la generazione di ulteriori tre spazi (posti superiormente, frontalmente e lateralmente rispetto alla metascatola piazzata) le cui

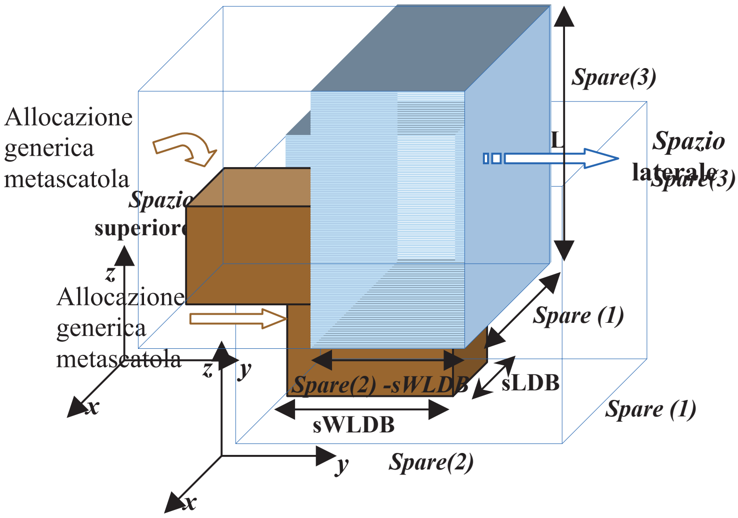

Figura 8.: Spazio superiore sovrastante la metascatola piazzata per il riempimento di un generico spazio d'indagine (Spare) di dimensioni spare(i), i = 1,2,3.

caratteristiche geometriche sono rappresentate nelle figg. 8., 9. e 10..

Figura 9.: Spazio generato lateralmente al piazzamento

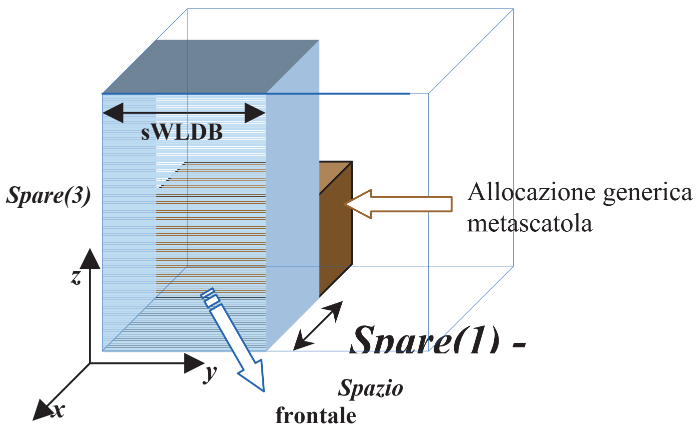

Figura 10.: Spazio generato frontalmente al piazzamento

Ad ogni iterazione tali spazi vengono piazzati in cima alla lista temporanea[20] da cui, frattanto, viene anche eliminato lo spazio generante. Il ciclo ha termine quando sono stati indagati tutti gli spazi della lista oppure quando, ad un certo momento, non ci sono più scatole da collocare. L'ultima osservazione riguarda la necessità di stabilire l'ordine (priorità) con il quale devono essere indagati gli spazi presenti in W; ebbene, dopo il piazzamento di ogni metascatola, la routine prima cercherà di colmare lo spazio superiore quindi gli

[20] Gestita con tecnica LIFO

altri due (laterale e frontale) dando la precedenza a quello con volume inferiore. Il ragionamento adottato è il seguente: uno spazio indagato per primo può, ai fini del suo riempimento, contare su una numerosità di scatole (appartenenti alle varie tipologie) superiore rispetto a quella su cui può invece contare uno spazio indagato successivamente e quindi, almeno teoricamente, ha maggiore probabilità di realizzare una migliore performance volumetrica. Con le priorità stabilite, pertanto, si vogliono dare maggiori chance dapprima allo spazio superiore (e ciò corrisponde ad una intenzione di rendere il più stabile possibile l'incolonnamento di metascatole) poi, dei restanti, a quello più piccolo (che avendo intuitivamente più difficoltà di essere colmato rispetto a quello più grande, è giusto che sia quello che, tra i due, possa fare affidamento su un numero di scatole maggiore).

Si entra infine nel merito delle caratteristiche e dei principi euristici su cui si fonda la procedura "Riemp_spaz" che, fissato uno spazio d'indagine preso dalla lista temporanea W (all'interno di uno dei cicli di riempimento degli spazi progenitori), ha il compito di ricercare la metascatola che meglio lo colmi. Rispetto alla procedura ("Iniz_muro") analizzata in occasione della descrizione della fase d'inizializzazione di un muro, e che aveva invece il compito di individuare la prima metascatola in assoluto da collocare al suo interno, la "Riemp_spaz" ha un'analogia ed una differenza fondamentali. La differenza è che mentre la prima ricerca la sua metascatola all'interno di un'unica tipologia[21], la seconda lo fa investigando all'interno di tutte quelle che, in quel momento, hanno disponibilità non nulla di pacchi. Tale diversità non dovrebbe stupire perché diverse sono anche le esigenze nei due casi d'inizializzazione di un muro e di riempimento di uno spazio generico. Si è infatti già detto che quando si avvia la costruzione di un muro, teoricamente, si può anche sfruttare tutto il volume del container ancora disponibile e ciò giustifica, appunto, il tentativo di piazzare prioritariamente le scatole della tipologia a volume totale maggiore; nel secondo caso, invece, si deve pensare che l'algoritmo è chiamato a riempire spazi di varie grandezze e poiché ogni volta può essere diversa la tipologia che per caratteristiche geometriche meglio si adatta a colmare lo spazio in esame, ogni volta sarà pertanto anche giusto guardare alle soluzioni offerte da tutte le tipologie!

L'aspetto che, invece, accomuna le due procedure è quello di valutare, laddove non esista il vincolo sul posizionamento in altezza, anche le rese volumetriche che si avrebbero considerando tutte le possibili orientazioni delle scatole. In questa ipotesi la procedura "Riemp_spaz" fissa, a turno, come altezza delle scatole una delle loro tre dimensioni e, ogni volta, incarica un'altra routine ("Permutaz_2") di individuare la più grossa unità logica tra quelle ottenibili dalla permutazione delle due dimensioni di base; quindi delle tre soluzioni ottenute (una per ciascuna delle volte che evoca la routine "Permutaz_2") sceglie quella che rappresenta la metascatola più voluminosa.

Fermo restando le definizioni di unità logiche date in occasione della descrizione della fase d'inizializzazione di un muro[22], immaginandole però riferite, ogni volta, alle dimensioni dello spazio analizzato piuttosto che a quelle del container, si elencano di seguito i passi attraverso cui si sviluppa la procedura "Permutaz_2":

1. Viene fissata come altezza una delle dimensioni delle scatole[23].
2. Si riorganizza la lista delle tipologie con disponibilità non nulle, per volumi unitari decrescenti[24] (la ragione di questa operazione verrà chiarita in seguito).
3. In base al numero delle scatole disponibili, si verifica anzitutto se si possono costruire unità logiche formate da un numero intero di pareti considerando, allo scopo, e per ciascuna tipologia, le soluzioni offerte dalle due possibili permutazioni delle dimensioni di base. Nell'ipotesi in cui esista più di una tipologia in grado di costruire almeno una parete allora si opterà naturalmente per quella che crea la metascatola più grande. Nell'ipotesi in cui, invece, non esista alcuna di siffatte tipologie, si passa al punto successivo.
4. Verificato che non esiste alcuna tipologia con un numero di pacchi sufficiente per costruire almeno una parete, la procedura prosegue valutando se esiste la possibilità di costruire unità logiche formate da

[21] Ovvero quella a volume totale maggiore al momento dell'inizializzazione del muro in esame
[22] Cfr. par. 6.4.1
[23] Cfr. nota n° 17
[24] Dopo tale riorganizzazione in testa alla lista ci sarà la tipologia le cui scatole hanno, singolarmente, volume superiore rispetto a quello delle scatole di tutte le altre tipologie

colonne (almeno una). In questo caso, dapprima si cerca una soluzione (metascatola) fissando l'orientazione delle scatole in modo che la dimensione (di base) maggiore sia parallela alla lunghezza del container[25], e solo nell'evenienza di un insuccesso, si passa a cercarne una dopo aver cambiato l'orientazione delle scatole. In entrambe le ipotesi, tra eventuali più tipologie rispondenti ai requisiti richiesti, si sceglie quella più *performante.* Se, invece, non si può costruire neppure una colonna in nessun modo e con nessuna tipologia, si passa al punto successivo.

5. Verificato che nessuna tipologia possiede un numero di pacchi sufficiente per costruire né una parete né una colonna, infine la procedura sceglie comunque quella in grado di realizzare la metascatola (che sarà una subcolonna o al limite un'unica scatola) più grande. Riguardo alle orientazioni delle dimensioni di base dei pacchi, valgono le stesse considerazioni fatte nel punto precedente.

6. Per le tipologie non soggette a vincolo, si cambia la dimensione fissata come altezza e si ripetono le operazioni dei punti 3,4 e 5 (quelle che, realmente, rappresentano la procedura "Permutaz_2").

Qualunque sia il tipo di metascatola (insieme di una o più pareti, insieme di una o più colonne, subcolonna) che la procedura ricerca, può sempre accadere che quella più voluminosa possa essere ottenuta contemporaneamente da due (o più!) tipologie. In questa poco probabile, ma pur sempre possibile, evenienza viene in soccorso il più volte evocato principio che suggerisce di collocare per primi gli oggetti più ingombranti, per cui, alla fine, si preferirà la tipologia che possiede le scatole a volume unitario maggiore. Per fare un esempio: se una tipologia T1 forma una metascatola di volume V utilizzando due scatole, mentre un'altra tipologia T2 forma una metascatola, diversa dalla prima ma sempre di volume V, utilizzando però dieci scatole, allora l'algoritmo sceglierebbe la metascatola creata da T1 perché, evidentemente, le sue singole scatole sono più voluminose di quelle di T2!

Si può ora capire lo scopo della riorganizzazione delle tipologie prevista dal punto 2 della *routine*: consentire in ogni momento all'algoritmo di individuare più facilmente la tipologia che contempla i pacchi a maggior volume unitario. L'individuazione avverrebbe, infatti, guardando semplicemente alla testa della lista.

Il paragrafo, così come la trattazione dell'intero metodo euristico proposto, si conclude con due osservazioni. La prima è che dopo la costruzione di un muro viene naturalmente aggiornato l'elenco delle scatole ancora da caricare e poiché, verosimilmente, la tipologia a volume totale maggiore non sarà più la prima in cima alla lista, in previsione dell'inizializzazione del muro successivo viene rieffettuata l'operazione di ordinamento per volumi totali decrescenti.

La seconda osservazione riprende un'affermazione fatta nel terzo paragrafo e cioè che la profondità dell'ultimo muro viene fissata, dopo il controllo di una certa condizione, da quella residua del container. Ciò ha un'importante conseguenza ai fini dell'iter da seguire per il suo riempimento. In effetti, in questo caso, non esiste una fase d'inizializzazione ma viene direttamente applicata quella di completamento: è come se si avesse uno spazio progenitore nullo (per esempio lo *sparez*) ed un altro (per esempio lo *sparew*) coincidente con l'ultima sezione verticale da colmare del container. Tale particolarità può anche essere apprezzata nel *flowchart* di figura 4.6 ove risulta collocata all'interno della strategia risolutiva generale dell'algoritmo ibrido-euristico.

[25] La giustificazione risiede nella volontà (quando si hanno almeno due colonne) di offrire, agli eventuali pacchi che dovessero posizionarsi su tale metascatola, una superficie d'appoggio con dimensioni più omogenee.

Applications of nonlinear dynamics to communications security

A. Şerbanescu, P. Ciotirnae, D. Andrei

Military Technical Academy Bucharest, Romania
Bd. G. Coşbuc 81-83 sector 5 Bucharest, Romania
Phone: +4021.335.46.60 ext.148
E-mail: serbal@mta.ro , ciotirnae@mta.ro , dandrei@mta.ro

Abstract. The fact that numerical sequences with chaotic behavior are very suitable for use in secure communications is proved. More improved results in use of them are found. An efficient data chaotic encryption algorithm and its hardware architecture design are proposed. Based on a chaotic system, an unpredictable binary sequence is generated and used to encrypt and decrypt the data message. The simulation results show that the proposed algorithm possesses the features of data security and simplicity in the required operations. The method possesses the desirable properties for high security data and voice-multiplexed transmissions. Moreover, the encrypted complex data signal is using a multi route through the network in order to increase the data security.

1. Introduction

In recent years there are several international centers of studies which are interested in solving the problem of a suitable use of nonlinear dynamical systems with chaotic behavior in secure communication scheme.

The basic ideas can be classified into three major groups: *individual data channel encryption*, *multiplexed data channel encryption* and *their combining form*. The *individual data channel encryption* algorithms scramble the original information and form a complex signal which is sent through the public or insecure channel. On the other hand, the *inverse transformation* algorithms transform the encrypted data value of the original signal. For example, a voice channel is partitioned into subbands and scrambled to transform it into an unintelligible noiselike signal. In this paper, a new chaotic encryption algorithm is proposed and its architecture is minutely described.

2. Method for cryptography with chaotical signal

Consider a chaotic system described by the Cauchy problem for

$$\dot{x} = Ax + bf(x) + c \tag{1}$$

where: $x \in \Re^n$, $A \in \Re^{n\times n}$, $b \in \Re^{n\times 1}$, $c \in \Re^{n\times 1}$ and $f : \Re^n \to \Re$

The transmitting part

For the information signal *i(t),* the crypto signal is

$$s(t) = s(p(t)\cdot K(t)) \tag{2}$$

where *s(·)* is a generic encryption function and *K(t)* in the key.

If a symmetric algorithm is adopted the information signal is decrypted as:

$$i(t) = d(s(t)\cdot K(t)) \tag{3}$$

where *d(·)* is the decryption function.

For the key we assume that:

$$K(t) = K(x(t)) \tag{4}$$

The resulting signal occurs in an equation, generating a dynamical system, described by

$$\dot{x} = Ax + bf(x) + c + bs(t) \tag{5}$$

The receiving part

For the receiver the most important objective is the **synchronization**. This goal is achieved by designing the decrypter as a nonlinear observer for the state of the encrypter.

The decrypter also occurs in a dynamical system described by

$$\dot{y} = Ay + bf(y) + c + g(h = r(y)) \tag{6}$$

where: $g : \Re \to \Re^n$ is a suitable chosen nonlinear function.

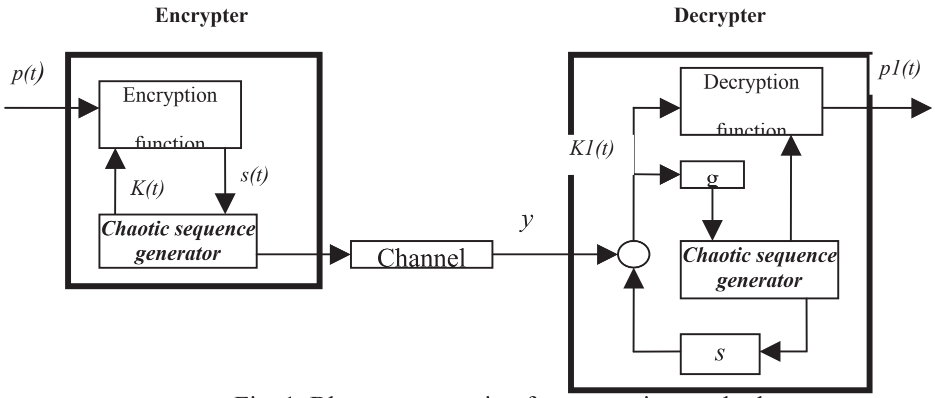

Fig. 1. Bloc representation for encryption method.

We must design the eq. (6) so that *y* converges to the state of the *x* as $t \to \infty$. We define the error signal as

$$e(t) = \|y(t) - x(t)\| \tag{7}$$

Therefore our intention is to have $e(t) \to 0$ as $t \to \infty$. If this is achieved for any initial condition $y(0), x(0)$ we say that the synchronization error system has a globally asymptotically stable equilibrium point for $e = 0$.

A graphical representation of the method proposed is presented in fig. 1.

Here is the proof for the assertion that the receiving signal is extract from coded signal with the K1(t) key.

$$K1(t) = K(y(t))$$

(8)

Let $s1(t) = h - r(y)$ be the crypto signal retrieved by the decrypter and let

$i1(t) = d(s1(t), K1(t))$ be the information signal obtained by the receiver.

If (6) is a global observer of the (5), it follows

$$s1(t) \to s(t) \tag{9}$$

because $y \to x$ as $t \to \infty$ for any initial condition.

As consequence $K(y(t)) \to K(x(t))$ so $K1(t) \to K(t)$ and the $s1(t) \to s(t)$. Finally, the comparison between (3) and (8) confirm that the assertion (9) is correct.

3. Data transmissions on EUROCOM multiple channels

Necessary conditions for military data transmissions are the assurances of integrity and protection of data. For these goals classical channel methods for protection can be used. Instead of these we use a hybrid method witch allows classical methods and involves new ones.

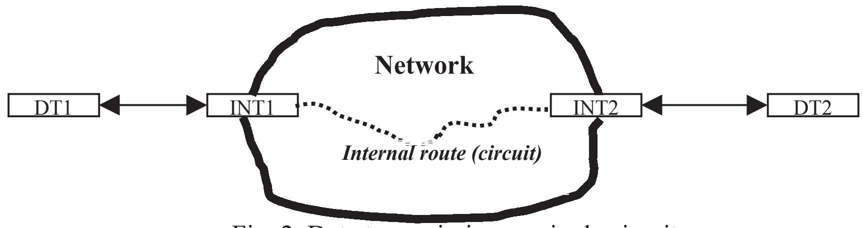

Fig. 2. Data transmission on single circuit.

In fig. 2. a classical transmission between two digital terminals (DT) through specific interface (INT) is described. On demand the network creates a single internal route. This route is exposed to jamming and interception.

We use a method which involves a multiple route. It is achieved a high degree of robustness against jamming and interception. For this it is necessary to create a special interface (M.R. int) which is capable to split the original source of information and to provide the network interface with a set of a multiple independent source of data.

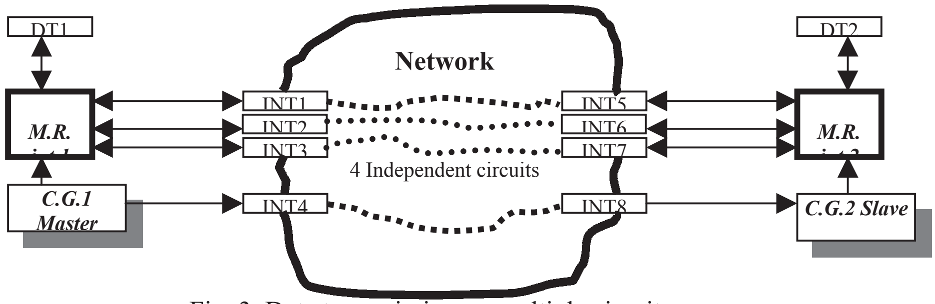

Fig. 3. Data transmission on multiple circuits.

The method is presented in fig. 3. In order to increase the “power” of the method splitting the message a chaotical numerical signal generators (C.G.) are involved.

The chaotical sequence is generated externally. In addition it is sent to the receiver through a separate channel (route).

The procedure of splitting the original message is represented in fig. 4. The method uses a chaotic sequence in order to determine the number of bits to route to the first circuit and so on.

The chaotic sequence is converted in hex numbers grouping sets of 4 bits, and it is validate if the number obtained is $7 \le x \le 13$. The receiver creates the number in the same manner.

Example: Let be the chaotical sequence to

0101 0101 1100 0110 1010 1101 0110 0101 1001 1001 0101 0110

Hex conversion is:

-05- -05- -12- - 06- -10- -13- -06- -05- -09- -09- -05- -06-

After validation with conditions $7 \le x \le 13$ we obtain a random sequence in the domain [7,13].

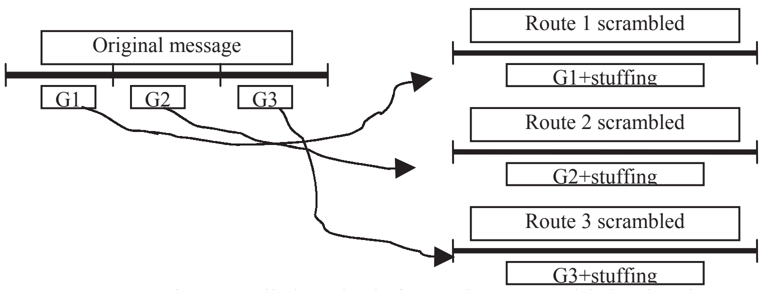

Fig. 4. Splitting the information on multiple circuits.

4. Comparison between classical and chaotic cryptography

Classical cryptography works on discrete values and in discrete time while in chaotic cryptography continuous-value systems that may operate in continuous or discrete time are used (Table 1).

Classical cryptography	*Chaotic cryptography*
- **integer values** on finite fields	- **continuous values** using fixed or floating point representation
- **algebraic methods**	- **analytic methods**
- digital realization by **integer arithmetic**	- digital realization by **non integer arithmetic**

Table 1. Comparison between classical and chaotic cryptography.

Chaotic maps and cryptographic algorithms (or more generally maps defined on finite fields) have also some similar properties: sensitivity to initial conditions and parameters, random like behavior and unstable orbits with long periods, depending upon the precision of the numerical implementation.

For example a block encryption algorithm can be re-written as a discrete time dynamical system

$$x_{n+1} = F(x_n) \tag{10}$$

where the initial condition x_0 is the plain text to be encrypted, and the final state x_k is the cipher text. Due to the fact that the chaotic map can be expressed by a similar equation, the property of the map being chaotic implies spreading out the influence of a single plaintext digit over many cipher text digits. In other words, any set of initial conditions of a chaotic map will eventually spread over the whole phase space as the system evolves.

5. Types of cryptographic algorithms or ciphers

The purpose of a cipher is to take unencrypted data (the plaintext) in order to produce an encrypted version of it called the cipher text. There are one major classes of ciphers: stream ciphers and block ciphers.

5.1. Chaotic stream cipher

The simplest example of a stream cipher is a bit of data is "xor-ed" with another bit of a stream generated by a pseudorandom generator. To decrypt the message the same pseudorandom bit stream is generated and the inverse operation (another "xor") is done.

Our chaotic stream cipher is based on a chaotic pseudorandom generator with the main part represented by a discrete time chaotic map known as "Piecewise Affine Markov Map" (PWAM).

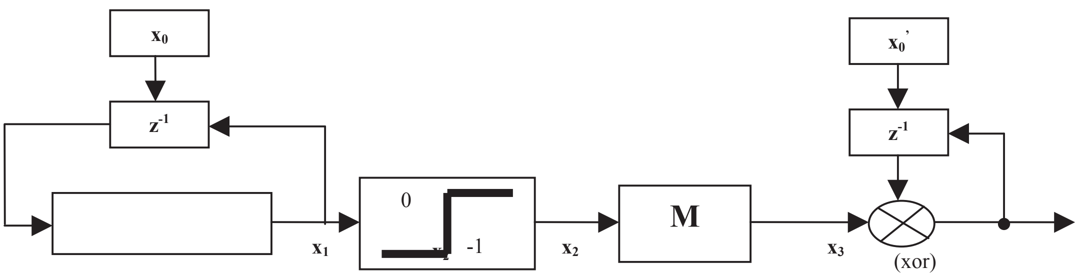

Fig. 6. Chaotic pseudorandom generator.

The chaotic map is defined by the following expression:

$$f_{M1}(x)=\begin{cases}B(D-|x|) & ,|x|<D\\ B(|x|-2D) & ,|x|\geq D\end{cases}, \tag{11}$$

where $B=3$, $D=1$, $x_0=0.1$.

The above function is defined on the real number domain such that the initial condition (x_0) and the output variable (x_1) belong to the interval *(-3,3)*. Keeping in mind the fact that the above chaotic map must be implemented on a finite precision machine we represent the real numbers x_0, x_1 in floating point single precision arithmetic (sign 1 bit, exponent 8 bits, mantissa 23 bits).

The second block stands for a selection logic so that only the values that lie in the subinterval *(-1,0)* are selected. This must be done in order to select a subinterval with a good distribution of generated values by the PWAM, because some of the chaotic properties are lost after imposing the precision of the numerical representation.

M is a mapping block described by the equation

$$x_3=\left[255\cdot\frac{x_2-a}{b-a}\right], \tag{12}$$

where *[ ]* stands for integer part function;

$a=-1$, $b=0$;

x_0', $x_3\in\{0,1,\ldots,255\}$ are integer numbers represented on 8 bits, $x_0'=255$.

Thus each of the single precision real numbers (x_2) is transformed into an 8 bit integer in order to generate the pseudorandom bit stream. The last transformation is applied on 8 bits once to ensure good statistical properties of the generated bit stream.

The encryption key is represented in our implementation by the initial condition of PWAM x_0 (32 bits) and the initial condition of the final "xor" operation x_0' (8 bits), that is a 40 bits key length, is used. As an example we present here the results obtained with the frequency test and the discrete Fourier transform test for a stream of *80000* bits length (figs. 7, and 8).

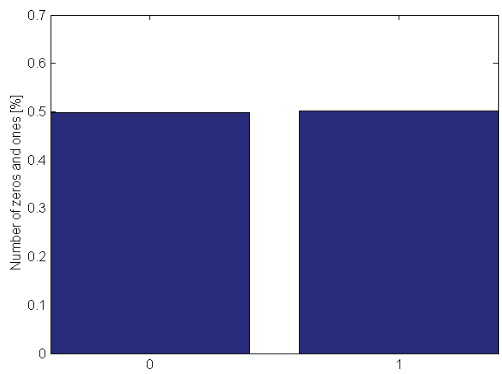

Fig. 7. Frequency test

(nb. of zeros: 39890; nb. of ones: 40110)

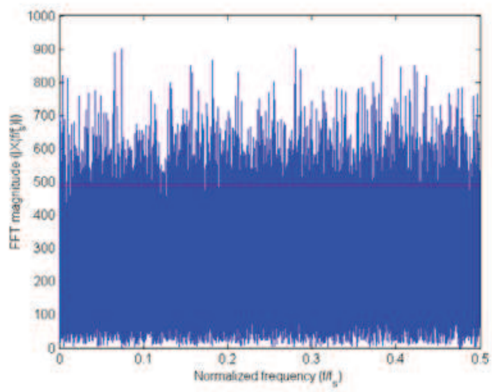

Fig. 8. Discrete Fourier transform test.

We have done several statistical tests and our generator has passed all such that we have concluded that the bit stream generated with the above structure has very good statistical properties and therefore it can be used in a stream cipher.

5.2 Chaotic block cipher (Generalized Chaotic Encryption Method)

A block cipher operates on blocks of data that are larger than one bit.

Here we present a chaos based secret key algorithm using the simple one-dimensional logistic map:

$$x_{n+1}=r\cdot x_n\cdot(1-x_n) \tag{13}$$

where $x_n\in(0,1)$ and $r\in(3.7,4)$ is the control parameter chosen such that (13) has a chaotic behavior.

The message to be transmitted is a text composed by some alphabet and we associate portions (e-intervals) of the attractor (*(0, 1)* domain) with alphabet characters. The cipher text of some character (plaintext) is the number of iterations applied in equation (13) to make its trajectory, departing from an initial condition x_0, reaches an e-interval associated with that character. If the attractor is divided into *S* intervals or sets, where *S* is also the character number of the alphabet, then each e-interval has the form

$$I_n = \left[x_{\min} + (n-1)\cdot e, x_{\min} + n\cdot e\right] \qquad (14)$$

where $n \in \{1,2,...,S\}$, $e = (x_{\max} - x_{\min})/S$ and $[x_{min}, x_{max}]$ represents the whole attractor or a portion of it.

As far as the number of iterations needed to reach a certain interval I_n is concerning we have numerically checked that this number can become quite large for certain initial conditions. Thus, in order to ensure a reasonably number of iterations in any situation, we have decided to divide first the whole attractor into *f* groups and then to divide each group into *S* e-intervals (fig. 9).

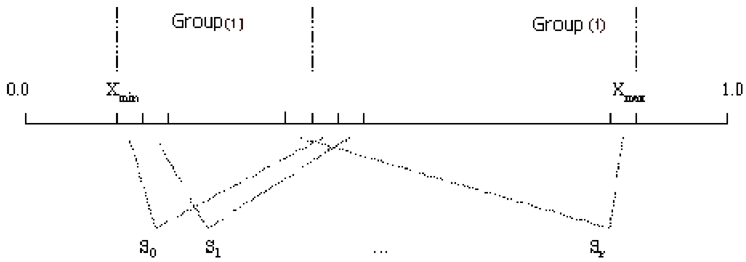

Fig. 9. Generalized association method.

A logic diagram of the above described generalized chaotic encryption method is given in fig. 10.

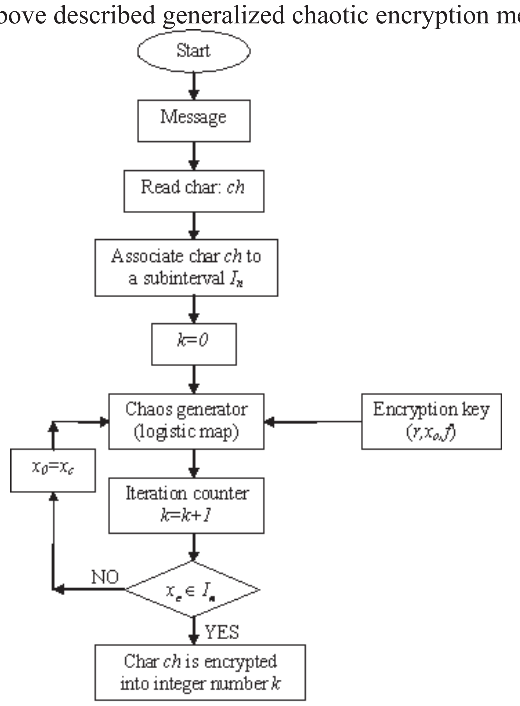

Fig. 10. Generalized chaotic encryption method.

To decrypt de message, at the receiver side equation, (4) is iterated with the same initial condition as much times as indicated by the cipher text.

6. Conclusions

In this paper, an efficient algorithm and its architecture have been proposed. The associated architecture possesses the following desirable features: high level of security, real-time processing capability, medium hardware cost, and low power consumption. Therefore, it is very suitable for military and private network implementation. Besides, the simulation results have indicated that the algorithm can easy make images to be in a chaotic state very soon.

The estimated processing speed achieves 2MHz, which can meet the requirement of first order real-time data/voice multiplexed encryption applications.

REFERENCES

[1] Baranovski, A.L., Daems, D., Design of 1-D chaotic maps with prescribed statistical properties. *Int. Journal of Bifurcations and Chaos*, **5**, 6 (1995), 1585-1598

[2] Blum, L, Schub M., A simple unpredictable pseudo-random number generator, *SIAM Journal of Computing.* **15**, 2 (1986), 364-383.

[3] Cernák, J. Digital generators of chaos. *Physics Letters A.* **214**, (1996), 151-160.

[4] Couture, R and L'Ecuyer, P., Distribution properties of multiply-with-carry random number generators, *Mathematics of Computation*, **66** (1997), 591.

[5] Couture, R and L'Ecuyer, P., Guest Editors' Introduction. *ACM transactions on Modeling and Computer Simulation,* **8**, 1 (1998), 1-2.

[6] Entacher, Karl., Bad Subsequences of well-known linear congruential pseudorandom number generators. *ACM transactions on Modeling and Computer Simulation,* **8**, 1 (1998), 61-70.

[7] W. J. Rugh., *Nonlinear System Theory, TheVolterra/Wiener Approach*. The Johns Hopkins University Press, 1981.

[8] D. D. Weiner, J. F. Spina., *Sinusoidal analysis and modeling of weakly nonlinear circuits,* Van Nostrand Reinhold, 1980.

[9] A. Abel, A. Bauer, K. Kelber, and W. Schwarz., Chaotic codes for CDMA applications, in *Proc. ECCTD*, vol. 1, Budapest, 1997. 306–311

[10] A. Abel, M. G¨otz, and W. Schwarz. Statistical analysis of chaotic communication schemes,. in *Proc. ISCAS*, Monterey,1998.

[11] S. S. Haykin., *Digital communications*. John Wiley & Sons, New York, 1988.

[12] M. K. Simon, J. K. Omura, R. A. Scholtz, and B. K. Levitt, *Spread spectrum communications handbook,* McGraw-Hill, New York, 1994.

Hydrodynamics of dispersed, multiphase flows by wave breaking

Ovidiu Tanasescu
SDB Bucuresti

Horatiu Tanasescu
ICEPRONAV Galati

Abstract. Our days CFD is routinely used in a huge variety of applications. However, there are some areas in which CFD has seriously limitations and active research is necessary to overcome them. Such a great limitation of CFD is represented by the dispersed, multiphase flows. Multiphase flows are commonly met in practice, and consequently their simulations is of great interest. In the same way like turbulent flows, multiphase flows (which may also be turbulent in one or more phases) can correspond to solutions of the equations of motion, and direct numerical simulation can be applied to them. However, in many practical problems, multiphase flows require additional special modeling. Still these additional models, tend to ignore or simplify a lot of important details of the flow, such as droplet or particle shape and their impact on interphase mass, momentum and energy transport. Our practical target is ship hydrodynamics wave breaking, tackled with very recently in the scientific world. Physically speaking bow breaking waves dissipate energy and affect forward hydrodynamic resistance of ship hull as a whole. Subsequent spray formation and air entrainment can be important for ship wake configuration. Additionally, from the safety point of view, breaking ocean waves interacting with ships are of main importance for ship capsizing. The global theme aims are: nonlinear three-dimensional water waves, wind-wave-turbulence and ocean waves – ship hull wave system interaction. Some subareas to be considered are: large amplitude and breaking waves, deterministic versus statistical models, stability of water waves, the role of turbulence in ocean dynamics and the implications of forcing and dissipation. The concerns of the present paper, which is the first one in a series, are focusing on:

- a 3D Galerkin weighted residuals finite element method for surface ships wave making resistance computation;
- experimental-analytical-numerical genesis and dynamics modeling of bow wave breaking influence on surface ships wave making resistance.

1. Introduction

Waves are a source of delight. They also cause and produce enormous destructions and drawbacks. We need to understand how they form and how they propagate, and find ways to harness their energy safely. Mathematic holds the key to this understanding. There are fascinating mathematical problems associated with water waves of great interest for both pure and applied mathematicians, and the water wave equations have spreaded and amplified everywhere in mathematics, as for example the D. J. Korteweg and G. de Vries equation (1895): if u is the particle displacement and the Ox is the axis in travelling direction, we have

$$\frac{\partial u}{\partial t} + u\frac{\partial u}{\partial x} = -b\frac{\partial^3 u}{\partial x^3}$$

where t is the time, and b is a positive constant. Of all various types of wave motion that occur naturally (created by the wind), artificially (generated by structure-water interaction) or both, surface water waves are not merely the most easily observed but of great scientific importance because of their special impact in ship hydrodynamics and not only. As we already mentioned in the abstract, the final theoretical target of this long cycle of papers, is hydrodynamics of dispersed, multiphase flows by wave breaking, with the practical application in ship hydrodynamics: the influence of bow waves on wave resistance and turbulent wakes, the action of breaking waves on moving ships, not to mention the capsizing of ships in heavy seas.

The wave resistance of surface ships is simulated by using field finite element method – Galerkin formulation. A theoretical – physical, analytical and numerical – three-dimensional model for free surface potential flow around surface ship hulls is considered. The spatial flow domain unstructured discretisation is performed by using curved boundaries hexahedron finite elements having twenty nodes, between parallel planes with the ship's central longitudinal plane). The special characteristic of the method is, in the authors opinion, that in considering the whole bulk of the fluid, the naval architecture potential flow problems could be discretised much more accurately. Moreover, having in view future developments, (unlike the boundary element method – Rankine sources – presently used for wave resistance computation almost everywhere in the world), the method described in this paper is not limited to the case of the potential flow, but it may be modified such that to include viscosity, in this way having also the possibility to take into account its influence on stern wave making. Ship bow breaking waves are investigated too.

The complex, competitive, rational process of selecting of a hull form that which is the best of all possible designs within a prescribed objective function (minimum forward hydrodynamic resistance) and a given set of constraints (of geometrical nature and practical design) is technically challenging. Until recently, the only way to evaluate ship's resistance performance was through experiment. The past ten years have, however, seen major achievements in a good numerical free surface potential flow prediction, inviscid flow models remaining the most important for naval architecture despite the recently increased abilities to predict the viscous flow in the boundary layer and wake. Application to inviscid flows are wave resistance computations, seakeeping, manoeuvring and propeller flows. From all applications to inviscid flows, the present work is focusing on the wave resistance problem only.

2. Physical and analytical model

Let us consider a ship hull model, piercing the free surface, moving steady horizontally in still water of infinite depth with a constant velocity U_∞ (upstream). We formulate the wave resistance problem in a Cartesian coordinate system fixed to the ship model (time-independent flow). The X-Y plane is at the design draft, the X axis is positive toward the stern and the vertical axis Z is positive upward.

Assumptions:

- fluid is ideal (inviscid);
- fluid (water) is considered incompressible;
- motion is irrotational;

Further down will try that all conditions of the physical model to be converted into analytical equations if possible.

By virtue of above mentioned assumptions, it is convenient to introduce the potential function ϕ (X,Y,Z), or velocity potential, such that, $U = grad\phi = \nabla\phi$. ϕ 's partial derivative in any direction gives the velocity component in that direction, $\phi_X = u$, $\phi_Y = v$, $\phi_Z = w$ The continuity equation (conservation of mass) for the steady flow of an incompressible fluid reads $\mathrm{div}\,\vec{U} = \nabla \cdot \vec{U} = 0$ in the case of potential flow becomes $\mathrm{div}U=\nabla\cdot\nabla\phi=\nabla^2\phi=\Delta\phi(X,Y,Z) = 0$, i.e. the Laplace's equation. Thus the potential ϕ satisfies the Laplace equation (i.e. it's a harmonic function). This is an elliptic partial differential equation. In view of the existence and uniqueness of its solution it must be supplemented with boundary conditions at all boundaries of the computational domain (the wetted hull surface, the water free surface and at infinity). Laplace equation together with the boundary conditions determine completely the motion.

2.1 Boundary conditions for the completely velocity potential ϕ

- on wetted hull surface: water does not penetrate the hull (Neumann condition), $n \cdot U = n \cdot \nabla\phi = 0$ (*n* is the unit vector normal to the hull) or

$$\phi_n = 0$$

- on the water free surface; physical nature of the water free surface requires two boundary conditions:
a. kinematical condition: water does not penetrate the water surface; thus at the surface$Z=\zeta$,

$$\nabla\phi \, .\nabla\zeta=\phi_Z \tag{1}$$

or

$$\phi_X.\zeta_X+\phi_Y\zeta_Y-\phi_Z=0; \tag{2}$$

b. dynamical condition: pressure on the water free surface must be atmospheric and independent of the position on it,

$$\frac{1}{2}(\nabla\phi)^2+g.\zeta = \frac{1}{2}U_\infty^2 , \tag{3}$$

or

$$g\zeta+\frac{1}{2}(\nabla\phi.\nabla\phi)-U_\infty^2)=0; \tag{4}$$

- decay (or regularity) condition: far away from the ship model, the flow is unperturbed and parallel, having a speed equal to ship model speed U_∞ , i.e,

$$\lim_{(X^2+Y^2+Z^2)\to\infty} \nabla\phi=(U_\infty,0,0);$$

- radiation condition: waves generated by the ship propagate only downstream (no upstream waves); this condition is introduced by the numerical method requiring a special treatment;
- equilibrium condition: the ship hull must be in equilibrium.

Combining of kinematical and dynamical boundary conditions (the equations (1) and (3)) and eliminating the unknown wave elevation ζ we are lead to the following non-linear free surface boundary condition,

$$\frac{1}{2}\nabla\phi\nabla(\nabla\phi)^2+g\phi_z=0$$

The exact problem formulated above is non-linear, since the free surface boundary condition itself is non-linear and should be exactly satisfied on the wavy surface $Z=\zeta(X,Y)$, which is unknown, and must be computed as a part of the solution. Thus, numerical methods, which have been applied to solve the problem usually entail some kind of linearization procedure.

The unknown pressures p on the hull and wavy surface $Z=\zeta(X,Y)$ will generate a potential ϕ and a wave elevation ζ, which fulfill the boundary conditions (2) and (4). Thus, for a mathematical consistent linearization we can introduce the following functions:

$$K(p,\zeta)=\phi_X.\zeta_X+\phi_Y.\zeta_Y-\phi_Z=0 \tag{5}$$

$$D(p,\zeta) = \zeta + \frac{1}{2g}[(\phi_X^2+\phi_Y^2+\phi_Z^2)-U_\infty^2]=0 \tag{6}$$

By introducing small perturbations δp, according to the classical Michell's theory, small $\delta\phi$ and $\delta\zeta$ are induced,

$$p=p'+\delta p \;\to\; \phi=\phi'+\delta\phi\,,\;\zeta=\zeta'+\delta\zeta$$

where: ϕ - the exact solution; ϕ' - an approximate solution; $\delta\phi$ - the potential difference; '- denotes a quantity from the immediate former iteration.

Expanding (5) and (6) in the first order Taylor series, we have

$$K(p,\zeta) \approx K(p',\zeta') + \Delta K(p,\zeta') + \Delta K(p',\zeta) \approx K(p',\zeta') + \frac{\partial}{\partial p}K(p,\zeta')\delta p + \frac{\partial}{\partial \zeta}K(p',\zeta')\delta\zeta \approx 0$$

where

$$K(p',\zeta')=\phi_X.\zeta'_X + \phi_Y.\zeta'_Y - \phi_Z,\ \ \Delta K(p,\zeta')=\delta\phi_X.\zeta'_X + \delta\phi_Y.\zeta'_Y - \delta\phi_Z$$

$$\Delta K(p',\zeta)=\phi'_X.\delta\zeta_X + \phi'_Y.\delta\zeta_Y + (\phi'_{XZ}.\zeta'_X + \phi'_{YZ}.\zeta'_Y - \phi'_{ZZ}).\delta\zeta$$

and

$$D(p,\zeta) \approx D(p',\zeta') + \Delta D(p,\zeta') + \Delta D(p',\zeta) \approx D(p',\zeta') + \frac{\partial}{\partial p}D(p,\zeta')\delta p + \frac{\partial}{\partial \zeta}D(p',\zeta')\delta\zeta \approx 0$$

where

$$D(p',\zeta') = \zeta' - \frac{1}{2}\left[U_\infty^2 - (\phi'_x + \phi'_y + \phi'_z)\right],$$

$$\Delta D(p,\zeta') = \frac{1}{g}(\phi'_X.\delta\phi_X + \phi'_Y.\delta\phi_Y + \phi'_Z.\delta\phi_Z),$$

$$\Delta D(p',\zeta) = \delta\zeta + \frac{1}{g}(\phi'_X\phi'_{XZ} + \phi'_Y\phi'_{YZ} + \phi'_Z\phi'_{ZZ})\delta\zeta\ .$$

ϕ'_Z and the second order derivatives in the Z direction (ϕ'_{XZ}, ϕ'_{YZ}, ϕ'_{ZZ}) being relative small are expected to go to zero and can be neglected. Thus the free surface boundary conditions become:

$$\phi_X\zeta'_X + \phi_Y\zeta'_Y - \phi_Z + \phi'_X\delta\zeta_X + \phi'_Y\delta\zeta_Y = 0 \tag{7}$$

and

$$\delta\zeta = \frac{1}{2g}\left[U_\infty^2 + \phi'^2_X + \phi'^2_Y - 2(\phi'_X\phi_X + \phi'_Y\phi_Y)\right] - \zeta' \tag{8}$$

By insertion of (7) in (8) the final mathematically consistent linearized boundary condition is obtained.

3. Numerical model

The Galerkin weighted residuals basically consists in:

$$\iiint_D \text{weighting function} \times \text{differential equation} = 0$$

Applying it to Laplace equation

$$\Delta\phi = 0$$

we have

$$\iiint_D N_i \left(\frac{\partial^2\phi}{\partial x^2} + \frac{\partial^2\phi}{\partial y^2} + \frac{\partial^2\phi}{\partial z^2}\right) dxdydz = 0,$$

where D is the spatial flow domain. Integrating by parts in order to reduce the order of the equation

$$\iiint_D \left(\frac{\partial N_i}{\partial x}\cdot\frac{\partial\phi}{\partial x} + \frac{\partial N_i}{\partial y}\cdot\frac{\partial\phi}{\partial y} + \frac{\partial N_i}{\partial z}\cdot\frac{\partial\phi}{\partial z}\right) dxdydz - \iint_S N_i \cdot \frac{\partial\phi}{\partial n} dS = 0 \qquad (9)$$

$i=1,...,m$; where m - the total number of nodes;

Taking into account that within the flow domain the surface integrals cancels at element interfaces, without loss of generality (4) can be rewritten, as follows

$$\iiint_D \left(\frac{\partial N_i}{\partial x}\cdot\frac{\partial\phi}{\partial x} + \frac{\partial N_i}{\partial y}\cdot\frac{\partial\phi}{\partial y} + \frac{\partial N_i}{\partial z}\cdot\frac{\partial\phi}{\partial z}\right) dxdydz = 0$$

Introducing trial functions to depict the spatial variation of ϕ , for each element, we have

$$\iiint_{D^e} \left(\frac{\partial N_i}{\partial x}\cdot\sum_{j=1}^{20}\frac{\partial N_j}{\partial x}\phi_j + \frac{\partial N_i}{\partial y}\cdot\sum_{j=1}^{20}\frac{\partial N_j}{\partial y}\phi_j + \frac{\partial N_i}{\partial z}\cdot\sum_{i=1}^{20}\frac{\partial N_j}{\partial z}\phi_j\right) dxdydz \ .$$

or in matrix form

$$A^e \cdot \phi^e$$

in which

$$a_{ij} = \iiint_{D^e} \left(\frac{\partial N_i}{\partial x}\cdot\frac{\partial N_j}{\partial x} + \frac{\partial N_i}{\partial y}\cdot\frac{\partial N_j}{\partial y} + \frac{\partial N_i}{\partial z}\cdot\frac{\partial N_j}{\partial z}\right) dxdydz,$$

leading to a 20x20 symmetric matrix $a_{ij} = a_{ji}$

$$\begin{bmatrix} a_{11}, a_{12}, \cdots, a_{1\,20} \\ a_{21}, a_{22}, \cdots, a_{2\,20} \\ \vdots \\ a_{20\,1}\cdots \quad \cdots, a_{20\,20} \end{bmatrix} \cdot \begin{Bmatrix} \phi_1 \\ \phi_2 \\ \vdots \\ \phi_{20} \end{Bmatrix}$$

$$\begin{Bmatrix} \dfrac{\partial N_i}{\partial x} \\ \dfrac{\partial N_i}{\partial y} \\ \dfrac{\partial N_i}{\partial z} \end{Bmatrix} = \begin{bmatrix} \hat{J}_{11} & \hat{J}_{12} & \hat{J}_{13} \\ \hat{J}_{21} & \hat{J}_{22} & \hat{J}_{23} \\ \hat{J}_{31} & \hat{J}_{32} & \hat{J}_{33} \end{bmatrix} \cdot \begin{Bmatrix} \dfrac{\partial N_i}{\partial \xi} \\ \dfrac{\partial N_i}{\partial \eta} \\ \dfrac{\partial N_i}{\partial \zeta} \end{Bmatrix},$$

$$\iiint_{D^e} dxdydz = \int_{-1}^{+1}\int_{-1}^{+1}\int_{-1}^{+1} |J| \cdot d\xi d\eta d\zeta \ ,$$

$$\int_{-1}^{+1}\int_{-1}^{+1}\int_{-1}^{+1} F(\xi,\eta,\zeta) d\xi d\eta d\zeta = I \, ,$$

$$I = \sum_{i=1}^{3}\sum_{j=1}^{3}\sum_{k=1}^{3} a_i a_j a_k F(\xi_i,\eta_j,\zeta_k) \, .$$

3.1 Practical succesion of the main steps necessary for elemental matrix coefficients evaluation (3D)

a. Evaluation of the shape functions N;
b. Evaluation of the local derivatives of the shape functions;
c. Evaluation of the Jacobian matrix J;
d. Evaluation of the determinant of the Jacobian Matrix det J;
e. Evaluation of the inverse of the Jacobian $|J|^{-1}$;
f. Evaluation of weighted volume:
The value of the weighted volume at each Gauss point is required in order to carry out the numerical integration, since from equations (11) and (12) we deduce

$$\iiint_{D^e} F(x,y,z)dxdydz = \int_{-1}^{+1}\int_{-1}^{+1}\int_{-1}^{+1} F(\xi,\eta,\zeta)\,|J|\,d\xi d\eta d\zeta = \sum_{i=1}^{3}\sum_{j=1}^{3}\sum_{k=1}^{3} a_i a_j a_k F(\xi_i,\eta_j,\zeta_k)\,|J|.$$

Therefore each of the terms $a_i a_j a_k |J|$ is computed at each Gauss point; later these terms can, be multiplied by the function value and summed over each Gauss point to perform the integration;
g. Evaluation of the global derivative of the shape functions $\partial N/\partial x$, $\partial N/\partial y$ and $\partial N/\partial z$
Having evaluated the local derivatives of the shape functions $\partial N/\partial \xi$, $\partial N/\partial \eta$ and $\partial N/\partial \zeta$ together with $\partial\xi/\partial x$, $\partial\eta/\partial x$, $\partial\zeta/\partial x$, $\partial\xi/\partial y$, $\partial\eta/\partial y$, $\partial\zeta/\partial y$ and $\partial\xi/\partial z$, $\partial\eta/\partial z$, $\partial\zeta/\partial z$ we can calculate now the global derivatives of the shape functions of the form $\partial N/\partial x$, $\partial N/\partial y$, $\partial N/\partial z$ using relations

$$\frac{\partial N}{\partial x} = \frac{\partial N}{\partial \xi}\cdot\frac{\partial \xi}{\partial x} + \frac{\partial N}{\partial \eta}\cdot\frac{\partial \eta}{\partial x} + \frac{\partial N}{\partial \zeta}\cdot\frac{\partial \zeta}{\partial x}$$

$$\frac{\partial N}{\partial y} = \frac{\partial N}{\partial \xi}\cdot\frac{\partial \xi}{\partial y} + \frac{\partial N}{\partial \eta}\cdot\frac{\partial \eta}{\partial y} + \frac{\partial N}{\partial \zeta}\cdot\frac{\partial \zeta}{\partial y}$$

$$\frac{\partial N}{\partial z} = \frac{\partial N}{\partial \xi}\cdot\frac{\partial \xi}{\partial z} + \frac{\partial N}{\partial \eta}\cdot\frac{\partial \eta}{\partial z} + \frac{\partial N}{\partial \zeta}\cdot\frac{\partial \zeta}{\partial z}$$

h. Evaluation of matrix coefficients a_{ij}
The coefficients, as given by equation (10), can now be calculated since

$$a_{IJ} = \sum_{i=1}^{3}\sum_{j=1}^{3}\sum_{k=1}^{3}\left(\frac{\partial N_I}{\partial x}\cdot\frac{\partial N_J}{\partial x} + \frac{\partial N_I}{\partial y}\cdot\frac{\partial N_J}{\partial y} + \frac{\partial N_I}{\partial z}\cdot\frac{\partial N_J}{\partial z}\right)\cdot |J|_{(\xi_i,\eta_j,\zeta_k)}\, a_i a_j a_k$$

in which the capitals I, J denote nodal numbers and i, j, k Gauss point numbers.

Once the governing equation and boundary conditions have been defined, the procedure is conceptually straightforward. It is highly dependent on the way in which both the geometry of the flow domain and spatial variation of the variables is defined. First the code is executed in single-body Neumann condition, at zero Froude number. In the next step, the linear solution is computed. Finally, non-linear effects on the free surface are taken into account by an iterative procedure (an Euler-Lagrange approach), always linearizing the free surface boundary conditions on the basis of the immediate former solution, until convergence is reached. Simultaneously, the finite elements are moved correspondingly so that the grid is adapted each step to follow the free surface. The infinity condition is fulfilled by using semi-infinite elements. For radiation condition a special treatment is applied.

4. Wave pattern analysis

The wave-pattern analysis is a valuable diagnostic tool, particularly when used with a measurement of the momentum defect in the viscous-wake region. This technique has led to the discovery of an additional drag component associated with wave breaking, and to a better understanding of the bulbous bows of full form big ships with low Froude number.

In fine high-speed vessels a bulbous bow promotes beneficial interference between the waves generated at different points along the length of the hull. Thus, for such vessels, the bow bulb reduces the wave resistance. Originally, bulbous bows of a similar form were fitted to certain ship types on the basis of experimental measurements indicating significant reductions in the total drag, but these reductions often exceed the total estimated resistance.

This apparent paradox has been reconciled by careful experimental measurements of the wave-energy flux and of momentum defect in the wake due to the viscous form drag. The latter measurement has revealed the existence of momentum associated with the breaking waves. Thus the wave-breaking resistance follows from the breaking of waves near the ship, predominantly at the bow. In this manner, the energy lost is convected downstream in the form of large-scale turbulence or eddies.

For full form giant ships, the bulbous bow is effective in reducing the magnitude of bow wave and thereby in avoiding wave breaking. For predicting the total drag, one may argue that it makes little difference whether the energy is wasted in wave radiation or in wave breaking, but only through an understanding of the mechanisms involved can the total drag be reduced intelligently and systematically. In this context we consider that using both a spatial moving boundary f.e.m. and an gaining insight into how waves break is the best solution.

4.1. Wave resistance computation

Once the field of velocities computed, the wave resistance can be obtained as follows

$$R_w = \rho\, U_\infty^2 \iint_{S_w} c_p\, n_x\, dx \text{, where } c_p = \frac{p - p_\infty}{0.5 \cdot \rho U_\infty^2} = 1 - \left(\frac{U}{U_\infty}\right)^2 .$$

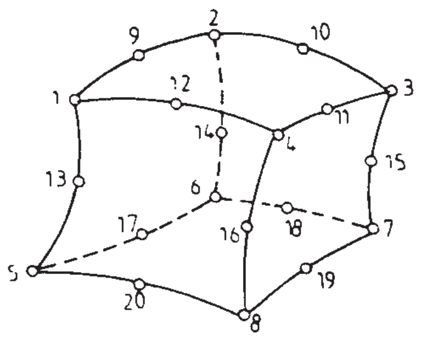

Hexahedron finite element
with curved boundaries
(see location of nodes)

5. Methodology of the experimental part

Three types of breaking waves must be investigated: plunging breaker; spilling breaker; breaker that start as a small scale plunging breaker and evolves further similar to a spilling breaker.

The surface geometry is measured by means of image analysis (spatial geometry), in addition to ordinary wave gauges (temporal geometry). The surface is described by a set of parameters, derived to best describe features of the wave geometry that are important to the physics in the breaking event. In addition to measuring the geometry of the free surface the kinematics is measured by using Particle Image Velocimetry. The measurements is conducted first in a wave laboratory and then in a towing tank laboratory.

6. Conclusion

It is hoped that, in this way, a new more accurate teoretical-numerical method for ships wave making resistance prediction will be found.

REFERENCES

[1] Bai, K.J., Kim, J.W., Kim, Y.H., Numerical computations for a nonlinear free surface flow problem.
[2] Batchelor, G.K., An introduction to fluid dynamics, Cambridge University Press, 1991.
[3] Bertram, V., Practical Ship Hydrodynamics, Butterworth-Heinemann, 2000.
[4] Chung, T.J., Finite element analysis in fluid dynamics", McGraw-Hill, New York, 1978.
[5] Dawson, C.W., A practical computer method for solving ship-wave problem, 2-nd International Conference on Numerical Ship Hydrodynamics, University of California, Berkley, 1977.
[6] Eggers, K., Sharma, S., Ward, L., An assessment of some experimental methods for determining the wave making characteristics of a ship form, Society of Naval Architects and Marine Engineers Transactions, **75**: 112-157.
[7] Fletcher, C.A.J., Computational techniques for fluid dynamics, Springer, Berlin, 1987.
[8] Jensen, G., Bertram, V., Sőding, H., Ship wave-resistance computations, 5-th International Conference on Numerical Ship Hydrodynamics, 1990.
[9] Jensen, G., Sőding, H., Rankine source methods for numerical solutions of steady wave resistance problem, 17-th Symposium on Naval Hydrodynamics, Hague, 1988.
[10] Jensen, P.S., On the numerical radiation condition in the steady-state ship wave problem, Journal of Ship Research, **31**, 1(1987), 14-22.
[11] Larsson, L.,Broberg, L.,Kim, K.J.,Zhang,D.H., New viscous and inviscid CFD Techniques for Ship Flows, 5th International Conference on Numerical Ship Hydrodynamics, Hiroshima, 1989.
[12] Longuet-Higgins, M.S., Progress toward understanding how waves break, 21-st Symposium on Naval Hydrodynamics, 1997.
[13] Pierson, J.W., Jean-Pierre Azed, Monte carlo simulations of nonlinear wave records with implications for models of breaking waves, Journal of Ship Research, **43**, 2(1999), 121-134.
[14] Tuck, E.O., Scullen, D.C., Lazauskas, L., Wave patterns and minimum wave resistance for high-speed vessels , 24-th Symposium on Naval Hydrodynamics, Fukuoka, Japan, 8-13 July, 2002.
[15] Tulin, M.P., Landrini, M., Breaking waves in the ocean and around ships, 23-rd Symposium on Naval Hydrodynamics, 2001.
[16] Washizu, K., Some applications of finite element techniques to nonlinear free surface fluid flow problems, Osaka, Japan, 1981.

Mathematics modelling of main process of polluants transport

Modelarea matematica a principalelor procese de transport al poluantilor. Metode de rezolvare si interpretare a solutiilor

Turcan Radu*, Turcan Viorica**
* Univ din Oradea, Fac.de Stinte, Departamentul de Matematica
** Colegiul Tehnic «Constantin Brancusi» - Oradea

Rezumat. Prezenta lucrare continua articolul [5] si prezinta în sectiunea 1 principalele metode analitice, si numerice pentru studiul miscarii uni si bidimensionale, in medii poroase. Am analizat in principal doua dintre aceste metode si anume: metoda diferentelor finite – pentru miscari unidimensionale si metoda elementelor finite in cazul dispersiei bidimensionale, deoarece metodele numerice au o mai mare aplicabilitate, inclusiv in cazurile in care domeniul de miscare este complex. Ambele metode presupun o discretizare pe intregul domeniu de miscare.

In sectiunea 2 este prezentat sub forma generala un program performant, corespunzator modelarii curgerii apelor subterane si a poluantilor prin acvifere.

1. Metode de rezolvare şi interpretare a soluţiilor

1.1. Metoda analitică pentru mişcări unidimensionale şi bidimensionale

Ecuaţia de transfer a poluanţilor în medii poroase are forma [4]

$$\frac{\partial C}{\partial t}+\frac{1}{R}\nabla\vec{u}C-\nabla\left(\frac{\vec{D}}{R}\nabla C\right)+\lambda C-\frac{q^{*}\rho_p C_p}{\rho m_e R}-\frac{\sigma^{*}}{\rho m_e R}=0 \tag{1}$$

1.1.1. Mişcarea unidimensională

În acest caz, ecuaţia (1), devine:

$$\frac{\partial C}{\partial t}+\frac{u}{R}\cdot\frac{\partial C}{\partial x}-\frac{D_C}{R}\cdot\frac{\partial^2 C}{\partial x^2}+\lambda C=0\,, \tag{2}$$

unde: C(x;t) = concentraţia poluantului la distanţa x de locul injectării şi la timpul t, de momentul injectării; D_L = coeficientul de dispersie longitudinală; t = timpul; u = viteza de mişcare reală a apei prin mediul poros; λ = rata de descompunere.

Pentru injecţia de poluant, de tip impuls, într-un acvifer infinit la ambele capete, i.e. $x\in(-\infty;\infty)$, la x = 0 şi t = 0; în acvifer se introduce o masă de poluant ΔM, ceea ce matematic se exprima prin conditia initiala

$$C_0(x_0;0)=\frac{\Delta M}{m_e T b R}\cdot\delta(x) \tag{3}$$

respective conditiile la mari distante

$$C(\pm\infty;t)=0 \tag{4}$$

unde: $C_0(x_0;0)=$ concentraţia poluantului în momentul injectării; $\Delta M=$ masa de poluant, în momentul iniţial; $m_e=$ porozitatea adimensională efectivă,T = grosimea stratului de acvifer, b = lăţimea; R = factor de întârziere; $\delta(x)$ = funcţia lui Dirac.

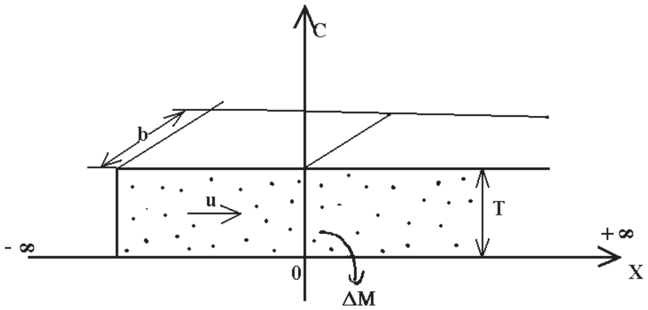

Fig.7.

Soluția analitică a problemei (2)-(4) a fost dată de Crank, în 1950, şi are forma

$$C(x;t) = \Delta M / (2bTm_e \sqrt{\pi D_L t / R}) \exp\{(x - ut/R)^2 / (4D_L t/R)\} \exp\{-\lambda t\}$$

unde $\Delta M \cdot e^{-\lambda t} = \int_{-\infty}^{\infty} bTm_e RC(x;t)dx$.

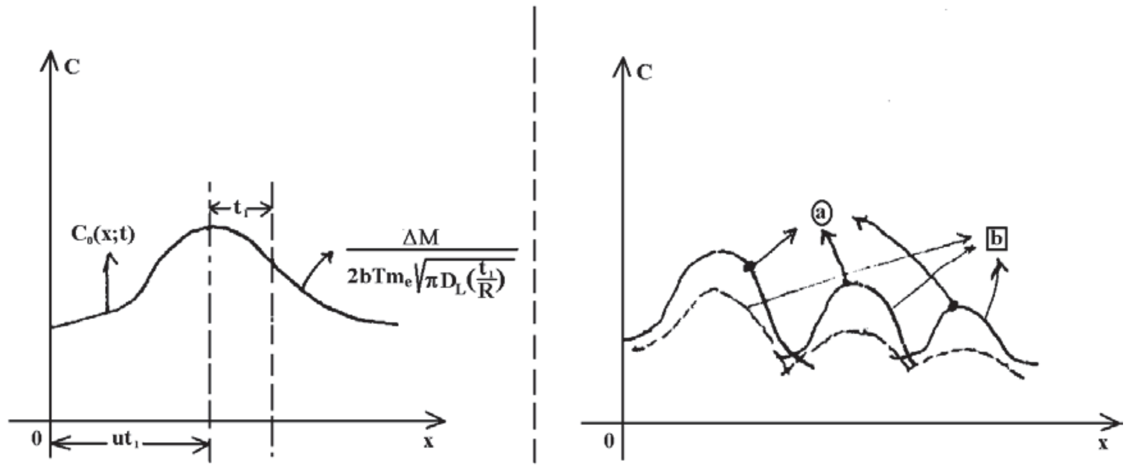

(a) (b)

Fig.1.

Evoluția în timp şi spațiu a concentrației poluantului, în stratul acvifer infinit şi în ambele sensuri, când poluantul este de tip conservativ (i.e. λ=0) sau de tip neconservativ (i.e. λ>0(b), (vezi fig.9).

1.1.2. Mişcarea bidimensională

Pentru mişcarea dimensională, ecuația (1) devine

$$\frac{\partial C}{\partial t} + \frac{u}{R} \cdot \frac{\partial C}{\partial x} - \frac{D_L}{R} \cdot \frac{\partial^2 C}{\partial x^2} - \frac{D_T}{R} \cdot \frac{\partial^2 C}{\partial y^2} = 0.$$

Sa consideram pentru injecția punctuală, cu poluant de tip impuls. In acest caz, în punctul de coordonate x=0 şi y=0 se efectuează injecția de poluant într-un acvifer constand dintr-un domeniu plan, infinit şi omogen. Condițiile la limită, la mari distante si cele initiale sunt respectiv

$$C^{(0)\to\lambda}(x=0;y=0;t)=\frac{\Delta M}{m_e\cdot T\cdot R}\cdot\delta(x)\delta(z)$$

$$\begin{cases} C^{(0)}(x=\pm\infty;y=\pm\infty;t)=0 \\ C^{(0)}(x=0;y=0;t=0)=0 \end{cases}$$

iar condiția de normare este se scrie ca

$$\int_{x=-\infty}^{+\infty}\int_{y=-\infty}^{+\infty} m_e TRC^0(x;y;t)dxdy=\Delta M$$

Soluția acestei probleme a fost dată de Csanady (1981) şi are forma

$$C^{(0)}(x,y;t)=\frac{\Delta M}{4\pi m_e T\cdot\sqrt{D_L\cdot D_L\cdot t}}\cdot\exp\left[-\frac{(x-ut/R)}{4D_L t/R}-\frac{y^2}{4D_T t/R}\right]$$

1.2. Metode numerice

1.2.1. Metoda diferențelor finite pentru mişcări unidimensionale

Fie ecuația cu derivate parțiale, a celei mai simple mişcări: dispersia unidimensională (într-un curent uniform):

$$\frac{\partial C}{\partial t}=u\cdot\frac{\partial C}{\partial x}+D\cdot\frac{\partial^2 C}{\partial x^2})$$

Metoda diferențelor finite constă în discretizarea intervalului unidimensional spațial $x\in[0;\infty)$ si a celui temporal $t\in[0;\infty)$ si înlocuirea ecuației cu derivate parțiale cu o ecuație algebrică, în valorile nodale spațio-temporale ale concentrației.

Prima variantă a metodei diferențelor finite este metoda explicită, care constă în determinarea concentrației C la momentul $t+\Delta t$ în funcție de valorile la *t*, ale acesteia în nodurile spațiale (vezi fig. 2).

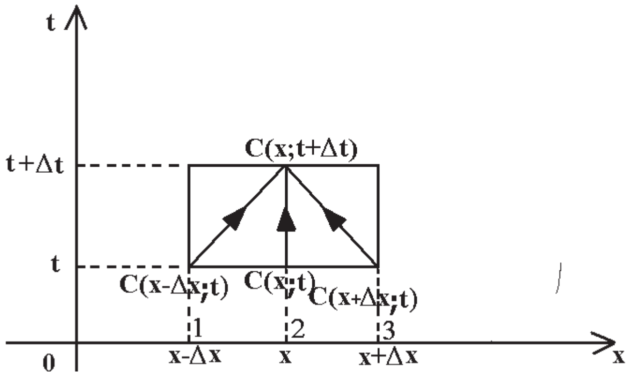

Fig. 2.

Pentru scrierea relațiilor cu diferențe finite, există mai multe posibilități: DIF – progresiv; DIF – central; DIF – regresiv.

Aceste 3 variante se referă la tipul aproximarii derivatelor parțiale de ordinul I. Astfel, în cazul DIF – progresiv, din dezvoltarea

$$C(x+\Delta x;t)=C(x;t)+\Delta x\cdot\frac{\partial C}{\partial x}+\frac{\Delta x^2}{2!}\cdot\frac{\partial^2 C}{\partial x^2}+.... \tag{5}$$

rezultă

$$\frac{\partial C(x;t)}{\partial x}=\frac{C(x+\Delta x;t)-C(x;t)}{\Delta x}-\frac{1}{2}\Delta x\cdot\frac{\partial^2 C}{\partial x^2}+0\cdot\left(\Delta x^2;\frac{\partial^3 C}{\partial x^3}\right)$$

În cazul în care avem DIF – regresiv, din dezvoltarea

$$C(x-\Delta x;t)=C(x;t)-\Delta x\cdot\frac{\partial C}{\partial x}+\frac{\Delta x^2}{2!}\cdot\frac{\partial^2 C}{\partial x^2}+.... \tag{6}$$

rezultă:

$$\frac{\partial C(x;t)}{\partial x}=\frac{C(x;t)-C(x-\Delta x;t)}{\Delta x}+\frac{1}{2}\Delta x\cdot\frac{\partial^2 C}{\partial x^2}+0\cdot\left(\Delta x^2;\frac{\partial^3 C}{\partial x^3}\right)$$

iar cazul DIF – central se obține din relațiile (5) şi (6), prin scăderea lor, i.e.

$$\frac{\partial C(x;t)}{\partial x}=\frac{C(x+\Delta x;t)-C(x-\Delta x;t)}{2\Delta x}+0\cdot\left(\Delta x^2;\frac{\partial^3 C}{\partial x^3}\right).$$

Pentru derivata a II-a se poate utiliza numai forma centrală, din relațiile (5) şi (6) rezultând, prin adunare,

$$\frac{\partial^2 C}{\partial x^2}=\frac{C(x-\Delta x;t)-2C(x;t)+C(x+\Delta x;t)}{\Delta x^2}+0\cdot\left(\Delta x^2;\frac{\partial^4 C}{\partial x^4}\right)$$

Pentru discretizarea temporală, în variantă explicită, se poate folosi numai DIF – progresiv

$$C(x;t+\Delta t)=C(x;t)+\Delta t\cdot\frac{\partial C}{\partial t}+\frac{\Delta t^2}{2!}\cdot\frac{\partial^2 C}{\partial t^2}+....$$

rezultând

$$\frac{\partial C(x;t)}{\partial t}=\frac{C(x;t+\Delta t)-C(x;t)}{\Delta t}-\frac{1}{2}\Delta t\cdot\frac{\partial^2 C}{\partial t^2}+0\cdot\left(\Delta t^2;\frac{\partial^3 C}{\partial t^3}\right).$$

1.2.2. Metoda elementelor finite (în cazul dispersiei bidimensionale)

Fie dispersia bidimensională simplă, i.e. mişcarea convectivă este uniformă, cu viteza constantă *u*, iar dispersia este bidimensională, având coeficientul de dispersie de forma

$$D_{i,j}=\begin{bmatrix}D_{xx} & 0\\ 0 & \mathrm{D}_{\mathrm{yy}}\end{bmatrix}=\begin{bmatrix}\alpha_L u & 0\\ 0 & \alpha_{\mathrm{T}} u\end{bmatrix}$$

În general $\alpha_L\neq\alpha_T$, i.e. dispersia longitudinală α_{L} este diferită de dispersia transversală α_{T}.

Ecuația generală a transportului poluanților într-un acvifer bidimensional are forma

$$\frac{\partial \mathrm{C}}{\partial \mathrm{t}}=-\mathrm{u}\frac{\partial \mathrm{C}}{\partial \mathrm{x}}+\frac{\partial}{\partial \mathrm{x}}\left(\mathrm{D}_{\mathrm{xx}}\frac{\partial \mathrm{C}}{\partial \mathrm{x}}\right)+\frac{\partial}{\partial \mathrm{y}}\left(\mathrm{D}_{\mathrm{yy}}\frac{\partial \mathrm{C}}{\partial \mathrm{y}}\right). \tag{7}$$

Derivata parțială a lui C în raport cu timpul se poate exprima într-o formă mai convenabilă (care să cuprindă câteva forme de interpolare) pornind de la formula de interpolare pentru valoarea medie:

$$C=\varepsilon C_0+(1-\varepsilon)C'. \tag{8}$$

Se observă că pentru: $\varepsilon=1/2$, rezultă $C=\dfrac{C_0+C'}{2}$, i. e. avem o interpolare constantă, cu valoarea medie a concentrației (fig. 3).

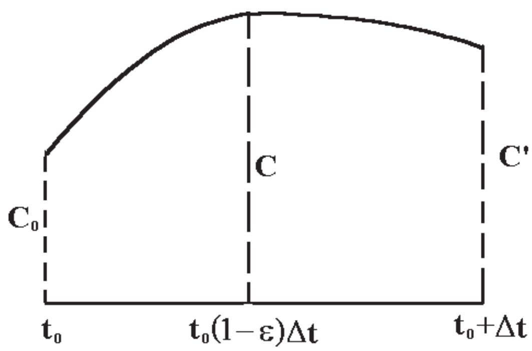

Fig.3.

Pentru concentrația C, exprimată prin formula (8), avem câteva cazuri particulare:

1) pentru $\varepsilon = 1 \Rightarrow C = C_0$ adevarata pentru $t = t_0$;

2) pentru $\varepsilon = 0 \Rightarrow C = C'$ adevarata pentru $t = t_0 + \Delta t$;

3) pentru $\varepsilon =$ arbitrar $\Rightarrow C = \varepsilon C_0 + (1-\varepsilon)C'$ adevarat pentru $t = t_0 + (1-\varepsilon)\Delta t$.

Atunci derivata lui *C* în raport cu timpul devine

$$\frac{\partial C}{\partial t} = \frac{C - C_0}{(1-\varepsilon)\Delta T} \tag{9}$$

Înlocuind (9) în (7) obținem

$$\frac{C - C_0}{(1-\varepsilon)\Delta t} = -u\frac{\partial C}{\partial x} + \frac{\partial}{\partial x}\left(D_{xx}\frac{\partial C}{\partial x}\right) + \frac{\partial}{\partial y}\left(D_{yy}\frac{\partial C}{\partial y}\right),$$

sau, echivalent

$$\frac{\partial}{\partial x}\left(D_{xx}\frac{\partial C}{\partial x}\right) + \frac{\partial}{\partial y}\left(D_{yy}\frac{\partial C}{\partial y}\right) - u\frac{\partial C}{\partial x} - \frac{C - C_0}{(1-\varepsilon)\Delta t} = 0,$$

i.e. ecuația generală de transport a poluanților printr-un acvifer bidimensional.

2. ASM (AQUIFER SIMULATION MODEL)

2.1. Descriere generală

2.1.1 Performanțele programului

Probleme pe care le rezolvă sunt: previziuni hidrogeologice; interpretarea datelor de pompare la puțuri; evaluarea testelor de pompare; simularea curgerii apelor subterane; interpretarea datelor de concentrație; simularea transportului poluanților în ape subterane.

2.1.2 Descrierea generală a ASM

ASM este un program ce simulează curgerea apelor subterane și transportul poluanților folosind metoda diferențelor finite în varianta sa celulară, i.e. toate mărimile fizice (hidraulice) sunt considerate în centrul celulei.

2.1.3. Schema bloc a programului

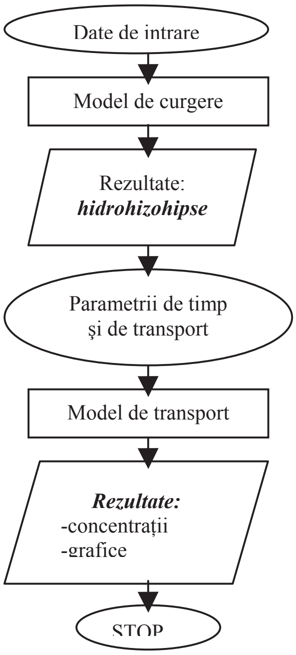

2.2. ASM – date de intrare pentru parametrii de curgere

- Tipul regimului de curgere permanent sau nepermanent;
- tipul acviferului: cu nivel liber sau sub presiune;
- mărimea acviferului: lungimea si latimea;
- mărimea celulelor: Δx (m), Δy (m);
- numărul celulelor: după axa Ox: $N_{x,}$, după axa Oy: N_y;
- grosimea acviferului: 2 m;
- caracterizarea acviferului prin: permeabilitatea [K(m/sec)] la cel cu nivel liber; transmisivitatea [T(m^2/sec)] la cel sub presiune; acvifer omogen (K sau T = constante); neomogen (K sau T = variabile);
- numărul şi poziţia puţurilor de: extragere (-m^3/sec), injecţie (+m^3/sec);
- alimentarea acviferului din precipitaţii cu debite constante sau variabile;
- condiţii la limită (înălţimi piezometrice, cunoscute pe frontiera domeniului);
- coeficienţii de înmagazinare pentru celulele acviferului:
  - 0 $\rightarrow$ pentru celulele la care nu se cunoaşte înălţimea piezometrică
  - 1 $\rightarrow$ pentru celulele situate pe frontiera domeniului

Cu aceste date de intrare, modulul de curgere poate fi rulat şi se obţin:

- înălţimile piezometrice în toate celulele din domeniu şi
- bilanţul apei (intrări, ieşiri de volume de apă)

2.3. ASM – date de intrare pentru parametrii de transport

- porozitatea efectivă ($0{,}18 \div 0{,}30$);
- factor de întârziere: R = 1 (fără întârziere) şi R>1 (cu întârziere);
- număr de particule, folosite în simulare;
- dispersivitatea longitudinală (1% din lungimea modelului);
- dispersivitatea transversală (1/10 din dispersivitatea longitudinală);
- tipul injecţiei (permanentă sau instantanee);

- rata de injecţie (pentru injecţia permanentă a unui poluant);
- masa de injecţie (pentru injecţia instantanee);
- poziţia surselor de poluare (în care celulă se află);
- timpul total de simulare (în zile);
- pasul de timp (în zile).

Cu aceste date de intrare (pentru parametrii de transport şi de timp) modulul de transport poate fi rulat, obţinând rezultate ale simulării transportului poluanţilor în acvifer.

Rezultatele oferite de modulul de transport sunt: concentraţii finale (după timpul total de simulare); variaţia concentraţiilor în puţuri de observaţie (în maxim 3 celule) stabilite anterior de utilizator; distanţele de la puţuri, pentru care timpul de transport convectiv are o valoare dată (pentru 20 de zile sau 50 de zile); traseul parcurs de o particulă de poluant dintr-un anumit punct, până la cel mai apropiat puţ de extracţie.

2.4. Alte precizări pentru ASM

Programul rulează sub MS – DOS; fişierul principal este: asm.exe; datele de intrare se salvează într-un fişier cu nume ales de utilizator; datele de ieşire (înălţimi piezometrice în celule) sunt create de program; rezultatele se pot vizualiza pe monitor; se pot capta (cu programe grafice).

BIBLIOGRAFIE

[1]. David, I., Grundwasserhydraulik, Vieweg, Wiesbaden, 1998.
[2]. Gheorghita, St. I., Metode matematice in hidrogazodinamica subterana, Ed. Academiei, Bucuresti,1966.
[3]. David, I., Sumalan, I., Carabet, A., Nitusca, A., Transportul poluantilor prin medii fluide, Universitatea „Politehnica” din Timisoara, 1966.
[4]. Turcan, R., Turcan, V. Modelarea curgerii apei si a transportului poluantilor prin acvifere – metode matematice, Conferinta Nationala de Analiza Matematica si Aplicatii, Universitatea „Babes-Bolyai”, Cluj-Napoca (8-9 nov 2002).
[5]. Turcan R., Turcan V., The transport in aquifers, în acest volum

Integrity in distributed database

Mădălina VĂLEANU
Department of Medical Informatics and Biostatistics,
Universitatea de Medicina si Farmacie „Iuliu Hatieganu" Cluj-Napoca

Grigor MOLDOVAN
Department of Computer Science,
Universitatea Babes-Bolyai Cluj-Napoca

Abstract. In this paper a proper terminology for discretionary models databases is defined and some integrity types for these models are specified. A modality for maintaining integrity of distributed databases is presented too.
Keywords: database, distributed database, database integrity, distributed database integrity, integrity level

1. INTRODUCTION

The database is now an integral part of our day-to-day life that often we are not aware using one. We can consider a database to be a collection of logically related data and a description of this data designed to meet the information needs of an organization [6,7].

The Database Management System (DBMS) is software that enables users to define, create and maintain the database and provides controlled access to this database. Data and database administration are the roles generally associated with the management and control of a DBMS and its data.

The Data Administrator (DA) is responsible for the management of the data resource including database planning, development and maintenance of standards, policies and procedures, and conceptual/logical database design.

The Database Administrator (DBA) is responsible for the physical realization of the database, including physical database design and implementation, security and integrity control, maintenance of the operational system, and ensuring satisfactory performance for the application and users.

Database integrity refers to the validity and consistency of stored data. Integrity is usually expressed in terms of constraints, which are consistency rules that the database is not permitted to violate. Constraints may apply to data items within a single record or they may apply to relationships between records. For example, an integrity constraint could state that an employee's salary cannot be grater than 10.000 $ or that the branch number contained in the employee's record, representing the branch that the employee works at, must correspond to an existing branch office. Again, integration allows the DBA to define, and the DBMS to enforce, integrity constraints.

Ensuring *integrity of information* means preventing/detecting/deterring the improper modification of information (Sandhu and Jajodia, 1990). For example, in a military environment the target coordinates of a missile should not be improperly modified. Also, in commercial environments, data integrity is a relevant aspect: the good working of an organization depends on correct operations a correct and coherent data. For example, an employee should not be able to modify his or her own salary, or improperly alter data regarding an electronic payment.

Integrity of the database concerns database protection from unauthorized access that could modify the contents of data, as well as from errors, viruses, sabotage or failures in the system that could damage stored data. This kind of protection is partly carried out by the DBMS through proper system controls, and various backup and recovery procedures, and partly through ad hoc security procedures.

Operational integrity of data aims to ensure the logical consistency of data in a database during concurrent transactions. The *concurrency manager* is the DBMS subsystem that fulfits this requirement.

The concurrency manager ensures the serializability properties of transactions. Serializability means that the outcome of a concurrent run of a set of transactions is the same as the one produced by a strict sequence of these transactions. Isolation means mutual independence among transactions, thus avoiding "domino effects", where an "abort transaction" causes other transactions to abort in a cascade.

The problem of ensuring that concurrent access to the same data item by different transaction does not lead to data inconsistency is a commonly solved through *locking* techniques.

Lock and unlock techniques consist, respectively, in blocking data items for the time needed to execute an operation, and in releasing the item once the operation has been completed. In this way, a transaction can lock a data item, making it inaccessible to other transactions. The item is accessible again at release time.

Semantic integrity of data is to ensure the logical consistency of modified data by controlling data values in the allowed range. Restrictions on data values (for example, attribute values in a relational database) are expressed as *integrity constraints*.

Constraints can be defined for the whole database (conditions defining the correct state of a database), or for transactions (conditions to be verified in order to execute a modification to the database).

2. DISCRETIONARY MODELS AND INTEGRITY

Each system subject is assigned three integrity levels [3,4,15]:

- *Absolute Integrity Level (AIL)* is the integrity level given to the data contained in the object and the subject upon its creation. It is fixed for the whole life cycle of the subject. Typically, this level will be the integrity level of the user on behalf of whom the subject is acting;
- *Read Integrity Level (RIL)* is the lowest integrity level from which the subject is allowed to read;
- *Write Integrity Level (WIL)* is the highest integrity level to which the subject is allowed to write.

Each object is assigned three integrity levels:

- *Absolute Integrity Level (AIL)* is the integrity level of the data contained in the object and the subject. It is fixed for the whole life cycle of the object;
- *Migration Integrity Level (MIL)* is the lowest integrity level to which data in the object may flow;
- *Corruption Integrity Level (CIL)* is the highest level from which data may flow into the object.

The TCB model

The TCB model defines multilevel relations [10]. A multilevel relation is defined as any relation where there exist classification attributes C_i for each attribute A_i and a classification attribute for each tuple. Formally, a multilevel relation is represented by a schema $R(A_1, C_1, \ldots, A_n C_n, T_C)$. An attribute A_i corresponding to C_i of a multilevel relation is single level iff, C_i is defined on a domain represented by a single class in the access class lattice; otherwise it is multilevel. A multilevel relation is single level if all attributes are single-level and of the same class.

Each tuple in a multilevel relation has the form $<a_1|c_1, \ldots, a_n|c_k, t>$, where $a_i|c_i$ indicates the value and the classification of attribute i respectively. Element t indicates the access class associated with the tuple: that is, the access class of the information in (or encoded in) the tuple.

Properties:

- *Database class integrity*: the access class of a relation schema must dominate the access class of the name of the database to which it belongs;
- *Visible data property*: the access of the relation schema must be dominated by the access class of the lowest data that can be stored in the relation. The greatest lower bound of the range of access classes specified for an attribute must dominate the access class of the relation schema;
- *View class integrity*: the access class of a view definition must dominate the access class of any relation or view named in the view definition;
- *Multilevel entity integrity*: let AK be the set of data attributes forming the primary key of a relation R. All classification attributes C_i corresponding to data attributes $A_i \in AK$ have the same value within any given tuple of R, and this class is dominated by the value of each classification attribute C_j whose data attribute $A_j \notin AK$. No tuple in an instance of R can have null values for any of the primary key attributes;

- *Multilevel referential integrity:* no tuple in a relation can have a non-null secondary key unless a tuple exist in the referenced relation with the corresponding primary key. Within a tuple, the access class of each element comprising a secondary key must be the same (that is, the secondary key attributes must be uniformly classified) and must dominate the access class of the primary key element(s) in the tuple referenced.

The Jajodia and Sandhu model

The Jajodia and Sandhu model is a model for the application of mandatory policies in relational database system.

A multilevel relation consists of the following parts:

- a state-independent multilevel relation scheme $R(A_1,C_1,\ldots,A_n,C_n,TC)$, where each A_i is a data attribute defined over domain D_i, each C_i is a classification attribute for A_i and TC is the tuple-class attribute;
- a collection of state-dependent relation instances $R_c(A_1,C_1,\ldots,A_n,C_n,TC)$,one for each access class c.

Properties:

Entity integrity: Let AK be the apparent key of a relation R. A multilevel relation R satisfies entity integrity if, and only if, for all instances R_c of R and $t \in R_c$

(1) $A_i \in AK \Rightarrow t[A_i] \neq null$,

(2) $A_i, A_j \in AK \Rightarrow t[C_i] = t[C_j]$,i.e. AK is uniformly classified, and

(3) $A_i \notin AK, t[C_i] \geq t[C_{AK}]$ (where C_{AK} is defined as the classification of the apparent key).

Null integrity: a multilevel relation R satisfies null integrity if for each instance R_c of R both the following conditions are satisfied:

(1)for all $t \in R_c, t[A_i] = null \Rightarrow t[C_i] = t[C_{AK}]$, that is null values are classified at the level of the key;

(2)R_c is subsumption free in the sense that it does not contain two distinct tuples such that one subsumes the other.

Polyinstantiation integrity property: a multilevel relation R satisfies polyinstantiation integrity iff, for ever R_c, for all A_i:AK, C_{AK}, $C_i \rightarrow A_i$.

3. Logical database design methodology for the relational model

The logical database design methodology for the relational model need two steps:

- build and validate local data model for each user view;
- build and validate global logical data model.

Integrity constraints are the constraints that we wish to impose in order to protect the database from becoming inconsistent. Note that, although DBMS control on integrity may or may not exist, this is not the question here. At this stage, we are concerned only with high-level design, that is specifying what integrity constraints are required, irrespective of how this might be achieved. Having identified the integrity constraints, we will have a local logical data model that is a complete and accurate representation of a user view. If necessary, we could produce a physical database design from the local logical data model, for example, to prototype the system for the user.[12,14]

We consider five types of integrity constraints:

- ✓ required data;
- ✓ attribute domain constraints;
- ✓ entity integrity;
- ✓ referential integrity;
- ✓ enterprise constraints.

Required data

Some attributes must always contain a valid value; in other words, they are not allowed to hold nulls. For example, every member of a staff has an associated job position (such as Manager, Assistants).

These constraints should have been identified when we documented the attributes in the data dictionary.

Attribute domain constraints.

Every attribute has a domain, which is a set of values that are legal. For example, the sex of a member of staff is either 'M' or 'F', so the domain of the Sex attribute is a single character string of 'M' or 'F'.

These constraints should have been identified when we choose the attribute domains for the data model

Entity integrity

The primary key of an entity cannot hold nulls. For example, each occurrence of the staff relation must have a value for the primary key attribute, namely Staff_No.

These constraints should have been considered when we identified the primary keys for each entity type.

Referential integrity

A foreign key links each occurrence in the child relation to the occurrence in the parent relation containing the matching candidate key value. Referential integrity means that, if the foreign key contains a value, that value must refer to an existing occurrence in the parent relation.

Enterprise constraints

Finally, we consider constraints known as enterprise constraints, sometimes called business rules. Updates to entities may be constrained by enterprise rules governing the 'real world' transaction that are represented by the updates.

4. DISTRIBUTED DATABASE

In a distributed DBMS, we need in addition a *global transaction manage*r or *transaction coordinator* at each site, to coordinate the execution of both the global and local transactions initiated at that site [2,5]. Inter-site communication is still through the *Data Communications* component (transaction manager at different sites do not communicate directly with each other).

When a transaction is submitted at some site, the transaction manager at that site breaks it up into a collection of one or more subtransactions that execute at different sites, submits them to transaction manager at the other site, and coordinates their activity [14].

We can consider aspects of concurrency control and recovery that require additional attention because of data distribution. There are many concurrency control protocols. Here appear the following issues[13]:

- **Distributed Concurrency Control:** how can locks for objects stored across several sites be managed? How can deadlocks be detected in a distributed database?
- **Distributed Recovery:** transaction atomicity must be ensured – when transaction commits, all its actions, across all the sites that it executes at, must persist. Similarly, when a transaction aborts, none of its action must be allowed to persist.

Distributed Concurrency Control

The choice of technique for implementing asynchronous replication determined *which* objects are to be locked. *When* locks are obtained and released is determined by the concurrency protocol. We now consider how lock and unlock requests are implemented in a distributed environment.

Lock management can be distributed across sites in many ways:

- *centralized*: a single site is in charge of handling lock and unlock requests for all objects.
- *primary copy*: one copy of each objects is designated as the primary copy. All requests to lock or unlock a copy of this object are handled by the lock manager at the site where the primary copy is stored.
- *fully distributed*: requests to lock or unlock a copy of an object stored at a site are handled by the lock manager at the site where the copy is stored.

Distributed Recovery

Recovery in a distributed DBMS is more complicated than in a centralized DBMS for the following reasons:

- new kinds of failure can arise, namely failure of communication link and failure of a remote site at which a subtransaction is executing;
- either all transactions of a given transaction must commit, or none must commit, and this property must be guaranteed despite any combination of site and link failures. This guarantee is achieved using a **commit protocol**.

Three-phase commit (3PC) is non-blocking for site failures, except in the event of the failure of all sites. Communication failure can, however, result in different sites reaching different decisions, thereby violating the atomicity of global transactions. The protocol requires that:

- no network partitioning can occur;
- at least one site must always be available;
- at most K sites can fail simultaneously (system is classified as K-resilient).

The 3PC protocol imposes a significant additional cost during normal execution, and requires that communication link failures do not lead to a network partition (wherein some sites cannot reach some other sites through any part) in order to ensure freedom from blocking

Maintaining integrity

Time	P_1	P_2
T_1	Begin_transaction	Begin_transaction
T_2	$Bal_x = Bal_x - 60$	$Bal_x = Bal_x - 50$
T_3	Write (Bal_x)	Write (Bal_x)
T_4	commit	commit

Successfully completed update operations by users in different partitions can easily violate integrity constraints, as illustrated in previous figure. Assume that a blank places a constraint on a customer account (with balance Bal_x) that it cannot go bellow 0. In partition P_1, a transaction has withdrawn 60 from the account and in partition P_2 a transaction has withdrawn 50 from the same account. Assuming at the start, both partitions have 100 in Bal_x, then on completion one has 40 in Bal_x and the other has 50. Importantly, neither has violated the integrity constraints. However, when the partitions recover and the transactions are both fully implemented, the balance of the account will be -10, and the integrity constraints will have been violated.

Processing in a partitioned network involves a trade-off in availability and correctness. Absolute correctness is easiest to provide if no processing of replicated data is allowed during partitioning. On the other hand, availability is maximized if no restrictions are placed on the processing of replicated data during partitioning [12].

In general, it is not possible to design a non-blocking atomic commit protocol for arbitrarily partitioned networks. Since recovery and concurrency control are so closely related, the recovery techniques that will be used following network partitioning will depend on the particular concurrency control strategy being used. Methods are classified as pessimistic or optimistic.

Pessimistic protocols

Pessimistic protocols choose consistency of the database over availability, and would therefore not allow transactions to execute in a partition if no guarantee the consistency can be maintained. The protocol uses a pessimistic concurrency control algorithms. Recovery using this approach is much more straightforward, since updates would have been confined to a single, distinguished partition. Recovery or reconnection of the network simply involves propagating all the updates to every other site.

Optimistic protocols

Optimistic protocols, on the other hand, choose availability of the database at the expense of consistency, and use an optimistic approach to concurrency control, in which updates are allowed to proceed independently in the various partitions. Therefore, when sites recover, inconsistencies are likely.

To determine whether inconsistencies exist, precedence graphs can be used to keep track of dependencies among data. While the network is partitioned, updates proceed without restriction, and precedence graphs are maintained by each partition. When the network has recovered, the precedence graphs for all partitions are combined. Inconsistencies are indicated if there is a cycle in the graph. The resolution of inconsistencies depends upon the semantics of the transactions, and thus it is generally not possible for the recovery to re-establish consistency without intervention.

5. Conclusions

For distributed databases are keep the classical (usual) integrity types and as a request can be added the integrity types referred to global transactions (concurrent) in inter-site communication.

References

[1] Bell, D., Grimson, J., Distributed database system, Addison-Wesley, 1992.
[2] Bobak, A., Distributed and multi-database systems , Bantam Books, 1993.
[3] Cartell, R., Object data management , Addison –Wesley – ACM Press Books, 1992.
[4] Castrano, S., Fugini, M., Martella, G., Samarati, P., Database security, Addison-Wesley, 1999.
[5] Ceri, S., Pelagatti, G., Distributed satabases. Principles and systems, International Student Edition, McGraw Hill, 1985.
[6] Connolly, T. M., Begg, C. E., Database systems, Addison-Wesley, 1999.
[7] Date, C. J., An introduction to database systems , Addison –Wesley – ACM Press Books, 1982.
[8] Fleming, C., B. von Halle, Handbook of relational database design, Adison-Wesley, 1989.
[9] Franklin, M., Concurrency control and recovery in Handbook of computer science, A.B. Tucker , CRC Press, 1996.
[10] Gilula, M., The set model for database and informational systems, Addison–Wesley – ACM Press Books, 1999.
[11] Gollmann, D., Computer security, John Wiley&Sons, 2000.
[12] Hoffer, J, George, J., Valacich, J., Modern system analysis & design ,3-rd ed., Prentice Hall, 2002.
[13] Ramakrishnan, R., Database management system, Mc Garw-Hill, 1998.
[14] Ozsu, M., Valduriez, P., Principles of distributed database systems, Prentice-Hall, 1991.
[15] Sandhu, R. S., Jajodia, S., Integrity mechanism in database management systems in Proc. 13th National Computer Security Conference, Oct. 1990.
[16] Vossen, G., Date Models, Database languages and database management systems, Addison–Wesley, 1991.
[17] Widom, J, Ceri, S., Active database system , Morgan Kaufmann, 1996.
[18] Zaniolo, C., Ceri, S., Faloutsos, C., Snodgrass, R, Subrahmanianv, Zicari, R., Advanced database systems, Morgan Kaufmann, 1997.

Some applications of the Perov's fixed point theorem

Ioan Dziţac, Simona Dziţac, Horea Oros,
University of Oradea, idzitac@uoradea.ro

Abstract. In this paper we will present an application of the Perov's fixed point theorem in the canonical n-Banach spaces and one consequence in the R^n space. A sequential simulation program in C++ for parallel asynchronous method RFAIM [Dzi 00] is presented for a numerical example of the [RCM 75].

Key words: fixed point theorem, numerical method, parallel asynchronous iterations, RFAIM method

1. PRELIMINARIES RESULTS

In this paper we shall denote $\mathbf{R}$ the real number set and $\mathbf{R^n}$ the natural ordonated real linear space: $R^n := (R^n, R, x+y, \lambda x, x \le y)$, where, for $x=(x_1,x_2,\ldots,x_n)\in\mathbf{R}^n$, $y=(y_1,y_2,\ldots,y_n)\in\mathbf{R}^n$ and $\lambda\in\mathbf{R}$, we have:

(1.1) $x=y \Leftrightarrow x_i=y_i, \quad i=1..n;$

(1.2) $x\le y \Leftrightarrow x_i \le y_i, \quad i=1..n;$

(1.3) $x+y=(x_1+y_1,x_2+y_2,\ldots,x_n+y_n);$

(1.4) $\lambda x=(\lambda x_1, \lambda x_2,\ldots,\lambda x_n);$

(1.5) $x \le y \Leftrightarrow x_i \le y_i, \quad i=1..n.$

Definition 1.1 [*n*-metric complete space]: Let *X* a nonempty set. A vector function $d_n: X\times X\to\mathbf{R^n}$ is called *n*-metric on *X*, if the following conditions are satisfied:

(1.6) $d_n(x,y)\ge 0_{\mathbf{R}}{}^n, \quad \forall x,y\in X;$

$d_n(x,y)= 0_{\mathbf{R}}{}^n \Leftrightarrow x=y,$

where $0_{\mathbf{R}}{}^{\mathbf{n}}$ is the null element from $\mathbf{R}^n$

(1.7) $d_n(x,y)= d_n(y,x), \quad \forall x,y\in X;$

(1.8) $d_n(x,y)= d_n(x,z)+d_n(y,z), \quad \forall x,y,z\in X.$

The couple (X,d_n) is named *n-metric space.* A *n*-metric space in which every fundamental sequence is convergent is called *n*-metric complete space.

Remarks:

1) A *1-metrical space* is a regular metric space, equipped with a scalar metric.

2) $\boldsymbol{R}^n$ is *n-metrical complete space*, in raport with te *n* – vector metric: $d_n:\mathbf{R}^n\times\mathbf{R}^n\to\mathbf{R}^n$,

(1.9) $d_n(x,y)=(|x_1-y_1|,|x_2-y_2|,\ldots,|x_n-y_n|).$

Definition 1.2 [*n*-normed space]: Let $(X,\mathbf{R},x+y,\lambda x)$ be a real vector space. A vector function $p_n(x):X\to\mathbf{R^n}$, $\forall x\in X$ is called a *n-norm* on X (or a *vector norm)*, if the following conditions are satisfied:

(1.10) $p_n(x)\ge 0_R{}^n, \quad \forall x\in X,$

$p_n(x)= 0_R{}^n \Leftrightarrow x= 0_X;$

(1.11) $p_n(x+y) \le p_n(x)+p_n(y), \quad \forall x,y\in X;$

(1.12) $p_n(\lambda x) =|\lambda| p_n(x), \quad \forall x\in X, \quad \forall\lambda\in\mathbf{R}.$

The couple (X,p_n) is called *n-normed space* (or *normed space with the vector norm).*

Remark: A *l-normed space* is a regular normed space, equipped with a scalar norm.

Definition 1.3 [*n*-metric induce by a *n*-norm]: Let (X,p_n) a *n*-norm space. If the vectorial function $d_n:X\times X\to\mathbf{R}^n$,

(1.13) $d_n(x,y)=p_n(x-y)$, $\forall x,y\in X$,
is a *n*-metric on X, then the function d_n is called the *n-metric induce by the n-norm* p_n.

Remark: The vector norm: $p_n:\mathbf{R}^n\to\mathbf{R}^n$,
(1.14) $p_n(x)=(|x_1|,|x_2|,\ldots,|x_n|)$, $\forall x\in\mathbf{R}^n$.
induces the *n*-metric given by relation (1.9).

Definition 1.4 [Banach *n*-space]: A *n*-normed space (X,p_n) which is complete with respect to the *n*- metric induce by the *n*-norm p_n is called *n- Banach space.*

Remark. The normed space $\mathbf{R}^n$ with *n*-norm (1.14) is a *n-Banach space.*

Definition 1.5 [Product of Banach spaces]: Let the Banach spaces (X_i,p_i), $i=1..n$, where $p_i:X_i\to[0\ \infty)$ are the scalar norms on the real vector spaces X_i. The product

(1.15) $$X=\prod_{i=1}^{n} X_i= X_1\times X_2\times\ldots\times X_n$$

with $x=(x_1,x_2,\ldots,x_n)\in X$, $x_i\in X_i$, $i=1..n$.

Theorem 1.1: Let X be a product of Banach spaces

$$X=\prod_{i=1}^{n} X_i= X_1\times X_2\times\ldots\times X_n,$$

and the scalar norms $p_i:X_i\to[0,\infty)$ on real Banach spaces X_i .
The vectorial function $\|x\|_{\to}:X\to\mathbf{R}^n$,

(1.16) $\|x\|_{\to}=(p_1(x_1),p_2(x_2),\ldots,p_n(x_n))$, $\forall x=(x_1,x_2,\ldots,x_n)\in X$,

is a *n*-norm on *X*

Proof:

1) Because X_i are real vector space and X their product shall be a real vector space, if we define for $x=(x_1,x_2,\ldots,x_n)\in X$, $y=(y_1,y_2,\ldots,y_n)\in X$ şi $\lambda\in\mathbf{R}$,
(1.17) $x+y=(x_1+y_1,x_2+y_2,\ldots,x_n+y_n)$, $\forall\ x,y\in X$;
(1.18) $\lambda\ x=(\lambda\ x_1,\lambda\ x_2,\ldots,\lambda\ x_n)$, $\forall x\in X$, $\forall\ \lambda\in\mathbf{R}$.

2) For all $i=1..n$ we have the following proprieties of the norms:
(1.19) $p_i(x_i)\geq 0_R$, $\forall\ x_i\in X_i$,
$p_i(x_i)=0_R \Leftrightarrow x_i=0_{Xi}$, ;
(1.20) $p_i(x_i+y_i)\leq p_i(x_i)+p_i(y_i)$, $\forall\ x_i,\ y_i\in X_i$;
(1.21) $p_i(\lambda\ x_i)=|\lambda|p_i(x_i)$, $\forall x_i\in X$, $\forall\lambda\in\mathbf{R}$.

It verifies immediately the proprieties:
(1.22) $\|x\|_{\to}\geq 0_{\mathbf{R}^n}$, $\forall x\in X$, $\|x\|_{\to}=0_{\mathbf{R}^n} \Leftrightarrow x=0_X$;
and
(1.23) $\|\lambda x\|_{\to}=|\lambda|p_n(x)$, $\forall x\in X$, $\forall\lambda\in\mathbf{R}$.

Further we have:

$$\|x+y\|_{\to} = (p_1(x_1+y_1), p_2(x_2+y_2), \ldots, p_n(x_n+y_n)) \le$$
$$(p_1(x_1)+p_1(y_1), p_2(x_2)+p_2(y_2), \ldots, p_n(x_n)+p_n(y_n)) =$$
$$(p_1(x_1), p_2(x_2), \ldots, p_n(x_n)) + (p_1(y_1), p_2(y_2), \ldots, p_n(y_n)) = \|x\|_{\to} + \|y\|_{\to}.$$

Therefore:

(1.24) $$\|x+y\|_{\to} \le \|x\|_{\to} + \|y\|_{\to}.$$

The relations (1.22), (1.23) and (1.24) shows that the vector norm $\|x\|_{\to}$ is a *n*-norm on the product of Banach spaces X.

Definition 1.6 [The canonical vector norm]:

Let $X=\prod_{i=1}^{n} X_i = X_1 \times X_2 \times \ldots \times X_n$ be a product of Banach spaces equipped with the *n*-norm:

(1.25) $\|x\|_{\to} : X \to \mathbf{R}^n$,

$$\|x\|_{\to} = (p_1(x_1), p_2(x_2), \ldots, p_n(x_n)), \quad \forall x=(x_1, x_2, \ldots, x_n) \in X.$$

where $p_i : X_i \to [0,\infty)$ are the scalar norms on the real Banach spaces X_i.
This vector norm is called the *canonical vector norm* on the product of Banach spaces X.

Theorem 1.2: The product of Banach spaces **:**

$$\boldsymbol{X=\prod_{i=1}^{n} X_i = X_1 \times X_2 \times \ldots \times X_n,}$$

with the canonical vector norm given by (1.25) , is a n-Banach space.

Proof.

We showed in theorem 1.1 that the product of Banach spaces X is a *n*-normed space in raport with the canonical vectorial norm defined by the relations (1.25). We shall show now that *X* is complete in raport with the *n*-metric induced by te canonical norm, i.e. *X* is a *n*-Banach space .

Let $d_n : X \times X \to \mathbf{R}^n$ be a *n*-metric induced by the canonical vectorial norm:

(1.26) $d_n(x,y) = \|x-y\|_{\to}, \quad \forall x,y \in X.$

We consider a fundamental sequence of elements from *X*,

$(x^m)_{m>0}$, where $x^m = (x_1^m, x_2^m, \ldots, x_n^m) \in X$, $x_i^m \in X_i$, $i=1..n$.

Therefore , $(\forall)\varepsilon = (\varepsilon_1, \varepsilon_2, \ldots, \varepsilon_n) > 0_{\mathbf{R}^n}$, exists $k=k(\varepsilon)$, $k \in \mathbf{N}^*$, such as: $d_n(x^{l+p}, x^p) < \varepsilon$, $(\forall) p>k$ and l natural. I.e. $d_n(x^{l+p}, x^p) = \|x^{l+p} - x^p\|_{\to} < \varepsilon$, :from where:

$$p_i(x_i^{l+p} - x_i^p) < \varepsilon_i, \quad i= 1..n,$$

which shows that the sequence $(x_i^m)_{m>0}$ is fundamental in X_i .

As X_i is complete (being a Banach space) implies the fact that exists $a_i \in X_i$, such as $x_i^m \to a_i$, for m that tends to infinite, $(\forall)$ $i= 1..n$: $x^m \to a$, $a=(a_1, a_2, \ldots, a_n) \in X$ and therefore this sequence is convergent in X, i.e. X is a *n*-Banach space, being complete in raport with the *n*-metric induced by the canonical vector norm.

Definition 1.7 [*n*-Banach canonical space]: We shall call a *n-Banach canonical space,* the *n*-Banach space $(X, \| x \|_{\rightarrow})$, defined on the product of Banach spaces:

$$X=\prod_{i=1}^{n} X_i = X_1 \times X_2 \times \ldots \times X_n,$$

equipped with the canonical vectorial norm: $\| x \|_{\rightarrow} : X \rightarrow \mathbf{R}^n$,

$\| x \|_{\rightarrow} = (p_1(x_1), p_2(x_2), \ldots, p_n(x_n)),\ \ \forall x=(x_1, x_2, \ldots, x_n) \in X.$

Definition 1.8 [*n*-euclidean norm on R^n]*: The canonical norm:*

(1.27) $\| x \|_{\rightarrow} :\ R^n \rightarrow R^n,\ \| x \|_{\rightarrow} = (|x_1|, |x_2|, \ldots, |x_n|),\ x=(x_1, x_2, \ldots, x_n) \in R^n,$

we shall name it n-euclidean norm on R^n

Theorem 1.3: *The space* R^n *is a* n-*canonical Banach space in raport with the* n-*euclidean norm.*

Proof.

Let R be a vector real space, equipped with te norm $\|x\| = |x|$. This norm induce the Euclid's metric, in raport with which R is a complete metrical space , i.e. is a Banach space.

So, the product of Banach spaces $(R^n, \|x\|_{\rightarrow})$ shall be a canonical n-Banach space, in accordance with theorem 1.2 and definition 1.7.

2. Perov's fixed point theorem for canonical contractions

The fixed points set of the map $f: X \rightarrow X$, is denoted by:

(2.1) $\boldsymbol{F_f = \{x \ /\ f(x)=x,\ x \in X\}.}$

Definition 2.1 [The spectral raze of a real matrix]: *Let M be the square matrix of n order with real numbers. We shall call the spectral raze of the matrix M, the real number denoted by* $\rho(M)$ *:*

(2.2) $\rho(M) = \max |\lambda_k|,\ k=1..n,$

where λ_k *are the proper values of matrix M.*

Definition 2.2 [A matrix converging to zero]*: A square* n-*order and non-negative* M *matrix is called convergent to zero if „the power matrix"* $M^m = \underbrace{M.M....M}_{m\ factors}$ *is* convergent to zero *(denoted by* $M \rightarrow O$, *convergent to the null matrix* O, *where* m *tends to infinite.*

Theorem 2.1*: Let M be a square n-order, real and non-negative matrix. Te following assertions are equivalent:*

(2.3) $\boldsymbol{M^m \rightarrow O;}$

(2.4) $\boldsymbol{\rho(M) < 1;}$

(2.5) $\boldsymbol{\det(E-M) \neq 0;}$

(2.6) $\boldsymbol{(E-M)^{-1} = E+M+M^2+\ldots,}$

where E is the unit n-*order matrix .*

The proof of this theorem is found in [Rus 79], on page 35-37 (with the corresponding terminological adaptation).

Definition 2.3 [The lipschitzian map in n-metric]: *Let* (X,d_n) *be a* n-*metric space. A map* $f:X\to X$ *is called* lipschitzian in a n-metric on X, *if there exits a matrix* L, *square of* n-*order and non-negative, so that te Lipschitz condition is satisfied:*

$$(2.7)\qquad d_n(f(x),f(y)) \le L\ d_n(x,y),\quad \forall x,y\in X.$$

The L *matrix is called* the Lipschitz matrix.

Definition 2.4 [The contracting map in n- metric]: *A lipschitzian map* $f:X\to X$ *in* n-*metric is called* contraction on X, *if the map admits a Lipschitz matrix* K *(in this case K named the contraction matrix), of spectral raze smaller then 1.*

Theorem 2.2 [Perov]: *Let* (X,d_n) *be a* n-*metric complete space and a contracting map* $f:X\to X$, *with te contraction matrix* K. *We have:*

(2.8) $F_f=\{x^*\}$;

(2.9) *The iterative sequence* $x^m=f^m(x^0)$, $\forall x^0\in X$, $m\in N^*$ *is convergent to a unique fixed point* x^* *of f;*

(2.10) *The estimation:* $d_n(x^m,x^*) \le K^m\ (E-K)^{-1}\ d_n(x^1,x^0)$;

(2.11) *If* $g:X\to X$ *is the approximation of f, i.e. exists in* R^n *a* $\varepsilon > 0$ *such that*

$$d_n(f(x),f(y)) < \varepsilon,\quad \forall x,y\in X,$$

then, for the iterative sequence $y^m=g^m(x^0)$, *we have the estimation:*

$$d_n(y^m,x^*) \le \varepsilon\ (E-K)^{-1}+K^m\ (E-K)^{-1}\ d_n(x^1,x^0).$$

The proof of this theorem can be found in [Rus 79, page 39] (with the corresponding terminological adaptations and notations).

Definition 2.5 [The canonical contraction]: *Let* $(X,\left\| x \right\|_{\to})$ *be a* n-*Banach canonical space with the canonical vectorial norm* $\left\| x \right\|_{\to}$. *A map* $f:X\to X$ *is named a* canonical contraction *on* X, *if there exists a non-negative matrix* K *with the spectral ray smaller then 1, such that:*

$$(2.12)\qquad \left\| f(x)-f(y) \right\|_{\to} \le K\ \left\| x-y \right\|_{\to},\ \forall x,y\in X.$$

Theorem 2.3: Let $(X, \left\| x \right\|_{\to})$ *a* n-*Banach canonical space and* $f:X\to X$ *a canonical contraction on* X, *with the contraction matrix* K.

In those conditions we have:

(2.13) $F_f=\{x^*\}$;

(2.14) *The sequence* $x^m=f(x^{m-1})$, $\forall x^0\in X, m\in N^*$ *is convergent to* x^*, *the unique fixed point of f ;*

(2.15) *It takes place the estimation:*

$$\left\| x^m - x^* \right\|_{\to} \le K^m\ (E-K)^{-1}\ \left\| x^1 - x^0 \right\|_{\to};$$

(2.16) *If* $g : X \to X$ *is an approximant of* f, *i.e. exists in* R^n *a* $\varepsilon > 0$ *such as* $\left\| f(x)-g(x) \right\|_{\to} < \varepsilon$, $\forall x\in X$, *then for the sequence we have the estimation:*

$$\left\| y^m - x^* \right\|_{\to} \le \varepsilon\ (E-K)^{-1}+K^m\ (E-K)^{-1}\ \left\| x^1 - x^0 \right\|_{\to}.$$

Proof.

According to the theorem 1.2 we have that X is a n-metric complete space in raport with the n-metric induced by the canonical vector norm. Because the map f is a canonical contraction on X, the conclusions of our theorem results from Perov's theorem.

Theorem 2.4*: Let* $X=R^n$ *and* $f:X\to X$ *be a canonical contraction on* X *with respect to the canonical vectorial norm:*

$$\left\| x \right\|_{\to} : R^n\to R^n,\ \left\| x \right\|_{\to} = (|x_1|, |x_2|, \ldots, |x_n|),\ x=(x_1,x_2,\ldots,x_n)\in R^n,$$

with the contraction matrix K.

In those conditions we have:

(2.17) $F_f=\{x^*\}$;

(2.18) *The sequence* $x^m=f(x^{m-1})$, $\forall x^0\in X$, $m\in N^*$ *is convergent to* x^*, *the unique point of* f;

(2.19) *It takes place the estimation:*

$$\left\| x^m - x^* \right\|_{\rightarrow} \le K^m \ (E-K)^{-1} \left\| x^1 - x^0 \right\|_{\rightarrow} ;$$

(2.20) *If* $g:X\rightarrow X$ *is an approximation of* f, *i.e. exists in* R^n *an* ε *with positive components, such that* $\left\| f(x)-g(x) \right\|_{\rightarrow} < \varepsilon$, $\forall x\in X$, *then for the sequence* $y^m=g(y^{m-1})$, $m=1,2,\ldots$, $y^0=x^0\in X$ *we have the estimation:*

$$\left\| y^m - x^* \right\|_{\rightarrow} \le \varepsilon \ (E-K)^{-1}+K^m \ (E-K)^{-1} \left\| x^1 - x^0 \right\|_{\rightarrow} .$$

Proof.

Appling the result of theorem 1.2 and theorem 2.3, the conclusions of our theorem results immediatly from Perov's theorem.

3. Numerical example

(3.1) In [RCM 73] it's gave the following example of ten nonlinear equations system, with ten real unknown:

```
x[i]=fi(x[1],x[2],x[3],x[4],x[5],x[6],x[7],x[8],x[9],x[10]), i=1..10,

x[1]=f1(x)=(x[1]+x[2])/4+x[3]/20
x[2]=f2(x)=(cos(x[1]+x[2]+x[4]-x[5]-x[8]-x[9]))/6.6
x[3]=f3(x)=0.5*cos(x[1]/2+x[3]/3-2*x[5]/3)+x[7]/5
x[4]=f4(x)=0.2*(sin(2*x[3])+cos(x[1]+x[4]))+x[5]/6
x[5]=f5(x)=(exp(-x[1]*x[1])+exp(-x[8]*x[8]))/2
x[6]=f6(x)=(x[1]-x[2]+x[8]+x[9]+3*x[10])/7.2
x[7]=f7(x)=exp(-x[1])+x[9]/11
x[8]=f8(x)=(cos(x[1]+x[3]+x[6]+x[9]))/5
x[9]=f9(x)=(sin(x[2]+x[4]+x[5]+x[8]))/5
x[10]=f10(x)=(exp(-x[3]*x[3])+exp(-x[8]*x[8]))/2-x[10]/11 .
```

Let $f=(f_1,\ldots,f_{10})$. It's showed that the $f:R^{10}\rightarrow R^{10}$ operator admits in private, the K contraction matrix, with the subunit spectral ray , $\rho(K)=0.7868\ldots$, where K is gave by the following table:

0,2500	0,2500	0,05000	0,0000	0,0000	0,0000	0,0000	0,0000	0,0000	0,0000
0,1520	0,1520	0,0000	0,1520	0,1520	0,0000	0,0000	0,1520	0,1520	0,0000
0,2500	0,0000	0,1670	0,0000	0,3340	0,2000	0,2000	0,0000	0,0000	0,0000
0,2000	0,0000	0,4000	0,2000	0,1670	0,0000	0,0000	0,0000	0,0000	0,0000
0,4289	0,0000	0,0000	0,0000	0,0000	0,0000	0,0000	0,4289	0,0000	0,0000
0,1390	0,1390	0,0000	0,0000	0,0000	0,0000	0,0000	0,1390	0,1390	0,4170
0,8579	0,0000	0,0000	0,0000	0,0000	0,0000	0,0000	0,0000	0,0910	0,0000
0,2000	0,0000	0,2000	0,0000	0,0000	0,2000	0,0000	0,0000	0,2000	0,0000
0,0000	0,2000	0,0000	0,2000	0,2000	0,0000	0,0000	0,2000	0,0000	0,0000
0,0000	0,0000	0,4289	0,0000	0,0000	0,0000	0,0000	0,42890	0,0000	0,0910

Program RFAIM SEQ_SIM (based of RFAIM method [Dzi00])

```
//Program  RFAIM_SEQ_SIM
//Sequential simulation of the asynchronous parallelism RFAIM

# include  <conio.h>
# include  <iostream.h>
# include  <iomanip.h>
```

```
# include  <math.h>
# include  <stdlib.h>

enum bool {false, true};
long double eps = 1.0e-9;
long double intervale
[][2]={{0.0,1.0},{0.0,1.0},{0.0,1.0},{0.0,1.0},{0.0,1.0},
{0.0,1.0},{0.0,1.0},{0.0, 0.2},{0.0,0.2},{0.0,1.0}];

bool finish (long double [ ], long double [ ], int);
void tipar (long double [ ], int);
void shuffle (unsigned [ ], int);
void genereaza (long double [ ], long double [ ], long double [ ], int);

long double f1 (long double [ ]);
long double f2 (long double [ ]);
long double f3 (long double [ ]);
long double f4 (long double [ ]);
long double f5 (long double [ ]);
long double f6 (long double [ ]);
long double f7 (long double [ ]);
long double g8 (long double [ ]);
long double f9 (long double [ ]);
long double f10 (long double [ ]);

int matherr (struct exception *e)
{
               switch (e->type)
               {
                       case DOMAIN:
                               cout << "Argumentul " << e->arg1<<"este eronat in"<<e->name;
                       break;
                       case OVERFLOW:
                               cout << "Argumentul " << e->arg1<<"este prea mare in functia
"<<e->name;
                       break;
                       case TLOSS:
                               cout << "Argumentul " << e->arg1<<"este prea mare in functia
"<<e->name;
                       break;
                       default:
                         cout << "eroare \ n " ;
               }
               exit (-1);
}
int main ( )
{
       clrscr ( ) ;
       //long double
x1[]={0.0,0.0,0.0,0.0,0.0,0.0,0.0,0.0,0.0,0.0};
       //long double
x2[]={0.0,0.0,0.0,0.0,0.0,0.0,0.0,0.0,0.0,0.0};
       //long double
x3[]={0.0,0.0,0.0,0.0,0.0,0.0,0.0,0.0,0.0,0.0};
       long double
x1[]={1.0,2.0,3.0,4.0,5.0,6.0,7.0,8.0,9.0,10.0};
       long double
x2[]={1.0,2.0,3.0,4.0,5.0,6.0,7.0,8.0,9.0,10.0};
long double
x3[]={1.0,2.0,3.0,4.0,5.0,6.0,7.0,8.0,9.0,10.0};
unsigned nr_comp=sizeof(x1)/sizeof(x1[0]),i,contor=0;
long double *x=x2;
       long double (*pf [ ]) , int) =
               {f1, f2, f3, f4, f5, f6, f7, f8, f9, f10} ;
       unsigned tab [ ] = {0, 1, 1, 2, 3, 4, 5, 6, 7, 8, 9};
       genereaza (x1, x2, x3, nr_comp);
       do {
               contor++ ;
```

```
               shuffle (tab, nr_comp);
               for (i = 0 ; i < nr_comp ; i++)
               {
                      x1[i] = x2[i] ;
               }
                    for (i = 0 ; i < nr_comp ; i++)
                   {
                      x2[tab[i]] = pf[tab [i] (x3) ;
                      x3[tab[i]] = x2[tab[i] ];
               }
}  while (!finish (x1, x2, nr_comp) ) ;

   cout <<"Am obtinut solutia dupa "<<contor>> "iterari simple"<< endl ;
   tipar (x2, nr_comp) ;
   return 0 ;
}
long double f1 (long double x[ ], int i)
{
       //long double ret = ((x[0]+x[1]) / 4 + x[2] / 20) ;
       long double ret = (x[1]) / 3 + x[2] / 15
       if (ret >intervale [i] [0] && ret< intervale [i] [1] )
              return ret ;
       else
              return intervale [i] [0] + (intervale [i] [1] - intervale [i] [0] * (long
double ) rand ( ) / RAND_MAX ;
}
long double f2 (long double x[ ], int i)
{
       long double
ret=((cos(x[0]+x[1]+x[3]-x[4]-x[7]-x[8]))/6.6);
if (x[i]>intervale [i] [0] && x[0]<intervale [i] [1] )
              return ret ;
       else
         return intervale [i] [0] + (intervale [i] [1] - intervale [i] [0] * (long double )
rand ( ) / RAND_MAX ;
}

long double f3 (long double x[ ], int i)
{
       long double ret = (0.5*cos (x[0] /2 +x[2] /3- 2*x[4] /3 + x[6] /5.0) ;
if (x[i] > intervale [i] [0] && x[0] < intervale [i] [1] )
              return ret ;
       else
         return intervale [i] [0] + (intervale [i] [1] - intervale [i] [0] * (long double )
rand ( ) / RAND_MAX ;
}

long double f4 (long double x[ ], int i)
{
       long double ret = (0.2*sin (2.0*x[2])+ 0.2*cos (x[0]) + x[3] + x[4] /6) ;
if (x[i] > intervale [i] [0] && x[0] < intervale [i] [1] )
              return ret ;
       else
         return intervale [i] [0] + (intervale [i] [1] - intervale [i] [0] * (long double )
rand ( ) / RAND_MAX ;
}

long double f5 (long double x[ ], int i)
{
       long double ret=((expl(-x[0]*x[0]+expl(-x[7]*x[7]))/2
if (x[i]>intervale [i] [0] && x[0]<intervale [i] [1])
              return ret ;
       else
         return intervale [i] [0] + (intervale [i] [1] - intervale [i] [0] * (long double )
rand ( ) / RAND_MAX ;
}

long double f6 (long double x[ ], int i)
```

```
{
        long double ret=(x[0]-x[1]+x[7]+x[8]+3*x[9]))/7.2;
if (x[i]>intervale [i] [0] && x[0]<intervale [i] [1] )
                return ret ;
        else
          return intervale [i] [0] + (intervale [i] [1] - intervale [i] [0] * (long double )
rand ( ) / RAND_MAX ;
}

long double f7 (long double x[ ], int i)
{
        long double ret = (expl (-x[0])+x[8] /11 ;
if (x[i] > intervale [i] [0] && x[0] < intervale [i] [1] )
                return ret ;
        else
          return intervale [i] [0] + (intervale [i] [1] - intervale [i] [0] * (long double )
rand ( )/RAND_MAX;
}

long double f8 (long double x[ ], int i)
{
        //long double ret=((cos(x[0]+x[2]+x[5]+x[8]))/5);
        long double ret = asin1 (5*x[8]))-(x[1]+x[3]+x[4];

if (x[i]>intervale [i] [0] && x[0]<intervale [i] [1] )
                return ret ;
        else
          return intervale [i] [0] + (intervale [i] [1] - intervale [i] [0] * (long double )
rand ( ) / RAND_MAX ;
}

long double f9 (long double x[ ], int i)
{
        //long double ret = ((sin (x[1] + x[3] + x[4] +x[7])) / 5 ;
        long double ret = acos1 (5*x[7]) - x[0] - x[2] - x[5];

if (x[i]>intervale [i] [0] && x[0]<intervale [i] [1])
                return ret ;
        else
          return intervale [i] [0] + (intervale [i] [1] - intervale [i] [0] * (long double )
rand ( )/RAND_MAX;
}
long double f10 (long double x[ ], int i)
{
//long double ret = (expl(-x[2]* x[2]+ expl(-x[7]* x[7])) /2 - x[9] /11 ;
long double ret = 11*(exp1(-x[2]*x[2])+exp1(-x[7]*x[7]))/24 ;
if (x[i] > intervale [i] [0] && x[0] < intervale [i] [1] )
                return ret ;
        else
          return intervale [i] [0] + (intervale [i] [1] - intervale [i] [0] * (long double )
rand ( ) / RAND_MAX ;
}

bool finish (long double x1[ ], long double x2 [ ], int nr)
{
    bool ret = true ;
    int i ;
    for (i = 0 ; i < nr ; i++)
{
        if ( fabs1 (x1[i] - x2[i]) > eps)
        {
                ret = false ;
                break ;
        }
}
    return ret ;
}
void tipar (long double x2[ ], int nr_comp)
```

```
{
        int i ;
        for (i = 0 ; i < nr_comp ; i++)
        {
           cout .setf (ios::fixed) ;
           cout << "x[" << setw(2) << (i+1)<<"] = " << setprecision (10) << x2[i] << endl ;
        }
}
void shuffle (unsigned tab [ ], int n)
{
        int i, j ;
        bool ok;
        randomize ();
        for (i = 0 ; i < n ; i++)
        {
                do{
                        ok = true;
                        tab [i] = random (10);
                        for (j = 0 ; j < i; j++)
                                if (tab [j] = = tab [i])
                                {
                                        ok = false;
                                        break;
                                }
                        } while (! ok);
        }
}
void genereaza (long double x1[ ], long double x2[ ], long double x3[ ],int nr_comp)
{
        for (int i = 0; i < nr_comp; i++)
        {
                x1[i] = (long double) rand ( ) / RAND_MAX;
                if ( i = = 7 || i = = 8)
                        x1[i] / = 5;
                x3[i] = x2[i] = x1[i];
        }
}
```

Numerical solution (the fixed point value) to be obtain after 10-12 vector iterations:

x[1]= 0.0853306672
x[2]= 0.1263607698
x[3]= 0.6466737693
x[4]= 0.5198021063
x[5]= 0.9768165122
x[6]= 0.3503781711
x[7]= 0.9308854467
x[8]= 0.1997436445
x[9]= 0.1394451735
x[10]= 0.7415213722

REFERENCES

[Dzi 00] Dzitac, I., Random–filtered asynchronous iterative methods, Bul. St. Univ. Baia Mare, Ser. B, Matematică – Informatică, Vol. XVI (2000), Nr. 1, pag. 17-24, ISSN 1222- 1201.

[RCM 75] Robert, F., Charnay, M., Musy, F., Iterations chaotique serie-parallele pour des equations nonlineaire de point fixe. Aplikace Matematiky 20 (1975), p.1-38 (French)

[Rus 79] RUS I.A.:O Principles and applications of the fixed point, Ed. Dacia, Cluj-Napoca, 1979. (Romanian)

Properties of the solutions of a parabolic equation of non divergent type

Aripov, M., Sadullaeva, Sh. A.
National University of Uzbekistan
E-mail: m.aripov@nuuz.uzsci.net
shahloaz@yahoo.com

Abstract. The properties of the weak solutions of an initial value problem is investigated for a quasilinear parabolic equation of non divergent type. Various similarity equations are constructed by an algorithm of nonlinear splitting. On the basis of some of these estimates solutions and fronts are obtained. The analogue of Fujita-Samarskii condition on a global solvability of an initial value problem is obtained.
Keywords: parabolic equation, not divergent type, asymptotic, week solution.
MSC 2000 Subject classification: 35K20, 35K55, 35K65.

1. Introduction

Consider, in a domain $Q = \{(t, x) : t > 0, x \in R^N\}$, the following Caushy problem

$$Au \equiv -\frac{\partial u}{\partial t} + u^p \nabla\left(|x|^m u^\sigma \nabla u\right) + \varepsilon\gamma(t)u^\beta = 0 \tag{1}$$

$$|x|^m u_0^{p+\sigma} \nabla u_0 \in C(0,\infty),\ \sup\ u_0(x) < \infty,\quad x \in R^N \tag{2}$$

where m>0, $\sigma > 0$, p>0, β≥1, are given numbers, $\varepsilon = \pm 1$, $0 < \gamma(t) \in C(0,\infty)$, $\nabla(\cdot) = \underset{x}{\mathrm{grad}}(\cdot)$.

The equation (1) describes various physical processes. It is of a degenerate type. Namely, when $u = 0$ the equation (1) degenerates into a first order equation. For this reason (1) can not have a classical solution. Consequently we shall study the weak solution which has the property $u \geq 0$ and $|x|^m u^{p+\sigma} \nabla u \in C(Q)$.

In the non degenerated case (p=0, when m=$\sigma = 0$, $\gamma(t) = 1$, $\varepsilon = +1$) this problem was considered first by Fujita ($\varepsilon = +1$) [1], and the conditions of global solvability $(\beta - 1)N > 2$ where obtained. In [2] more general conditions of global solvability for the divergent case of the equation (1) were obtained while in [5-9] the same results were obtained for equations more general than equation of divergent type. The problem (1) - (2) began to be studied intensively rather recently (see [4] and references).

The present work is devoted to investigation of the properties of the solutions of the problem (1) - (2). One manner of construction of the various similarity equations by algorithm of nonlinear splitting [4-6] is provided.

2. The similarity solutions; approximation similarity solutions

We consider at first more simple case when $\gamma(t) = 0$ in (1)

Lemma 1. *Equation (1) has a similarity solution of the following form*

$$u(t,x) = f(\xi),\ \xi = \frac{\phi(x)}{(T+t)^{1/2}},\ \phi(x) = \frac{2}{2-m}|x|^{\frac{2-m}{2}}$$

$$f^p\left[\xi^{1-S}\frac{d}{d\xi}\left(\xi^{S-1} f^\sigma \frac{df}{d\xi}\right)\right] + \frac{\xi}{2}\frac{df}{d\xi} = 0 \tag{3}$$

where T>0 , and

$$\bar f(\xi)=\left(c-\frac{p+\sigma}{4}\xi^2\right)_+^{1/p+\sigma},\ (m)_+=\max(0,m),\quad s=\frac{2N}{2-m} \tag{4}$$

(c>0 *is constant*, 0<p<1) *is a function which, in* $|\xi|<2\sqrt{\frac{c}{p+\sigma}}$ *, satisfies the equation*

$$\bar f^{\,p}\left(\xi^{1-s}\frac{d}{d\xi}\left(\xi^{s-1}\bar f^{\,\sigma}\frac{d\bar f}{d\xi}\right)\right)+\frac{\xi}{2}\frac{d\bar f}{d\xi}+\frac{s}{2(1-p)}\bar f=0\,. \tag{5}$$

$\bar f(\xi)$ is an upper solution of a problem (1),(2), if

$$u_0(x)\le \bar f(\xi|_{t=0})\ ,\quad x\in R^N\,.$$

It is easy to see that $\xi^{s-1}f^{p+\sigma}\nabla f\in C(0,\infty)$.

We denote by $D=\{(t,x):t>0,|x|<l(t)\}$ that part of a domain Q, where a function *l(t)* is continuous, i.e. $l(t)\in C(0,\infty)$.

Let us construct other similarity solutions.

Lemma 2. *The equation (1) has the following similarity type solution*

$$u(t,x)=(T\pm t)^{-\alpha}f(\xi)$$

where $\xi=\begin{cases}\dfrac{\phi(x)}{[\tau(t)]^{1/2}} & \text{if } 1-\alpha(p+\sigma)\ne 0\\ \sum\limits_{i=1}^{N_a}\alpha_i x_i-c_1\ln(T\pm t),\ a=\sum\limits_{i=1}^{N}a_i^2\ne 0 & \text{if } 1-\alpha(p+\sigma)=0,\ m=0\end{cases}$

$$\tau(t)=\begin{cases}\pm\dfrac{(T\pm t)^{1-\alpha(p+\sigma)}}{1-\alpha(p+\sigma)}+c_2, & \text{if } 1-\alpha(p+\sigma)\ne 0\\ \pm\ln(T\pm t), & \text{if } 1-\alpha(p+\sigma)=0\end{cases}$$

and the function $\bar f(\xi)$ *satisfy the equations*

$$f^p\left(\xi^{1-s}\frac{d}{d\xi}\left(\xi^{s-1}f^\sigma\frac{df}{d\xi}\right)\right)+\frac{\xi}{2}\frac{df}{d\xi}\pm\frac{\alpha}{1-\alpha(p+\sigma)}f=0,\ \textit{if}\ 1-\alpha(p+\sigma)\ne 0$$

(6)

and

$$af^p\frac{d}{d\xi}\left(f^\sigma\frac{df}{d\xi}\right)\pm c_1\frac{df}{d\xi}\pm\alpha\cdot f=0,\ \textit{if}\ 1-\alpha(p+\sigma)=0\,,$$

respectively.

We notice that the equation (1) has the week solution

$$u(t,x)=(T+t)^{-\alpha}f(\xi)\,,\ \bar f(\xi)=\left(c-\frac{p+\sigma}{4}\xi^2\right)_+^{1/p+\sigma},\ \xi=\frac{\phi(x)}{(T+t)^{1/2}},\quad \phi(x)=\frac{2}{2-m}|x|^{2-m/2}$$

$$\alpha=\frac{N}{(2-m)(1-p)+N(p+\sigma)},\quad (0<p<1),\qquad \tau(t)=\frac{1}{1-\alpha(p+\sigma)}(T+t)^{1-\alpha(p+\sigma)}\,.$$

On basis of these preliminaries we shall prove the theorem on the global solvability of the problem (1) - (2) for $\gamma(t) \neq 0$.

3. GLOBAL SOLVABILITY AND ESTIMATION OF THE SOLUTIONS.

Theorem 1. *Let, in (1)* $\varepsilon = -1$, $0 < p < 1$, *m<2,*

$$[\bar{u}(t)]^{\beta-(p+1)}\gamma(t)\tau(t) \leq \frac{N}{(1-p)(2-m)}. \tag{7}$$

Then the problem (1) - (2) has a global solution, for which, in Q, the estimation

$$u(t,x) \leq z_+(t,x)$$

holds

Proof. Let us construct the upper solution $z_+(t,x)$ by method of nonlinear splitting [5-7], according to which first we find the solution of the simple equation

$$\frac{d\bar{u}}{dt} = -\gamma(t)\bar{u}^{\beta}, \text{ i.e. } \bar{u}(t) = (T + (\beta-1)\int_0^t \gamma(t)dt)^{-\frac{1}{\beta-1}} \tag{8}$$

and then look for the solution $u(t,x)$ of equation (1) in the form

$$u(t,x) = \bar{u}(t)W(\tau(t),x), \tag{9}$$

where

$$\tau(t) = \int [\bar{u}(t)]^{p+\sigma} dt = \begin{cases} \dfrac{(\beta-1)(T+(\beta-1)\cdot t)^{\frac{\beta-(p+\sigma+1)}{\beta-1}}}{\beta-(p+\sigma+1)} & ,if \quad \beta \neq p+\sigma+1 \\ \dfrac{1}{(p+\sigma)}\ln(T+(p+\sigma)\cdot t) & ,if \quad \beta = p+\sigma+1 \end{cases}.$$

Then for $W(\tau(t),x)$ from (1) taking into account (9), we obtain the equation

$$\frac{\partial W}{\partial \tau} = W^p \nabla\left(|x|^m W^{\sigma}\nabla W\right) + [\bar{u}(t)]^{\beta-(p+\sigma+1)}\gamma(t)\left(W \pm W^{\beta}\right). \tag{10}$$

By Lemma 1 the main part of equation (10) is similarity. Hence, putting

$$W(\tau,x) = f(\xi), \quad \xi = \frac{\phi(x)}{\tau^{1/2}}, \; \phi(x) = \frac{2}{2-m}|x|^{2-m/2} \tag{11}$$

in (10), simple algebra lead to the approximately similarity equation.

Then substituting (12) in (11), we obtainthe the approximation selfsimilar equation

$$f^p\left(\xi^{1-s}\frac{d}{d\xi}\left(\xi^{s-1}f^{\sigma}\frac{df}{d\xi}\right)\right) + \frac{\xi}{2}\frac{df}{d\xi} + [\bar{u}(t)]^{\beta-(p+\sigma+1)}\gamma(t)\tau(t)\left(f \pm f^{\beta}\right) = 0$$

(12)

where $s = 2N(2-m)$.

Remark. Let $\gamma(t)$ be a function of Hardy class. Then it is easy to see that $\gamma(t)\tau(t)[\bar{u}(t)]^{\beta-(p+1)} \sim c$ as $t \sim +\infty$, where c is some constant. Indeed, by Hardy theorem we have

$$\tau(t) = \int_0^t [\bar{u}(t)]^{p+\sigma} dt \sim [\bar{u}(t)]^{p+\sigma} \sim [\gamma(t)\, t]^{\frac{p+\sigma}{\beta-1}} t, \quad t \sim \infty$$

$$\left[\bar{u}(t)\right]^{\beta-(p+\sigma+1)} = \left[T + \int_0^t \gamma(t)dt\right]^{-\frac{\beta-(p+\sigma+1)}{\beta-1}} \sim \left[t\gamma(t)\right]^{-\frac{\beta-(p+\sigma+1)}{\beta-1}}, \quad \text{for } t \sim \infty .$$

Hence (12) is an asymptotic similarity equation for a function $\gamma(t)$ of Hardy class.

Theorem 2. *Let the conditions of Theorem 1 hold, let* $\varepsilon = +1$ *and let*

$$\left(c^{\frac{1}{\beta-1}} + 1\right)\left[u(t)\right]^{\beta-(\sigma+p+1)}\gamma(t)\tau(t) \le \frac{N}{(2-m)(1-p)}, \quad t > 0, \textit{ where}$$

$$c^{\frac{1}{\beta-1}} = \max \bar{f}^{\frac{1}{\beta-1}}(\xi)$$

Then the problem (1)-(2) has a global solution for which, in Q, the estimate $u(t,x) \le z_+(t,x)$ *holds.*

Theorem 3. *Let in (1) be* $1-\alpha(p+\sigma)=0,$ *m=0, N=1* $\gamma(t)=1$*, where the number α is defined by (6). Then, for the free boundary of solution we have the asymptotic expansion* $\sum_{i=1}^{N_a} a_i x_i \approx c_1 \ln t$ *, where* $a_i \quad (i=1,N)$*. and* $c_1 > 0$ *- are constants.*

Proof. In a domain $|\xi| < \dfrac{c}{p+\sigma}$, where $\xi = \sum_{i=1}^{N_a} a_i x_i - c_1 \ln t$, consider a function $\tilde{f}(\xi) = A\xi^{\frac{1}{p}}$, where $A^p = \pm pc_1/a(p-1)$. The solution of the second equation of (6) is looked in the form $f = \tilde{f}\cdot y(\eta)$, where $\eta = -\ln\xi$. Then the obtained equation for $y(\eta)$ has a solution, which tends to the constant $c_3 > 0$ as $\xi \to 0, \quad (\eta \to +\infty)$, because $f = \tilde{f}\cdot c_3$. That finishes the proof of Theorem 3.

Theorem 4. *Let be the condition* $[\bar{u}(t)]^{\beta-(p+\sigma+1)}\gamma(t)\tau(t) \le C$ *t>0, where C is a constant. Then in a neighborhood of a front a finite solution of the equation (12) has the asymptotic*

$$f(\xi) \approx \bar{f}(\xi) = a\left(c - \frac{p+\sigma}{4}\xi^2\right)_+^{1/p+\sigma}$$

where a, c>0 are some constants.

This asymptotic behaviour reflects well the physics of the studied process. In particular, as p and σ→0 (linear case) this formula shows that front of temperature tends to infinitye. In linear case the asymptotic

$$f(\xi) \approx \bar{f}(\xi) = \exp\left(-\frac{\xi^2}{4}\right)$$

of the solution was obtained by A. Samarskii in the monograph [1].

4. Some corollaries.

In particular case of equation (1) when $\gamma(t) = 1$ we have the following Corollaries

Corollary 1. *Let* ε=-1, N>1, 0<p<1, $\beta > \sigma + p + 1 + \dfrac{(2-m)(1-p)}{N}$, $\quad u_0(x) \le z_+(0,x),\ x \in R^N$, *where* $z_+(t,x)$ *is the above defined function*

$$\bar{u}(t) = \left(T + (\beta - 1)t\right)^{-\frac{1}{\beta-1}},\ \xi = \frac{\phi(x)}{[\tau(t)]^{1/2}},\ \tau(t) = \frac{1}{\beta - (1 + p + \sigma)}\left(T + (\beta - 1)t\right)^{\frac{\beta-(1+p+\sigma)}{\beta-1}},$$
$$\beta - (1 + p + \sigma) \neq 0$$

Then for the solution $u(t,x)$ *of (1)-(2) the estimate* $u(t,x) \le z(t,x)$ *is holds in Q.*

Corollary 2. *Let, in (1),* $\varepsilon=-1$, $m=-2(N-1)$, $N>1$, $u_0(x) \le z_+(0,x)$, $x \in R^N$. *Then, for a front* $x_f(t)$ *is valid the asymptotic expansion* $|x_f(t)| \approx a(\ln t)^N$ *, t>1 , where a>0 holds.*

This result was early were obtained by J.Lions, M.Bertsch, R.Kersner.

5. Localization of the solution in the case $\beta = 1$

In the following we establish a condition of localization of the solution by constructing an exact solution.

Choosing $u(t,x) = e^{-\int_0^t \gamma(t)dr} w(\tau(t),x)$, $\tau(t) = \int_0^t e^{(p+\sigma)\int_0^\eta \gamma(\eta)d\eta} d\eta$ reduce the equation (1) to the form

$$\frac{\partial w}{\partial t} = w^p \nabla\left(|x|^m w^\sigma \nabla w\right)$$

which, as shown in the above, has a solution

$$w(\tau, x) = [T + \tau(t)]^{-\alpha} \bar{f}(\xi),\ \ \alpha = \frac{N}{(2-m)(1-p) + (p+\sigma)N}$$

where T>0-is a constant,

$$\bar{f}(\xi) = A\left(a - \frac{p+\sigma}{4}\xi^2\right)_+^{\frac{1}{\sigma+p}},\ \ A^p = \frac{1}{1-p},\ \ \xi = \phi(x)/(\eta(\tau))^{1/2},$$

$$\phi(x) = \frac{2}{2-m}|x|^{\frac{2-m}{2}},\ \eta(\tau) = \frac{1}{1-(p+\sigma)}(T + \tau(t))^{1-\alpha(p+\sigma)}.$$

The condition $\tau(\infty) < +\infty$ is the condition of localization of the solution of equation (1).

Let N=1, m=0 and $\tau(\infty) < +\infty$. Then the equation (1) has a temperature wave type localized solution

$$u(t,x) = \begin{cases} A(c\tau - |x|)^{\frac{1}{p+\sigma}}, & 0 \le x \le c\tau \\ 0, & |x| \ge c\tau \end{cases},$$

where $A^p = \dfrac{cp}{1-p}$. It the multidimensional case, when m=-2(N-1), $N \ge 2,$ equation (1) also has a temperature wave type weak solution

$$u(t,x) = A\left(c\tau(t) - \frac{|x|^N}{N}\right)^{\frac{1}{p+\sigma}},\ \ A^{p+\sigma} = \frac{c(p+\sigma)}{1-p},\ 0<p<1$$

where $\tau(t)$ is the above defined function. In this case the temperature wave is concentrated only in a domain

$$|x| \le Nc\tau^{\frac{1}{N}} < \infty, \quad N \ge 2,$$

where the constant c is a velocity of a temperature wave. This is a new nonlinear effect.

6. STRONG ABSORPTION CASE ($0<\beta<1$).

A. A. Samarskii [2] notice that the case $0<\beta<1$ is very difficult and it is not studied enough. In this case we prove the following theorem about global solvability of the solution of problem (1)-(2).

Theorem 5. *Let* $u_0 \le T^{-1/(\beta-1)}\bar{f}(\xi)_{t=0}$, $x \in R^N$, *$0<p<1$, $m<2$,*

where $\overline{f}(\xi) = \left(a - \frac{\sigma+p}{4}\xi^2\right)_+^{\frac{1}{\sigma+p}}$, $\quad \xi = \frac{2}{2-m}|x|^{\frac{2-m}{2}} / (\tau(t))^{1/2}$, *a>0 is a constant,*

$$\tau(t) = \int \left[T + (1-\beta)\int \gamma(t)dt\right]^{\frac{\sigma+p}{1-\beta}} dt \quad \textit{and}$$

$$\gamma(t)\tau(t)\left[T + (1-\beta)\int \gamma(t)dt\right]^{\frac{\beta-2+p+\sigma}{1-\beta}} \le \frac{N}{(1-p)(2-m)}, \quad t > 0$$

Then the problem (1)-(2) has a global solution for which in Q the estimate

$u(t,x) = [(T+(1-\beta)\int \gamma(t)dt)]^{-1/(1-\beta)}\,\overline{f}(\xi)$, $\mathrm{T}>0$ *is valid.*

Corollary 3. Let $\gamma(t) = \gamma = const$. *Then the condition of global solvability is*

$$2N - [\sigma + p + (2-m)(1-p)] \le \beta < 2 - (p+\sigma).$$

REFERENCES

[1] Fujita B. H. On the blowing up of solutions to the Cauchy problem for $u_t = \Delta u + u^{1+\alpha}$, J. Fac. Sci. Univ. Tokio, 1966., Sect. IA. **13** 1(1966), 109-127.
[2] Samarskii, A. A., Kurdyumov, S. P., Galaktionov, V. A., Mikhajlov, A.P., Blow up in a problem for quasiliniear parabolic equations, Moscov,. Science 1987.
[3] Galaktionov, V. A., Kurdyumov, S. P., Mikhajlov, A.P., Samarskii, A. A,. On the unbounded solutions of a Cauhy problem for the parabolic equation $u_l = \nabla(u^{\sigma}\nabla u) + u^{\beta}$., RAS, USSR, 252 6(1980), 1362-1364.
[4] Yuxiang Li, Weibing Deng, Chunhong Xie. Global Existence and nonexistence for degenerate parabolic systems. Proc. Am. Math. Soc. ISO (2002). 3661-3670.
[5] Aripov, M., Asymptotics of a solution of the non-Newtonian polytrophic filtration equations. ZAMM, supl.3 (2000), **80**. 767-768
[6] Aripov, M., Methods of the standard equations for the solution of nonlinear boundary problems. Fan.Tashkent. 1988.
[7] Aripov, M., Approximate self-similar approach for solving quasiliniar parabolic equation, in "Experimentation, Modeling, Computation in Flow Turbulence and Combustion." Willey & Sons, New York, 1997. vol.2, p. 19-26.
[8] Aripov, M., Sadullaeva. Sh.A, Vichislitelnaya Technologiya, 4 (2003), **8**, 72-78.
[9] Aripov, M., Kabiljanova. F.A., Khaydarov, A., Vichislitelnaya Technologiya, 4(2003), **8**, 79-84.

Modelarea agregatelor hidroenergetice prin metoda elementelor finite

Mircea Vereş
Universitatea din Oradea

Abstract. The paper presents problematics of modelling the operation of energy equipment (machines) by the finite element method.

1. NOȚIUNI TEORETICE

1.1. Analiza statică

Problemele statice sunt acelea în care încărcările şi condițiile de frontieră nu se schimbă. Ecuațiile care descriu aceste tipuri de probleme, sunt de forma:

$$K \cdot U = F \ , \tag{1}$$

în care: K este matricea de rigiditate, F sunt încărcările exterioare şi U sunt deplasările rezultate în urma aplicării încărcărilor.

1.2. Analiza dinamică

Modelul matematic al unei probleme de analiză dinamică are forma:

$$M\ddot{u} + C\acute{u} + Ku = F(t), \tag{2}$$

în care: K este matricea de rigiditate, F sunt încărcările exterioare, M este matricea maselor, C matricea de amortizare. Dacă numărul de noduri ale unui element este „ndf" (number of degrees of freedom), deplasarea în interiorul fiecărui element poate fi exprimată prin funcția de formă:

$$u = N^T \cdot u_K \ ,$$
$$N^T = \left[N_1; N_2; ......; N_{ndf}\right] \ , \tag{3}$$
$$u_K = \left[u_1; u_2; ....; u_{ndf}\right]^T \ .$$

Matricea maselor, pentru o anumită aplicație, poate fi calculată folosind funcțiile de formă şi densitatea materialului:

$$M = \int_{-1}^{1}\int_{-1}^{1} N_0^T \cdot \rho \cdot N_0 \cdot r \det(I) d\xi dn \ , \tag{4}$$
$$N_0 = \left[N^T .....N^T\right].$$

Pentru determinarea matricelor amortizărilor se presupune că aceasta este o combinație liniară între matricea de rigiditate şi cea a maselor:

$$C = \alpha \cdot M + \beta \cdot K \tag{5}$$

Valori ridicate ale coeficientului α vor amortiza frecvențele joase, iar valori mari ale coeficientului β vor amortiza frecvențele înalte.

1.3. Determinarea frecvențelor proprii

Frecvențele proprii sunt definite ca soluții ale ecuației (2) în care lipseşte termenul de amortizare:

$$M\ddot{u} + Cu = 0, \tag{6}$$
$$u = \acute{u} \cdot e^{i\omega t} \ . \tag{7}$$

Substituind (7) în ecuația (6) se obține expresia în ω:

$$(-\omega^2 M + K)u = 0\ . \tag{8}$$

Prin rezolvarea ecuației se determină frecvențele proprii:

$$f = \frac{\omega}{2\pi}\ . \tag{9}$$

Modurile proprii vor avea forma:

$$\Phi^{T\cdot} M \cdot \Phi = I. \tag{10}$$

1.4. Analiza răspunsului în frecvență

Răspunsul în frecvență se studiază în cazul soluției staționare pentru încărcări cu forțe de excitație armonice. Toate încărcările armonice vor excita sistemul simultan, cu aceleaşi frecvențe. În acest sens, cea mai folosită metodă de analiză a răspunsului în frecvență este metoda descompunerii modale.

Pornind de la ecuația dinamică:

$$M\ddot{u} + C\acute{u} + Ku = p(t), \tag{11}$$

deplasările nodale sunt exprimate în funcție de modurile proprii φ_l în cazul analizei frecvențelor proprii şi în funcție de coordonatele generalizate q_l.

$$u = \sum q_l(t) \cdot \varphi_l(x, y) \tag{12}$$

Modurile proprii posedă următoarele proprietăți:

$$\Phi^{T\cdot} M \cdot \Phi = I\ , \qquad \Phi^{T\cdot} K \cdot \Phi = \mathrm{diag}(\omega_l^2). \tag{13}$$

Pentru a descompune termenul de amortizare al ecuației, se presupune ortogonalitatea matricei de amortizare dată de relația:

$$\Phi^{T\cdot} C \cdot \Phi = \mathrm{diag}(2\xi_l \cdot \omega_l), \tag{14}$$

în care ξ_l este coeficientul de amortizare pentru modul l.

După înlocuiri şi transformări succesive se obține relația coordonatelor generalizate:

$$\ddot{q} + 2\xi \cdot \omega_l \cdot \dot{q}_l + \omega^2 \cdot q_l = \varphi_l^T p(t) \tag{15}$$

Folosind exprimarea în domeniul complex a încărcărilor armonice, se obține:

$$p(t) = \acute{I}_{mag}[p \cdot e^{i\Omega t}] \tag{16}$$

Substituind (16) în ecuația (15), rezultă:

$$\ddot{q} + 2\xi_l \cdot \omega_l \cdot \dot{q}_l + \omega_l^2 \cdot q_l = \varphi_l^T \cdot \overline{p} \cdot e^{i\Omega t}\ , \tag{17}$$

cu soluția staționară:

$$q_l(t) = \overline{q}_l \cdot e^{i\Omega t}\ , \tag{18}$$

din care rezultă:

$$(-\Omega^2 + 2\xi_l \cdot \omega_l \cdot \Omega_i + \omega_l^2) \cdot \overline{q}_l \cdot e^{i\Omega t} = \varphi_l^T \cdot \overline{p} \cdot e^{i\Omega t} \,. \tag{19}$$

Din relația (19) se obțin coordonatele generalizate q_l cu ajutorul cărora se calculează deplasările, folosind transformarea de coordonate:

$$\overline{u} = \overline{\phi} \cdot \overline{q} \,, \tag{20}$$

Pentru a exprima partea reală a soluției complexe a răspunsului în frecvență, se utilizează relațiile:

$$u(t) = \dot{I}_{mag}(\overline{u} \cdot e^{i\Omega t}) \,,$$

$$u(t) = \dot{I}_{mag}(\overline{u}) \cdot \cos(\Omega t) + \mathrm{Re}\,al(\overline{u}) \cdot \sin \Omega t \,,$$

$$u(t) = |\overline{u}| \cdot \sin(\Omega t + \gamma) \,, \tag{21}$$

$$\gamma = a \tan \frac{\dot{I}_{mag}(\overline{u})}{\mathrm{Re}\,al(\overline{u})} \,.$$

2. DETERMINAREA MODURILOR PROPRII DE VIBRAȚIE PENTRU HIDROAGREGATUL CU PUTEREA P=9MW

2.1. Parametrii modelării

Parametrii utilizați în cadrul realizării modelului dinamic sunt :

- \- Material :
  - **modulul lui Young : 2*10^{11}N/m^2;**
  - **Coeficientul lui Poisson: 0,266.**
- \- Structura modelului :
  - **numărul de noduri : 1853;**
  - **numărul de elemente : 7328;**
  - **numărul de grade de libertate : 5778;**
  - **numărul relațiilor cinematice : 420**
- \- Coordonatele centrului de greutate :
  - **Xg : 585,7 mm;**
  - **Yg : -585,3 mm;**
  - **Zg : -713,6 mm.**
- \- Tensorul de inerție în origine :

2.450e+009	7.140e+006	9.616e+006
7.140e+006	6.749e+010	-4.198e+006
9.616e+006	-4.198e+006	6.750e+010

2.2.Rezultatele modelării

Rezultatele simulării au fost obținute luând în considerare următorii parametrii :

- numărul de moduri proprii calculate : 10;
- numărul de iterații :44;
- toleranța valorilor proprii obținute : 2.089*10^{-4}

Modurile proprii rezultate sunt prezentate în tabelul 1, iar coeficienții de formă proprie de vibrație sunt prezentați în tabelul 2, unde: Tx,Ty,Tz,Rx,Ry,Rz reprezintă încărcările și reacțiunile din lagărele hidroagregatului.

Tabelul 1. Caracterizarea modurilor proprii de vibrație

Marcarea (numerotarea) MPV	Frecvența proprie [Hz]	Caracterizarea MPV după domeniul de :	
		frecvență	deformare
1	3,3692	foarte mică	Vibrații axiale ale ansamblului rotor-arbore
2	138,61	mică	Vibrații radiale în LR și LT; încovoierea ușoară a arborelui
3	143,66	mică	Vibrații radiale în LR și LT; încovoierea puternică a arborelui între LR și RT
4	447,36	medie	Vibrații radiale mari în LRA, și mai mici în LR și LT; încovoierea arborelui în LRA
5	462,55	medie	Vibrații pronunțate în LRA cu încovoierea arborelui în LRA și foarte reduse în LR și LT
6	528,82	medie	Vibrații reduse în LR și mai mari în LT, îcovoierea arborelui între LR și LT
7	935,75	mare	Vibrații longitudinale, reduse radial în toate lagărele
8	961,26	mare	Vibrații puternice în LR și LT pe direcția radială cu încovoierea arborelui între LR și LT
9	1075,3	foarte mare	Vibrații longitudinale mari și radiale în LR și LT, încovoierea arborelui între LR și LT
10	1093,0	foarte mare	Vibrații foarte puternice în LR și LT pe direcție radială cu încovoierea arborelui între LR și LT

MPV – mod propriu de vibrație; LRA – lagăr radial-axial; LR – lagăr radial; LT – lagăr turbină

Tabelul 2. Valorile încărcărilor și a reacțiunilor din lagăre

Mod propriu	Frecvența [Hz]	Tx [%]	Ty [%]	Tz [%]	Rx [%]	Ry [%]	Rz [%]
foarte mică	**3,3692**	**0.00**	**0.14**	**0.59**	**99.6**	**0.56**	**0.08**
mică	**138,61**	**0.00**	**7.90**	**79.86**	**0.23**	**68.84**	**6.78**
	143,66	**0.00**	**79.98**	**7.74**	**0.03**	**6.66**	**69.03**
Medie	**447,36**	**0.01**	**0.00**	**0.00**	**0.04**	**7.79**	**0.87**
	462,55	**0.00**	**0.00**	**0.00**	**0.00**	**0.82**	**7.81**
	528,82	**0.00**	**0.00**	**0.00**	**0.00**	**0.07**	**0.08**
mare	**935,75**	**0.14**	**0.45**	**5.20**	**0.00**	**3.30**	**0.29**
	961,26	**0.02**	**5.18**	**0.44**	**0.00**	**0.27**	**3.32**
foarte mare	**1075,3**	**87.15**	**0.00**	**0.01**	**0.00**	**0.00**	**0.00**
	1093,0	**0.10**	**0.03**	**0.02**	**0.00**	**0.01**	**0.01**

În figurile următoare sunt sugerate deformațiile ansamblului la frecvențele proprii calculate.

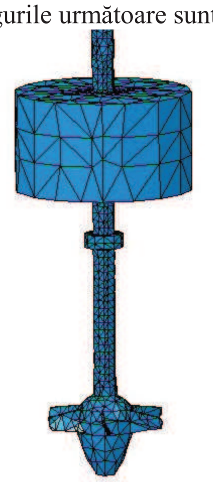

Fig. 1. Mod.1 Deformația arborelui la frecvența de 3,3692 Hz.

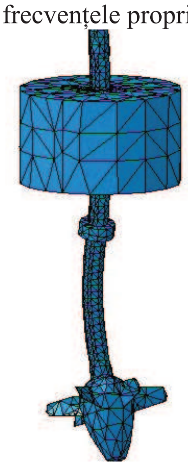

Fig. 2. Mod.2 Deformația arborelui la frecvența de 138,61 Hz

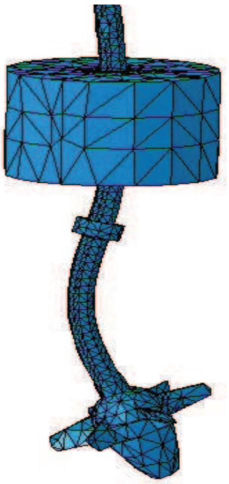

Fig. 3. Mod.3 Deformația arborelui la frecvența de 143,66 Hz.

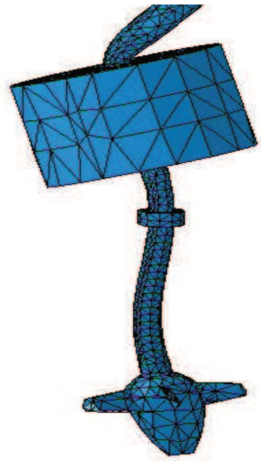

Fig. 4. Mod.4 Deformația arborelui la frecvența de 447,36 Hz

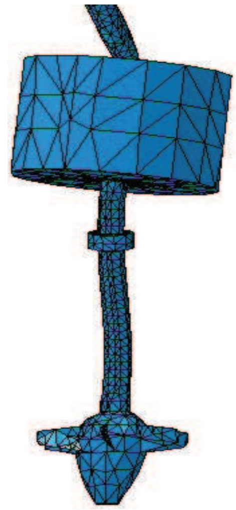

Fig.5. Mod.5 Deformația arborelui la frecvența de 462,55 Hz

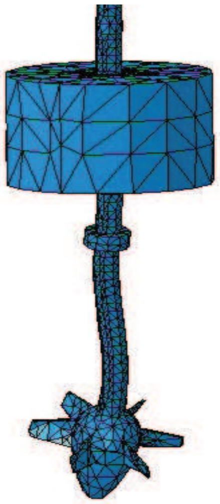

Fig. 6. Mod.6 Deformația arborelui la frecvența de 528,82 Hz

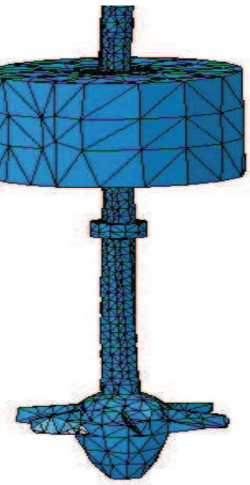

Fig. 7. Mod.7 Deformația arborelui la frecvența de 935,75 Hz.

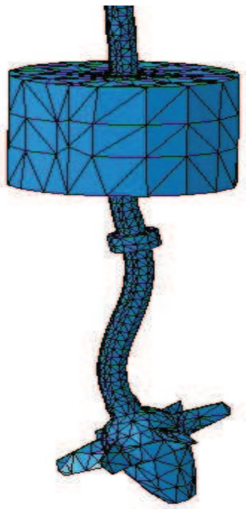

Fig. 8. Mod.8 Deformația arborelui la frecvența de 961,26 Hz

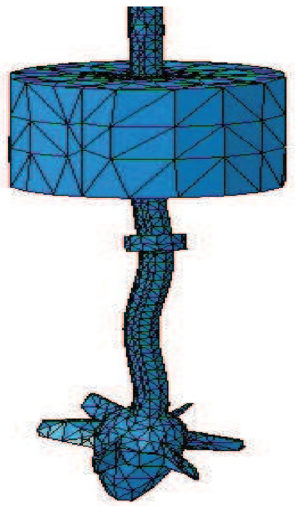

Fig. 9. Mod.9 Deformația arborelui la frecvența de 1075,3 Hz

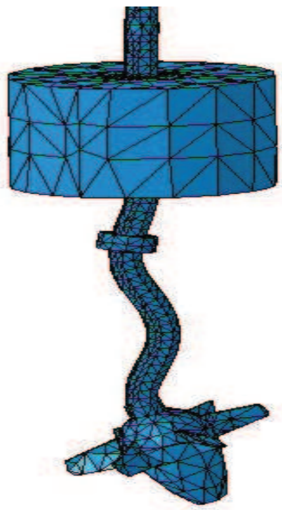

Fig. 10. Mod.10 Deformația arborelui la frecvența de 1093,0 Hz

3. CONCLUZII

1. Modelarea funcționării sistemului experimental pentru cazul utilizării unor lagăre cu alunecare şi respectiv, a unor lagăre cu sustentație hidrostatică, permite, în cazul obținerii unui model corect, predicția funcționării sistemului şi în alte condiții decât cele testate experimental. Cu ajutorul modelelor se poate stabili răspunsul sistemului în situații limită ce pot duce la defecte majore.

2. Pentru simulare se impune utilizarea unui soft adecvat, cum este programul de simulare "System Identification Toolbox" din cadrul modelului de programare MATLAB al firmei Math Works, şi a unor

semnale de excitație sinusoidale generate, de asemenea, pentru un program de calculator; în corelație cu amplitudinea şi frecvența excitației reale.

3. Pentru determinarea modurilor proprii de vibrație (MPV) ale unui agregat hidroenergetic se va face uz de modelul dinamic şi de un program de calcul adecvat (CATIA).

4. Se apreciază că, pentru studiul efectelor fenomenelor vibraționale asupra gradului de deformare al ansamblului rotor-lagăre (ARL) din structura unui hidroagregat sunt acoperitoare un număr de 10 MPV, corespunzătoare la 10 valori ale frecvenței proprii, aparținând la 5 domenii (foarte mică, mică, medie, mare, foarte mare).

4. BIBLIOGRAFIE

[1] Felea, I., Coroiu, N., *Fiabilitatea şi mentenanța echipamentelor electrice*, Ed. Tehnică, Bucureşti, 2002.
[2] Felea, I*., Ingineria fiabilității în electroenergetică*, Ed. Did. şi Ped., Bucureşti, 1996.
[3] Felea, I., Vereş, M., Bendea, G., Boja, I., *Considerații privind diagnoza tehnică a echipamentelor electrice*, Analele Universității din Oradea, Fascicula Energetică, nr. 9, Oradea, 2003.
[4] Gârbea, D., *Analiză cu elemente finite*, Ed. Tehnică, Bucureşti, 1990
[5] Vereş M., *Considerații privind hidrodinamica lagărelor radiale şi axiale*, Analele Universității din Oradea, Fascicola Energetică, Nr.8 vol. I, pag. 271-274, Oradea, 2002.
[6] Vereş, M., *Cercetări vizând identificarea principiilor şi metodelor de diagnoză tehnică a echipamentelor hidroenergetice*. Referat nr.2 de doctorat, Universitatea din Oradea, 2000.
[7] Vereş, M., *Cercetări privind diagnoza tehnică a echipamentelor hidroenergetice*, Teză de doctorat, Universitatea din Oradea, 2003.

A computer package for analysis of variance

Maria PÂRV
University of Agricultural Sciences and Veterinary Medicine
Faculty of Veterinary Medicine
Calea Mănăştur 3-5, RO 3400 Cluj-Napoca, Romania
e-mail: maria_parv@yahoo.com

Abstract. This paper presents a computer package for analysis of variance, running under Microsoft Windows. The programs POLIFACT, PATRLAT, and DREPTLAT have a common user interface for entering data and displaying the results. Based mainly on the general algorithm presented in [3] and [4], POLIFACT is an ANOVA-type program, performing analysis of variance for a randomised complete polyfactorial design (see [1], [2], [5] and [7]). The other two programs in the package do computations in two particular situations, where the experimental designs are latin squares and latin rectangles [6]. Besides the usual output of ANOVA, the programs produce additional information like comparison tables based on limit differences DL and Duncan tests.

1. Terminology

The analysis of variance (or *dispersional analysis*, [7], AV for short) is a statistical method for the analysis of observational data which depend on several factors acting simultaneously, in order to establish the most important factor and to estimate their influence. This method was introduced in the agricultural research by R.A. Fisher and is based on the additive property of variance: it can be written under the form of a sum in which each term represents the variance due to one of the factors considered.

Suppose that Y is a random real variable whose values depend on p *factors* $x_1, x_2, ..., x_p$, qualitative or quantitative. Every factor has a finite number of values, called *levels*. The cardinal of the set of values of the factor j ($1 \le j \le p$), i.e. the *number of levels* of j^{th} factor, is denoted by J_j. The p factors considered, $x_1, x_2, ..., x_p$ have the number of levels $J_1, J_2, ..., J_p$.

An important component of AV deals with experiment planning; various experimental plans or schemes use the terms *block* and *cell*. A *cell* is a p-uple $(i_1, i_2, ..., i_p)$, where i_j, $1 \le j \le p$, is a fixed level of j^{th} factor, $1 \le i_j \le J_j$. There are in all $J_1 \cdot J_2 \cdot \ ... \cdot J_p$ cells for a so-called *complete* classification or experimental scheme. If not all cells are considered, we have an *incomplete* classification or experimental scheme.

A system of cells is called *block*; sometimes, the notions of cell and block are synonimous. For example, all the cells corresponding to the same level of the first factor belong to a *big block*; there are in all J_1 big blocks. Every big block is divided into J_2 *middle-sized blocks*; every such a intermediate block corresponds to a separate level of the second factor, and so on. In this setting, the cell is the *small block*; all experiments performed in the same cell (called *repetitions*) have in common the same combination of factor levels. An experimental scheme is *balanced* if the same number of repetitions are performed in each cell.

Usual application domains of AV include experimental sciences: chemistry, biology, psychology, sociology, medicine, but especially agricultural science.

2. Notation and formulae

In what follows, AV for a complete and balanced experimental plan is considered, with p factors and r repetitions. The total number of observations, N, is computed by

$$N = r \cdot \prod_{i=1}^{p} J_i \ . \tag{1}$$

The observational data are represented in a $(p+1)$-dimensional table, denoted by X. In every cell $(i_1, i_2, ..., i_p)$ r experiments (repetitions) are performed; the measured value of the j^{th} experiment is denoted by $x_{i_1 i_2 \cdots i_p j}$, with $1 \le i_k \le J_k$, $1 \le k \le p$, and $1 \le j \le r$.

2.1. Effects and interactions

In order to better understand the notions presented further down, we shall consider $p = 4$; the names of factors are A, B, C, and D, while the repetitions (considered as a *fictitious* factor) are denoted by R. For these five factors, the summation indices and their levels will be i, j, k, l, m, and I, J, K, L, M, respectively. The observational data will be x_{ijklm} , with $1 \le i \le I$, $1 \le j \le J$, $1 \le k \le K$, $1 \le l \le L$, and $1 \le m \le M$.

In order to further simplify the notations, we shall specify at the summation symbol Σ only the index (indices) of summation; the absence of such an index, marked by an $*$, signifies the average (or mean) with respect to the corresponding factor.

For instance, the average of all observations, denoted by $\bar{x}$, is expressed by

$$\bar{x} \equiv x_{*****} = \frac{\sum_{i,j,k,l,m} x_{ijklm}}{I \cdot J \cdot K \cdot L \cdot M} \ , \tag{2}$$

the average of the i^{th} level of the A factor ($1 \le i \le I$) has the form

$$x_{i****} = \frac{\sum_{j,k,l,m} x_{ijklm}}{J \cdot K \cdot L \cdot M} \ , \tag{3}$$

the average of the k^{th} level of the C factor ($1 \le k \le K$) is computed by

$$x_{**k**} = \frac{\sum_{i,j,l,m} x_{ijklm}}{I \cdot J \cdot L \cdot M} \ , \tag{3'}$$

while the average of the combination between the i^{th} level of the A factor ($1 \le i \le I$) and the j^{th} level of the B factor ($1 \le j \le J$) is expressed by

$$x_{ij***} = \frac{\sum_{k,l,m} x_{ijklm}}{K \cdot L \cdot M} \ . \tag{4}$$

The averages of the combinations of three and four factors can be defined in a similar way.

We call *main effect* of the i^{th} level of the A factor ($1 \le i \le I$) the quantity [7]

$$\alpha_i^{\mathrm{A}} = x_{i****} - \bar{x} \ . \tag{5}$$

The main effects of levels j, k, and l for the factors B, C, and D, respectively, are defined analogously

$$\alpha_j^{\mathrm{B}} = x_{*j***} - \bar{x} \ , \tag{6}$$

$$\alpha_k^{\mathrm{C}} = x_{**k**} - \bar{x} \ , \tag{7}$$

$$\alpha_l^{\mathrm{D}} = x_{***l*} - \bar{x} \ . \tag{8}$$

In order to point out the cooperative effects of the factors, their interactions are also considered; one defines the 2nd, 3rd and 4th order *interactions*. For instance

$$\alpha_{ij}^{\mathrm{AB}} = x_{ij***} - \alpha_i^{\mathrm{A}} - \alpha_j^{\mathrm{B}} - \bar{x} \tag{9}$$

represents the interaction between the i^{th} level of the A factor and the j^{th} level of the B factor,

$$\alpha_{ijk}^{\mathrm{ABC}} = x_{ijk**} - \alpha_{ij}^{\mathrm{AB}} - \alpha_{ik}^{\mathrm{AC}} - \alpha_{jk}^{\mathrm{BC}} - \alpha_i^{\mathrm{A}} - \alpha_j^{\mathrm{B}} - \alpha_k^{\mathrm{C}} - \bar{x} \tag{10}$$

represents the interaction between the i^{th} level of the A factor, the j^{th} level of the B factor, and the k^{th} level of the C factor, while

$$\begin{aligned} \alpha_{ijkl}^{\mathrm{ABCD}} = x_{ijkl*} &- \alpha_{ijk}^{\mathrm{ABC}} - \alpha_{ijl}^{\mathrm{ABD}} - \alpha_{ikl}^{\mathrm{ACD}} - \alpha_{jkl}^{\mathrm{BCD}} - \alpha_{ij}^{\mathrm{AB}} - \alpha_{ik}^{\mathrm{AC}} - \alpha_{il}^{\mathrm{AD}} \\ &- \alpha_{jk}^{\mathrm{BC}} - \alpha_{jl}^{\mathrm{BD}} - \alpha_{kl}^{\mathrm{CD}} - \alpha_i^{\mathrm{A}} - \alpha_j^{\mathrm{B}} - \alpha_k^{\mathrm{C}} - \alpha_l^{\mathrm{D}} - \bar{x} \end{aligned} \tag{11}$$

represents the interaction between the i^{th} level of the A factor, the j^{th} level of the B factor, the k^{th} level of the C factor, and the l^{th} level of the D factor.

The equation (11), rewritten in the form

$$x_{ijkl*} = \bar{x} + \alpha_i^{\mathrm{A}} + \alpha_j^{\mathrm{B}} + \alpha_k^{\mathrm{C}} + \alpha_l^{\mathrm{D}} + \alpha_{ij}^{\mathrm{AB}} + \alpha_{ik}^{\mathrm{AC}} + \alpha_{il}^{\mathrm{AD}} + \alpha_{jk}^{\mathrm{BC}} + \alpha_{jl}^{\mathrm{BD}} + \alpha_{kl}^{\mathrm{CD}} + \alpha_{ijk}^{\mathrm{ABC}} + \alpha_{ijl}^{\mathrm{ABD}} + \alpha_{ikl}^{\mathrm{ACD}} + \alpha_{jkl}^{\mathrm{BCD}} + \alpha_{ijkl}^{\mathrm{ABCD}}, \quad (12)$$

represents the decomposition of the average of the cell (i, j, k, l) into: average of the whole experiment, main effects of the factor levels and their interactions.

2.2. Variances

In order to point out the effects and interactions, the sums of squares of the corresponding deviations are computed. By means of the fictitious factor R, one can introduce, among the parameters α, defined in section 2.1, other parameters which measure the experimental errors.

The *variance* σ^2 is defined as

$$\sigma^2 = \frac{SS}{\nu}, \quad (13)$$

where SS represents the sum of squares, while ν denotes the number of degrees of freedom. Table 1 contains the equations for those quantities, where the subscripts A, B, C, D, R have the same meaning as the superscripts for main effects and interactions.

Table 1. Equations for *SS* and ν

SS	ν	Analogously for
$SS_{\mathrm{A}} = \sum_i (\alpha_i^{\mathrm{A}})^2$	I – 1	B, C, D, R
$SS_{\mathrm{AB}} = \sum_{i,j} (\alpha_{ij}^{\mathrm{AB}})^2$	(I - 1)·(J - 1)	AC, AD, AR, BC, BD, BR, CD, CR, DR
$SS_{\mathrm{ABC}} = \sum_{i,j,k} (\alpha_{ijk}^{\mathrm{ABC}})^2$	(I - 1)·(J - 1)·(K - 1)	ABD, ABR, ACD, ACR, ADR, BCD, BCR, BDR, CDR
$SS_{\mathrm{ABCD}} = \sum_{i,j,k,l} (\alpha_{ijkl}^{\mathrm{ABCD}})^2$	(I - 1)·(J - 1)·(K - 1)·(L - 1)	ABCR, ABDR, ACDR, BCDR
$SS_{\mathrm{ABCDR}} = \sum_{i,j,k,l,m} (\alpha_{ijklm}^{\mathrm{ABCDR}})^2$	(I - 1)·(J - 1)·(K - 1)·(L - 1) ·(M - 1)	

The sum of squares of the experimental errors SS_e is computed by summing up all SS sums which contain the R factor:

$$SS_e = SS_{\mathrm{R}} + SS_{\mathrm{AR}} + SS_{\mathrm{BR}} + SS_{\mathrm{CR}} + SS_{\mathrm{DR}} + SS_{\mathrm{ABR}} + SS_{\mathrm{ACR}} + SS_{\mathrm{ADR}} + SS_{\mathrm{BCR}} + SS_{\mathrm{BDR}} + SS_{\mathrm{CDR}} + SS_{\mathrm{ABCR}} + SS_{\mathrm{ABDR}} + SS_{\mathrm{ACDR}} + SS_{\mathrm{BCDR}} + SS_{\mathrm{ABCDR}}, \quad (14)$$

while the number of degrees of freedom ν_e is the sum of the degrees of freedom corresponding to the sums SS in (14).

The sum (14) can be rewritten as

$$SS_e = SS_{e\mathrm{A}} + SS_{e\mathrm{B}} + SS_{e\mathrm{C}} + SS_{eD} + SS_{e\mathrm{R}}, \quad (15)$$

where the first four terms in the right-hand side represent the sums of the squares of the errors referred to the four factors. Table 2 lists the equations for these sums and the corresponding degrees of freedom.

Table 2. Sum of squares of the errors and the corresponding degrees of freedom

SS	ν
$SS_{e\mathrm{A}} = SS_{\mathrm{AR}}$	$\nu_{e\mathrm{A}} = \nu_{\mathrm{AR}}$
$SS_{e\mathrm{B}} = SS_{\mathrm{BR}} + SS_{\mathrm{ABR}}$	$\nu_{e\mathrm{B}} = \nu_{\mathrm{BR}} + \nu_{\mathrm{ABR}}$
$SS_{e\mathrm{C}} = SS_{\mathrm{CR}} + SS_{\mathrm{ACR}} + SS_{\mathrm{BCR}} + SS_{\mathrm{ABCR}}$	$\nu_{e\mathrm{C}} = \nu_{\mathrm{CR}} + \nu_{\mathrm{ACR}} + \nu_{\mathrm{BCR}} + \nu_{\mathrm{ABCR}}$
$SS_{e\mathrm{D}} = SS_{\mathrm{DR}} + SS_{\mathrm{ADR}} + SS_{\mathrm{BDR}} + SS_{\mathrm{CDR}} + SS_{\mathrm{ABDR}} + SS_{\mathrm{ACDR}} + SS_{\mathrm{BCDR}} + SS_{\mathrm{ABCDR}}$	$\nu_{e\mathrm{D}} = \nu_{\mathrm{DR}} + \nu_{\mathrm{ADR}} + \nu_{\mathrm{BDR}} + \nu_{\mathrm{CDR}} + \nu_{\mathrm{ABDR}} + \nu_{\mathrm{ACDR}} + \nu_{\mathrm{BCDR}} + \nu_{\mathrm{ABCDR}}$

2.3. Checking the statistical hypotheses

As the other chapters of experimental statistics, AV also needs the settlment of the extent to which the differences in the results of an experiment are (or not) placed between the limits of the experimental error. In order to point out the statistical significance of the results, we use three tests: the *t* test, the *F* test and the Duncan test.

Theoretical values of the Student's test *t* are used for computing the theoretical *limit differences DL*

$$DL = t_e \cdot s_d \,, \tag{16}$$

where s_d is the standard error of differences, and t_e is taken from statistical tables, as function of the degrees of freedom of the error *e*. The equations for s_d are given in Table 4.

In order to compare the different variants of a polyfactorial experiment, one usually determine the theoretical *DLs* corresponding to the confidence limits P 5%, P 1% and P 0,1%. Denoting by Δ the difference between the averages of comparing variants (also called *deviation*), and by *DL* P 5%, *DL* P 1%, and *DL* P 0,1% the corresponding limit differences, the interpretation of results is given in Table 3.

Table 3. Comparing the deviations in average by using the *t* test and limit differences *DL*

Case	Statistical significance
$\lvert\Delta\rvert < DL$ P 5%	The deviation does not exceed the limits of experimental error.
$\lvert\Delta\rvert \in [DL$ P 5%, DL P 1%)	The deviation is *statistically* significant
$\lvert\Delta\rvert \in [DL$ P 1%, DL P 0,1%)	The deviation is *distinct* significant.
$\lvert\Delta\rvert \geq DL$ P 0,1%	The deviation is *very* significant.

The *F* (Fisher-Snedecor) test, computed by:

$$F_{\text{computed}} = \frac{\sigma^2}{\sigma_e^2} \,, \tag{17}$$

where σ^2 denotes the variance of some variant (factor or factor combination), while σ_e^2 is the corresponding variance of the error, is used to determine the homogenity of the compared variances. The computed *F* value, F_{computed} is compared with the theoretical *F* value, $F_{\text{theoretical}}$ taken from statistical tables, as a function of the corresponding degrees of freedom and a given confidence limit. The variances are homogeneous if $F_{\text{computed}} < F_{\text{theoretical}}$, i.e. the casual and systematic factors have a comparable contribution to the result. If $F_{\text{computed}} \geq F_{\text{theoretical}}$, the deviation is statistically significant into the considered confidence interval.

The *F* test indicates only the presence or absence of certain effects, being therefore a quantitative indicator. In the presence of effects, the AV processing continues normally with the comparison of variances based on limit differences *DL*.

The general formula (16) which computes *DL* is made explicit by Table 4 and equations (18) - (23). Table 4 contains formulae (taken from [1]) for the main effects and the second- and third-order interactions, where the order of considered factors matters.

Table 4. Computing the limit differences *DL* with (16)

The factors/factor combination	t_e	s_d	Analogously for
A – compares the means of the levels of A factor	$t_{e\mathrm{A}}$	$s_{d_\mathrm{A}} = \sqrt{\dfrac{2 \cdot SS_{e\mathrm{A}}}{\mathrm{J \cdot K \cdot L \cdot M}}}$	B, C, D
BA – compares the means of the levels of B to the same level of A	$t_{e\mathrm{B}}$	$s_{d_\mathrm{BA}} = \sqrt{\dfrac{2 \cdot SS_{e\mathrm{B}}}{\mathrm{K \cdot L \cdot M}}}$	CA, DA, CB, DB, DC
AB – compares the means of the levels of A to the same level of B	eq. (18)	eq. (19)	AC, AD, BC, BD, CD
CAB – compares the means of the levels of C to the same levels of A and B	$t_{e\mathrm{C}}$	$s_{d_\mathrm{CAB}} = \sqrt{\dfrac{2 \cdot SS_{e\mathrm{C}}}{\mathrm{L \cdot M}}}$	DAB, DAC, DBC
BAC – compares the means of the levels of B to	eq. (20)	eq. (21)	BAD, CAD, CBD

the same levels of A and C			
ABC – compares the means of the levels of A to the same levels of B and C	eq. (22)	eq. (23)	ABD, ACD, BCD

In the following equations, the values t_{eA}, t_{eB} şi t_{eC} are taken from statistical tables (t values) for the degrees of freedom ν_{eA}, ν_{eB} and ν_{eC} and the desired significance threshold

$$t_{eAB} = \frac{(J-1)\cdot SS_{eB}\cdot t_{eB} + SS_{eA}\cdot t_{eA}}{(J-1)\cdot SS_{eB} + SS_{eA}}\ , \qquad (18)$$

$$s_{d_{AB}} = \sqrt{\frac{2\cdot(J-1)\cdot SS_{eB} + SS_{eA}}{J\cdot K\cdot L\cdot M}}\ , \qquad (19)$$

$$t_{eBAC} = \frac{(K-1)\cdot SS_{eC}\cdot t_{eC} + SS_{eB}\cdot t_{eB}}{(K-1)\cdot SS_{eC} + SS_{eB}}\ , \qquad (20)$$

$$s_{d_{BAC}} = \sqrt{\frac{2\cdot(K-1)\cdot SS_{eC} + SS_{eB}}{K\cdot L\cdot M}}\ , \qquad (21)$$

$$t_{eABC} = \frac{J\cdot(K-1)\cdot SS_{eC}\cdot t_{eC} + (J-1)\cdot SS_{eB}\cdot t_{eB} + SS_{eA}\cdot t_{eA}}{J\cdot(K-1)\cdot SS_{eC} + (J-1)\cdot SS_{eB} + SS_{eA}}\ , \qquad (22)$$

$$s_{d_{ABC}} = \sqrt{\frac{2\cdot J\cdot(K-1)\cdot SS_{eC} + (J-1)\cdot SS_{eB} + SS_{eA}}{J\cdot K\cdot L\cdot M}}\ . \qquad (23)$$

The comparison of variants by using limit differences *DL* is valid only inside the groups of factors/factor combination given in Table 4 which differ by the levels of the first factor considered, called *neighbours with respect to the classification*. In order to compare the means of other variants, multiple comparison methods need to be used. Among these methods, the Duncan test is based on the notion of significant difference *DS*, computed by

$$DS\ 5\% = s_{\bar{x}}\cdot q_{5\%} \qquad (24)$$

where $s_{\bar{x}}$ is the *mean error*, generically given by $s_{\bar{x}} = \frac{s_d}{\sqrt{2}}$, s_d being the error of differences, given in Table 4.

In this case the place of the variant in the classification does not matter, as Table 5 shows.

Table 5. Computing the significant differences with (24)

The factors/factor combination	Degrees of freedom	Mean error $s_{\bar{x}}$	Analogously for
A – compares the means of the levels of A factor	ν_{eA} (Table 2)	$s_{\bar{x}_A} = \sqrt{\frac{SS_{eA}}{J\cdot K\cdot L\cdot M}}$	B, C, D
BA – compares the means for all combinations of levels of B and A	ν_{eB} (Table 2)	$s_{\bar{x}_{BA}} = \sqrt{\frac{SS_{eB}}{K\cdot L\cdot M}}$	CA, DA, CB, DB, DC
CAB – compares the means for all combinations of levels of C, A and B	ν_{eC} (Table 2)	$s_{\bar{x}_{CAB}} = \sqrt{\frac{SS_{eC}}{L\cdot M}}$	DAB, DAC, DBC

The Duncan test uses the notion of *studentized range*, explained below. The considered range contains values (means) sorted in ascending order. The theoretical value is computed by $q = W/s$, where W is the size of the range (the difference between the largest and the smallest value), and s is the standard deviation of the error, with ν degrees of freedom. The value of q also depends on the number of the values in the considered range, d, and on the significance threshold (usually 5%).

When comparing the means of variants VM, the variants are identified by their position within the considered range. Multiple comparisons are performed: the variant at the i^{th} position is compared with all variants at the j^{th} position ($j > i$), and the number of comparisons is given by $d = j–i+1$. The theoretical values $q(\nu, d)$ are taken from two-entry tables and are used to compute the significant differences $DS(d)$ with the aid of equation (24).

If $|\mathrm{VM}(j) - \mathrm{VM}(i)| \geq DS(j\text{-}i+1)$ then the difference of means for the variants i and j is considered significant. The next step is to group all variants which have no significant differences, producing as a final result a classification of variants into non-disjoint groups.

3. SPECIAL CASES OF AV

The general algorithm described in the previous section refers to the AV processing for a polyfactorial, complete and balanced experimental plan. This sections introduces two other special cases.

3.1. One-factor experiments in a latin square design

The latin square experimental design has the following features [6]:

- the general plan is a square, where both rows and columns denote a complete repetition;
- the number of blocks (b), columns (l), variants (v), and repetitions (n) are equal;
- a row (column) cannot contain two identical variants;
- the AV processing allows to eliminate both the differences between blocks and the differences between columns.

Table 6 illustrates this design, in which a cell is identified by the pair (ib, ic), where ib represents the block index, while ic is the column index, both varying from 1 to $b = l = v$. Every cell contains two distinct informations: the index of the variant $iv_{ib,\ ic}$ and the observed value $val_{ib,\ ic}$. The variant indices attached to the cells in the row (block) i dnote a complete repetition; this means that ($iv_{i,I}$, $iv_{i,II}$, ..., $iv_{i,l}$) is a permutation of (1, 2, ..., v). Analogously, the variant indices attached to the cells in the column j also contain a complete repetition.

The AV processing in this special case is close to the general algorithm; for details, see [6].

3.2. One-factor experiments in a latin rectangle design

The latin rectangle experimental design has the following features [6]:

- the general plan is a rectangle, where both rows and columns denote a complete repetition;
- the columns are divided into sub-columns; the number of sub-columns (s) is the same for all columns;
- the number of blocks (b), columns (l), and repetitions (n) are equal;
- the total number of sub-columns ($l \cdot s$) is equal to the number of variants;
- a row (column) cannot contain two identical variants;
- the AV processing allows to eliminate both the differences between blocks and the differences between columns.

The latin square is a particular case of the latin rectangle, where the number s of sub-columns is equals to 1. The AV computations in these two special experimental designs are almost identical.

4. THE COMPUTER PACKAGE

Three programs constitute the current version of the computer package for AV: POLIFACT, DREPTLAT, and PATRLAT. The user interacts with them via a common user interface, discussed below.

4.1. The user interface

The user interface of the programs is using Romanian language. All programs in the package have some common features with respect to the user interface, as follows:

- input data from keyboard can be stored in a file;
- the produced results are displayed in a separate window and can be either saved in a text file or printed.

The main window of each program exposes the full functionality of it, being primarily dedicated to entering and visualization of the input data, while the output is displayed in a separate editor-like window.

The input data of every AV program are corresponding to a specific experiment, and can be classified into three categories:

- the general data identifying the experiment;
- the data describing the factors;
- the observational data.

A detailed description of the input data is given below; there are slight variations from program to program. The main window has two areas:

- the data area, containing the input data; the factor and observational data are displayed in a spreadsheet-like way;
- the command area, in the right part of the window, with five command buttons: **Încarcă** (**Load**) for loading data from a file, **Salvează** (**Save**) for saving the current data in a file; **Prelucrează** (**Process**) for performing the computations and displaying the results; **Afişează** (**Display**) which shows **Results Window** (see below); **Închide** (**Close**) which ends the execution of the program.

The buttons **Încarcă** and **Salvează** display standard Microsoft Windows dialog boxes **Open** and **Save As**. The button **Afişează** shows **Results Window** (see Figures 1 and 2).

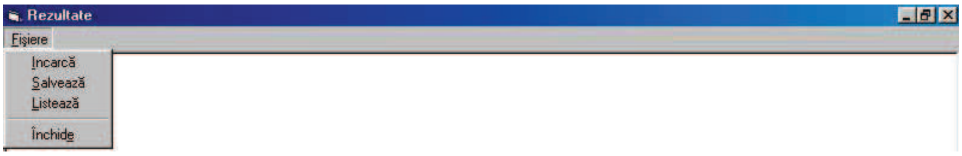

Fig. 1. The **Results Window** with its menu visible.

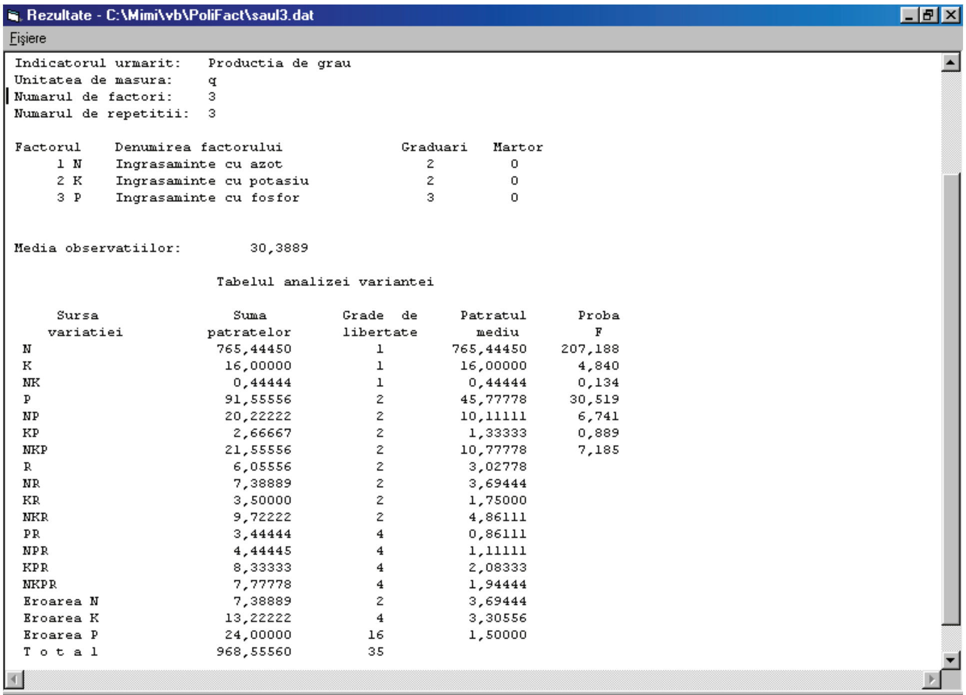
Rezultate - C:\Mimi\vb\PoliFact\saul3.dat

Fişiere

Indicatorul urmarit: Productia de grau
Unitatea de masura: q
Numarul de factori: 3
Numarul de repetitii: 3

Factorul	Denumirea factorului	Graduari	Martor
1 N	Ingrasaminte cu azot	2	0
2 K	Ingrasaminte cu potasiu	2	0
3 P	Ingrasaminte cu fosfor	3	0

Media observatiilor: 30,3889

Tabelul analizei variantei

Sursa variatiei	Suma patratelor	Grade de libertate	Patratul mediu	Proba F
N	765,44450	1	765,44450	207,188
K	16,00000	1	16,00000	4,840
NK	0,44444	1	0,44444	0,134
P	91,55556	2	45,77778	30,519
NP	20,22222	2	10,11111	6,741
KP	2,66667	2	1,33333	0,889
NKP	21,55556	2	10,77778	7,185
R	6,05556	2	3,02778	
NR	7,38889	2	3,69444	
KR	3,50000	2	1,75000	
NKR	9,72222	2	4,86111	
PR	3,44444	4	0,86111	
NPR	4,44445	4	1,11111	
KPR	8,33333	4	2,08333	
NKPR	7,77778	4	1,94444	
Eroarea N	7,38889	2	3,69444	
Eroarea K	13,22222	4	3,30556	
Eroarea P	24,00000	16	1,50000	
T o t a l	968,55560	35		

Fig. 2. The **Results Window** showing the computed results.

The **Results Window** contains a text box which fills all its client area and a menu **Fişiere** (**File**). The text box shows all the results produced by the program; the user can scroll in both horizontal and vertical directions. The **Fişiere** menu has the following menu options:

- **Încarcă** (**Load**) – loads in the text box the content of a text file, previously saved with **Salvează**;
- **Salvează** (**Save**) – saves the content of the text box in a text file;
- **Listează** (**Print**) – print the content of the text box;
- **Închide** (**Close**) – close **Results Window** and redisplays main window.

4.2. What results are displayed

Most of the results computed by the general AV algorithm described in Section 2 are presented in a tabular form, and are displayed in the client area of the **Results Window**, shown in fig. 2:

- the general data of the problem, the factor data, and the observational matrix (optional, the check box **Datele experientei**);
- the arithmetic mean of the observed data;
- the AV table, containing columns for the source of the variation, sum of squares, degrees of freedom, mean square and F test; there are rows for main effects, and interactions of two and three factors, as well as the errors introduced by each factor;
- (optional, the check box **Diferentele limita**) a table with t values and the corresponding limit differences DL for the significance thresholds P 5%, P 1%, and P 0,1%, and all variants given in Table 4;
- (optional, the check box **Interactiuni factori**) comparison tables, one table for each variant in Table 4. There are columns for the variant identification, the averages being compared, the deviation from the witness variant (absolute value and percentual value) and the significance of the deviation;
- (optional, the check box **Testul Duncan**) Duncan test results, for each variant in Table 5. The results are included in three tables. The first table contains the differences in means; its rows and columns contain the means of variants considered, sorted in ascending order, while a cell on row i and column j ($j > i$) contains the difference between the mean of the variant i and variant j. The second table refers to the significant differences DS, with rows for the mean errors, theoretical q values, and theoretical DS values. Finally, the third table contains the final results, with rows corresponding to the compared variants and columns for variant identification, its mean, and classification. The variant classification is a single letter or a group of letters. All variants which have a common letter in the classification form a cluster in the sense that their differences in means are not statistically significant.

The frame **Parametri de afisare** (**Display parameters**), disposed in the right side of the main window, contains the already referred check boxes which control the display of the above-described tables.

4.3. The POLIFACT program

The POLIFACT program performs the AV computations for randomised complete polyfactorial designs.

The *general data* identifying the experiment are disposed in the upper part of the main window (fig. 3), in the frame **Datele problemei** (**Problem data**). They are:

- the name of the experiment (the text box labeled **Denumirea experientei**);
- the place of the experiment (the text box labeled **Locul experienței**);
- the date of the experiment (the text box labeled **Perioada experienței**);
- the author(s) of the experiment (the text box labeled **Autorul experienței**);
- the significance of observed data (the text box labeled **Indicatorul urmărit**);
- the unit of measure (the text box labeled **UM indicator (per ha)**);

- the number of factors (the text box labeled **Numărul de factori**);

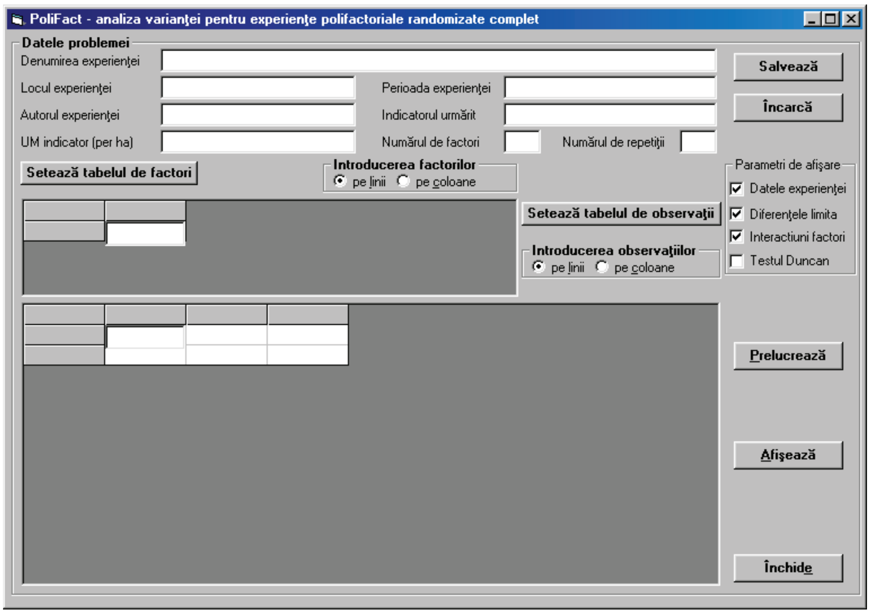

- the number of repetitions (the text box labeled **Numărul de repetitii**).

Fig. 3. The main window of the POLIFACT program – initial view.

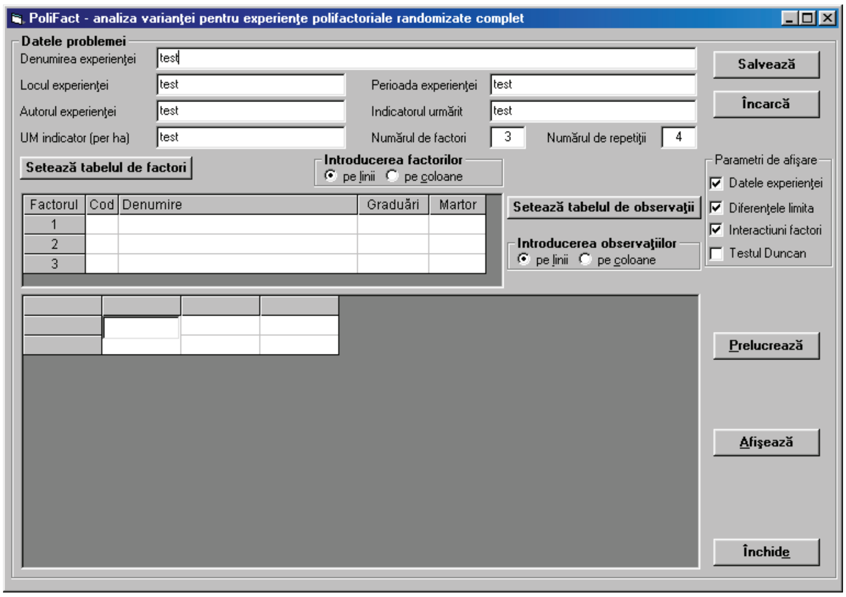

Fig. 4. The main window of the POLIFACT program after entering the general data and pressing the button **Setează tabelul de factori**

The *data describing the factors* are contained in a table disposed in the middle part of the **Datele problemei** frame. This table is configured after the general data are already set, by pressing the command button **Setează tabelul de factori** (**Set factor table**); every line of the table describes a separate factor, having the following columns (fig. 4):

- the factor identifier (code), a letter used to unique by identify the factor in the displayed results; every upper-case letter is allowed, the letter **R** identifies the repetitions;
- the factor name;
- its number of levels – at least two;
- the index of the witness level, with valid values between 0 (the mean with respect to the current factor) and the number of levels.

Factor data can be entered rowwise (**pe linii** option button, default) or columnwise (**pe coloane**), as the frame **Introducerea factorilor** (**Entering factor data**) specifies.

Observational data are contained in a separate table, in the lower part of the **Datele problemei** frame. This table is configured after the factor data are already in place, by pressing the button **Setează tabelul de observații** (**Set observation table**). Its number of rows equals the number of factor combinations, whereas the number of columns equals the number of repetitions (see Figure 5). Table header contains (from left to right) columns with factor identifiers, followed by columns for repetitions. The cells in the factor columns contain the factor levels, being automatically generated, while those in the repetition columns contain the observed data.

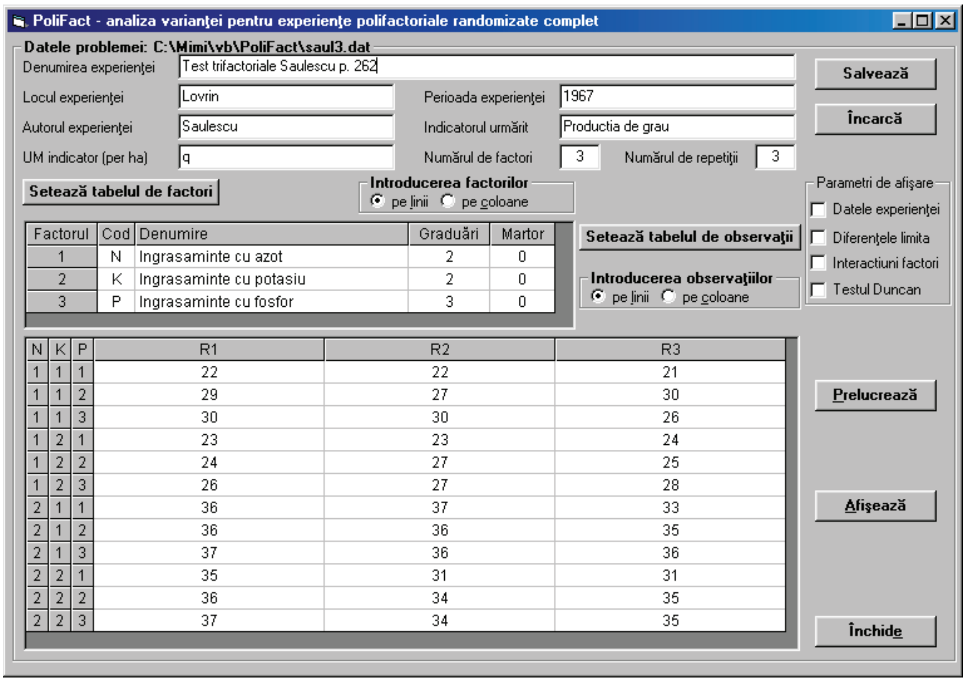

Fig. 5. The main window of the POLIFACT program after entering the factor data and pressing the button **Setează tabelul de observații.**

Observational data can be entered rowwise (**pe linii**, default) or columnwise (**pe coloane**), as the frame **Introducerea observatiilor** (**Entering observational data**) specifies. After all the data are in place, the main window looks as Figure 6 shows. The name of the current data file is shown in the caption of data area frame.

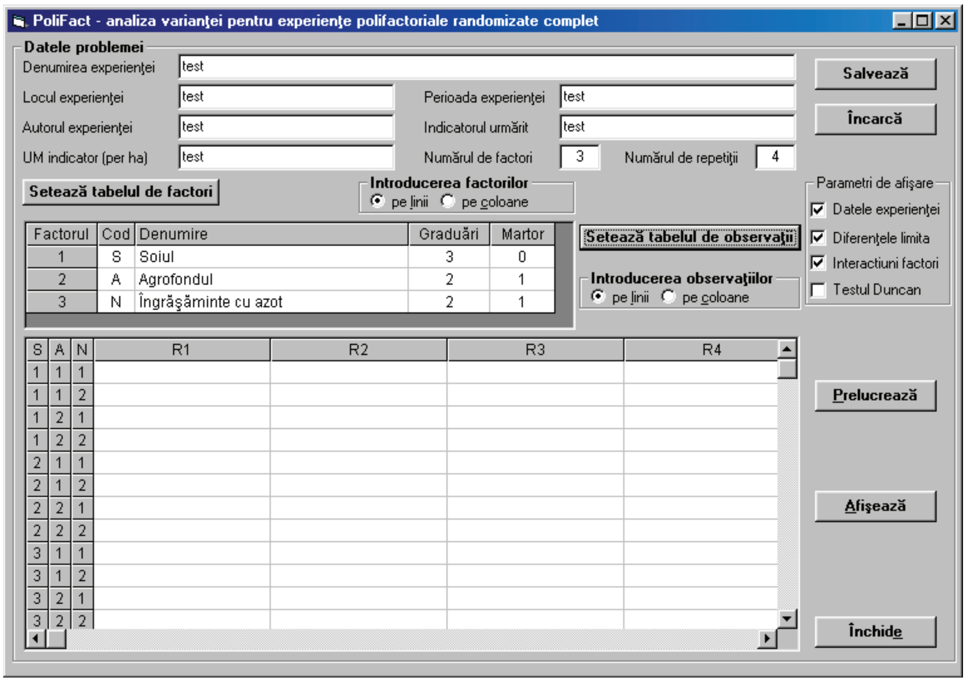

Fig. 6. The main window of the POLIFACT program – input data loaded from a file.

4.4. The PATRLAT program

The PATRLAT program performs the AV computations for latin square experimental designs. Its main window is shown in fig. 7; the command area resembles well those in POLIFACT main window, whereas the data areas are different.

The new controls contained in the *general data area* are as follows:

- the number of variants (the text box labeled **Numărul de variante**);
- the number of blocks (the text box labeled **Numărul de blocuri**);
- the significance of the variants (the text box labeled **Semnificația variantelor**);
- the index of the witness variant, with valid values between 0 (the mean with respect to the mean of the experiment) and the number of variants (the text box labeled **Varianta martor**).

As fig. 7 shows, there is no factor table, because the experiments are considered monofactorial. There are data for a sole factor - called here variant – (the significance, the number of levels, and the witness variant) included in the general data area.

Observational data are contained in a separate table, in the lower part of the **Datele problemei** frame. This table is configured after the factor data are already in place, by pressing the button **Setează tabelul de observații** (**Set observation table**). Its number of rows and columns are the same, i.e. the number of blocks, respectively columns. The first column denotes the block, while the next ones are denoting the columns of the experimental plan (Roman numerals). The cells in the columns part contain the observed data. Every cell contains two values, separated by a semicolon: the index of the variant set in the current block and column, and the observed value, as discussed in Section 3.1.

Validations include both formal (numerical values) and logical (the variant indices lying between 0 and the number of variants) tests.

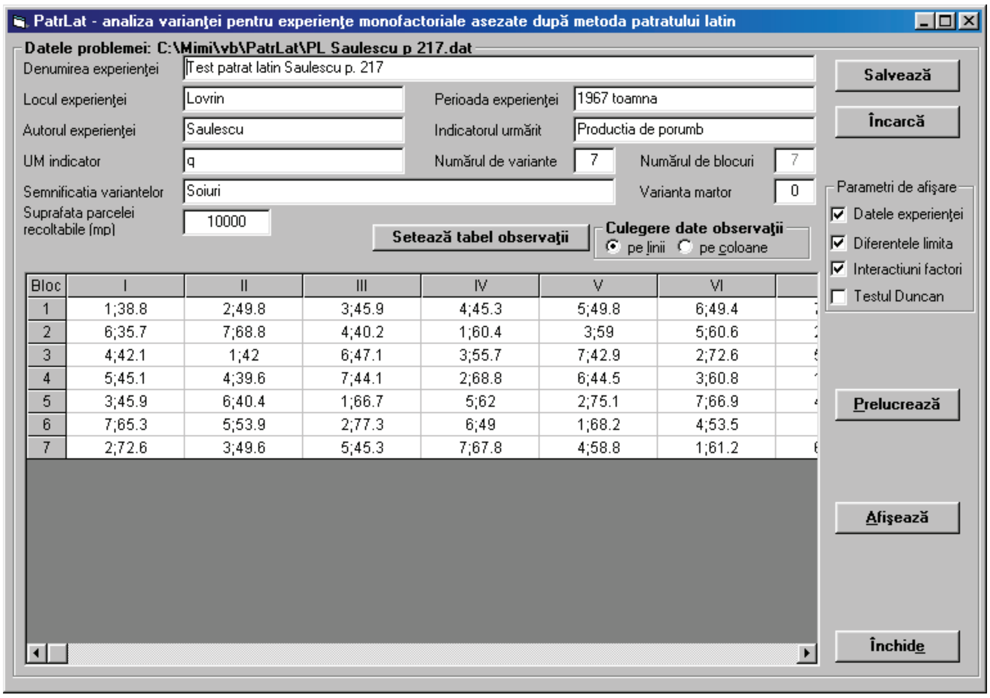

Fig. 7. The main window of the PATRLAT program.

4.5. The DREPTLAT program

The DREPTLAT program performs the AV computations for latin rectangle experimental designs. Its main window is shown in fig. 8. The only differences with respect to the PATRLAT main window are:

- an additional text box placed in the data area, which contains the number of columns (the text box labeled **Numarul de coloane**);
- the columns in the table of observed data are splitted into sub-columns. A typical sub-column header is of the form *C*-*s*, where *C* is the column index (Roman numeral), and *s* is the sub-column index (Arab numeral).

The number of columns must divide the number of variants, as discussed in 3.2. Every cell in the sub-column area contains two values, separated by a semicolon: the variant index and the observed value.

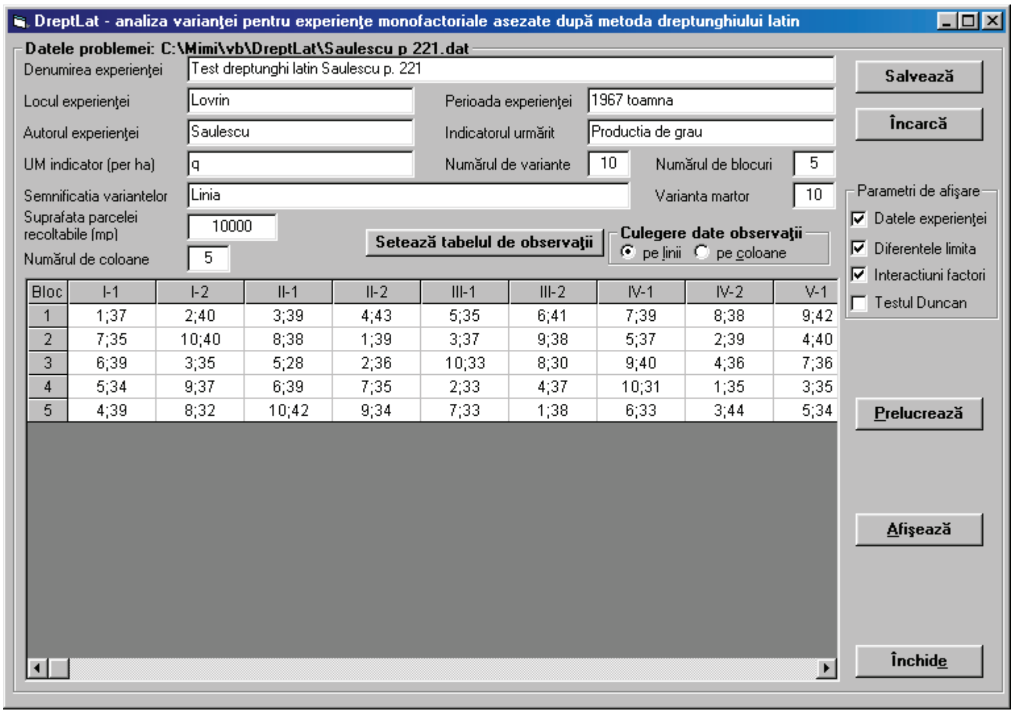

Fig. 8. The main window of the DREPTLAT program.

5. Conclusions and further work

The programs described in this paper are used currently in our University. The users of the old versions [4, 5] appreciate both the user-friendly graphical interface and their new features. Future versions of the package will include new programs dedicated to other special cases of AV.

REFERENCES

[1] Cochran, W.G, C. Cox, *Experimental designs*, 2nd ed., John Wiley and Sons, 1957.

[2] Hartley. H.C., *Varianzanalyse*, in *Mathematische Methoden für Digitalrechner* (eds. Ralston, A., Wilf, H.S.), R. Oldenbourg Verlag, München, 1972. (German)

[3] IBM Scientific Subroutine Package (SSP), IBM Corp., 1969.

[4] Pârv, B., M. Pârv, *ANVAR – A Software package for analysis ofvVariance*, in *Lucrările Conferinţei Naţionale de Matematică Aplicată şi Mecanică*, 20-23 oct. 1988, Institutul Politehnic Cluj-Napoca, vol. II, 513-522.

[5] Pârv, B., D. Stegăroiu, G. Morar, M. Pârv – *Ghid de utilizare: AVEPRC Analiza varianţei privind experienţele polifactoriale randomizate complet*, Sistem-model-calculator. Aplicaţii, Tipo Agronomia, Cluj-Napoca, 1988.

[6] Săulescu, N.A., N. N. Săulescu, *Câmpul de experienţă*, ed. a II-a, Ed. Agro-Silvică, Bucureşti, 1967.

[7] Văduva, I., *Analiza dispersională*, Ed. Tehnică, Bucureşti, 1970.

EDUCATION SECTION
(SECTIUNEA DIDACTICA)

Inegalități algebrice folosite în demonstrarea unor inegalități geometrice

Liliana Antonescu,
Şcoala "Liviu Rebreanu" Mioveni-Arges

Inegalitățile sunt importante în toate domeniile matematicii, uneori chiar mai mult decât egalitățile.

Inegalitățile geometrice sunt attractive în special, deoarece pot fi uşor înțelese şi în acelaşi timp ele reprezintă o introducere excelentă în gândirea matematică creativă şi în spiritul matematicii moderne. De multe ori inegalități geometrice sau trigonometrice se demonstrează cu ajutorul unor inegalități algebrice.

Inegalitatea mediilor ne ajută să demonstrăm multe inegalități legate de elementele unui triunghi sau ale altor figuri sau corpuri geometrice.

Teorema 1. *Dacă $x_1, x_2, \ldots, x_n$ sunt numere pozitive, atunci*

$$\min_{1\le i\le n}\{x_i\} \le m_h \le m_g \le m_a \le m_p \le \max_{1\le i\le n}\{x_i\} \qquad (1)$$

unde $m_h = \dfrac{n}{\dfrac{1}{x_1}+\dfrac{1}{x_2}+\ldots+\dfrac{1}{x_n}}$ *este media lor armonică,* $m_g = \sqrt[n]{x_1 \cdot x_2 \cdot \ldots \cdot x_n}$ *este media lor geometrică,* $m_a = \dfrac{x_1+x_2+\ldots+x_n}{n}$ *este media lor aritmetică şi* $m_p = \sqrt{\dfrac{x_1^2+x_2^2+\ldots+x_n^2}{n}}$ *este media lor pătratică.*

Să dăm câteva aplicații ale inegalității (1) .

Problema 1. *Dintre toate paralelipipedele dreptunghice cu arie totală dată, cubul are volumul cel mai mare.*

<u>*Demonstrație*</u>. Să notăm cu a, b şi c lungimea, lățimea şi înălțimea unui paralelipiped dreptunghic cu aria totală S şi volumul V. Evident, V=abc and S=2(ab+bc +ca). Din ipoteza că S este constantă rezultă că suma celor trei numere ab, bc şi ac este constantă. Putem aplica Teorema 1 pentru aceste numere şi avem că $(ab\cdot bc\cdot ca)^{1/3} \le \dfrac{ab+bc+ca}{3}$ sau $(V^2)^{1/3} \le S/6$. Astfel, $V \le (S/6)^{3/2}$. Egalitatea are loc dacă şi numai dacă ab=bc=ac. De aici rezultă că volumul este maxim dacă a=b=c, i.e. atunci când paralelipipedul dreptunghic este cub.

Problema 2. *Un cilindru circular drept cu volumul V are arie minimă dacă diametrul său este egal cu înălțimea.*

<u>*Demonstrație*</u>. Notând cu S, r şi h, respectiv aria, raza şi înălțimea unui cilindru circular drept cu volumul V, avem că $S=2\pi(r^2 + rh)$ şi $V = \pi r^2 h$. Deci, $S = 2\pi\left(r^2 + \dfrac{V}{\pi r}\right) = 2\pi\left(r^2 + \dfrac{V}{2\pi r}+\dfrac{V}{2\pi r}\right)$. Putem considera, astfel, că $S/(6\pi)$ este media aritmetică a numerelor r^2, $V/(2\pi r)$ şi $V/(2\pi r)$, deci cu Teorema 1, obținem $\dfrac{S}{6\pi} \ge \left(\dfrac{V^2}{4\pi^2}\right)^{1/3}$. Membrul drept al inegalității este constant. Deci S este minimă când are loc egalitate, şi anume $r^2 = V/(2\pi r)$ sau $V = 2\pi r^3$. Astfel, S este minimă când 2r = h.

Să ne întoarcem acum la figurile geometrice.

Problema 3. *Să se demonstreze că în orice triunghi ABC avem* $6Rr \le \sqrt[3]{a^2b^2c^2}$ *, unde notațiile sunt cele obişnuite*.

<u>*Demonstrație*</u>. Să observăm că putem scrie abc=4RS=4Rpr=2Rr(a+b+c). Deci [Rr(a+b+c)]/(abc)=1/2 sau (Rr)/(bc)+(Rr)/(ca)+(Rr)/(ab)=1/2. Inegalitatea dintre media geometrică şi media aritmetică a numerelor (Rr)/(bc), (Rr)/(ca), (Rr)/(ab) şi egalitatea precedentă conduc la $(R^3r^3)/(a^2b^2c^2) \le 1/6^3$, de unde $6Rr \le \sqrt[3]{a^2b^2c^2}$.

Problema 4. *Să se arate că într-un triunghi oarecare ABC are loc inegalitatea $\sin A+\sin B+\sin C\geq 3[S/(2R^2)]^{1/3}$, unde notațiile sunt cele obişnuite.*

<u>Demonstrație</u>. Să folosim inegalitatea $m_g \leq m_a$, pentru n=3, i.e. $\sqrt[3]{x_1x_2x_3} \leq \frac{x_1+x_2+x_3}{3}$. Să alegem $x_1=\sin A$, $x_2=\sin B$, $x_3=\sin C$ şi să înlocuim $\sin A + \sin B + \sin C \geq 3\sqrt[3]{\sin A\sin B\sin C}$, dar (folosind Teorema sinusurilor) $\sin A\sin B\sin C=S/(2R^2)$, de unde rezultă inegalitatea cerută.

Problema 5. *Se dă rombul ABCD. Sa se demonstreze că $2\sqrt{2}\,AB \geq AC + BD$.*

<u>Demonstrație</u>. Fie $AC \cap BD = \{O\}$. $AO = AC/2$, $BO = BD/2$. În triunghiul AOB avem $AB^2=AO^2+BO^2$, deci $AB = \sqrt{\frac{AC^2+BD^2}{4}}$, $AB = \frac{1}{\sqrt{2}}\sqrt{\frac{AC^2+BD^2}{2}}$.Aplicând Teorema 1 avem AB = $\frac{1}{\sqrt{2}}\sqrt{\frac{AC^2+BD^2}{2}} \geq \frac{1}{\sqrt{2}}\cdot\frac{AC+BD}{2}$. Deci $2\sqrt{2}\,AB \geq AC + BD$.

Problema 6. *Să se demonstreze că în orice triunghi ABC este satisfăcută inegalitatea $a\cdot tg(A/2) + b\cdot tg(B/2)+c\cdot tg(C/2) \geq 6p\, tg(A/2)tg(B/2)tg(C/2)$.*

<u>Demonstrație</u>. Numerele $a\cdot tg(A/2)$, $b\cdot tg(B/2)$, $c\cdot tg(C/2)$ sunt pozitive. De aceea inegalitatea mediilor ne permite să scriem $a\cdot tg\frac{A}{2}+b\cdot tg\frac{B}{2}+c\cdot tg\frac{C}{2}\geq 3\sqrt{abc\cdot tg\frac{A}{2}tg\frac{B}{2}tg\frac{C}{2}}$. Calculând produsul P al tangentelor jumătăților de unghiuri, găsim $P = tg(A/2)tg(B/2)tg(C/2) = S/(p^2) = r/p$. Cantitatea de sub radical (cu $abc = 4RS$, $S = p^2P$, $1/p = P/r$) se scrie
$4RSP = 4R\cdot p^2P\cdot P = 4Rp^3\cdot(1/p)\cdot P^2 = =p^3\cdot 4R\cdot(P/r)\cdot P^2 = p^3\cdot P^3\cdot 4(R/r)$. Relația lui Euler, care dă distanța d dintre centrele cercurilor circumscris şi înscris într-un triunghi şi anume $d^2 = R^2 - 2Rr$ (≥ 0), ne arată că $(R/r) \geq 2$.

Teorema 2. *Dacă $x_1, x_2,\ldots,x_n$ sunt numere pozitive, atunci $(x_1+x_2+\ldots+x_n)[(1/x_1)+(1/x_2)+\ldots+(1/x_n)]\geq n^2$.* Această inegalitate este de fapt $m_h \leq m_a$, scrisă puțin altfel. Scriind această inagalitate pentru n = 3, avem $(x_1+x_2+x_3)[(1/x_1)+(1/x_2)+(1/x_3)] \geq 9$.

Această ultimă inegalitate are foarte multe aplicații, cu ajutorul ei putându-se demonstra multe inegalități relative la elementele unui triunghi.

Problema 7. Sa se a*rate că într-un triunghi ABC există relația $h_a+h_b+h_c\geq 9r$, notațiile fiind cele obişnuite.*

<u>Demonstrație</u>. Să alegem $x_1 = h_a$, $x_2 = h_b$, $x_3 = h_c$ şi să ținem cont că aria unui triunghi poate fi scrisă $S= (1/2)ah_a=(1/2)bh_b=(1/2)ch_c =pr$, şi deci $1/h_a=a/(2S)$, $1/h_b=b/(2S)$, $1/h_c=c/(2S)$, $1/r=(2p)/(2S)$. Obținem că $(1/h_a)+(1/h_b)+(1/h_c)=1/r$. Folosind inegalitatea din Teorema 2 avem $(h_a+h_b+h_c)[(1/h_a)+(1/h_b)+(1/h_c)] \geq 9$, deci $(h_a+h_b+h_c)/r \geq 9$.

Problema 8. *Să se arate că într-un triunghi are loc inegalitatea $r_a+r_b+r_c \geq 9r$, unde r_a, r_b, r_c sunt razele cercurilor exânscrise triunghiului.*

<u>Demonstrație</u>. Este uşor de demonstrat că aria triunghiului, S, se mai poate scrie şi astfel
$S = r_a(p-a) = r_b(p-b) = r_c(p-c) = pr$ şi, deci, $(1/r_a)+(1/r_b)+(1/r_c) = [(p-a)/S]+[(p-b)/S]+[(p-c)/S] = =(3p-2p)/S = 1/r$. Inegalitatea cerută este acum evidentă.

Să demonstrăm acum, cu ajutorul inegalităților algebrice o inegalitate cunoscută ca inegalitatea lui Euler $R\geq 2r$. Folosim tot Teorema 2, unde drept x_1, x_2, x_3 luăm tot razele cercurilor exînscrise triunghiului. Atunci $(r_a+r_b+r_c)(r_ar_b+r_br_c+r_cr_a) \geq 9r_ar_br_c$. Pe de altă parte, $r_a+r_b+r_c = 4R + r$, $r_ar_b+r_br_c+r_cr_a = p^2$, $r_ar_br_c = p^2r$. Deci $(4R + r)p^2 \geq 9p^2r$, de unde rezultă imediat ca $R \geq 2r$.

O altă inegalitate algebrică, folositoare în multe situații este:

Inegalitatea lui Jensen. *Fie E un interval $f:E\rightarrow$**R**. Dacă f este convexă pe E, atunci oricare ar fi $x_1, x_2, \ldots,x_n \in E$ şi oricare ar fi numerele pozitive $p_1, p_2,\ldots,p_n$, are loc inegalitatea*

$$f\left(\frac{p_1x_1+p_2x_2+\ldots+p_nx_n}{p_1+p_2+\ldots+p_n}\right)\leq\frac{p_1f(x_1)+p_2f(x_2)+\ldots+p_nf(x_n)}{p_1+p_2+\ldots+p_n}.$$

Să aplicăm inegalitatea lui Jensen în:

Problema 9. *Să se arate că într-un triunghi oarecare are loc inegalitatea sinA + sinB + sinC* $\leq \dfrac{3\sqrt{3}}{2}$, *egalitatea având loc când triunghiul este echilateral.*

<u>Demonstrație</u>. Se ia funcția f(x) = sin x pe intervalul [0 , π]. Funcția este concavă pe acest segment. Atunci, luând două puncte x_1, x_2 $\in [0,\pi]$, relația $[f(x_1)+f(x_2)]/2 = (\sin x_1 + \sin x_2)/2$, devine $[f(x_1)+f(x_2)]/2 = \sin[(x_1+x_2)/2]\cos[(x_1-x_2)/2] \leq \sin[(x_1+x_2)/2]$, deoarece $0 \leq \cos[(x_1-x_2)/2] \leq 1$, pentru orice $(x_1-x_2)/2$. Deci $(\sin x_1+\sin x_2)/2 \leq \sin[(x_1+x_2)/2]$. Inegalitatea lui Jensen, aplicată pentru sin x ,x $\in [0, \pi]$ si $x_i \in [0, \pi]$, i =1,2,…,n, ne dă $\dfrac{1}{n}\sum_{i=1}^{n} \sin x_i \leq \sin\left(\dfrac{1}{n}\sum_{i=1}^{n} x_i\right)$. Atunci, luând x_1= A, x_2 = B, x_3 = C cu A + B + C = π, A, B, C >0, avem imediat (sinA + sinB + sinC)/3 ≤ sin(π/3) = $\dfrac{\sqrt{3}}{2}$ şi deci inegalitatea cerută a rezultat imediat.

Acest rezultat se poate aplica imediat şi în:

Problema 10. *În orice triunghi se verifică inegalitatea* $(r_a/a)(r_b/b)(r_c/c) \leq \left(\dfrac{\sqrt{3}}{2}\right)^3$.

<u>Demonstrație</u>. Inegalitatea din enunț se transformă succesiv $(pS^2)/S^3 \leq \dfrac{3\sqrt{3}}{8}abc \Leftrightarrow \dfrac{p}{R} \leq \dfrac{3\sqrt{3}}{2} \Leftrightarrow \sin A + \sin B + \sin C \leq \dfrac{3\sqrt{3}}{2}$. Ultima inegalitate este cea demonstrată anterior cu ajutorul inegalității lui Jensen.

O altă inegalitate algebrică, inegalitatea *Cauchy-Buniakovski-Schwartz*, poate fi de asemenea folosită în demonstrarea unor inegalități geometrice. Folosind această inegalitate obținem

$$\sin\alpha\cos\beta + \sin^2\beta \leq \sqrt{\sin^2\alpha + \sin^2\beta}\cdot\sqrt{\cos^2\beta + \sin^2\beta}, \forall\alpha,\beta \in R$$

$$\sin\beta\cos\alpha + \sin^2\alpha \leq \sqrt{\sin^2\alpha + \sin^2\beta}\cdot\sqrt{\cos^2\alpha + \sin^2\alpha}, \forall\alpha,\beta \in R$$

Adunând cele două inegalități membru cu membru obținem inegalitatea

$$\forall\alpha,\beta \in R, \sin^2\alpha + \sin^2\beta + \sin(\alpha+\beta) \leq 2\sqrt{\sin^2\alpha + \sin^2\beta}, \qquad (2)$$

egalitatea având loc dacă $\alpha = k_1\pi$, $\beta = k_2\pi$, $k_1, k_2 \in Z$ sau $\alpha + \beta = 2k\pi + (\pi/2)$, $k \in Z$.

Să indicăm acum două aplicații ale acestei inegalități şi anume:

Problema 11. *În orice triunghi ABC are loc inegalitatea*

$$\sin^2 A + \sin^2 B + \sin C \leq 2\sqrt{\sin^2 A + \sin^2 B}, \qquad (3)$$

egalitatea având loc dacă $m(C) = 90^0$.

<u>Demonstrație</u>. Se alege α = A, β = B şi se aplică inegalitatea (2) ținând cont că sin(A+B)=sinC.

Problema 12. *Să se arate că în orice triunghi ABC avem* $a^2 + b^2 + 2Rc \leq 4R\sqrt{a^2+b^2}$.

<u>Demonstrație</u>. Această inegalitate se obține uşor folosind (3) şi Teorema sinusurilor.

Inegalitățile algebrice sunt o sursă importantă de rezultate în domeniul geometriei şi în special în cel al geometriei triunghiului.

BIBLIOGRAFIE

[1] Georgescu-Buzău, E., Onofraş, E., Metode de rezolvare a problemelor de matematică in liceu, Editura Didactică şi Pedagogică, Bucuresti, 1983.
[2] Kazarinoff, N., Geometric inequalities, New Mathematical Library,1961.
[3] Voda, V., Triunghiul – ringul cu trei colțuri, Editura Albatros, Bucuresti, 1979.
[4] Tudor, I., Probleme de geometrie pentru gimnaziu, Editura Paco, 1992.
[5] Gazeta Matematica, Nr.7-8/1993, Societatea de Ştiinte Matematice din Romania.
[6] Gazeta Matematica, Nr.4/1981, Societatea de Ştiinte Matematice din R.S.R.

Mulțimea lui Mandelbrot

Ștefăniță Hăbuc
Școala „Liviu Rebreanu” Mioveni-Argeș

Studiul sistemelor dinamice în planul complex a luat amploare odată cu apariția calculatorului și reprezentări grafice. Surprinzătoarele imagini obținute au incitat și mai mult studiul atât din punct de vedere matematic, cât și din cel informatic furnizând o teorie în acest sens. Bazele matematice au fost pornite încă de la începutul secolului XX de către matematicianul francez Gaston Julia, dezvoltată mai apoi de Benoit Mandelbrot al cărui nume îl poartă mulțimea la care vom face referire.

Plecând de la spațiul complex C organizat ca un spațiul topologic și alegând o funcție polinomială $f: C \to C$, $f(z) = a_0 + a_1 z + a_2 z^2 + ... + a_n z^n$, cu $n \geq 2$ și $a_k \in C$ pentru $k = \overline{0,n}$, în spațiul fazelor *C* funcția *f* genereaza un sistem dinamic sau semidinamic discret.

Fie *w* un punct periodic de perioadă *p*, cu $(f^p)'(w) = \lambda$. Punctul *w* este numit: *superatractiv* dacă $\lambda = 0$, *atractiv* dacă $0 \leq |\lambda| < 1$, *indiferent* dacă $|\lambda| = 1$ si *repulsiv* dacă $|\lambda| > 1$. Închiderea mulțimii punctelor repulsive a sistemului discret si deci a funcției *f* se numește *mulțime Julia* și va fi notată cu *J(f)*.

Vom considera cazul când funcția f este $f(z) = z^2 + c = f_c(z)$. Numim **mulțime Mandelbrot** (notată cu **M**), mulțimea parametrilor *c* pentru care mulțimea Julia a lui f_c este conexă. Adică avem **M** = $\{c \in C \mid J(f_c)$ este conexă$\}$. La prima vedere **M** apare ca o mulțime rezultată dintr-o restricție impusă mulțimii *J(f)*, de fapt, după cum vom vedea, **M** conține o mulțime de informații referitoare la structura mulțimilor Julia.

Definiția dată este destul de incomodă pentru scopurile noastre de a face reprezentarea pe calculator. De aceea vom da o definiție echivalentă cu aceasta, care este mult mai comoda pentru a investiga forma cu totul excepțională a mulțimii Mandelbrot și de a determina efectele reprezentării acesteia în planul complex al parametrului *c*.

Se poate demonstra că mulțimea Mandelbrot poate fi caracterizată în funcție de șirul de iterate al funcției f_c în punctul zero. Astfel **M** = $\{c \in C \mid \{f_c^k(0)\}_{k \geq 1}$ este mărginit$\}$ sau **M** = $\{c \in C \mid f_c^k(0) \to \infty$ când $k \to \infty\}$.

Dinamica punctelor este studiată cu ajutorul mulțimilor de nivel. Alegem o rețea de puncte $c \in C$ și testăm pentru fiecare punct dacă după N iterații termenul corespunzător șirului $0 \to c \to c^2 + c \to \ldots$, depășește sau nu un disc centrat în origine de rază suficient de mare. Această rețea se va găsi în interiorul unui dreptunghi ale cărui dimensiuni $x_{\min}, y_{\min}, x_{\max}, y_{\max}$ vor fi citite inițial de la terminal. Așadar, pentru un punct *(x,y)* din rețea se va parcurge următoarea procedură:

```
Procedura Mandelbrot
  k ← 0
  xn ← x
  yn ← y
  cat timp (xn*xn+yn*yn<M) si (k<N) repetă
        k ← k+1
        aux ← xn*xn - yn*yn + x
        yn ← 2*xn*yn + y
        xn ← aux
stop procedura
```

Parametrii M și N vor fi aleși astfel încât convergența să fie destul de rapidă dar să se obțină și o imagine cât mai bună. De exemplu în experiențele noastre (realizate în limbajele Pascal și C) am folosit M=100 și N=64. Vom observa că dacă mărim pe N imaginea devine din ce în ce mai bună, iar convergența nu este mai rapidă și, în consecință, timpul de redare al imaginii este mai mare.

În funcție de valoarea lui *k* se va face şi colorarea punctului din interiorul porțiunii dreptunghice aleasa pentru reprezentare. Este indicat să alegem o schemă de culori astfel încât pentru valori foarte mari ale lui *k* se va calcula *k* mod *nrcul*, unde *nrcul* reprezintă numărul maxim de culori alese.

Analizând reprezentarea din fig. 1 a mulțimii Mandelbrot observăm mai întâi o regiune delimitată prin o cardioidă, simetrică față de o axă centrală cu adâncitura de +0.25 şi cuprinsă la stânga până la -0.75. Urmează apoi un disc cu centrul în -1 şi raza 0.25, tangent la cardioidă. Mai observăm o mulțime infinită de discuri tangente la **M**, iar pentru ele există de asemenea o infinitate de discuri tangente.

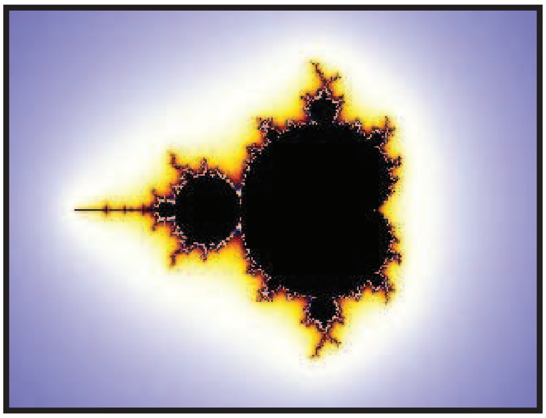

Fig. 1. Mulțimea Mandelbrot

Mergând mereu în stânga, pornind din cardioidă, se ajunge la punctul numit Myrbert-Feigenbaum, situat la – 1.401. În acest punct se poate observa apariția primei noi cardioide. Segmentul conținut între acest punct şi -2 este conținut în mulțimea lui Mandelbrot. Pe acest segment se găsesc o infinitate de componente cardioide, foarte mici.

Ceea ce este interesant, este apariția mulțimilor Julia în structura mulțimii Maldelbrot. Folosind poziționarea parametrului *c* se pot observa următoarele cazuri:

- dacă *c* este în interiorul corpului principal al lui M, care are forma unei cardioide, mulțimea Julia se prezintă ca un cerc deformat fractal în jurul unui punct fix atractiv;
- dacă *c* este în interiorul unui „mugure”, mulțimea Julia constă dintr-o mulțime infinită de cercuri deformate fractal în jurul unui atractor periodic şi a preimaginilor sale;
- dacă *c* este în punctul de germinație al unui „mugure”, avem aşa numitul caz parabolic: frontiera se prezintă asemenea unor „cârcei” care se îmbogățesc spre margine în raport cu un atractor stabil;
- dacă *c* este pe frontiera cardioidei sau a unui mugur, avem cazul numit *discurile lui Siegel*, în interiorul regiunii limitate de mulțimea Julia găsim cercuri în jurul unor puncte fixe.

Descompunerea binară

O reprezentare interesantă a mulțimii lui Mandelbrot se poate obține folosind o tehnică denumită **descompunerea binară**. În acest caz colorarea nu se va mai face în funcție de parametru k, această tehnică constând în colorarea anumitor zone în negru şi a altora în alb în funcție de condiția $y \leq 0$ ce va pusă la ieşirea din ciclu. Astfel se realizează împărțirea fiecărui nivel de atracție în benzi, ce vor creste de la nivelul exterior către cel interior. Fiecare nivel va prezenta 2^{k} benzi, unde k reprezintă numărul nivelului de atracție calculat de la exterior către interior, de fapt numărul de iterate ce va calculat prin procedura Mandelbrot.

Aceasta tehnică va fi realizată folosind următoarea procedură de calcul:

```
Procedura Mandelbrot
  k ← 0
  xn ← x
  yn ← y
  cat timp (xn*xn+yn*yn<M) si (k<N) repetă
        k ← k+1
        aux ← xn*xn - yn*yn + x
        yn ← 2*xn*yn + y
        xn ← aux
 daca yn>= 0 atunci culoare ← alb
             altfel culoare ← negru
stop procedura
```

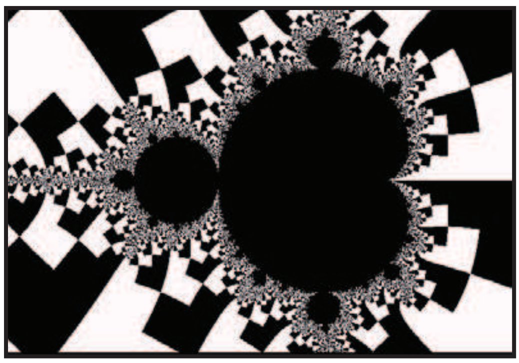

Fig. 2. Mulțimea lui Mandelbrot – descompunere binară.

Colorarea se face numai pentru punctele din exteriorul mulțimii, nu şi pentru cele din interior.

În ceea ce privește limbajul de programare, este mai indicat să folosim C-ul deoarece acesta are inclusă o bibliotecă de funcții pentru numere complexe, față de limbajul Pascal ce nu prezintă acest lucru. Programul pentru realizarea unei imagini pentru mulțimea Mandelbrot în descompunere binară este următorul:

```
#include<iostream.h>
#include<conio.h>
#include<graphics.h>
#include<math.h>
#include<complex.h>

const M=100;
const N=64;
const xmin=-2.5;
const xmax=1.5;
const ymin=-1.5;
const ymax=1.5;

complex f(complex z)
 {
  return z*z;
 }

int mandelbrot(complex z)
 {
  int k=0;
  complex zn=z;
  while ((norm(zn)<M)&&(k<N))
  {
   k=k+1;
   zn=f(zn)+z;
   }
  if (norm(zn)>=M)
    if (imag(zn)<=0)  k=0;
            else k=15;
  return k;
 }

void main()
 {
  clrscr();
  int gm;
  int gd=DETECT;
  initgraph(&gd,&gm,"C:\BORLANDC\BGI");
  int w=640; double sx=(xmax-xmin)/double(w);
  int h=480; double sy=(ymax-ymin)/double(h);
  double s=sx; if (sy>s) s=sy;
  h=int((ymax-ymin)/s);
  w=int((xmax-xmin)/s);
  double x=xmin,y;
  int i,j;
  complex z;
  for(i=0;i<=w;i++)
  {
   y=ymin;
   for(j=0;j<=h;j++)
```

```
    {
     z=complex(x,y);
     putpixel(i,h-j,mandelbrot(z));
     y=y+s;
    }
  x=x+s;
  }
  getch();
}
```

BIBLIOGRAFIE

[1] Holmgen, R. A., A First course in discrete dynamical systems, Springer, New York, 1994.

[2] Peitgen, H.O., Richter, P.H., The beauty of fractals. Images of complex dynamical systems, Springer, New York, 1996.

[3] Niculescu, C. P., Sisteme dinamice haotice, Univ. Craiova, 1995.

[4] Vlada, M., Nistor, I., Postea, A., Constantinescu, C. Grafică pe calculator în limbajele Pascal şi C, Ed. Tehnică, Bucureşti, 1992.

[5] Retrisor, E., Sisteme dinamice haotice, Editura Universitatii din Timisoara, 1992.

[6] Constantinescu, C.-P., Haos, fractali si aplicatii, Ed. The Flower Power, Pitesti, 2003

Probleme distractive de matematică

Gruia Monica
Sc. „ L. Rebreanu”, Mioveni, Arges

Problemele rezolvate cu ajutorul matematicii sunt foarte variate şi, pe lângă probleme tradiţionale de algebră sau geometrie, apar probleme cu tablouri cu numere sau culori aranjate în diferite feluri, cu lăcuste sau purici care sar dintr-un loc în altul, cu piese de şah şi deplasări de obiecte. În spatele acestei matematici făcute cu zâmbetul pe buze găsim autori celebri şi teoreme „serioase”.

În această lucrare propunem câteva probleme de determinare a numărului de metode pentru atingerea unui scop.

Probleme cu sărituri

I) În câte moduri un săritor, care stă în faţa unor celule desenate pe pământ, poate să ajungă la celula n, dacă el sare de la celula 1 la celula n, atingând pământul numai în interiorul celulelor, iar lungimea salturilor este arbitrară?

Fie u_s numărul de moduri prin care se poate ajunge în celula s. Pentru rezolvarea problemei trebuie să ţinem seama că săritorul are posibilitatea (una singură) de a sări în celula a n-a, fără să atingă pământul în vreo celulă intermediară. Dacă el sare întâi prin k celule intermediare, el o poate face în C^k_{n-1} moduri. Prin urmare, avem

$$u_n = 1 + C^1_{n-1} + C^2_{n-1} + \dots + C^{n-1}_{n-1} = 2^{n-1}. \qquad (1)$$

Observaţia 1. Evident, cu acest prilej am găsit numărul diverselor reprezentări ale numărului n sub forma unei sume de termeni pozitivi întregi (inclusiv cazul „ sumei” formate dintr-un singur termen), două reprezentări fiind considerate distincte dacă diferă fie prin natura termenilor, fie prin ordinea lor.

Observaţia 2. Dacă săritorul are voie să atingă pământul numai de un număr par de ori, atunci el va dispune de $1 + C^2_{n-1} + C^4_{n-1} + \dots$ adică de 2^{n-2} moduri.

II) În câte moduri un săritor poate să ajungă în celula a n-a dacă el are voie să efectueze numai salturi simple (până în celula vecină) şi duble (sărind din două în două) ?

Să notăm cu v_s numărul de moduri prin care se poate ajunge în celula cu nr. s. Deoarece săritorul poate ajunge în celula s numai din celulele cu numerele $s-1$ şi $s-2$, iar pentru a ajunge aici el dispune respectiv de v_{s-1} şi de v_{s-2} moduri, rezultă că, pentru $s>2$, are loc egalitatea

$$v_s = v_{s-1} + v_{s-2}. \qquad (2)$$

Ne convingem uşor că

$$v_1 = 1 \text{ şi } v_2 = 2. \qquad (3)$$

Plecând de la (3), cu ajutorul relaţiei (2), putem determina consecutiv valorile lui $v_3, v_4, v_5, \dots$, adică să scriem soluţia problemei sub forma tabelului

s	1	2	3	4	5	6	7	8	9	10	11	12	13	14
v_s	1	2	3	5	8	13	21	34	55	89	144	233	377	610

(4)

Ecuaţia (2) este un caz particular al ecuaţiilor denumite *cu diferenţe finite*

$$v_{x+m} = F(v_x, v_{x+1}, \dots, v_{x+m-1}), \qquad (5)$$

care formează obiectul de studiu al calculului cu diferenţe finite.

Fiind cunoscute valorile lui $v_0, v_1, v_2, \dots, v_{x+m-1}$, este uşor să găsim consecutiv, cu ajutorul egalităţii (5), care este şi ea o relaţie de recurenţă pentru funcţia v_x, valorile lui v_m, v_{m+1}, v_{m+2}, …, adică să obţinem soluţia ecuaţiei (5) cu ajutorul unui tabel. Ar fi, însă, incomod să căutăm pe această cale, de exemplu, pe v_{1000}, astfel că, de obicei, căutăm să reprezentăm soluţia sub forma $v_x = f(x)$.

Ne convingem uşor că ecuaţiile (2) şi (3) sunt satisfăcute de funcţia

$$v_n = (1/5^{1/2})\{ [(1 + 5^{1/2})/2]^{n+1} - [(1 - 5^{1/2})/2]^{n+1} \} \qquad (6)$$

Calculând cu ajutorul ei valorile lui $v_3, v_4, v_5, \ldots$, vom obţine aceleaşi numere ca în tabelul (4).
Observaţia 3. În prima problemă cu săritorul am fi putut stabili relaţia

$$u_s = 1 + u_1 + u_2 + \ldots + u_{s-1}\ , \qquad (7)$$

de unde rezultă uşor (pentru $u_1 = 1$) egalitatea $u_n = 2^{n-1}$.
Observaţia 4. În problema cu săritorul putem varia condiţiile după cum vrem: de exemplu, putem să admitem în general salturile simple, duble şi triple, făcând însă restricţia că din celulele ale căror numere de ordine sunt multipli de cinci (inclusiv din poziţia iniţială) se pot face numai salturi simple.

În aceste condiţii, să notăm cu w_s numărul de moduri în care se poate ajunge la celula nr. s; atunci, în locul unei singure ecuaţii, vom avea sistemul

$w_s = w_{s-1} + w_{s-2} + w_{s-3}$ pentru $s = 5k$ şi pentru $s = 5k + 1$ (sau $s = 5k - 1$),
$w_s = w_{s-1} + w_{s-3}$ pentru $s = 5k + 2$,
$w_s = w_{s-1} + w_{s-2}$ pentru $s = 5k + 3$; unde $w_1 = 1,\ w_2 = 1,\ w_3 = 2$.

Să trecem acum la probleme în care funcţia căutată depinde de două sau mai multe argumente care sunt numere întregi.

Problema turnului

În câte moduri (cu cel mai mic număr de mutări) putem trece un turn de pe câmpul (0, 0) în câmpul (m, n) dacă îl deplasăm prin mutări simple, adică mutări în care turnul trece în câmpul vecin pe orizontală sau pe verticală ?

Numerele dintre paranteze marchează respectiv numărul coloanei şi numărul liniei la intersecţia cărora se află câmpul; coloanei din stânga şi liniei de jos li se atribuie numărul 0 (m şi n sunt întregi pozitivi).

Să notăm cu $u_{x,y}$ numărul de moduri prin care se poate trece din câmpul (0, 0) în câmpul (x, y). Evident, oricare ar fi numerele pozitive x şi y, avem

$$u_{x,\,0} = 1 \text{ şi } u_{0,\,y} = 1. \qquad (8)$$

Deoarece, pentru $x > 0$ şi $y > 0$, turnul poate ajunge în câmpul (x, y), fie din câmpul $(x\text{-}1, y)$, fie din câmpul $(x, y\text{-}1)$, în care el poate ajunge, respectiv, în $u_{x-1,\,y}$ şi $u_{x,\,y-1}$ moduri, rezultă că

$$u_{x,\,y} = u_{x-1,y} + u_{x,\,y-1}. \qquad (9)$$

Am obţinut o relaţie de recurenţă pentru funcţia $u_{x,\,y}$, care depinde de două argumente întregi. Scriind în fiecare câmp (x ,y) al tablei de şah valoarea lui $u_{x,\,y}$ corespunzătoare, atunci, în virtutea relaţiilor (8) şi (9), toate câmpurile din coloana din stânga şi din linia de jos vor putea fi completate imediat cu cifra 1. Apoi vom putea completa treptat celelalte câmpuri, scriind în ele numere egale cu suma a două numere vecine (de jos şi din stânga).Tabelul reprezintă soluţia ecuaţiei (9) în condiţiile (8).

1						
1	5					
1	4	10				
1	3	6	10			
1	2	3	4	5		
	1	1	1	1	1	1

Problema turnului poate fi rezolvată mai simplu, rezolvare care, totodată, va reprezenta soluţia ecuaţiei (9) printr-o formulă comodă.

Să remarcăm că pentru a trece turnul din câmpul (0, 0) în câmpul (m, n) sunt necesare în total $m + n$ mutări; m pe orizontală şi n pe verticală. Fiecare mod de a deplasa turnul poate fi caracterizat printr-o schemă formată din literele o şi v, care ne arată în ce ordine trebuie să efectuăm mutările orizontale şi pe cele verticale. Pentru a alege cele m locuri·ocupate de litera *o* (dintre cele $m + n$ locuri existente în schemă), avem în total $C^{m}_{m+n}=\dfrac{(m+n)!}{m!n!}$ posibilități distincte, ceea ce ne dă soluția problemei turnului de şah.

Soluția ecuației (9) în condițiile (8) este funcția

$$u_{x,y} = \frac{(x+y)!}{x!y!} \tag{10}$$

Problema păianjenului

În câte moduri un păianjen aflat în originea coordonatelor poate să treacă (pe drumul cel mai scurt!) în nodul k, l, m al unei rețele spațiale ? (Într-o rețea spațială orice nod, adică orice punct cu coordonate întregi, este legat cu mici bare paralele cu axele de coordonate de cele şase noduri vecine). Această problemă este o generalizare naturală a problemei turnului.

Notând *cu* $u_{x, y, z}$ numărul de moduri prin care se poate ajunge în nodul *(x, y, z*), atunci pentru valori naturale ale numerelor *x, y, z*, avem

$$u_{x, y, z} = u_{x-1, y, z} + u_{x, y-1, z} + u_{x, y, z-1} \tag{11}$$

Pe lângă această ecuație cu diferențe, care contine o funcție necunoscută depinzând de trei argumente întregi, avem şi condițiile

$$u_{x,y,0} = \frac{(x+y)!}{x!y!};\ u_{x,0,z} = \frac{(x+z)!}{x!z!};\ u_{0,y,y} = \frac{(y+z)!}{y!z!}$$

care rezultă din soluția problemei precedente.

Orice mod concret prin care păianjenul poate trece din nodul (0, 0, 0) în nodul *(k, l, m*) poate fi caracterizat prin şirul de litere *x, y, z*, care arată în ce ordine se succed deplasările păianjenului după direcțiile axelor *Ox, Oy, Oz*; de aceea, $u_{k, l, m}$ va fi egal cu numărul de moduri în care putem completa $k + l + m$ locuri, cu *k* litere „*x*”, cu *l* litere „*y*” şi cu *n* litere „*z*”.

Dintre cele $k + l + m$ locuri de care dispunem, putem alege *k* locuri pentru a le umple cu litera „*x*” în $\dfrac{(k+l+m)!}{k!(l+m)!}$ noduri; fiecăruia din aceste noduri îi corespund $\dfrac{(l+m)!}{l!m!}$ posibilități de a alege *l* locuri (dintre cele $l + m$ rămase libere) pentru a le completa cu litera „*y*”. Prin urmare, numărul total de posibilități de a alege *k* locuri în schemă (pentru a le umple cu litera „*x*”) şi *l* locuri (pentru a le umple cu litera „*y*”) este

$$\frac{(k+l+m)!}{k!(l+m)!}\cdot\frac{(l+m)!}{l!m!} = \frac{(k+l+m)!}{k!l!m!}$$

Aşadar, soluția ecuației (11) în condițiile limită (12) va fi funcția $u_{x, y, z} = \dfrac{(x+y+z)!}{x!y!z!}$

Probleme multidimensionale

Problema păianjenului poate fi generalizată la o rețea cvadridimensională, ale cărei noduri se obțin din nodurile rețelei tridimensionale, deplasând-o cu una, cu două, cu trei etc. unități de lungime în direcția celei de-a „ patra axe” *Ou.* Nu este necesar să orientăm axa *Ou* perpendicular pe axele *Ox, Oy, Oz*, căci pentru aceasta ar trebui „ să ieşim în spațiul cvadridimensional”, ci este suficient să ne imaginam o serie de rețele tridimensionale, ale căror noduri sunt unite prin mici bare „ unitare”, adică egale cu unitatea, şi „ paralele” cu axa *Ou.*

Pentru rețele tridimensionale cu număr finit de noduri aceasta se poate realiza sub forma unui model, unind efectiv prin „ sârme unitare” nodurile corespunzătoare ale rețelelor tridimensionale de ordinul „zero”, de ordinul întâi, al doilea etc.

Într-o astfel de rețea cvadridimensională, fiecare nod va fi caracterizat prin patru numere întregi (coordonatele sale).

Păstrând terminologia geometrică, un ansamblu de *m* numere reale $a_1, a_2, \ldots, a_m$ reprezintă coordonatele unui punct în „ spațiul *m* dimensional” $\mathbf{R}^m$.

Dacă numerele $a_1, a_2,..., a_m$ sunt întregi şi pozitive şi considerăm drept vecine nodurile în care numai una dintre coordonate diferă cu o unitate, pe când toate celelalte sunt egale, atunci pentru $a_1 + a_2 +... + a_m = n$, trecerea de la nodul O (0, 0,…, 0) la nodul A ($a_1, a_2, ..., a_m$) se poate efectua în n mutări (trecând de fiecare dată în câte un nod vecin).

Dacă mutările în cadrul cărora creşte numai prima coordonată sau numai a doua etc. sunt notate respectiv cu literele x_1, x_2 etc., atunci numărul de moduri pentru a trece prin n mutări din nodul O (0,0,...0) în nodul A ($a_1, a_2, ...,a_m$) este egal cu numărul de „ permutări cu repetiție” care se pot face cu n elemente:

$$\underbrace{x_1, x_1, ..., x_1}_{a_1 \text{ elemente}} \;; \qquad \underbrace{x_2, x_2, ..., x_2}_{a_2 \text{ elemente}} \;; \qquad \ldots \;; \qquad \underbrace{x_m, x_m, ..., x_m}_{a_m \text{ elemente}}$$

Ca exemplu de problemă multidimensională este problema umplerii cu apă a unor butoaie: butoaiele cu numerele de ordine 1, 2, … , m au respectiv capacitățile $a_1, a_2, ..., a_m$ căldări; în câte moduri se pot umple toate butoaiele dacă trebuie respectată condiția că apa dintr-o căldare plină se toarnă în întregime într-unul din butoaie ?

Acest număr este egal cu: $\dfrac{(a_1 + a_2 + \cdots + a_m)!}{a_1! a_2! \cdots a_m!}$.

Studiul matematic şi fizic al centrului de greutate al unui corp: teorie, experiment, metodică

Consuela Luiza Voica şi Elena Popescu
Şcoala cu clasele I-VIII nr.12, Sector I, Bucureşti.

În prezenta lucrare încercăm să răspundem la întrebările: Există o legătură între noţiunile matematice şi cele fizice cu denumiri asemănătoare? Putem utiliza proprietăţi fizice în demonstrarea unor rezultate de geometrie? Pot fi realizate orele de curs prin colaborarea unor profesori de specialităţi diferite? În lucrare sunt prezentate modalităţile practice, rezultate dintr-un experiment cu elevii, de realizare a unor ore de curs, în care se leagă cunoştinţele de matematică cu cele de fizică. Sunt arătate atât implicaţiile studiului matematic asupra modelului fizic, şi invers, cât şi modul în care pot colabora profesorii de matematică cu cei de fizică. Prin aceasta se urmăreşte din punct de vedere metodic modul de pregătire al elevilor pentru abordarea în viitor a unor probleme interdisciplinare şi modalităţi de conlucrare a unor specialişti din discipline diferite.

1. Introducere

Lucrarea realizează o legătură între premodelarea matematică şi cea fizică într-o problemă implicând calculul centrului de greutate al unui tetraedru şi al unui paralelipiped dreptunghic. Acest centru joacă un rol important în alunecarea corpului pe un plan înclinat. De aceea lucrarea de faţă arată modalitatea concretă şi metodica prin care se induce aceasta elevilor.

În accepţiunea didacticii contemporane, o componentă majoră a procesului didactic o constituie aplicarea cunoştinţelor şi competenţelor dobândite într-un context dat, prin transferarea acestora în contexte noi, variate. În acest sens, exersarea se poate realiza prin "interconectarea diferitelor tipuri de reprezentări, construirea relaţiilor dintre reprezentare şi obiect, privirea conceptelor în lumina noilor experienţe" [1, p.26], ceea ce aratăm în lucrarea de faţă. Experimentul nostru concordă cu programele şcolare care solicită printre altele "identificarea utilizării unor concepte şi metode matematice studiate, în diferite domenii" şi "aplicarea cunoştinţelor dobândite prin studiul fizicii în domenii conexe acesteia" [2].

2. Scopul şi obiectivele experimentului

Primul constă în realizarea transferului de cunoştinţe între diferite discipline din aria curriculară matematică şi ştiinţe, evidenţiindu-se legăturile dintre noţiunile matematice şi fizice cu aceeaşi denumire dar cu conţinut diferit, specific ştiinţei respective. În plus, arătăm posibilitatea utilizării unor proprietăţi fizice în demonstrarea unor rezultate de geometrie, abordare rar întâlnită în literatura matematică. Dintre puţinele lucrări în acest domeniu menţionăm [3].

Experimentul reprezintă o premieră, realizând ore de curs cu colaborarea unor profesori de specialităţi diferite. Uneori, această colaborare se foloseşte şi la cursurile de matematică aplicată din universităţi [4].

Obiectivele experimentului sunt: identificarea unor posibilităţi de colaborare între profesori de discipline diferite; organizarea şi desfăşurarea unor ore de curs, în care doi profesori de discipline diferite au rol de conducere a învăţării; identificarea legăturilor dintre proprietăţi învăţate în contexte diverse; aplicarea unor metode matematice în rezolvarea problemelor practice, precum şi utilizarea proprietăţilor fizice în demonstrarea unor rezultate matematice; utilizarea lucrului în grup, ca metodă de dinamizare a clasei şi de eficientizare a activităţii; crearea unui cadru ambiental atractiv şi agreabil de desfăşurare a orelor (prin audiţii muzicale în timpul realizării de către elevi a modelului decupat din hârtie); determinarea desfăşurării unor experimente de acelaşi tip, prin popularizarea modului de organizare şi a concluziilor obţinute.

Considerăm că aceste obiective vor crea premiza grupurilor mixte de cercetare formate din matematicieni aplicaţi, fizicieni, chimişti, ingineri etc.

3. PROIECTAREA EXPERIMENTULUI ŞI PREMODELAREA

În proiectarea experimentului, am plecat de la următoarea întrebare, adresată elevilor: “care este legătura dintre centrul de greutate învăţat la matematică, şi aceeaşi noţiune din fizică?” Am constatat că elevii nu pot realiza legături între aceste noţiuni; pentru ei, centrul de greutate înseamnă sau “punctul de intersecţie a medianelor” (la matematică) sau “punctul de aplicaţie a forţei de greutate “ (fizică).

Situaţii-problemă au apărut şi la matematică, şi la fizică, în cazul în care am încercat să lucrăm cu configuraţii plane sau spaţiale mai complicate. De exemplu, am întrebat: “Ce punct ar putea să fie denumit centru de greutate al unui tetraedru? Dar al unui paralelipiped oblic?” Deoarece elevii nu au putut formula răspunsuri coerente, ne-am propus să organizăm ore în comun, în care să evidenţiem legăturile dintre concepte cu denumire comună, dar cu definiţii diferite, din matematică şi din fizică. În acest fel, am putut explica coerent modul în care apar unele definiţii în matematică şi în fizică, ceea ce depăşeşte, de fapt, simpla legătură dintre matematică şi fizică. Într-adevăr astfel se abordează şi problema mult mai dificilă a derivării unor rezultate matematice din cele fizice (e.g. în mecanică [3]).

Experimentul s-a derulat pe parcursul ultimilor 2 ani şcolari, cu diferite clase a VIII-a. De la un an la altul, precum şi de la o clasă la alta, am modificat atât modul de organizare a clasei, cât şi sarcinile de lucru.

Modelul fizic: centrul de greutate a două puncte materiale de mase egale este punctul de aplicaţie al rezultantei forţelor de greutate. Poziţia centrului de greutate se determină din relaţia fizică de egalitate a momentelor forţelor de greutate faţă de centrul de greutate, i.e. $\mathbf{G} \cdot b_1 = \mathbf{G} \cdot b_2 \Rightarrow b_1 = b_2$. Rezultă că acest centru de greutate G se află la mijlocul segmentului imaginar ce uneşte cele două puncte (fig.1).

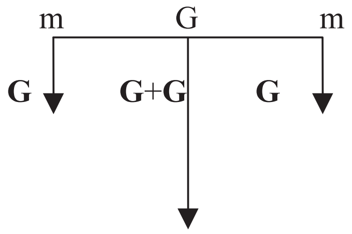

Fig.1.

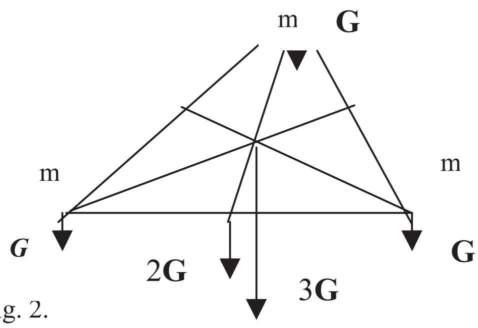

Fig. 2.

Pentru trei puncte materiale necoliniare, de mase egale, centrul de greutate al triunghiului determinat de cele trei puncte este şi punctul de aplicaţie al fortei de greutate a sistemului format de cele trei puncte (fig. 2). Acesta reprezintă punctul de intersecţie al medianelor triunghiului şi, scriind relaţia de egalitate a celor două momente, obţinem

$$2\mathbf{G} \cdot b_1 = \mathbf{G} \cdot b_2 \Rightarrow 2\, b_1 = b_2 \,.$$

Modelul matematic: Ultima relaţie arată că acest centru se află pe fiecare mediană la o treime de baza şi două treimi de vârf [5]. Prin urmare, modelul matematic al centrului de greutate este acelaşi cu cel din fizică.

Cazul tetraedrului. Firesc, ne întrebăm dacă putem aplica aceeaşi metodă pentru determinarea poziţiei centrului de greutate al unui tetraedru. Mai întâi elevii au fost solicitaţi să demonstreze matematic afirmaţia: “medianele” tetraedrului se intersectează într-un punct situat pe fiecare din ele la ¼ de bază şi ¾ de vârf ” (fig.3).

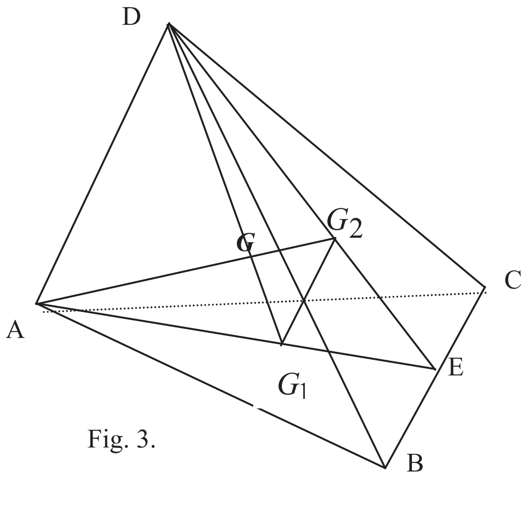

Fig. 3.

Demonstraţia matematică pentru medianele AG_2 şi DG_1 s-a făcut asfel: în triunghiul ADE, avem $\frac{EG_1}{AG_1} = \frac{EG_2}{DG_2} = \frac{1}{3}$, G_1 şi G_2 fiind centrele de greutate ale feţelor ABC şi DBC. Conform reciprocei teoremei lui Thales rezultă că $G_1G_2 \,//\, AD$ şi $\frac{G_1G_2}{AD} = \frac{1}{3}$. Aplicând apoi teorema fundamentală a asemănării pentru triunghiurile AGD şi G_2GG_1 obţinem $\frac{GG_1}{DG} = \frac{GG_2}{AG} = \frac{1}{3}$. Deci AG = 3$GG_2$.

Aplicând acelaşi raţionament pentru medianele CG_3 şi BG_4, unde G_3 şi G_4 sunt centrele de greutate respective ale feţelor ABD si DAC, am demonstrat afirmaţia de mai sus.

Apoi, demonstraţia acestui rezultat s-a făcut utilizând metode fizice şi s-a dovedit a fi mult mai uşoară. Ea se bazează pe ideea prezentată anterior pentru un triunghi.

Astfel, considerând că în vârfurile tetraedrului se află puncte materiale de aceeaşi masă (fig.4) şi aplicând raţionamentul fizic prezentat anterior pentru fiecare faţă a tetraedrului, obţinem poziţia centrului de greutate al fiecărei feţe, în care acţionează o greutate de modul 3G şi este chiar cea găsită matematic.

Pentru fiecare vârf şi centrul de greutate al feţei opuse aplicăm relaţia fizică de egalitate a momentelor faţă de centrul de greutate, i.e. $3G \cdot b_1 = G \cdot b_2 \Rightarrow 3b_1 = b_2$, fapt ce demonstrează afirmaţia facută.

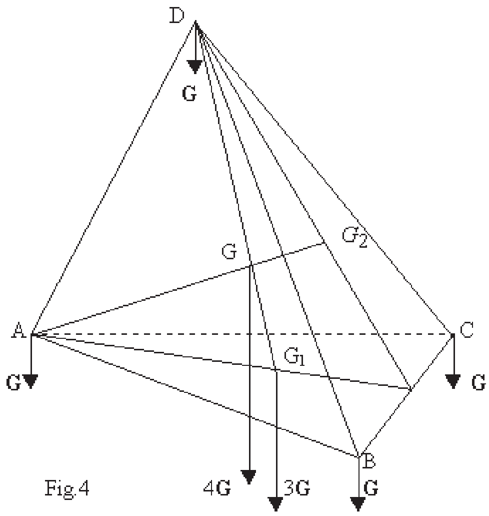

Fig.4

Centrul de greutate al unui sistem de puncte materiale se poate determina, prin gruparea arbitrară a punctelor date. În rezolvarea anterioară, am grupat trei puncte, lăsând unul dintre puncte separat.

Elevii au fost întrebaţi " Ce proprietate geometrică obţineţi dacă grupaţi punctele două câte două şi utilizaţi rezultatul cunoscut din fizică?"

Punctul M, mijlocul segmentului AD, este centrul de greutate al sistemului format din punctele A şi D iar punctul N, mijlocul segmentului BC, este centrul de greutate al sistemului format din punctele B şi C iar în fiecare din ele acţionează o forţă de modul 2G. Din egalitatea momentelor forţelor de greutate faţă de centrul de greutate, obţinem că G se află la mijlocul lui MN. Analog se demonstrează că G este mijlocul segmentelor PQ şi RS, unde P, Q, R, S sunt mijloacele segmentelor: AB, CD, AC şi BD.

Astfel, utilizând raţionamente fizice am demonstrat următoarea proprietate matematică:" Într-un tetraedru, segmentele ce unesc mijloacele laturilor opuse sunt concurente."

Demonstraţia matematică se bazează pe proprietăţile paralelogramului şi este mai lungă iar experimentul nostru este o pledoarie pentru realizarea obiectivului: "aplicarea unor metode matematice în rezolvarea problemelor practice, precum şi utilizarea proprietăţilor fizice în demonstrarea unor rezultate matematice."

În particular, pentru un tetraedru regulat, centrul de greutate şi centrul de simetrie coincid, ceea ce ne induce ideea de generalizare a afirmaţiei pentru corpurile cu centru de simetrie. Deci pentru un paralelipiped centrul de greutate se va afla la intersecţia diagonalelor lui.

4. PREMODELAREA FIZICĂ A ALUNECĂRII UNUI CORP PE PLANUL ÎNCLINAT

Să considerăm următoarea problemă: un paralelipiped dreptunghic confecţionat din lemn cu volumul de 54 cm^3 şi densitatea de 600 kg/m^3 alunecă pe un plan înclinat de unghi $\alpha = 30°$. Să se calculeze valoarea forţei de frecare ştiind că $\mu = 0{,}2$ şi g =10 N/kg. Pentru rezolvarea problemei confecţionăm un paralelipiped dreptunghic din carton având dimensiunile de 3 cm, 2 cm, 9 cm [6, p.21] şi îl lăsăm să alunece pe planul înclinat, având $\alpha = 30°, 45°, 60°$. Apoi procedăm la fel cu un paralelipiped din lemn şi cu unul din aluminiu. Observăm că forţa de frecare depinde de : natura suprafeţelor de contact; valoarea unghiului planului înclinat şi greutatea corpului.

Experimentul a pus în evidenţă pe de o parte o realitate fizică: existenţa unei legături între forţa de alunecare şi câţiva factori de care ea depinde, iar pe de altă parte, modalitatea de definire empirică , experimentală, a aşa-numitelor legi de material, care în cazul corpurilor rigide sunt tocmai legile de frecare. Desigur, în cazul simplu de mai sus, această lege este liniară, constanta de material fiind μ . Prin aceasta am pus în evidență şi o modalitate uşoară de înțelegere ulterioară a unor legități fizice profunde.

Revenind la problema dată, acum avem o bază fizică pentru calcularea forței de frecare. Pentru rezolvarea problemei reprezentăm forțele care acționează asupra corpului lăsat să alunece pe planul înclinat (fig.5) şi deducem formula forței de frecare

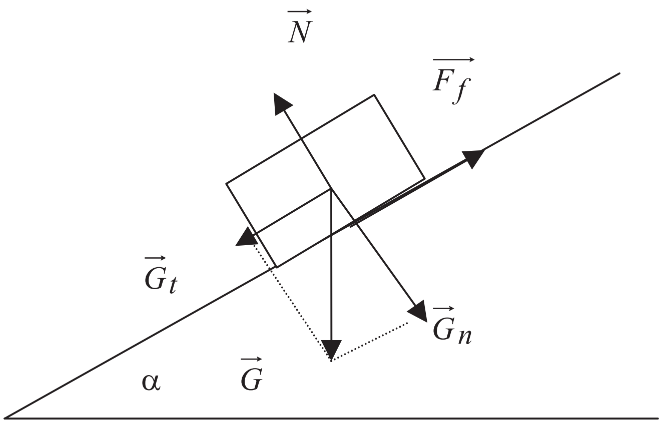

Fig.5.

$$F_f = \mu \cdot N = \mu \cdot G_n = \mu \cdot G \cdot \cos\alpha = \mu \cdot m \cdot g \cdot \cos\alpha = \mu \cdot \rho \cdot V \cdot g \cdot \cos\alpha .$$

Înlocuind datele de mai sus ale problemei în acestă formulă rezultă valoarea forței de frecare: $F_f = 0{,}2 \cdot 600 kg/m^3 \cdot 54 \cdot 10^{-6} m^3 \cdot 10 N/kg \cdot \frac{\sqrt{3}}{2} = 560{,}52 \cdot 10^{-4} N$, direcția ei fiind tangentă la suprafața planului înclinat (suprafața de contact).

5. Evaluarea experimentului

Am evaluat experimentul prin intermediul unor fişe cu întrebări, adresate elevilor şi profesorilor asistenți. În urma prelucrării răspunsurilor, am constatat următoarele: elevii au apreciat ca bună colaborarea cu colegul de bancă, orele le-au plăcut mult, iar întrebările au avut grad de dificultate mediu. Din acest experiment ei au aflat lucruri interesante: cum se pot îmbina cunostințele dobândite la fizică cu cele de la matematică, au înțeles mai bine noțiunea de centru de greutate şi au recapitulat în acest fel mai uşor lucruri studiate separat la cele două materii. Au aflat despre paralelipipedul oblic şi cel drept, au vizualizat un model al lor şi o realizare practică a unei probleme de fizică , rezolvarea devenind astfel mai uşoară. Profesorii au găsit experimentul foarte interesant de urmat, iar colaborarea dintre elevi şi respectiv dintre profesori a fost bună şi foarte bună.

Toate aceste premize ne-au determinat să prezentăm acest experiment şi să ne formulăm ca obiectiv popularizarea lui. În plus, încercarea de a prefigura modelarea matematică de la facultăți şi conlucrarea unor grupuri eterogene dar unitare de specialişti din cercetarea de mai târziu, a fost şi ea un real succes.

Bibliografie

[1] ***, *Ghiduri metodologice pentru aplicarea programelor de matematică, fizică, chimie, biologie,* editate de CNC şi MEC, Ed.Aramis, Bucureşti, 2001.

[2] ***, *Curriculum naţional. Programe şcolare pentru clasele a V-a -a VIII-a. Aria curriculară matematică şi ştiinţe ale naturii, e*Editate de MEC şi CNC, Bucureşti, 1999.
[3] *Iacob C,, Matematică aplicată şi mecanică,* Ed. Acad. R. S. R. , Bucureşti 1989.
[4] *Comunicare particulară cu doamna Prof. dr. Adelina Georgescu*.
[5] *Pufu, E. – C., Elemente de geometrie a maselor – centre de greutate,* în această carte.
[6] *Singer,M.,. Voica, C., Voica, C.-L., Decupează, construieşte şi verifică!* Ed.Sigma, Bucureşti, 2000.

Nota asupra unor relaţii trigonometrice

Valerian Oprişor,
„Liviu Rebreanu” Mioveni-Argeş

În unele aplicaţii industriale (e.g. în aviaţie), cunoaşterea exactă a valorii unor funcţii se poate dovedi deosebit de importantă.

Pe de altă parte, stimularea gândirii geometrice a elevilor mici este un obstacol în calea pericolului ca aceştia, folosind calculatorul, să nu mai fie convinşi de utilitatea acestei gândiri. Cum nu elevul este cel care ştie ce-i va folosi în profesiunea sa, profesorul are datoria să-i furnizeze elevului mic astfel de motive, una din surse dovedindu-se CAIM-ul.

În acelaşi timp la CAIM, Secţia de Învăţământ trebuie să dezbată printre altele, probleme metodologice de formare a gândirii matematice a elevului, posibil matematician, fizician sau inginer de mâine. De aceea, lucrarea noastră prezintă două metode de calcul, geometric şi trigonometric, al valorilor funcţiilor trigonometrice ale unghiurilor de 18^o şi de 15^o, reliefându-se avantajul uneia faţă de cealaltă, ca şi complementaritatea lor.

Problema 1. a) *Arătaţi că există punctele* O,A,B,C *astfel încât* $A\in(OC)$, $[OA]\equiv[AB]\equiv[BC]$ *şi* $[OB]\equiv[OC]$. b) *Demonstraţi că în situaţia de mai sus are loc relaţia* : $2\cdot|AC|=(\sqrt{5}-1)\cdot|OA|$.

c) *Deduceţi relaţiile*: $4\cdot sin18^o=\sqrt{5}-1$ şi $4\cdot cos\,36^o=\sqrt{5}+1$.

Soluţie. a) Pentru un unghi $\angle AOB$ de măsură $u<45^o$ rezultă $m(\angle OBA)=u$, $m(\angle BAC)=2\cdot u$, $m(\angle OCB)=2\cdot u$, $m(\angle ABC)=180^o-4\cdot u$ (fig.1). Are loc $[OB]\equiv[OC]$ dacă (şi numai dacă) $\angle OBC\equiv\angle OCB$, i.e. $u=180^o/5=36^o$.

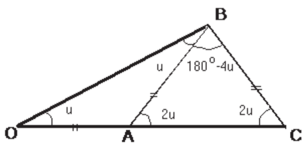

Fig. 1

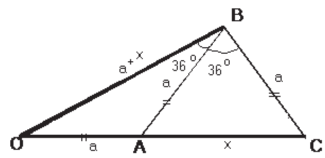

Fig. 2

b) Notând $|OA|=a$ şi $|AC|=x$ rezultă $|OB|=a+x$ (fig. 2). În ΔOBC, unde BA este bisectoarea $\angle OBC$, aplicând teorema bisectoarei obţinem $(a+x)/a=a/x\Leftrightarrow x^2+a\cdot x-a^2=0\Leftrightarrow(2\cdot x+a)^2=5\cdot a^2$ de unde $2\cdot x=a\cdot\sqrt{5}-a$, de unde rezultă relaţia cerută.

c) Fie D mijlocul segmentului (AC) (fig.3). Cunoscând lungimile tuturor segmentelor din fig. 3 se calculează $sin\,18^o$ din ΔDBC şi $cos36^o$ din ΔDBO şi se obţin relaţiile cerute.

Observaţie. Putem calcula valori ale funcţiilor trigonometrice şi pentru unghiurile cu măsurile de 54^o şi 72^o.

Folosirea mai multor procedee pentru rezolvarea unei aceleiaşi probleme permite să se constate mai uşor eficienţa unei anumite metode, să se decidă în care din situaţii se realizează o mai mare economie de timp în rezolvare sau se obţine o soluţie mai simplă şi elegantă. Astfel, la trigonometrie la clasa a IX-a sunt frecvente aplicaţiile de tipul:

Problema 2. *Să se calculeze fără tabele trigonometrice sin* 18^o *sau cos* 18^o.

Soluţie. Li se poate sugera elevilor, ca aplicaţii la formulele învăţate, abordabile de altfel şi la nivelul clasei a VII-a, să găsească o ecuaţie care să aibă drept necunoscută pe *sin* 18^o. În acest sens observăm că $2\cdot18^o=36^o$, $3\cdot18^o=54^o$ iar $36^o+54^o=90^o$. Prin urmare arcele $2\cdot18^o$ şi $3\cdot18^o$ sunt complementare, deci $sin\,2\cdot18^o=cos\,3\cdot18^o$. Utilizând formulele trigonometrice care dau funcţiile arcului dublu şi triplu se găseşte relaţia: $2\cdot sin18^o\cdot cos18^o=4\cdot cos^3 18^o-3\cdot cos18^o$, din care prin împărţire cu $cos18^o\neq0$ şi ţinând cont că avem $cos^2 18^o=1-sin^2 18^o$, se obţine $4\cdot sin^2 18^o+2\cdot sin18^o-1=0$, de unde rezultă $sin18^o=(\sqrt{5}-1)/4$. De aici , prin utilizarea formulelor trigonometrice învăţate, se pot deduce valorile şi ale altor funcţii

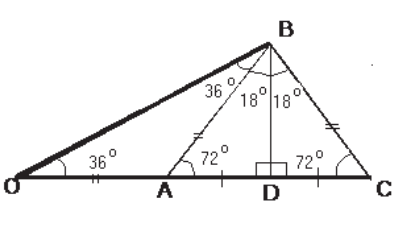

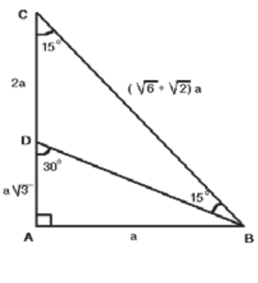

Fig. 3 Fig. 4

Problema 3. *Aplicând definițiile funcțiilor trigonometrice în triunghiul dreptunghic, calculați sin* 15^o.

Soluție. Fie ρABC cu m($\angle$ A)= 90^o, m($\angle$ C)= 15^o şi D $\in$ (AC) astfel încât m($\angle$ DBC)= 15^o (fig.4).

Notând |AB| = a şi având m($\angle$ ADB) = 30^o, rezultă că |BD| = |DC| = $2 \cdot a$, |AD| = $a \cdot \sqrt{3}$ şi utilizând teorema lui Pitagora avem că : |BC| =($\sqrt{6} + \sqrt{2}$) $\cdot$ a. În ρABC cu m($\angle$ A)= 90^o avem: *sin*($\angle$ ACB)= |AB| / |BC| , i.e. $sin 15^o = a / (\sqrt{6} + \sqrt{2}) \cdot a \Leftrightarrow sin 15^o = (\sqrt{6} - \sqrt{2}) / 4$.

Problema 4. *Calculați fără tabele trigonometrice sin* 15^o.

Soluție. Utilizând formula $sin 2 \cdot x = 2 \cdot sin x \cdot cos x$ şi punând $x=15^o$ obținem : $4 \cdot sin 15^o \cdot cos 15^o = 1$. Ținând cont că $sin^2 15^o + cos^2 15^o = 1$, obținem : $sin^2 15^o - 4 \cdot sin 15^o \cdot cos 15^o + cos^2 15^o = 0$ de unde prin împărțire cu $cos^2 15^o \neq 0$ şi notând *sin* x / *cos* x = t obținem $t^2 - 4 \cdot t + 4 = 3 \Leftrightarrow t = 2 - \sqrt{3}$.

De aici rezultă $sin 15^o / cos 15^o = 2 - \sqrt{3} \Leftrightarrow cos 15^o = (2 + \sqrt{3}) \cdot sin\ 15^o$. Înlocuind în $4 \cdot sin 15^o \cdot cos 15^o = 1$ obținem $4 \cdot sin^2 15^o = 2 - \sqrt{3} \Leftrightarrow 16 \cdot sin^2 15^o = (\sqrt{6} - \sqrt{2})^2$, de unde găsim $sin 15^o = (\sqrt{6} - \sqrt{2}) / 4$.

Ştiind *sin* 15^o, putem deduce *cos* 15^o, respectiv *cos* 75^o şi *sin* 75^o.

Spiritul creator ca şi originalitatea gândirii pot fi evidențiate în cadrul multor altor probleme.

BIBLIOGRAFIE

[1] Barbu R., Barbu N., Valențe educative ale lecțiilor de matematica, Revista de pedagogie, 1987.
[2] Brânzei D., Negrilă A., Negrilă M., Algebră şi geometrie, Ed. Paralela 45, Pitesti, 2001.
[3] Cuculescu I., Ottescu C., Geometrie, manual pentru clasa a VII-a, E.D.P., Bucuresti, 1985.
[4] Cota A., Marta R., Mariana R., Vornicescu F., Geometie si trigonometrie, manual pentru clasa a IX-a, E.D.P., Bucureşti, 1992.

Geometria maselor şi centre de greutate

Elena – Camelia Pufu
Şcoala „Liviu Rebreanu" – Mioveni

Ana Moşteanu
Liceul „Dacia" – Piteşti

1. INTRODUCERE

Studiul fizicii începe obligatoriu cu cel al mecanicii, ale cărei noţiuni fundamentale: traiectorie, viteză, acceleraţie, forţă, masă, lucru mecanic, energie, impuls, moment cinetic etc. şi ale cărei legi fundamentale (principiile mecanicii): ale impulsului, momentului cinetic, energiei cinetice, conservării energiei mecanice, sunt apoi folosite în toate capitolele fizicii.

În mecanică s-a făcut cea dintâi aplicaţie a matematicii la studiul cantitativ şi calitativ al fenomenelor naturii. Mecanica este cea mai matematizată ştiinţă, mult timp ea fiind considerată drept o ramură a matematicii.

În această lucrare evidenţiem necesitatea cunoaşterii noţiunilor matematice pentru rezolvarea problemelor fizicii, legate de determinarea centrelor de greutate ale corpurilor.

Se poate arăta, atât teoretic, cât şi experimental că poziţia centrului de greutate este bine determinată pentru fiecare corp şi nu depinde de orientarea lui în spaţiu. Existenţa sa ne arată că forţa gravitaţională acţionează asupra unui corp ca şi cum ar fi aplicată într-un anumit punct cu toate că forţa este un vector alunecător.

Centrele de greutate ale corpurilor omogene, cu forme geometrice regulate, care posedă axe sau plane de simetrie, sunt întotdeauna situate pe axa, respectiv pe planul de simetrie.

Pentru corpuri de formă mai complicată pentru determinarea centrului de greutate este necesară divizarea acelui sistem de puncte materiale în mai multe subsisteme distincte şi compunerea forţelor paralele de greutate ale punctelor materiale ce alcătuiesc corpul şi care sunt supuse acţiunii greutăţii.

Consideraţiile privind centrul de greutate al unui sistem discret de puncte materiale pot fi extinse şi la cazul sistemelor materiale continue care ocupă un segment de dreaptă, un arc de curbă sau un domeniu plan sau tridimensional. Ele stau la baza însăşi a calculului integral.

2. CENTRUL DE GREUTATE AL UNUI SISTEM RIGID DE PUNCTE MATERIALE

Să considerăm un sistem alcătuit din n puncte materiale A_1, A_2, …., A_n de mase m_1, m_2, …, m_n, ce au poziţiile fixe unele faţă de altele deci sistemul este nedeformabil şi plasat în câmp gravitaţional uniform. Fiecare punct al sistemului este supus acţiunii unei forţe de greutate $\mathbf{G}_i=m_i\boldsymbol{g}$, unde $\boldsymbol{g}$ este un vector constant oricare ar fi poziţia punctului material.

Aşa cum am menţionat, acest sistem de forţe paralele ce au direcţia şi sensul verticalei descendente este întotdeauna echivalent cu o forţă unică aplicată în centrul acelor forţe paralele.

Centrul forţelor de greutate paralele se numeşte **centrul de greutate** al sistemului, iar forţa unică **G**, echivalentă cu forţele sistemului, se numeşte **greutatea sistemului de puncte materiale.**

Modulul forţei **G** este dat de relaţia

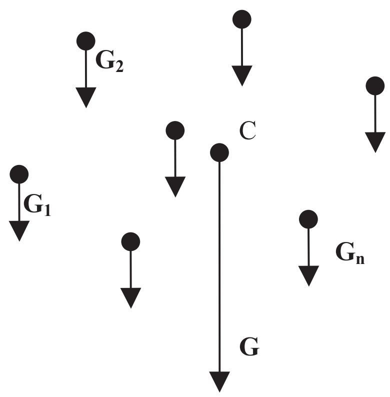

Fig. 1. Centrul de greutate al unui sistem rigid de puncte materiale.

$$G = m_1 g + m_2 g + ... + m_n g = (m_1 + m_2 + ... + m_n)\, g$$

sau

$$G = M \cdot g$$

unde $M = m_1 + m_2 + ... + m_n$ reprezintă masa sistemului de puncte materiale.

3. Determinarea poziției centrului de greutate al unui sistem de două puncte materiale în raport cu un sistem de coordonate

Cele două puncte materiale ale sistemului au masele m_1 şi respectiv m_2 şi coordonatele x_1, y_1 şi respectiv x_2, y_2 în raport cu un sistem de axe perpendiculare *xOy* (fig. 2).

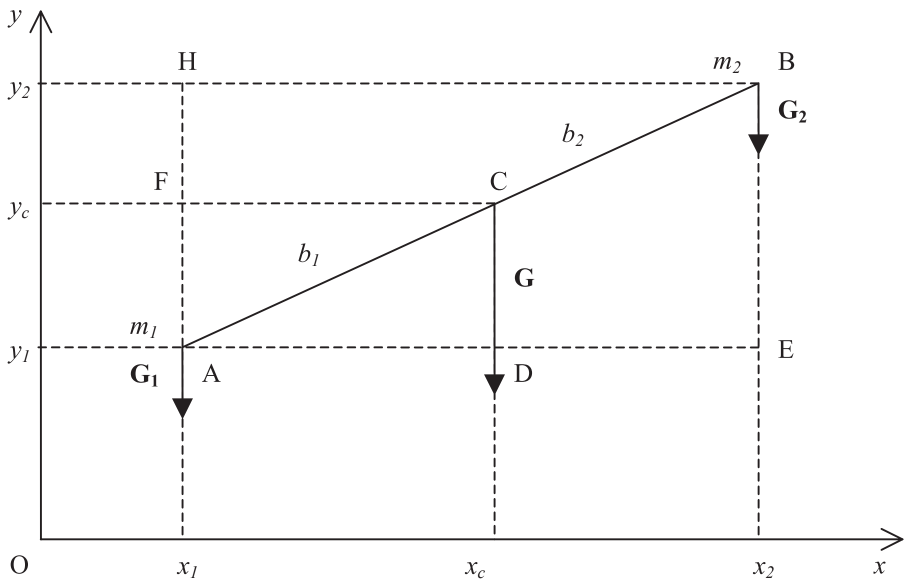

Fig. 2. Centrul de greutate al unui sistem de două puncte materiale de coordonate x_c şi y_c.

$$\mathbf{G_1} = m_1 \boldsymbol{g}$$
$$\mathbf{G_2} = m_2 \boldsymbol{g} \tag{2.1}$$
$$\mathbf{G} = \mathbf{G_1} + \mathbf{G_2}$$

Să notăm AC=b_1 şi CB=b_2. Ținând seama de compunerea forțelor paralele de acelaşi sens avem

$$G_1 \cdot b_1 = G_2 \cdot b_2 \quad \text{sau} \quad \frac{b_1}{b_2} = \frac{G_2}{G_1}. \tag{2.2}$$

Din asemănarea triunghiurilor AEB şi ADC, ca şi a triunghiurilor AHB şi AFC obținem

$$\frac{x_c - x_1}{x_2 - x_c} = \frac{b_1}{b_2} \ \text{şi}\ \frac{y_c - y_1}{y_2 - y_c} = \frac{b_1}{b_2}. \tag{2.3}$$

Utilizând şi relația (2.2) găsim

$$\frac{x_c - x_1}{x_2 - x_c} = \frac{G_2}{G_1} \ \text{şi}\ \frac{y_c - y_1}{y_2 - y_c} = \frac{G_2}{G_1}, \tag{2.4}$$

relații ce ne permit să determinăm coordonatele centrului de greutate

$$x_c = \frac{G_1 x_1 + G_2 x_2}{G_1 + G_2}\ ;\ y_c = \frac{G_1 y_1 + G_2 y_2}{G_1 + G_2}. \tag{2.5}$$

Raportând sistemul de puncte materiale la trei axe de coordonate obținem şi a treia coordonată a centrului de greutate

$$z_c = \frac{G_1 z_1 + G_2 z_2}{G_1 + G_2}\,. \tag{2.6}$$

Relațiile (2.5) şi (2.6) se pot generaliza la cazul unui sistem format dintr-un număr oarecare de puncte materiale şi obținem coordonatele centrului de greutate al acestui sistem

$$\begin{aligned} x_c &= \frac{G_1 x_1 + G_2 x_2 + \ldots + G_n x_n}{G_1 + G_2 + \ldots + G_n}\,, \\ y_c &= \frac{G_1 y_1 + G_2 y_2 + \ldots + G_n y_n}{G_1 + G_2 + \ldots + G_n}\,, \\ z_c &= \frac{G_1 z_1 + G_2 z_2 + \ldots + G_n z_n}{G_1 + G_2 + \ldots + G_n}\,. \end{aligned} \tag{2.7}$$

4. Determinarea poziției centrului de greutate (centrul de masă) pentru un sistem de trei puncte materiale situate în vârfurile unui triunghi ABC

Teoremă. *Centrul maselor* G *corespunzător maselor* m_1, m_2, m_3 *plasate respectiv în vârfurile* A, B, C *ale triunghiului* ABC *se găseşte în interiorul triunghiului.*

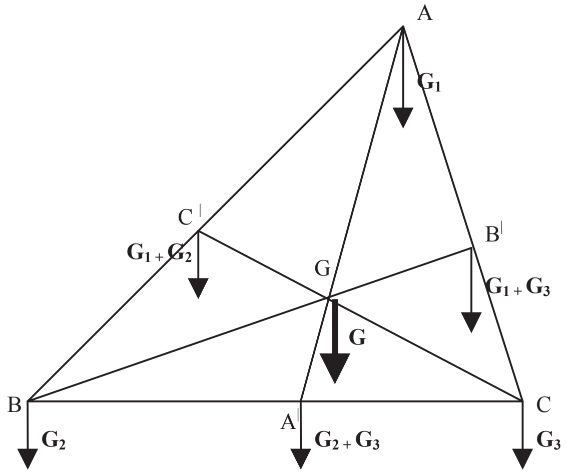

Fig. 3. Centrul de greutate al unui sistem de trei puncte materiale.

În vârfurile triunghiului ABC avem plasate masele m_i (i = 1, 2, 3) şi greutățile **G**$_i = m_i \cdot g$ (i = 1, 2, 3).

Compunând greutățile $\mathbf{G}_2$ şi $\mathbf{G}_3$, aplicate în B şi C, se găseşte la greutatea $\mathbf{G}_2 + \mathbf{G}_3$ aplicată în punctul $A^{|} \in BC$ astfel încât

$$m_2 \mathrm{BA'} = m_3 \mathrm{CA'}\ . \tag{3.1}$$

Centrul de greutate al celor trei greutăți se va afla în punctul G de pe segmentul $AA^{|}$ şi va fi dat de

$$m_1 \mathrm{AG} = (m_1 + m_2)\mathrm{A'G}\,. \tag{3.2}$$

Dacă am fi compus întâi greutățile $\mathbf{G}_3$ şi $\mathbf{G}_1$ aplicate respectiv în C şi A, ar fi rezultat greutatea $\mathbf{G}_3 + \mathbf{G}_1$ aplicată în punctul $B^{|} \in$ (CA). Dacă apoi pe aceasta am fi compus-o cu greutatea $\mathbf{G}_2$ aplicată în B am fi obținut acelaşi centru G situat pe segmentul $BB^{|}$ şi am fi avut

$$m_3\mathrm{CB'} = m_1\mathrm{AB'};\ m_2\mathrm{BG} = (m_3 + m_1)\mathrm{B'G}. \tag{3.3}$$

În mod analog, compunând întâi greutăţile $\mathbf{G}_1$ din A şi $\mathbf{G}_2$ din B, am fi obţinut greutatea $\mathbf{G}_1 + \mathbf{G}_2$ aplicată în $C' \in (AB)$. Aceasta compusă cu greutatea $\mathbf{G}_3$ aplicată în C, ar fi condus la centrul de greutate G $\in (CC')$. Avem astfel

$$m_1\mathrm{AC'} = m_2\mathrm{BC'};\ m_1\mathrm{CG} = (m_1 + m_2)\mathrm{C'G}. \tag{3.4}$$

Dreptele AA', BB', CC' se intersectează evident în punctul G care se găseşte în interiorul triunghiului ABC.

Putem enunţa şi demonstra următoarea teoremă reciprocă.

Teoremă. *Fiind dat un punct oarecare* G *în interiorul triunghiului* ABC, *există întotdeauna o distribuţie de mase* m_1, m_2, m_3 *plasate respectiv în* A, B, C *astfel ca* G *să fie centrul acestor mase*.

Această teoremă constituie o sursă de nenumărate aplicaţii geometrice privind în special concurenţa de drepte (aplicaţii la geometria triunghiului).

Prin urmare:

- medianele unui triunghi se intersectează într-un punct G interior acestuia, care este centrul maselor egale plasate în vârfuri. Punctul G de intersecţie al medianelor se numeşte centrul medianelor triunghiului;
- bisectoarele triunghiului ABC se intersectează în centrul de greutate al maselor plasate în vârfuri numit şi *ortocentrul triunghiului*.

După cum s-a arătat, într-un câmp gravitaţional omogen, centrul de greutate coincide cu centrul de masă. Totuşi noţiunea de centru de masă este mai generală decât cea de centru de greutate, deoarece centrul de masă al unui sistem fizic se poate determina întotdeauna independent de forţele gravitaţionale, ceea ce nu este adevărat pentru centrul de greutate.

În determinarea centrului maselor unui sistem material (S) putem întotdeauna să divizăm acel sistem în două sau mai multe subsisteme disjuncte (S_j), j=1,2,3,….,n, să determinăm centrele maselor G_j ale acestor sisteme, să le atribuim apoi acestora masele totale ale sistemelor (S_j). Centrul G al maselor sistemului (S) va fi atunci şi centrul maselor sistemului material format din punctele G_j dotate cu masele m_j (j=1,2,……n).

De exemplu, în spaţiul cosmic un experimentator va putea determina centrul de masă al unui corp, dar centrul său de greutate nu, deoarece forţa gravitaţională nu are nici un efect în locul în care se face experimentul.

Cele prezentate arată că se impune o corelare a programei de fizică cu cea de matematică astfel încât elevii să aibă noţiuni elementare de geometrie şi de analiză matematică atunci când studiază fenomenele mărimile fizice.

BIBLIOGRAFIE

[1] Hristev, A., Mecanică şi acustică, Editura Didactică şi Pedagogică, Bucureşti, 1984.
[2] Compediu de fizică, Editura Ştiinţifică şi Enciclopedică, Bucureşti, 1988.
[3] Brenneke, R., Schuster, G., Fizică – Manual pentru cursul superior al liceului, Editura Didactică şi Pedagogică, Bucureşti, 1973.
[4] Iacob, C., Matematică aplicată şi mecanică, Editura Academiei, Bucureşti, 1989.
[5] Manualele de fizică pentru clasa a VIII-a şi a IX-a.

Contents

Preface 3
A. Bica - The remainder estimation in terms of the third derivative for the successive approximations method applied to ODE's 5
E. Codeci, D. Codeci - The bifurcation codimension for the Goodwin's model 13
M. Gâta - Authentication of the message as part of the protocol with public key 15
C. Georgescu, A. Georgescu - On the saddle-node bifurcations in the demand-supply model 19
E. Laslo, D. Noje - Amorphous Viral Operator 24
B.V. Loginov, K.M. Petrov - Bifurcation problems for the equation div $(g(|\nabla f|^2)\nabla f)+\lambda f=0$ 28
D. Noje, B. Bede, V. Kos - Image contrast modifiers using vectorial MV-algebras 32
G.I. Oros, A. Cătaş - On a differential inequality 37
G.I. Oros - A new differential inequality I 40
F. Todor - A probability interpretation for the zeta function of Riemann and some technical regularization for spectral representation 43
M. Trifan - Some mathematical models in cancer theory 48
A. Ionescu - On the variation of the stationary states for an excitable model 52
I. Miodrag - Determination of an exremal domain for the functions of class *S* 55
L. Ungureanu - Cusp bifurcation in a problem of microeconomic dynamics 61
L. Antonescu, G.I. Oros - Observatii metodice asupra compunerii functiilor 65
O.D. Makinde, M.O. Adebayo - Fluid dynamics of expanding and contracting tube: a case study of methods of series summation 68
L. Marra - Project of a hybric-heuristical algorithm 79
A. Şerbanescu, P. Ciotirnae, D. Andrei - Applications of nonlinear dynamics to communications security 92
O. Tanasescu, H. Tanasescu - Hydrodynamics of dispersed, multiphase flows by wave breaking 99
R. Turcan, V. Turcan - Mathematics modelling of main process of polluants transport 107
M. Văleanu, G. Moldovan - Integrity in distributed database 114
I. Dzițac, S. Dzițac, H. Oros - Some applications of the Perov's fixed point theorem 120
Aripov, M., Sadullaeva, Sh. A - Properties of the solutions of a parabolic equation of non divergent type 130
M. Vereş - Modelarea agregatelor hidroenergetice prin metoda elementelor finite 136
M. Parv - A computer package for analysis of variance 143

Education section

L. Antonescu - Inegalități algebrice folosite în demonstrarea unor inegalități geometrice 157
Ş. Hăbuc - Mulțimea lui Mandelbrot 160
G. Monica - Probleme distractive de matematică 164
C.L. Voica, E. Popescu - Studiul matematic şi fizic al centrului de greutate al unui corp: teorie, experiment, metodică 168
V. Oprişor - Nota asupra unor relații trigonometrice 173
E.C. Pufu, A. Moşteanu - Geometria maselor şi centre de greutate 175